

Some pages of this thesis may have been removed for copyright restrictions.

If you have discovered material in Aston Research Explorer which is unlawful e.g. breaches copyright, (either yours or that of a third party) or any other law, including but not limited to those relating to patent, trademark, confidentiality, data protection, obscenity, defamation, libel, then please read our [Takedown policy](#) and contact the service immediately (openaccess@aston.ac.uk)

THE INFLUENCE OF CUTTING TOOL GEOMETRY UPON ASPECTS
OF CHIP FLOW AND TOOL WEAR

A Theoretical, Three Dimensional Examination of
the Cutting Geometry and the Shape of
the Twist Drill

PETER MARTIN WEBB

Doctor of Philosophy

THE UNIVERSITY OF ASTON IN BIRMINGHAM

July 1990

This copy of the thesis has been supplied on condition that anyone who consults it is understood to recognise that its copyright rests with its author and that no quotation from the thesis and no information derived from it may be published without the author's prior, written consent.

THE UNIVERSITY OF ASTON IN BIRMINGHAM

THE INFLUENCE OF CUTTING TOOL GEOMETRY UPON ASPECTS
OF CHIP FLOW AND TOOL WEAR

PETER MARTIN WEBB
Doctor of Philosophy
1990

This work is undertaken in the attempt to understand the processes at work at the cutting edge of the twist drill. Extensive drill life testing performed by the University has reinforced a survey of previously published information. This work demonstrated that there are two specific aspects of drilling which have not previously been explained comprehensively.

The first concerns the interrelating of process data between differing drilling situations. There is no method currently available which allows the cutting geometry of drilling to be defined numerically so that such comparisons, where made, are purely subjective. Section one examines this problem by taking as an example a 4.5mm drill suitable for use with aluminium. This drill is examined using a prototype solid modelling program to explore how the required numerical information may be generated.

The second aspect is the analysis of drill stiffness. What aspects of drill stiffness provide the very great difference in performance between short flute length, medium flute length and long flute length drills? These differences exist between drills of identical point geometry and the practical superiority of short drills has been known to shop floor drilling operatives since drilling was first introduced. This problem has been dismissed repeatedly as over complicated but section two provides a first approximation and shows that at least for smaller drills of 4.5 mm the effects are highly significant.

Once the cutting action of the twist drill is defined geometrically there is a huge body of machinability data that becomes applicable to the drilling process. Work remains to interpret the very high inclination angles of the drill cutting process in terms of cutting forces and tool wear but aspects of drill design may already be looked at in new ways with the prospect of a more analytical approach rather than the present mix of experience and trial and error.

Other problems are specific to the twist drill, such as the behaviour of the chips in the flute. It is now possible to predict the initial direction of chip flow leaving the drill cutting edge. For the future the parameters of further chip behaviour may also be explored within this geometric model.

TWIST DRILLING / METAL CUTTING / THREE DIMENSIONAL CUTTING
/ GEOMETRIC MODELLING / STRESS ANALYSIS

Acknowledgements

I should like to thank my supervisor,
Dr. J.D. MAIDEN, and Dr. D.P. UPTON of
Aston University, the Staff of S.K.F.
& DORMER and LUCAS AEROSPACE for their
help and guidance.

LIST OF CONTENTS

	PAGE
THEESIS SUMMARY	1
ACKNOWLEDGEMENTS	2
LIST OF CONTENTS	3
LIST OF FIGURES	7
CHAPTER 1	
1. THE TWIST DRILL	12
1.1. A BRIEF HISTORY OF DRILLS	12
1.2. THE MANUFACTURE OF TWIST DRILLS	20
1.3. TESTING OF DRILL PERFORMANCE	25
1.4. DRILL GEOMETRY - CURRENT LIMITATIONS	30
1.5. DRILL DYNAMICS - LIMITED APPRECIATION	32
1.6. INTRODUCTION TO THE ANALYSIS OF DRILLING	35
CHAPTER 2	
2. LITERATURE SURVEY	38
2.1. LITERATURE COVERING DRILL GEOMETRY	38
2.2. LITERATURE DESCRIBING FLEXIBILITY	
2.3. FLEXIBILITY AND VIBRATION	46
2.3. CONCLUSIONS	50
2.3.1. CURRENT STUDIES OF GEOMETRY	50
2.3.2. FLEXIBILITY	55
2.4. STATEMENT OF RESEARCH OBJECTIVES	57
PART ONE - INTRODUCTION OF GEOMETRIC ANALYSIS	59
CHAPTER 3	
3. GEOMETRIC WORK	61

	PAGE
PART TWO - INTRODUCTION OF STRESS ANALYSIS	167
CHAPTER 7	
7. DRILL RIGIDITY	169
7.1. DRILL STIFFNESS	169
7.2. THE ANALYSIS OF TORSION	171
7.2.1. CIRCULAR SECTIONS	172
7.2.2. NON-CIRCULAR SECTIONS	172
7.3. THE LONGITUDINAL EFFECT	177
7.4. THE DYNAMIC DRILLING MODEL	178
7.5. FINITE ELEMENT ANALYSIS	184
7.6. CONCLUSIONS	188
CHAPTER 8	
8. STRESS ANALYSIS	190
8.1. FINITE DIFFERENCE ANALYSIS OF TORSION	190
8.2. ANALYSIS OF LONGITUDINAL STRAIN BY	
FINITE DIFFERENCE EQUATIONS	202
8.3. CONCLUSIONS	206
CHAPTER 9	
9. TOTAL DRILL DEFORMATION	210
9.1. THE TOTAL SOLUTION	210
9.2. TORSION AND BENDING MODELS	211
9.3. WARPING FUNCTION OF THE TORSION MODEL	229
9.4. CONCLUSIONS	230
CHAPTER 10	
10. DRILL DYNAMIC RESPONSE	232
10.1. NATURAL FREQUENCY AND THE VALUE	
OF VIBRATION ANALYSIS	232

	PAGE
10.2. SUPPORTING OBSERVATIONS FROM DRILL TESTING	238
10.3. CONCLUSIONS	244

CHAPTER 11

11. DISCUSSION AND CONCLUSIONS	247
11.1. DEFINITION OF THE GEOMETRIC PROBLEM	248
11.2. ENUMERATE TOOL GEOMETRY	248
11.3. IDENTIFY THE CUTTING ANGLES	249
11.4. MODIFICATION FOR TOOL FLEXIBILITY	251
11.5. SUMMARY OF CONCLUSIONS	255
11.6. FUTURE WORK	256

LIST OF REFERENCES	258
--------------------	-----

APPENDIX A

LISTING OF COMPUTER PROGRAMS AND SPREADSHEETS

16.2. Orthographic Projection for Fig. 17.1	INSIDE BACK COVER
---	-------------------

17. Intersections of the Ellipses of the Ellipsoids	
---	--

18. Calculating the Area of the Ellipsoids	
--	--

19. Ellipsoidal Intersections	
-------------------------------	--

20. Ellipsoidal Intersections	
-------------------------------	--

21. Ellipsoidal Intersections	
-------------------------------	--

22. Ellipsoidal Intersections	
-------------------------------	--

23. Ellipsoidal Intersections	
-------------------------------	--

24. Ellipsoidal Intersections	
-------------------------------	--

25. Ellipsoidal Intersections	
-------------------------------	--

26. Ellipsoidal Intersections	
-------------------------------	--

27. Ellipsoidal Intersections	
-------------------------------	--

28. Ellipsoidal Intersections	
-------------------------------	--

LIST OF FIGURES

	PAGE
1. Lip or Flat Drill	13
2. Twisted Flat Drill	14
3. A. Whitworth Twist Drill B. Morse Twist Drill	15
4. Photograph of Drill Types	19
5. Flow Chart of Drill Manufacture	22
6. Example Force Data	27
7. Geometric Reference Values of Drill Form	29
8. Galloway's Chart of Factors Involved in Drilling	33
9. Proposed Additions to Galloway's Chart	34
10. Extract from Billau and McGoldrick [4]	44
11. Schaterin's Torque Tube	48
12. Fundamental Cutting Geometry	52
13. Grinding Cones and Drill Parameters	62
14. Family of Ellipses or Tool Rake Angle	66
15. Geometry of Major and Minor Axes of Ellipse	67
16. Z Ordinate Routine for Tip of Tool	68
17. Interception of the Ellipses at the Tool Point	71
18. Cutting Edge as a Cone Generator	72
19. Side Elevation Normal to Cutting Edge	75
20. Side Elevation of Outer Corner	76
21. Tool Rake (not True Rake)	77
22. Sketch vs Simple Computer Representation of Chip Flow [14]	80
23. Optimisation of Drill Stiffness [15] by Optimisation of Angle θ	82
24. Examples of Flute X-Section	85

	PAGE
25. Figure of Face Normals	90
26. Spherical Representation of Tool Wedge Angle	92
27. Velocity Vector	94
28. Spherical Representation of Inclination Angle	95
29. Stereographic Projection	98
30. Typical 'P Z X' Triangle	100
31. Stereographic Representation of the Cutting Action	
32. of a Straight Cutting Edge Twist Drill [14]	102
32. Point Shape [2]	104
33. Webthickness Parameter vs Actual Webthickness	108
34. Helical Milling	110
35. Spreadsheet Display of Drill Data	116
36. Periphery Clearance Angle [4]	117
37. Spreadsheet Histogram of Clearance Angle	119
38. Line Graph of Helix or Tool Rake Angle	120
39. Range of Point Face Clearance Angles	121
40. Representation of Drill Flank Face Distribution	
41. of Clearance Angle for Zero Feed	124
41. Representation of Drill Flank Face Distribution	
42. of Clearance Angle for 0.2mm/Rev Feed	125
42. Representation of Drill Flank Face Distribution	
43. of Clearance Angle for 0.4mm/Rev Feed	126
43. Representation of Drill Flank Face, Comparison of Zero Clearance Angle for Range of Feed Rates	127
44. Turbo Pascal Program - Input Parameters	129
45. Turbo Pascal Program - Output Data	130
46. Parabolic Drill Flute	132

	PAGE
47. Cubic Drill Flute Lay of Torsional Stress	133
48. Wu's Drill Point [3]	134
49. Set of Drill Flute Data	137
50. Flute Data Change of Origin	138
51. Grinding Wheel Profile	139
52. Inclination Angle	141
53. Tool Wedge Angle	142
54. Rake Angle Normal	143
55. Flank Angle Normal	144
56. Chisel Inclination Angle	146
57. Chisel Wedge Angle	147
58. Chisel Rake Angle Normal	148
59. Chisel Flank Angle Normal	149
60. Chip Flow 2-D Graphic Display	150
61. Optical Sectioning of Drill Point	155
62. Graph of Rake Angle of Combined Flutes	157
63. Grinding Wheel Profile - Combined Flutes	159
64. Sketch vs Simple Computer	
65. Turbo Drill Representation of Chip Flow [14]	160
65. Filon's Cross Section with Circular Notch	176
66. Graphs of Drill Torque Test & Drill Twisting	179
67. Graph of Drill Extension per Torque	180
68. Dynamic Drilling model	182
69. Helical Tube	183
70. Cross Section showing Drill Mesh used for	
71. evaluation of Finite Difference Equations	195
71. Cross Section of the Two Drill Models	196

	PAGE
72. Turbo Pascal Display of Torsional Shear Stress Distribution	198
73. Contour Lines of Membrane under the Influence of Torsion	199
74. SC4 Display of Torsional Shear Stress in Flute	200
75. Points of Interest	201
76. Turbo Pascal Display of Longitudinal Shear Stress Distribution	207
77. SC4 Display of Longitudinal Shear Stress in Flute	208
78. Bending Model Strain Distribution & Cross Section of Drill under the Influence of Torsion	214
79. Triangle of Helix Angle and Drill Extension	215
80. Bending Model/Real System Longitudinal Strain	217
81. Bending Model Radius of Curvature : Drill Twist	219
82. Bending Model Curvature : Drill Twist	220
83. Turbo Pascal Display of Combined Shear Stress Distribution - Quick Spiral Helix	223
84. SC4 Display of Combined Shear Stress in Flute	224
85. Turbo Pascal Display of Combined Shear Stress Distribution - Slow Helix Drill	226
86. Warping Distribution	228
87. Photograph of Broken Drill in Test Block	236
88. Drill Torque Testing Machine	239
89. Drill Extension Testing Machine	240
90. Drill Modification Design	241
91. Drill Mounting Design	242
92. Boundary Value Partial Differential Equations	252

	PAGE
1.0 THE TWIST DRILL	12
1.1 A BRIEF HISTORY OF DRILLS	12
1.2 THE MANUFACTURE OF TWIST DRILLS	20
1.3 TESTING OF DRILL PERFORMANCE	25
1.4 DRILL GEOMETRY - CURRENT LIMITATIONS	30
1.5 DRILL DYNAMICS - LIMITED APPRECIATION	32
1.6 INTRODUCTION TO THE ANALYSIS OF DRILLING	36

Drilling is

process of

removing

material

from a workpiece

The twist drill is using the cutting action of

flutes which are

specialized flutes. Flat

edges on the drill

will first come

probably about 1920

The

is

part

of

1. THE TWIST DRILL

The first two chapters provide an introduction to the subject of twist drilling. There is a complete lack of fundamental data that may be used to examine the cutting action of the drilling process. At the end of Chapter 2 this lack of data is crystallised into two objectives for which the main body of the thesis proposes novel solutions.

1.1. A BRIEF HISTORY OF DRILLS

Drilling is one of the most common of all production processes. There are thousands of drilling machines and many more lathes and milling machines which are frequently used for drilling. Millions of holes are produced with a vast consumption of drills.

The twist drill is among the oldest of tools and one of the first which necessitated a complex shape to perform a specialist function. Flat drills were made and used as long ago as the Neolithic Period. The date when the modern twist drill first came into use is not absolutely certain, but is probably about 1860.

The original drills were simply rough bars of steel which, in the blacksmith's shop, were flattened and angularly pointed at one end. The technical name for them being 'lip' or 'flat' drill, figure 1. The flat drill was a very

unsatisfactory tool, because if the hole were of any depth, the drill had to be frequently withdrawn to clear away the chips. The holes easily became clogged and this also prevented the coolant from getting to the point. These drills required constant redressing and grinding to get them to run at all true in use. Drills of this old type would not stand the strain of a heavy feed and the amount of cutting done per revolution was therefore small. The spear point had to be wholly re-made after a few sharpenings. The general development of manufacturing efficiency led to a demand for speedier results. One must not forget, however, that for some materials flat drills are still used today.

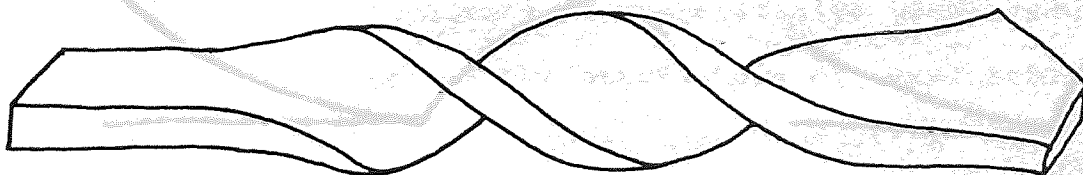


Figure 1 - Lip or Flat Drill

Flat drills failed to meet the more modern requirements of the industrial age for several reasons. It was necessary to repeatedly stop the work to clear the chips out of the hole, also, the drills quickly lost their sharp cutting edge so causing frequent breakage. These problems hindered

production and lost time. The major cause of the loss of cutting edge was heat, bluntness produced excessive heat, heat drew the temper of the steel, and loss of temper caused the cutting edge to break down. Heat generation became excessive as soon as the point lost its first sharpness, generated heat was then kept from dispersing by the accumulation of chips. High-speed steel had not yet been invented so some way of reducing the build up of chips, and so improving the tool, was required.

An intermediate stage was the invention, by person or persons unknown, of a twisted drill. This was made by twisting a flat bar of steel while hot until its shape was that of a worm-screw feeder, figure 2. For a time these drills figured side by side with the flat drills in engineering shops, but, as with many intermediate inventions, they did not provide the answer. This



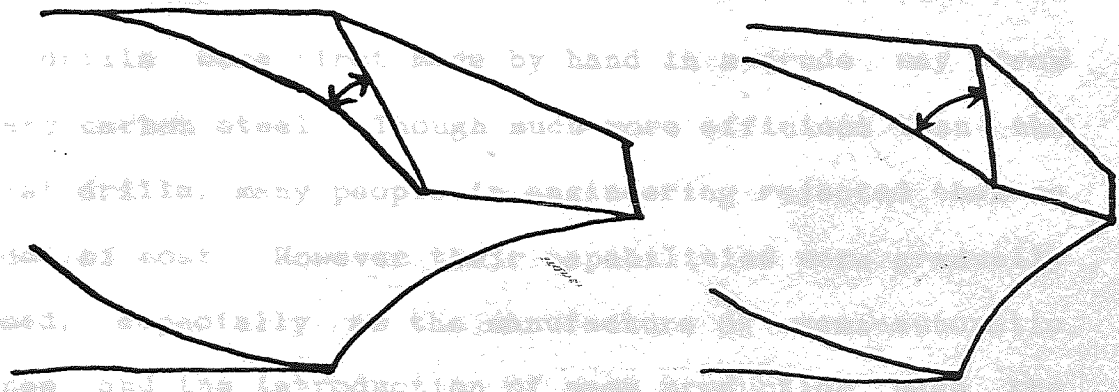
Sides very sharp, wedge angle very small.

Have moderate equal strength

Figure 2 - Twisted Flat Drill

configuration still occurs in the twisted bits used in wood-working shops and some rock drills used in mining. The designs were made by Sir Joseph Whitworth, figure reason for their failure was that they did not clear away their cuttings, as the modern twist drills do, in long chips. The drill broke the chips up into little pieces and was subsequently not very efficient in removing them. The geometry is utilised in order to produce the cutting hole still became clogged.

The next stage of development was to put spiral grooves in the drill body to provide generous rake and clearance, the drill body to provide at least a partial remedy for the swarf problem. The corkscrew action of the spiral flutes conveyed the cuttings away from the point, and also removed with the cuttings was the heat which they engendered. This was the first recognisable twist drill.



Edge very sharp, wedge angle very small.

More moderate sharpness, much stronger edge.

Figure 3A - Whitworth Twist Drill 3B - Morse Twist Drill

In the year 1860 or thereabouts, during work to improve the gun barrel, twist drills of a design approximating closely to modern designs were made by Sir Joseph Whitworth, figure 3A. The new tool overcame many of the difficulties experienced with the old type of drill. The major breakthrough was the way the combination of the flute and point geometry is utilised in order to produce the cutting edge. In America their manufacture was begun by the Manhattan Firearms Company. The first drills had a small wedge angle in order to provide generous rake and clearance. This resulted in a weak cutting edge with poor performance and tool life. Morse reduced the cutting angles and manufactured more robust twist drills capable of far better work than flat drills, figure 3B. Morse went on to devise several early specialised drills purporting to increased performance.

Twist drills were first made by hand in a crude way from ordinary carbon steel. Though much more efficient than the old flat drills, many people in engineering rejected them on grounds of cost. However their capabilities were gradually realised, especially as the manufacture of semi-automatic machines and the introduction of mass production made the adoption of an improved drill a necessity.

Even the crude, imperfect tools first produced had great advantages over the flat drill. The grooves of a twist drill are an important part of the cutting edge. Their uniform

shape along the whole of the fluted portion makes it possible to re-grind and re-use the the tool time after time without greatly reducing the length or diameter or lowering the efficiency. This prolonged the life of the tool and lent economic argument for their use. The face of the drill, being placed at an acute angle, gives decreased resistance to the cut, and a wedge-like action helps to feed the tool. Less power is needed to bore a hole with a twist drill than to bore the same hole with a flat drill, i.e. the same hole could be drilled faster with less effort.

Though twist drills have greater penetrative power than flat drills, there is a limit to the speed at which they can be run. Initially this was the point at which their temper was lost by overheating. When a drill lost temper, it had either to be re-hardened, or to have all the material that had become soft ground away. (Another effective cutting edge could only be obtained in the still hardened material well back from the softened point). The new carbon steel twist drill, although a great improvement on its predecessor, still left much to be desired. It had to be run at speeds only moderate in comparison with present day standards.

Once the problem of successful manufacture had been solved subsequent development of twist drills was dependent on economic incentive for a tool that many users considered expensive already. One aspect that did receive a lot of attention was the metallurgy of the alloy steels used in

their production. The introduction of alloy steels, which retained their temper even when red hot, increased the potential output to such an extent that a whole new generation of drilling machines had to be designed to permit the full realisation of the new tool's cutting ability. The first applications of high speed steel, HSS, were successful for lathe tools and soon a high speed steel specially suitable for twist drills became available. It combined toughness with great keenness of temper. With this steel the drill could be run almost at red heat without loss of edge so allowing higher cutting speeds and much greater output. Drilling machines underwent rapid development culminating in automatic machines and high speed multi spindle drilling machines.

The twist drill was thus able to combat the first prejudice against it. Its greater accuracy and length of service were the major points in its favour. The higher cost of manufacture was redeemed by greater efficiency, and eventually the discovery of high speed steel established the twist drill permanently in favour. Now Carbon Steel drills are a rarity, they are almost entirely superceded by H.S.S. There are some applications where carbon steel tools are still preferred but the required raw material, in wire form, is also scarce.

Modern H.S.S. drills come in two forms, bright finish and steam tempered, they may also be a H.S.S. substrate with a



Figure 4 - Photograph of Drill Types

ceramic coating of Titanium Nitride, figure 4. Experiment with TiN coated drills indicates an ability to be run at 10% higher feed per drill revolution, feed per rev, and 3 times spindle speed, i.e. 330% increase in drilling rate, as reported by Upton and Thornley [1], requiring the introduction of yet a new range of higher performance drilling machines. Solid Carbide Drills have also become available and are run with low feed but at even higher spindle speeds so similarly requiring drilling machines of great rigidity and high spindle speed capability.

1.2. THE MANUFACTURE OF TWIST DRILLS

Historically the manufacture of the twist drill was restricted to those few who mastered the kinematics/kinetics of the manufacturing process. For example with flute grinding, the helical grinding operation required knowledge of how to modify a standard machine tool to perform the required operation. Drill manufacturing equipment was so 'out of the ordinary' that normal machine tools had to be extensively altered before they could be used for drill manufacture. Different companies used different modifications which were all kept secret. The solution to the problem of how to manufacture drills was the valuable experience of the drill companies. Nowadays it is possible to purchase 'off the peg' special machines, purpose designed for the manufacture of twist drills.

Any country can now buy these machines and set up a drill manufacturing factory. The new machines are set fairly arbitrarily, because no direct relationship between the machine settings and the drills produced has been available. Once running they 'mass produce' a general purpose drill form. As with so many other industries the ability to understand the performance of the drill form, to design the correct drill form for the job and then to produce quality drills of precisely the designed form is the only asset left to enable the old established drill manufacturers to compete with the new Third World factories.

Drills are manufactured in as large a batch size as is possible. General purpose designs are used which minimise variation on the manually set up machines. The automated machinery for a flexible drill manufacturing facility which allows the so called "mass production of a batch size of one" is only just beginning to appear in the market place. The manufacturing process for small general purpose drills is as close to mass production as possible, working against very strong competition. For the specials and larger drills the market is much smaller and the industry must now respond to the need for purpose designed tools in this area.

Small general purpose drills are produced from a single piece of tool steel bar. A common raw material is molybdenum alloy bar, M2. This is cropped to size and roughly shaped

SMALL DRILLS

LARGE DRILLS

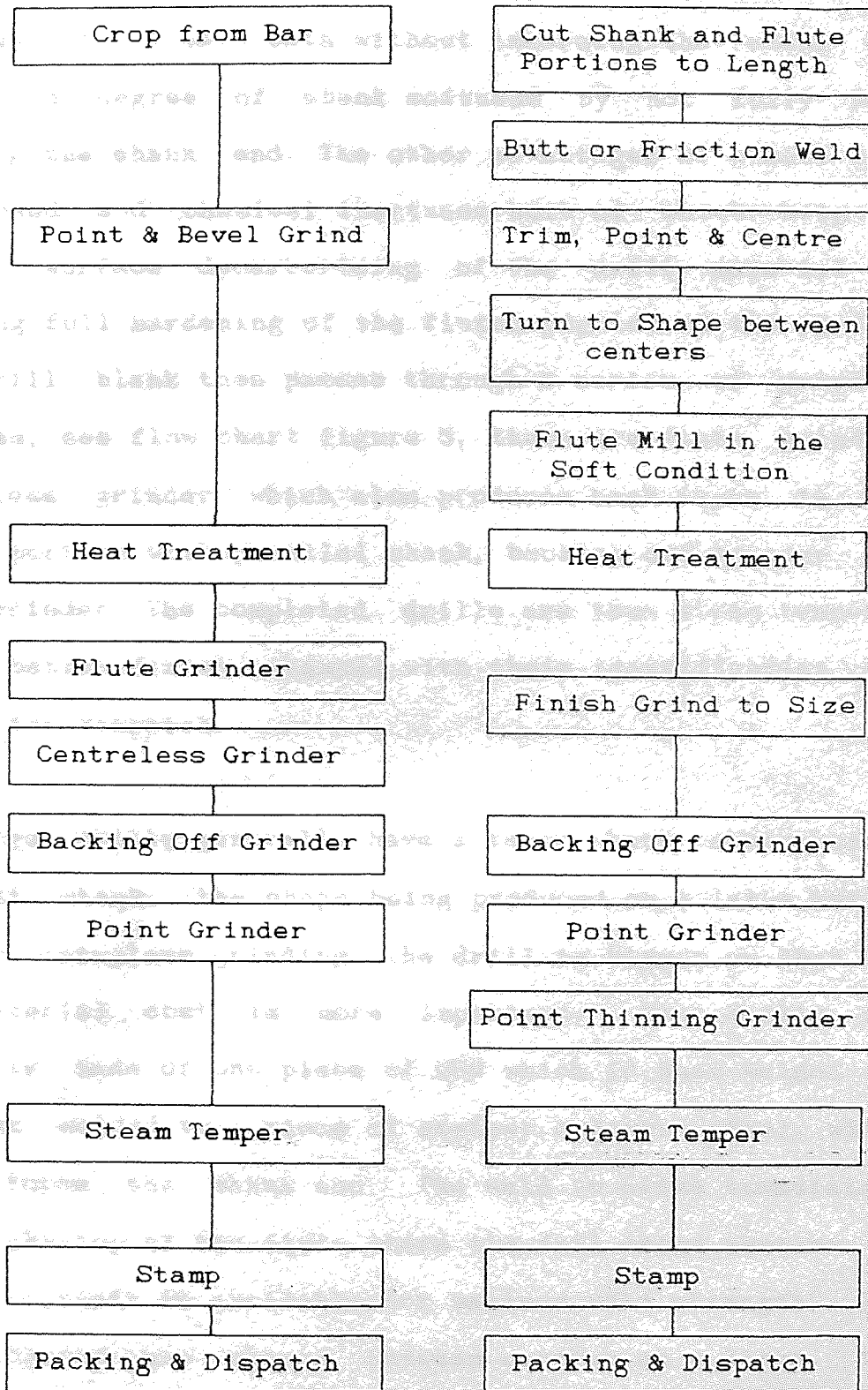


Figure 5 - Flow Chart of Drill Manufacture

with a point at one end and bevelled at the other. Heat treatment in a salt bath without immersing the shank end ensures a degree of shank softness by not fully heat treating the shank end. The other advantages of a salt bath are speed and chemical inertness both of which help to prevent surface decarburising of the drill material so ensuring full hardening of the fluted portion of the drill. The drill blank then passes through a series of grinding machines, see flow chart figure 5, these are flute grinder, centreless grinder which also produces back taper in the fluted portion with parallel shank, backing off grinder and point grinder. The completed drills are then steam tempered for a better finish, stamped with their identification and packed for dispatch.

The larger drills generally have a taper shank rather than a straight shank, the shape being produced on a lathe rather than by centreless grinding. The drill is bigger so that the raw material cost is more important. The drills are generally made of one piece of HSS which is butt welded or friction welded to a piece of cheaper ordinary steel which piece forms the shank end. The weld is sited immediately above the top of the flute where the full cross section of the drill shaft is available for maximum weld strength. The drill blanks are shaped between centres on a lathe, the tapered shank requiring a much more intricate shape. The drill flutes are milled soft and the drills are then heat treated. This time there is no requirement to avoid heating

the shank end. The grinding processes often including point thinning, the drills are then finished as described above.

One method of improving the H.S.S. twist drill is by applying a low surface friction ceramic coating. This alters the cutting characteristics of the cutting faces of the drill and produces a drill with enhanced performance and tool life.

Ceramic TiN coating is performed by specialist companies on a sub-contract basis rather than in house by a drill manufacturer. The drills used currently are the same as the uncoated drills but they are produced without finishing operations. These blanks are then supplied for TiN coating on a batch basis. Plasma Vapour Deposition is a process used to put a thin coating of ceramic material onto a metallic substrate. The coating chamber is evacuated of air and an electric potential is established between an electrode and the target tool. At a controlled pressure a plasma of gas is created electrically around the target. Titanium is then vapourised into the plasma by striking an electric arc onto a titanium surface. The tool, being the cathode, attracts the metallic and nitrogen ions from the gas plasma. P. V. D. coating is used in preference to Chemical Vapour Deposition, a high temperature process used for coating ceramic tool inserts, because the temperature reached by the tool whilst inside the coating chamber is lower, low enough not to degrade the heat treatment of the tool steel substrate.

1.3. TESTING OF DRILL PERFORMANCE

The monitoring and testing of the drilling process is complicated by two factors. First, although drilling may be performed by turning the workpiece, in general the tool is turning. Second the process is taking place at the bottom of the hole being generated by the drilling operation. To overcome the first factor the monitoring sensors must be mounted either on the drilling machine spindle or in the base of the drilling fixture or mounting. This places the sensors further away from the tool work interface than is generally the case for more accessible metal cutting processes. The inaccessibility caused by the second factor means that several forms of sensor suitable for other methods of metal cutting may not be used in drilling.

The following two aspects of drill performance may be monitored during the drilling operation:-

i, The Drilling Torque.

The drilling torque is the summation of three components. The first is the torque required by the drill cutting edges in performing their metal removal operation. The second is the friction force between the drill shaft and the hole sides. The last is the friction force between the swarf material contained within the drill flute and the hole sides.

ii, The Drilling Thrust.

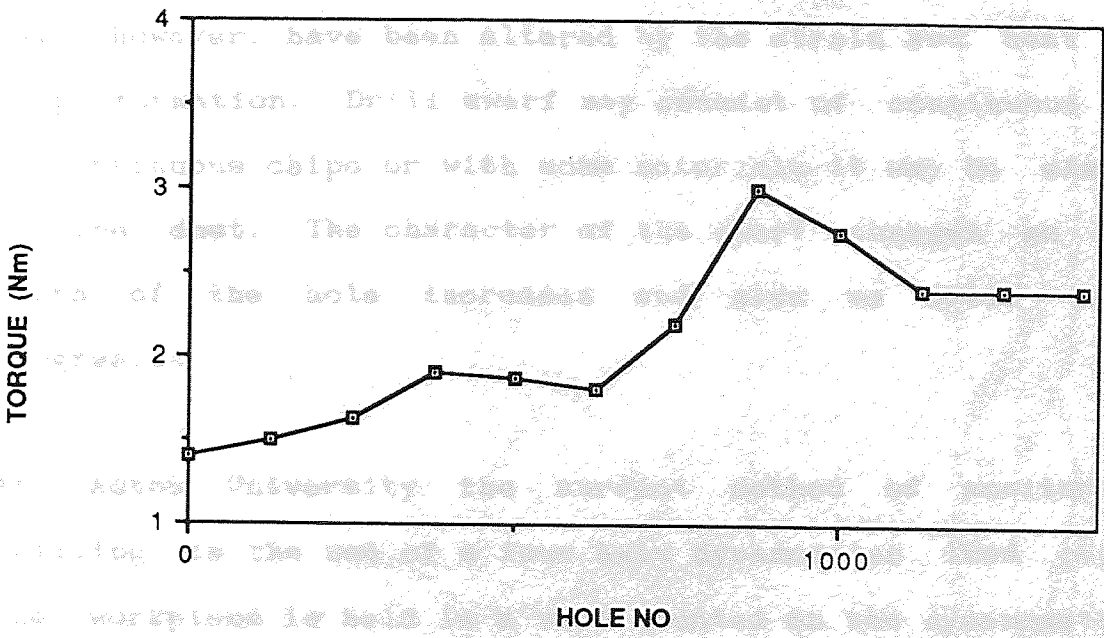
The drilling thrust is the summation of two components. The first is the thrust required by the cutting edges in performing their metal removal operation. The second is the thrust generated by the drill point or flank faces due to their lack of a positive cutting clearance towards the centre of the drill point.

Off line from the drilling process it is possible to assess the drill wear. This usually requires removing the drill and examining it optically. The drill wear is usually assessed by measuring the drill flank wear. During life testing, after an initial rapid build up, drill wear progressively increases until the end of the test. Consistent drill wear patterns have been observed for the same drill/workpiece combinations but these wear patterns vary for different drill/workpiece combinations. To date no research has been able to offer an analysis of these relationships.

Hole surface finish and hole diameter may be sampled from the finished holes. The measured statistics show some variations as drill wear progresses. The use of ceramic coated tools produces marked improvement in general hole quality including surface finish. Initial hole oversize is dependent on both the accuracy of the drill shape and the drilling machine kinematics.

chip formation. Chip formation is another indicator of the progress of the drilling process. Drilling starts in the workpiece which covers the cutting edge with material that is removed by the drill. The metallurgical properties of the workpiece have been altered by the stress and heat of the process. Drill starts with removal of material by chip formation. Drill starts with removal of material by chip formation. Drill starts with removal of material by chip formation.

Drilling Torque



Drilling Thrust

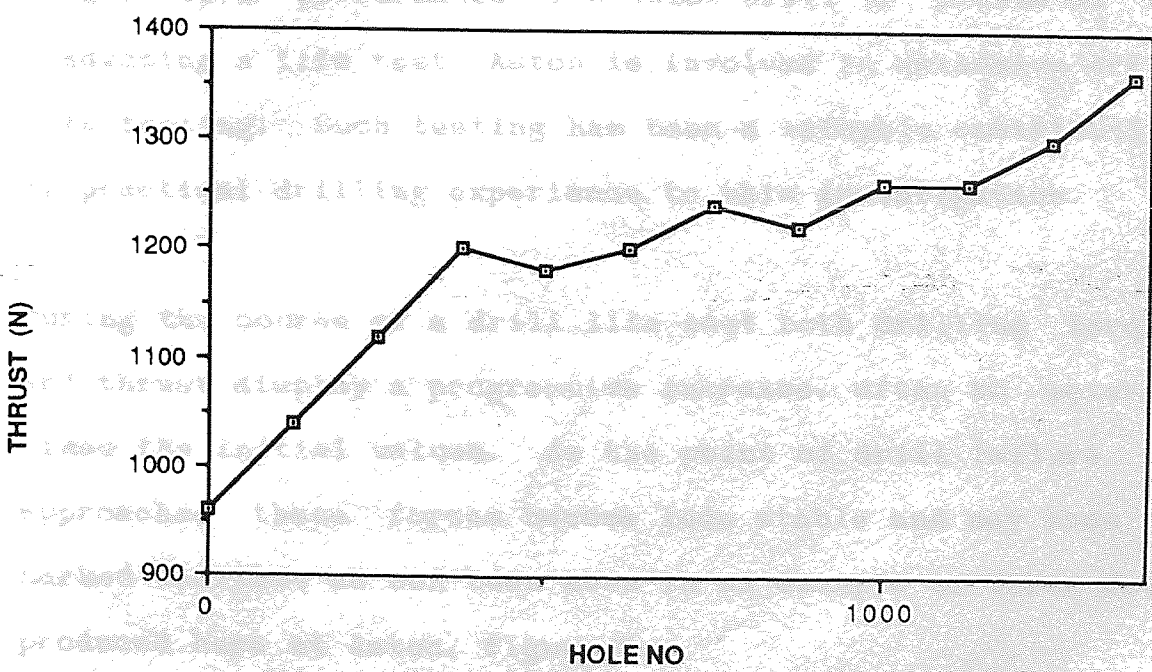


Figure 6 - Example Force Data

Drilling swarf or chips are another indicator of the progress of the drilling process. Drilling swarf is the waste material which consists of the workpiece material that has been removed by the drill. Its metallurgical properties may, however, have been altered by the strain and heat of chip formation. Drill swarf may consist of continuous or discontinuous chips or with some materials it may be simply a fine dust. The character of the swarf changes as the depth of the hole increases and also as drill wear progresses.

At Aston University the current method of monitoring drilling is the use of a four axis dynamometer load cell. The workpiece is held in a vice mounted on the dynamometer. This allows the torque and thrust force of the process to be measured and recorded throughout the drilling operation. The longer term performance of a twist drill is evaluated by conducting a life test. Aston is involved in extensive drill life testing. Such testing has been a valuable contribution of practical drilling experience to this investigation.

During the course of a drill life test both drilling torque and thrust display a progressive increase, often to several times the initial values. As the point of drill failure is approached these forces become less stable and may show a marked increase as can be seen in an example of force data produced here at Aston, figure 6.

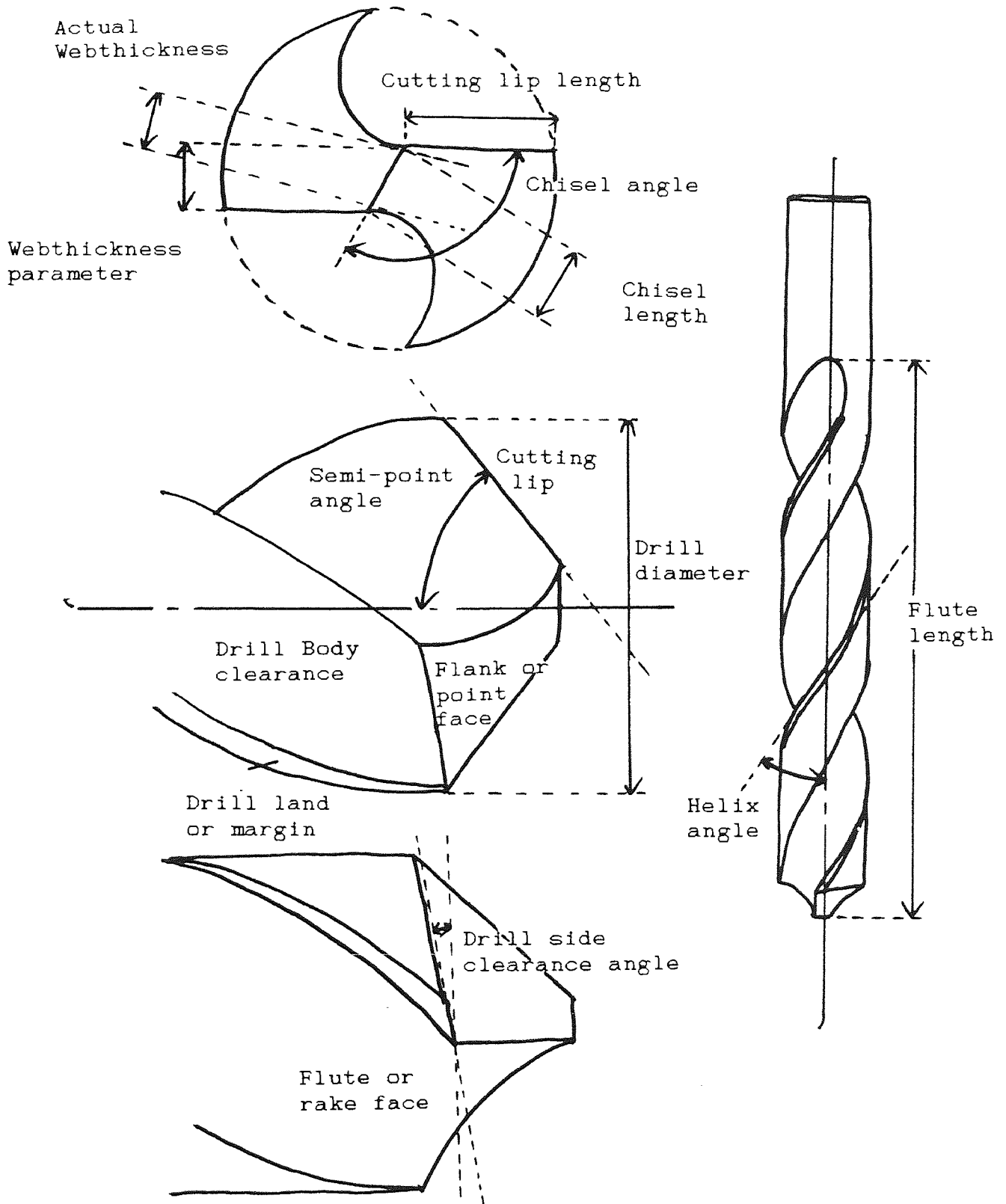


Figure 7 - Geometric Reference Values of Drill Form

1.4. DRILL GEOMETRY - CURRENT LIMITATIONS

Since its inception the twist drill has been described by a set of geometric references, figure 7. A full set uniquely describes a specific drill form by a method recognised throughout the industry. The geometric references on the drill occur as a result of complex interactions between the various aspects of the drill manufacturing process. Over the years the individual drill manufacturers have built up their own sets of data by trial and error. These sets of data are kept secret and detail the machine settings and tool form requirements for the generation of the companies' drills to specific geometric reference values. These drill forms have then been tested and selected, again by trial and error. Particular drills have either proved themselves suitable or unsuitable for the performance of specific drilling operations.

In this way, in a number of different forms, the twist drill works in a generally satisfactory manner. It is certainly not necessary for the user to be aware of the very complex, three dimensional, nature of the cutting action of the twist drill. Such knowledge is, however, increasingly being required in order to make best use of the drilling process.

The drill testing that has been performed has generally been after careful tool selection. A range of drills is assembled where the forms are generally similar but where one value,

for example the point angle, varies across the range. Practical testing then indicates the influence of that geometric property. It is however impossible to isolate one value as all the geometric properties are inter-related. These examinations are therefore subjective and provide only empirical estimations of influences.

Almost all of the published information on drilling is thus specific to particular drill/workpiece combinations. To understand these results it has been found necessary to have a practical understanding of the drilling process, and the mechanisms of drill wear and drill failure, otherwise it is impossible to assess the, sometimes, limited value of these published works. As technology advances, with the accompanying requirement to carefully explain how processes work in the simple terms that are required before that process may be programed into a computer, there is a requirement for a more educated and accurate assessment of the drill cutting process to be made.

The major advance that currently requires fundamental reassessment is in the application of plasma ceramic coatings to drilling, i.e. Titanium Nitride. The large increases in spindle speed, RPM, required to achieve the higher cutting speeds possible with such ceramic coatings have in general made current drilling machines out of date. The less obvious consequence is a need to redefine the best cutting geometry. This change is required by the large

reduction in the friction of the coated tool surface. Such change is now coming faster than the historical, trial and experience method of development can cope with. Currently the same tool geometries are being used for both coated and uncoated drills.

1.5. DRILL DYNAMICS - LIMITED APPRECIATION

Drilling is the greatest used of all the machining processes but is in some ways the least understood as a metal cutting process. Most of the research effort involving drilling has concentrated on specific situations where measurements are made and empirical relationships devised that fit the measurements. Two commercial publications typical of such an approach are "Short versus Long" and "Torsional Rigidity", in 'Metal Cutting' and by the 'National Twist Drill and Tool Company'. Such results are then put forward as the mathematical solutions to the general drilling problem.

Papers like these have long described the dynamic nature of twist drilling but always in subjective terms. There is some general agreement, for example, a short drill performs better than a long drill and a thick webbed drill better than a less stiff, thin webbed drill. Nowhere, however, is there a simple and logical explanation of the dynamic process. This aspect of drilling remains to be explored theoretically and it appears to be unique within metal cutting.

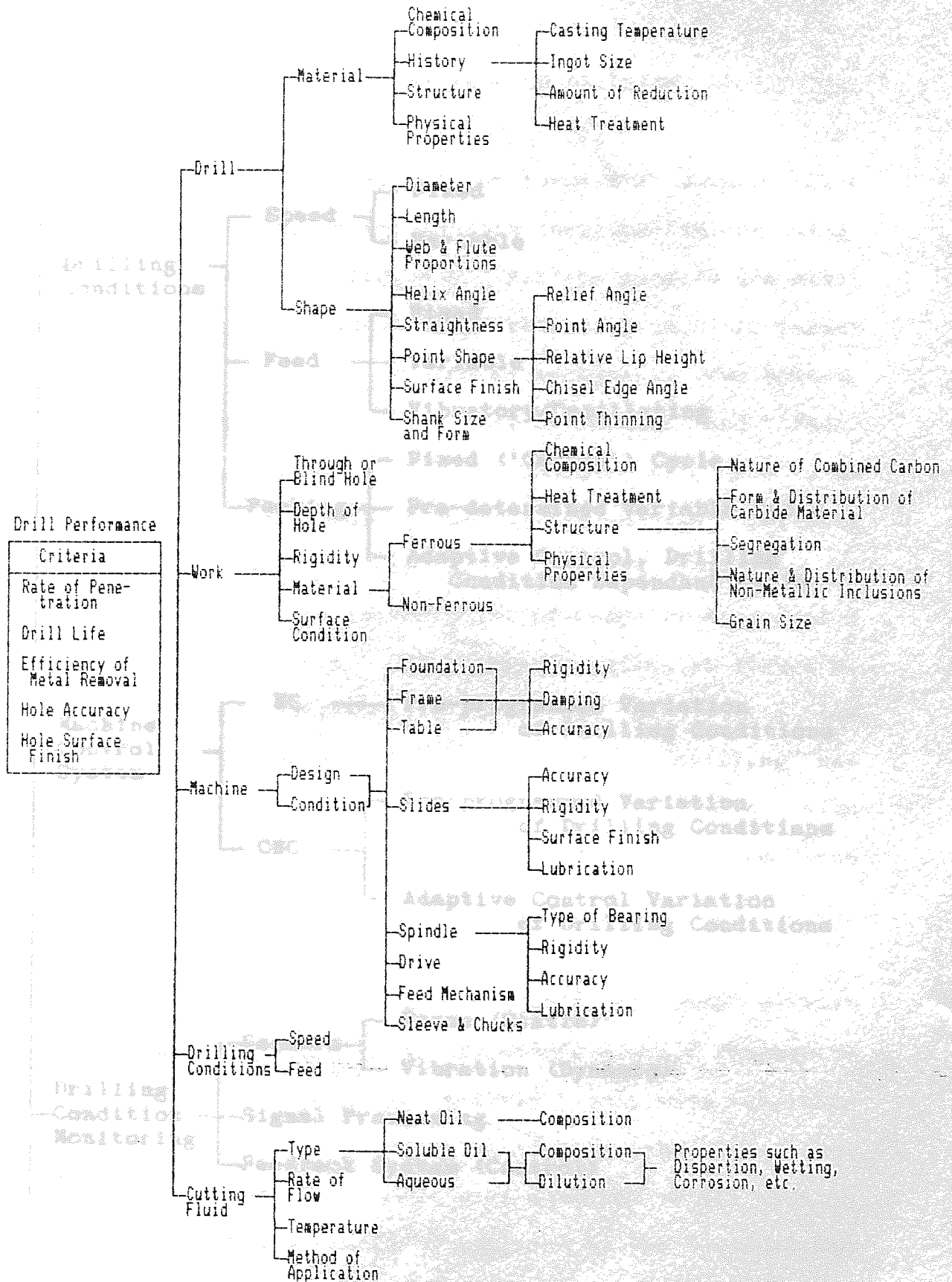


Figure 8 - Galloway's Chart of Factors Involved in Drilling

CONTRIBUTIONS TO THE ANALYSIS OF DRILLING

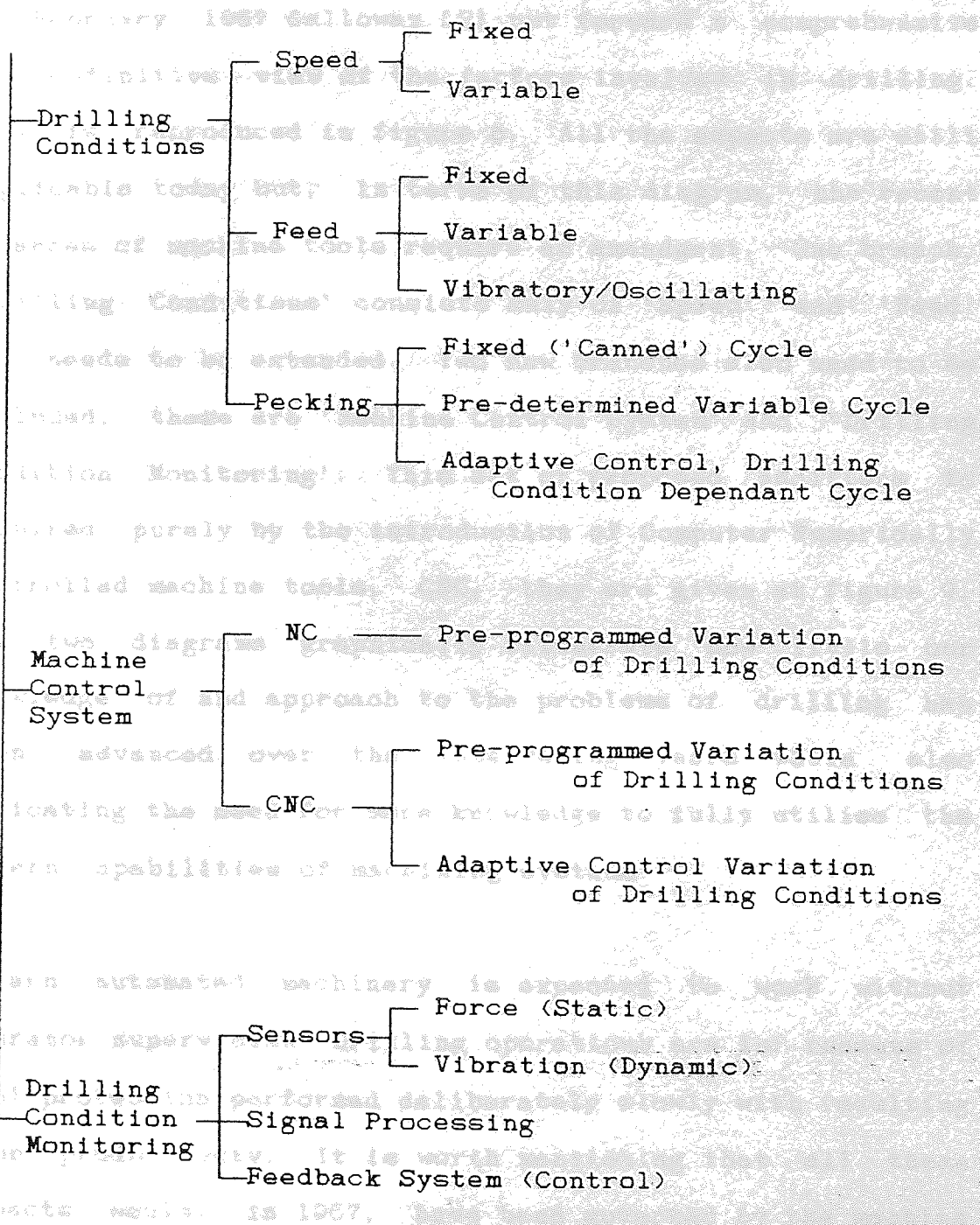


Figure 9 - Proposed Additions to Galloway's Chart

1.6. INTRODUCTION TO THE ANALYSIS OF DRILLING

In February 1957 Galloway [2] put forward a comprehensive and definitive view of the factors involved in drilling. This is reproduced in figure 8. All the aspects are still applicable today but, in terms of this diagram, the recent advances of machine tools require an amendment. One branch, 'Drilling Conditions' consists only of 'Speed' and 'Feed' and needs to be extended. Two new branches also need to be included, these are 'Machine Control System' and 'Drilling Condition Monitoring'. This set of proposed additions is required purely by the introduction of Computer Numerically Controlled machine tools, CNC, they are given at figure 9. The two diagrams graphically illustrate how little our knowledge of and approach to the problems of drilling has been advanced over the intervening years while also indicating the need for more knowledge to fully utilise the modern capabilities of machining systems.

Modern automated machinery is expected to work without operator supervision. Drilling operations are for reasons of tool protection performed deliberately slowly with resulting poor productivity. It is worth mentioning that all these aspects would, in 1957, have been governed by the machine operator. His actions should be replaced by the computer and his sight, smell, hearing and touch should be replaced by the sensors of the monitoring system.

In many ways the CNC machine tool has failed to utilise the power currently available in smaller and cheaper microprocessor systems. Such power may not only be used to ensure the geometric accuracy of the tool path but also to monitor and control its progress. The requirement to monitor and control becomes the specification for an adaptive control system for the drilling process. Adaptive control is possible in a metal cutting situation that is mathematically predictable but is not possible in drilling where the mathematical relationships are currently based purely on a set of simplistic empirical equations that are unable to cope with the large variations present in the real world.

2 LITERATURE SURVEY CHAPTER 2

	PAGE
2. LITERATURE SURVEY	38
2.1. LITERATURE COVERING DRILL GEOMETRY	38
2.2. LITERATURE DESCRIBING FLEXIBILITY AND VIBRATION	46
2.3. CONCLUSIONS	50
2.3.1. CURRENT STUDIES OF GEOMETRY	50
2.3.2. FLEXIBILITY	55
2.4. STATEMENT OF RESEARCH OBJECTIVES	57

2. LITERATURE SURVEY.

2.1. LITERATURE COVERING DRILL GEOMETRY

In the extensive body of literature covering the drilling process only a few develop limited mathematical approaches to the geometry of the twist drill. None developed any form of comprehensive system to examine drill geometry. These papers now are examined in turn.

Galloway [2] points out that drilling is used very extensively in the Engineering Industry and is therefore a basic process to the Engineering Industry as a whole. His paper describes various drill tests where Torque and Thrust were measured with a Dynamometer.

The dynamometer Galloway used in 1957 was made 'in house' with sensing elements in the form of steel diaphragms. These have greater compliance than more modern load cells. This lack of rigidity prompted one critic to query whether drill performance had been evaluated without the dynamometer as he had noticed a 40% reduction in drill life using a similar dynamometer compared with a rigid base.

Extensive hole and drill geometry measurement was also made. He examined relief and feed angles along the drill cutting lips, the difference giving the effective clearance. Both these values vary across the drill lips and chisel. Optimum penetration rate is described as that which gives an even

distribution of wear along the cutting edge. Too high a penetration rate was seen to cause accelerated wear of the corners. Too low a penetration rate reached a point of sudden rise in both torque and thrust due to wear. Both changes led to a reduction in the number of inches depth of material drilled over an 'optimum' penetration rate.

Optimum point grinding geometry was investigated for a range of workpiece materials, point angle and point thinning especially. Vibration behaviour, effect of drill geometry and effect of a bush are also investigated.

Galloway provides the first account found describing the point using solid geometry. He gives a geometric description of the conical method of point grinding defining the parameters of the grinding cone. The cutting edge is assumed straight. The z axis is assumed collinear with the drill axis. The x and y axes are parallel and perpendicular to the projection of the cutting edge onto a x-y plane perpendicular to the drill axis. An analysis is presented, developing various trigonometric formulae to calculate the related cutting geometry. As with all such efforts to obtain formulae, the mathematics is highly complicated and difficult to apply.

Galloway's work is a comprehensive account of drilling holes and has become an important reference for researchers in this area. It is limited only by the extremely primitive

equipment and restricted analytical power available at that time, for example, as seen from the discussion quoted above, the compliance of a contemporary mechanical dynamometer was sufficient to greatly influence the results. All the new areas indicated by figure 9 technically post date this analysis.

The next reference found which uses a similar approach is Tsai and Wu [3]. They make use of a computer and process basically similar geometry. They wished to evaluate mathematically the performance of a Twist Drill with what Tsai and Wu describe as conical, ellipsoidal and hyperboloidal drill point shapes.

Galloway [2] developed a fairly complex mathematical expression for the drill point based on his interpretation of the co-ordinate axes. This is used as the starting point of several subsequent analyses including that of Tsai and Wu. It is reproduced below:-

$$\frac{1}{a^2} \left[(x \cos \theta + z \sin \theta) + (a^2 - \delta \frac{a^2}{c^2} d^2 - S^2)^{\frac{1}{2}} \right]^2 + \frac{1}{a^2} (y - S)^2 + \frac{1}{c^2} (z \cos \theta - x \sin \theta + d)^2 = 1$$

This describes the flank face as a quadratic surface in the three dimensional space represented by the cartesian co-ordinates (x, y, z). a, c, d, θ and S are the grinding parameters, a and c determine the shape of the quadratic

surface and θ determines the direction of the drill axis with respect to the axis of the quadratic surface. δ equals +1 for the ellipsoidal drill and -1 for the conical drill and the hyperboloidal drill. d and S determine the location of the drill point on the grinding surface.

The drill flank contour so described is a set of elliptical curves obtained as the intersection of cutting planes orthogonal to the drill axis and the drill flank. This equation simplifies to the following:-

$$Ax^2 + By^2 + Cx + Dy + E = 0$$

in the orthogonal (x, y) plane

As the elevation becomes smaller the contour ellipse becomes larger, the centre of the ellipse shifts towards the +x direction. With the conical flank the ellipses are equally spaced, with the hyperboloidal flank the ellipses are spaced with increasing separation from the chisel to the outer corner and with the ellipsoidal flank the ellipses are spaced with decreasing separation from the chisel to the outer corner

The drill point is mapped in the x,y plane at equal intervals of z. An 'end on' diagram of the drill point shape is produced. This evaluation of the conical drill point shape has not been improved by any subsequent researchers. This drill end representation is an efficient way of generating an accurate end view in a simple system. The

geometry is a set of equally spaced ellipses of progressively increasing size overlaid with a series of representations of the drill flute cross section with angles of rotation corresponding to their particular z level. No attempt is made to create a model of the drill and its cutting action, no use is made of the simple representation of the drill cutting edge to examine the cutting process.

The next paper, by Billau and McGoldrick [4], looks at drill clearance around the drill circumference. Their work examines what are described as conical and cylindrical point drills. The drill point is again described by Galloway's mathematics. A system of ellipses is generated as before, but for the so called cylindrical point, the ellipses are equally spaced and all of the same size. In the paper they derive several complicated mathematical equations which are used purely to calculate the clearance angle around the periphery. They make no attempt to calculate the cutting clearance across the flank face and make no allowance for drill feed. Ignoring feed reduces the value of the analysis because, of the two major forces in drilling, namely torque and thrust, the thrust may be attributed to the absence of cutting clearance not at the periphery but towards the centre of the drill flank face.

The conical drill point is again approached as a system of ellipses where the cutting lip is assumed to be a cone generator, i.e. any straight line on the surface of the cone

must pass through the apex of the cone. The analysis looks at drill point angle with reference to a diagram reproduced as figure 10 herein, along with a reproduction of the cones from [2] for comparison. Analysis of the drill point by overcomplicated mathematics leads to misinterpretations such as the one highlighted in this figure. It indicates the cutting lip cone generator. Figure 10 shows the extent of the drill flank and of the grinding cone at this point. The flank area, part of the cone surface, is not totally enclosed by the cone area and cannot therefore exist. It is impossible for the flank to be a portion of the indicated cone surface. This particular problem casts doubt on this solution and formula for point angle, such situations are not unique in the literature.

The above three papers are the only papers found that attempt parts of the analysis drill geometry. Lacking a geometry base there have been no papers found which analyse the drill cutting geometry.

Radhakrishanan et al [5] also examine the drill geometry and examine the problems of generating a specific flute shape. They start by assuming the basic requirement that the cutting edge of a twist drill is straight. They utilise Galloway's mathematics and mathematical models for the orthogonal flute shape corresponding to a straight cutting edge. They propose the calculation of the oblique flute profile from which the wheel profile may be obtained. They



Aston University

Illustration has been removed for copyright restrictions

Figure 10 - Extract from Billau and McGoldrick [4]

state that the oblique flute form bears more direct comparison with the wheel profile required to create it but they do not explain how the problem of interference, common to all helical grinding/milling operations, is to be avoided.

The 'secondary' flute shape is dependent on factors such as land width, web thickness, maximum chip-removing capacity and the grinding wheel thickness. This is the half of the flute corresponding to the non-cutting edge. This paper is the earliest in which these aspects are included or at least mentioned in the analysis. As with previous studies simple mathematical curves are assumed for the shape of the secondary flute.

Radhakrishanan uses Galloway's mathematical model of the primary flute orthogonal profile. It is described by the following equation using cylindrical co-ordinates with a r- θ polar reference system in the x-y orthogonal plane. Correction for the helix is built into the formula:-

$$r = t \operatorname{cosec} Y$$

$$v = Y + \frac{t}{R_0} (\tan \alpha_0) (\cot Y) (\cot \beta)$$

t = half web thickness

R_0 = is the radius of the drill

α_0 = helix angle at drill periphery

β = semi point angle

Y = angle between OP' and OX

By solving this equation the orthogonal profile of the flute in the x-y plane may be determined. A co-ordinate transformation is then used to produce from these values the required oblique profile using an iterative technique.

Radhakrishanan describes the secondary half of the flute by a formula determining its end points. The shape in between is assumed:-

$$f(x,y) = 0$$

a function involving two or more unknown constants.

By assuming an elliptical or circular curve only two unknowns are present. He solves the equation with two initial conditions, ie the positions of the two end points. More advanced curves are not attempted. This leads to a lack of continuity between the cutting and non-cutting halves of the flute.

2.2. LITERATURE DESCRIBING FLEXIBILITY AND VIBRATION

There is limited literature that looks at the dynamic nature of the drilling process. The fluted structure of the twist drill enhances drill flexibility. This aspect has been noted by only a few researchers.

Kirilenko [6] looks at a stiffness and strength calculation procedure for twist drills which make an allowance for the helical arrangement of the swarf flutes. Although the cross

section of a twist drill may be described mathematically by circles and parabolas, the resulting partial differential equation is not one that may be solved by any of the standard stress theory solutions. Prior to the easy availability of computers the method of solution of such equations was limited to time consuming numerical iteration techniques. Kirilenko dismisses the numerical approach and proposes a series of factors or constants. These he calculates for a particular cross section by integration and graphical methods. He claims good correlation between theoretical and experimental results. The equations and the calculations of the constants are, however, neither easy to understand nor easy to apply.

Schaterin [7] examines tool flexibility for a 20mm twist drill. This report is a translation into German of Scharetin's original paper published in Russia. He measures flexibility in terms of constants and proportionality factors. The longitudinal effects due to twisting deformation of the drill and the twisting effects due to longitudinal deformation of the drill are measured with an experimental rig. The problem concerns the drilling of plates of difficult to machine material. The deformation effects are reduced by comparing standard drills with special drills having increased web thickness, "erhöhter Steifigkeit" in the title translates as enhanced stiffness. A set of arbitrary proportionality factors of stiffness are tabulated for the range of web thicknesses studied.

Schaterin attributes chatter vibration in drilling to this effect.

A second paper also by Schaterin [8] is also translated from the Russian original and continues the investigation of the first. In it he measures the dynamic effect of the drill deformation while drilling 20mm plates of manganese steel. The upper portion of the drill flute is fitted with a thin walled torque tube clamped to the drill at each end of the tube. The tube deforms by association with the drill and this deformation is detected by wire strain gauges, figure 11. In this way measurement of the drill vibration, or rather dynamic deformation, while drilling, is possible. The torque tube only increased the drill's rigidity by a small percentage. A sinusoidal vibration at a frequency of the drill's natural frequency of twisting deformation is

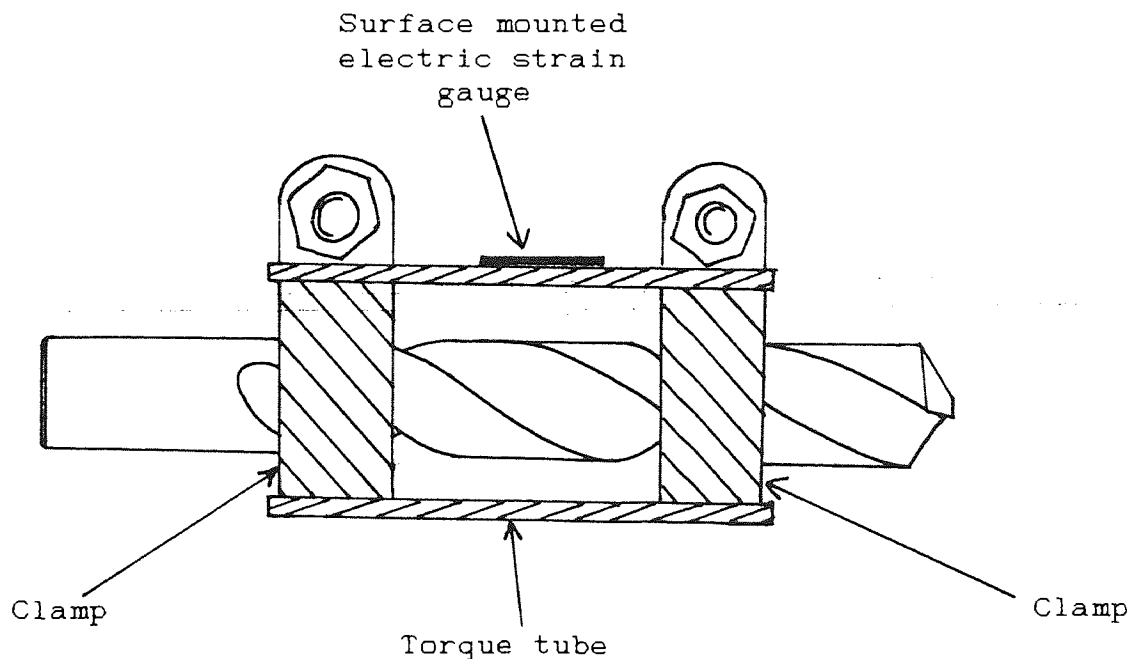


Figure 11. - Schaterin's Torque Tube

reported. This is modulated, at increased cutting speed, feed or wear, by a lower frequency saw tooth vibration of much greater amplitude which is very detrimental to tool life.

K. Narasimha et Al [9] investigated what they describe as the "torque-thrust coupling effect in twist drills". Once again the paper states that the complexities of shape of the twist drill make an analytical static deformation model elusive and takes an experimental approach. The range of drill diameter, helix angle and web thickness used is greater than that used by Schaterin [7]. They emphasise that the deformation effects are linear over the range of measurements made. The conclusion states that the stiffest construction of drill is a drill with a helix of 28° . This does coincide with the industry standard helix for a general purpose drill as developed over the last 100 years.

Kirilenko [6] has made the only attempt found at analysis of the deformation of the drill form and his paper is offered only as an 'interesting' mathematical exercise.

Chandrupatlia and Webster [10] present a highly simplistic attempt to look at the deformation present in the twist drill by the use of Finite Element Analysis. The whole of the end of the twist drill is modelled by two symmetrical 3-D FEA building blocks joined along the centreline of the drill web. The drill shape logically divides here into two

sections. The drilling torque is distributed among the three nodes making up each cutting edge, the drilling thrust is ignored. Details of the deformation, specifically of the outer corners, is obtained.

The FEA mesh has used a complex building block, a 20 node curved side brick element, that requires substantial computer processing, this is offset by the simplicity of the approach in using only one block. The analysis should be very informative of the deformation of a twist drill but the very nature of the FEA process leads one to doubt the accuracy of the nodal deformations, which are markedly nonlinear. In any FEA analysis the sophistication of the displacement model limits the accuracy of the resulting nodal deformations and this is a one element model. The nodal deformations are calculated within the computer during the finite element analysis but these deformations are accurate at a set of points within each element at positions between a node and the element centre. The deformations are least accurate at the extremities, ie. at the nodes themselves, which is the location for where they are reported.

2.3. CONCLUSIONS

2.3.1. CURRENT STUDIES IN GEOMETRY

The deficiency of all the work found that examined drill geometry is that none of the information is transferable

between different shapes of drills and to other forms of cutting. This deficiency is the one addressed in Part One of this thesis but one must first define what is to be measured.

Cutting angles are defined within Stabler's paper [11] which proposes the requirement that metal cutting theory be based on 'Fundamental' angles. This is restated by Stabler in the discussion of a later paper, Galloway [12]. Three angles are put forward as the fundamental angles of cutting theory, figure 12. In order of importance they are:-

1. The Rake Angle or 'Primary Rake Angle' measured normal to the rake face and normal to the cutting edge. The rake angle is stated as being directly proportional to the efficiency of cutting.
2. The Obliquity or Inclination Angle of the edge with respect to the relative direction of workpiece motion. The inclination controls the direction of chip flow by Stabler's law "Inclination angle of approach, β , = inclination angle of leaving, γ ." Stabler tested this law up to 60° inclination and 40° primary rake.
3. Clearance Angle is stated as necessary to the cutting process but so long as it is present it's magnitude is immaterial. This angle should, according to Stabler, be measured in the plane containing the direction of relative motion of the workpiece.



Aston University

Illustration has been removed for copyright restrictions

Stabler - 1951 Extension to Oblique Cutting

Figure 12 - Fundamental Cutting Geometry

page 52

The vast majority of the research effort involving drilling has concentrated on specific situations where measurements are made and empirical relationships devised. Descriptions are given in terms of the drill geometric references so precluding any fundamental analysis of the processes. [2..5] do attempt to deal with the geometry of the twist drill. Plane trigonometry is used to develop fairly complex equations which describe the various surfaces of the drill form. None of the results include any means of correcting for drill feed, they are not given in terms of the above fundamental angles, nor are they in a form allowing the subsequent calculation of fundamental angles. Such an approach does not offer the universal numerical solution required for mathematical predictability.

The four references [2..5] construct a framework within which it is possible to measure rake, inclination, and clearance angles but, assuming the drill axis vertical, these calculations are restricted to the horizontal and vertical planes only. It would be possible only after the calculation of the necessary intermediate planes to use such a plane trigonometry approach to calculate the 'Fundamental' angles. The calculation of the plane orthogonal to the cutting edge is required as the 'Fundamental' angles are all situated in or measured from this plane. Drill feed has to be ignored as it would move the approaching velocity vector of the workpiece out of the horizontal plane by a variable angle related to the feed rate and radius, so greatly

increasing the complexity of the problem.

This research, [2..5], has attempted a mathematical solution that is continuous across the drill cutting edge. This leads to an overcomplicated set of mathematical equations. The modern approach is a piecewise examination of the tool surface using the power of the computer to generate and regenerate a set of discrete co-ordinate points about which the required geometry may be calculated. Such a system uses only simple mathematics and is able to define the surface mesh of the point and shank of the drill. The data is generated in terms that are unambiguous to a computer.

In reviewing current research on drill geometry and the complexities of the methods that have been proposed it is considered that the use of spherical trigonometry would lead to a clear and viable solution to the problem of defining the cutting geometry of the drill and particularly defining the fundamental cutting angles. Spherical trigonometry is used for the solution of problems with spherically curved surfaces, such as navigation. It allows direct calculations within a problem of directions in three dimensions. The result of adding spherical trigonometry to a geometric model of the drill will be to allow direct calculation of the three 'Fundamental' metal cutting angles as applicable to the twist drill, making full allowance for drill feed. The derived angles may then be used for further calculations as required.

All four previous works derive complex equations which seek to define a few specific aspects of the drill cutting action. A piecewise system is of adequate accuracy and simplifies the mathematics. Coupled with the use of a modern personal computer it is much more applicable to the problem. The mesh of data may be regenerated, for any variation of the drill form parameters, in seconds. Without this complete knowledge as a basis, further work looking at the chip production process at the drill cutting edge is impossible.

2.3.2. FLEXIBILITY

Historically tool flexibility has been regarded as insignificant and over complicated. A few papers have been published in Russia which measure flexibility. No other papers offering a contribution to fundamental knowledge of drill flexibility have been found. The general approach is to assume the drill as a rigid body where the rotation of the drilling spindle and the speed of penetration of the drill into the hole are the only two factors to control the cutting process i.e. to assume the drill point moves in unison with the machine spindle.

On the workshop floor the practical effects of flexibility have been recognised since drilling first came into use. It has been a recurring theme in the literature that in attempting to drill holes in difficult situations, normal length drills continually fail to perform, while the

substitution of shorter flute length drills has provided a total solution. Machine operators have been known to cut brand new drills in half before use or have kept an old stub in a back pocket to be produced when all else fails.

From the above it is obvious that tool flexibility is important, but what are the important aspects of drill structure? What aspects of drill stiffness provide the difference in performance between a short and a long drill?

The rigidity of a drill is related to its cross sectional area. Torsional theory states that the torsional stiffness is proportional to the cross sectional area and inversely to the second moment of area. The area is largely dependent on the drill size but the shape, and therefore the 2nd moment of area, may be varied. Theory states that the stiffest cross section is a circle but the unfortunate fact is that part of the circular drill cross section has to be cut away to make the drill flutes. Without the flutes there is no path for the waste material of the cutting process to escape. The flutes allow extensive warping deformation to take place so turning the rigid drill into a structure more closely resembling a coil spring.

The introduction of three dimensional tool flexibility converts the static situation to a very dynamic one, nowhere has the twist drill been described in these terms.

2.4. STATEMENT OF RESEARCH OBJECTIVES

The literature survey reveals a complete lack of any capability of describing the 'fundamental' geometry of the twist drill. The practical effect of this is to prevent accurate interpolation or extrapolation between sets of test data. Each and every new drilling situation therefore requires the performance of a new testing program with subjective results produced by trial and error.

There is little or no attempt at a fundamental evaluation of the dynamic flexibility of the twist drill shape. Some work on drill flexibility and an even smaller volume on drill deformation exists, but nowhere is the basic dynamic stability of the drilling process examined. There are several dynamic and vibrational properties of the drilling process that have been shown to be valid indicators for use in condition monitoring. These effects have not been explained and even a limited understanding of the dynamic processes will aid the progress towards economic drilling automation.

The objectives of the proposed research are therefore twofold:-

1. The provision of a computer based system able to create a geometric model of the drill form and calculate the 'fundamental' cutting geometry of that form. This

system must be driven by the minimum number of parameters.

2. To examine drill flexibility and the stability of the drilling process. To identify basic parameters within the cutting mechanism that govern the mechanisms of tool flexibility phenomena.

The direct application of this prototype work is to allow the power of computer aided design, CAD, to be used to improve the design of the twist drill. This facility is not currently available even though it has been recognised by drill manufacturers as desirable. The contribution of shape to both the metal cutting process and to the dynamic instability during that process may be assessed. This new design aid will allow drills to be looked at in new ways, it will enhance the 'experience' of the drill manufacturing industry and will remove the need for design by trial and error.

The thesis is divided into two parts corresponding to the two objectives. Where computer programs have been used to explore aspects of the mathematics then the computer output has been 'screen dumped' to a printer for inclusion in the thesis. The programs are found in Appendix A.

PART ONE

The true cutting geometry of the cutting edges of the twist drill must exist, there is a flank face and a rake face with a flow of workpiece material across them. It must therefore be possible to describe this cutting geometry in numerical terms. The motivation for pursuing the geometric nature of the drilling process is based on the shortcomings of current practical testing as described in chapter one, especially in the attempts to analyse the data.

Chapter 3 totally reworks the mathematics from a similar foundation to that laid down by the literature. This approach to the basic shape of the twist drill is shown to be valid. The modifications are desirable to simplify the piecewise application on a computer.

Chapter 4 takes the basic drill form and explores the fundamental cutting geometry of the twist drill. There is an accepted interpretation of cutting geometry and it is in these terms that the drill must be expressed.

Chapter 5 describes the prototype computer systems. These are designed to explore an example twist drill through the above calculations and look at the cutting geometry and chip flow information that is generated for that example.

Chapter 6 summarises the output of this form of analysis and discusses future work required to provide valid cutting force and wear information. It is proposed that this method is equally applicable to other three dimensional situations.

This thesis proposes a new solution to the complex geometry of the twist drill offering equivalent mathematical information about any drill form. This solution therefore offers mathematical predictability of the drilling process.

The output of prototype computer programs has been 'screen dumped' to a printer for inclusion in the thesis.

	PAGE
3. GEOMETRIC WORK	61
3.1. THE GEOMETRIC MODEL BASED ON	
GALLOWAY'S GRINDING CONES	61
3.2. RELATING THE SOLID GEOMETRY TO A REAL DRILL	73
3.3. THE DRILL FLUTE	78
3.4. CONCLUSIONS	83

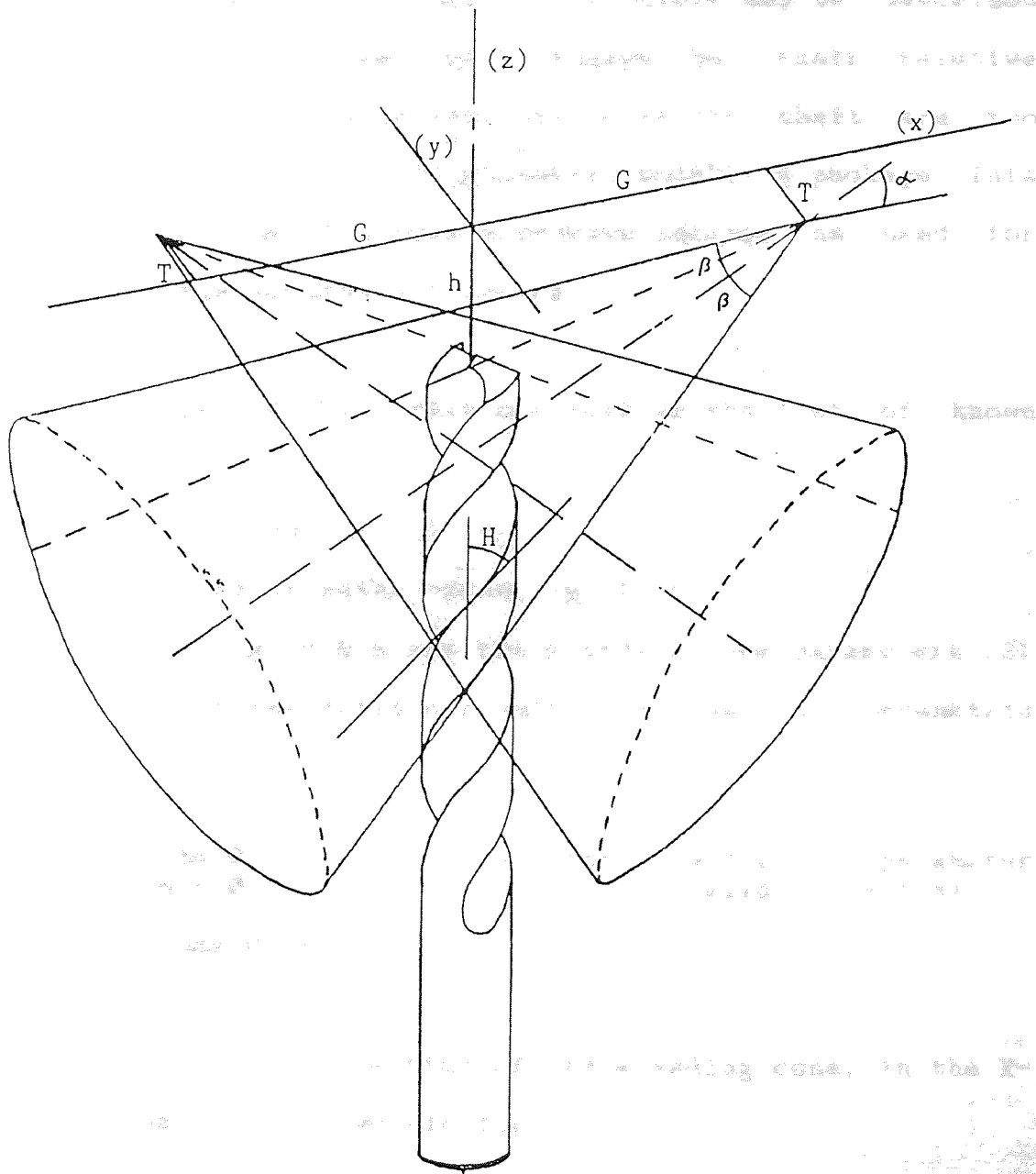
3. GEOMETRIC WORK.

3.1. GEOMETRIC MODEL BASED ON GALLOWAY'S GRINDING CONES.

This thesis proposes a solution for the geometry of the twist drill. The starting point is the same solid geometry as described in Galloway's paper, [2]. The alternative approach proposed here, however, is a solution based on the calculation of a sequence of discrete points. These points form a mesh which, when complete, describes the entire surface of the drill. For convenience a different orientation of the axes is used. A large number of numerical values are generated but they are held and processed within a personal computer and may best be reported to the operator by graphical display. This method allows much greater flexibility in the variation of the form of the modelled drill combined with ease of determining the associated cutting geometry.

The analysis must be based on the most suitable co-ordinate system. The system used is shown at figure 13 and is now described. The z axis is positioned collinear with the longitudinal axis of the drill. The x and y axes are orthogonal, and they are parallel and perpendicular to the projection of the axis of the grinding cones in the x-y plane. The tip of the tool is assumed to be $(0, 0, 0)$. This co-ordinate system is similar to that of Galloway [2] but has been identified as more suitable for this geometric modelling method.

Figure 13 - Drill



- The apex co-ordinates G, T & h
- The cone inclination α
- The cone semi-angle β
- The Flute Helix Angle H

Figure 13 - Grinding Cones and Drill Parameters

Using this cartesian co-ordinate system it is possible to determine the point shape and flute contour with simple plane trigonometry. The drill point shape may be described with the use of a few basic solids but their relative orientation and the helical nature of the shaft are too complex for a standard CAD geometric modelling package. This may not be true of a more expensive package as used for example in the aerospace industry.

The starting point for this analysis is the list of known points:-

The tip of the tool, $(0, 0, 0)$

The apex of the grinding cones, (g, t, h)

- g, t & h are the grinding cone parameters [2]

The locus of the drill circumference has the parametric form:-

$$\left. \begin{aligned} x &= r \cos \theta \\ y &= r \sin \theta \end{aligned} \right\} \begin{array}{l} r \text{ is a constant and } \theta \text{ is a parameter} \\ \text{(this locus is valid for all } z \text{)} \end{array}$$

$\Rightarrow (r \cos \theta, r \sin \theta, z)$

The locus of a conic section of the grinding cone, in the X-Y plane, has the parametric form:-

$$\left. \begin{aligned} x &= p + A \cos \theta \\ y &= q + B \sin \theta \end{aligned} \right\} \begin{array}{l} p \text{ \& } q \text{ are constant and } \theta \text{ is a parameter} \\ \text{(this is valid at a specific value of } z \text{)} \end{array}$$

The conic section is an ellipse with major axis = A and minor axis = B .

$$\Rightarrow (p + A \cos \theta, q + B \sin \theta, z)$$

The following is a list of the minimum number of parameters, as set out in the objective, required to determine the drill point geometry, the fluted shaft geometry and the cutting geometry:

- | | | | |
|-----------------------|---------------------|---|--------------------|
| The apex co-ordinates | $g, t,$ | } | point geometry |
| | (h is dependent) | | |
| The cone inclination | α | } | point geometry |
| The cone semi-angle | β | | |
| The Drill Radius | R | | |
| The Web Thickness | W | | |
| The Flute Helix Angle | H | | - fluted shaft |
| The Feed Rate per rev | a | | - cutting geometry |

Given the list of parameters one must now start to calculate the three dimensional surfaces that make up the drill form.

Each flank face of the drill point is part of the surface of its respective grinding cone. The cones are placed symmetrically about the drill axis so it is sufficient to calculate only one side.

The drill point or flank surface is investigated as a series of conic sections taken in the x-y plane and at successive values of z. If the cone surface is projected onto an x-y plane orthogonal to the drill axis then the locus of the intersection of the cone with an x-y plane is an ellipse. The loci of successive z levels relative to the drill are successive geometrically similar ellipses, figure 14. The ellipses are centred on the projection of the cone axis in the x-y plane which has been defined as parallel to the x axis. The ellipses originate at the cone apex and are distributed along the projection of the cone axis. The size of the ellipse is dependent on the z level, distance from

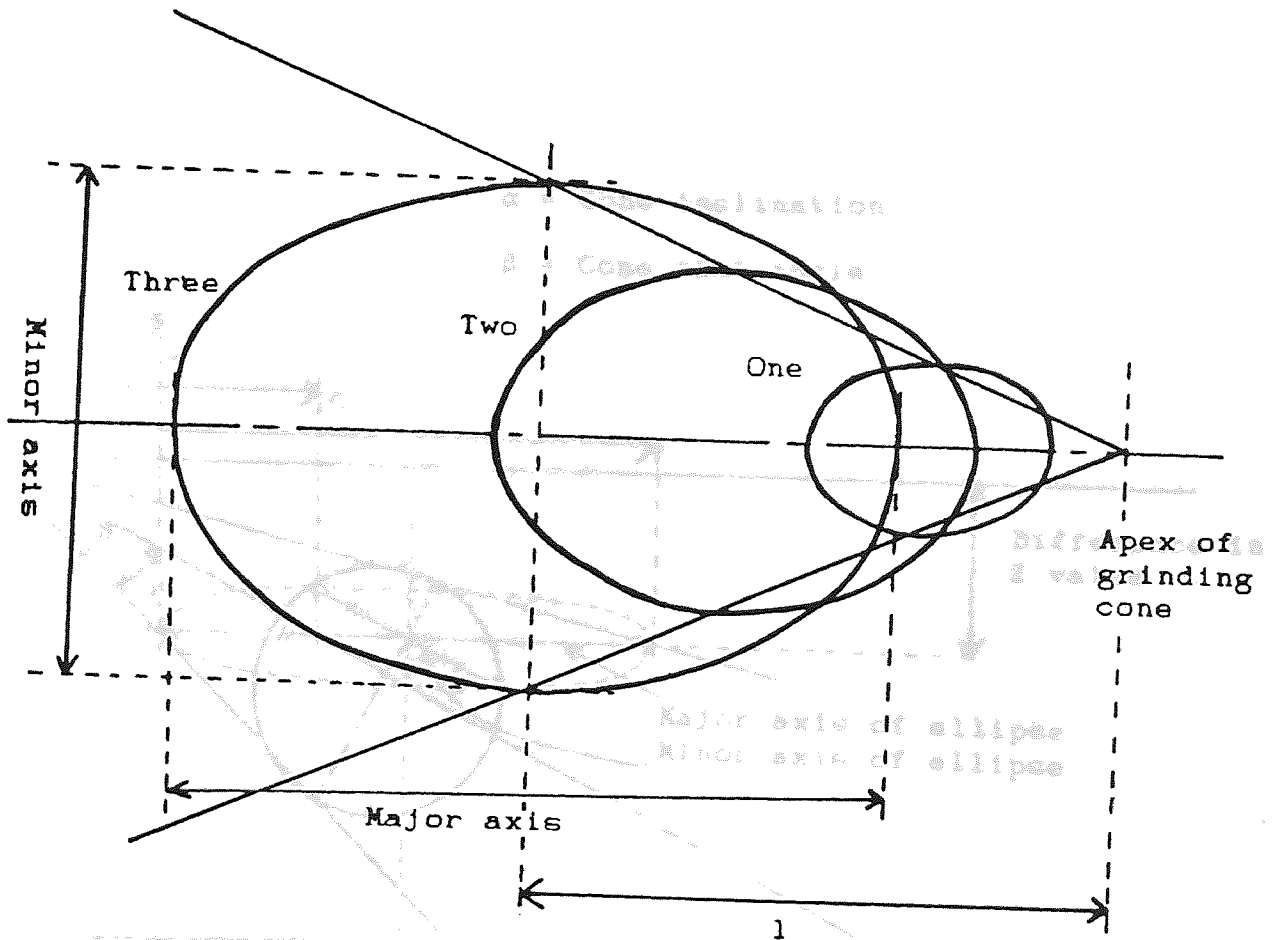
the apex along the z axis, which is proportional to the x ordinate, distance from the apex along the x axis, of the ellipse centre from the cone apex. The cones are geometrically similar so the ratio of the Major and Minor axes is constant, figure 15. The ratios of the Major and Minor axes to the distance from the cone apex, axially, in the z direction or in the x direction are also constant. The obvious starting point is, therefore, to describe the values of the Major and Minor axis of the conic section for a value of $l = 1$ unit in the x direction. This allows the Major and Minor axis to be described as multiples of 1, i.e., $A = A'1$ and $B = B'1$.

As an example let us examine the situation for the tip of the drill, figure 16. The parameters of the grinding cones are the position of the apex, (g, t, h) , the inclination and semi-angle, (α, β) . The solution of figure 16 is a standard trigonometrical exercise. Let us assume g and t are known:-

$$\text{ellipse parametric form} \begin{cases} A \cos(\mu) = A'1 \cos(\mu) \\ B \sin(\mu) = B'1 \sin(\mu) \end{cases}$$

This point indicates the tip of the drill but the equation is equally valid for any other pair of co-ordinates on the drill flank face. The mathematical solution is as follows:-

$$\begin{aligned} A'1 \cos(\mu) &= g - 1 \\ B'1 \sin(\mu) &= t \\ 1 (A' \cos(\mu) + 1) &= g \\ 1 (B' \sin(\mu)) &= t \end{aligned}$$



Distance in
size () for

Family of Ellipses

Figure 14 - Family of Ellipses

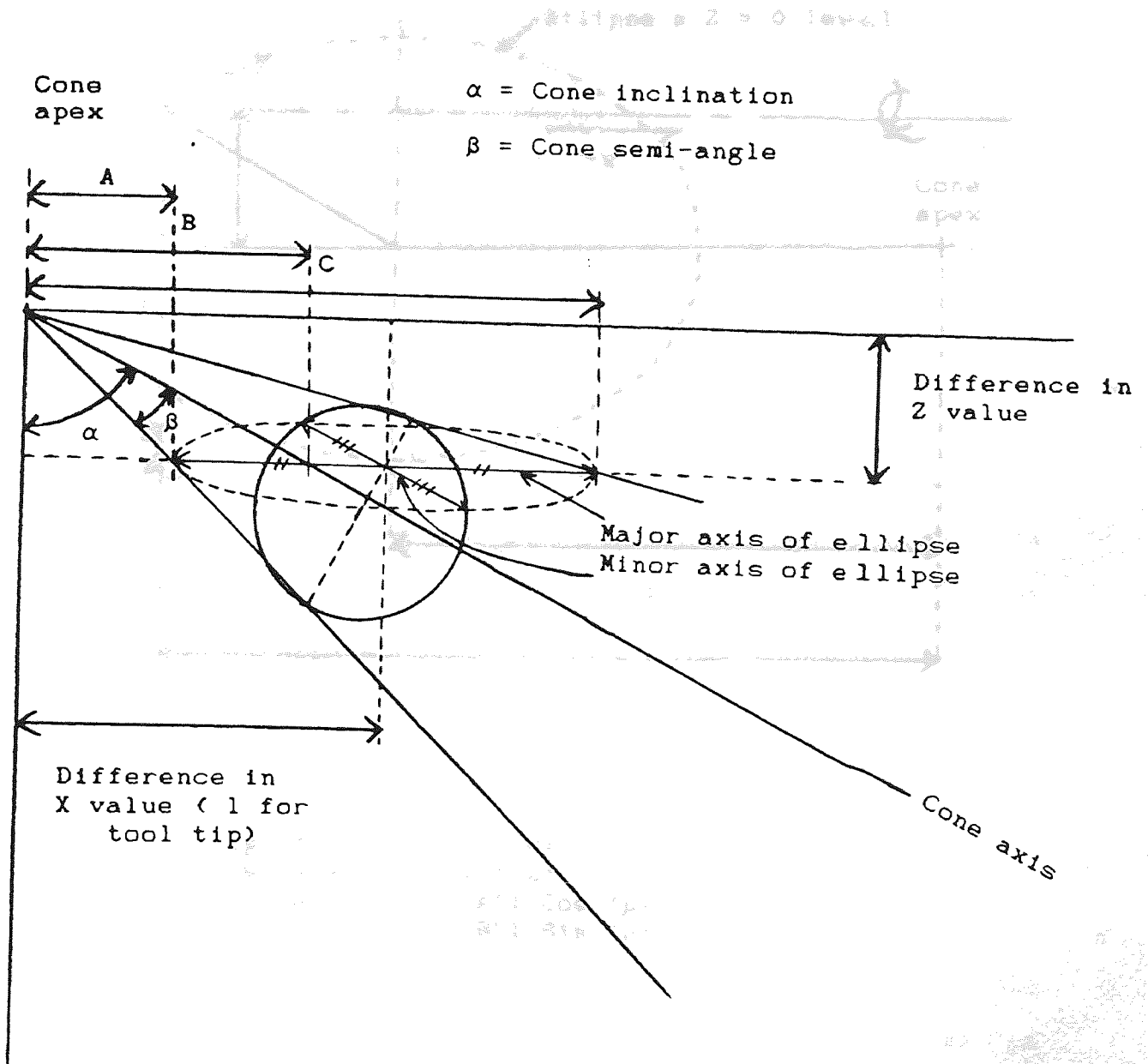
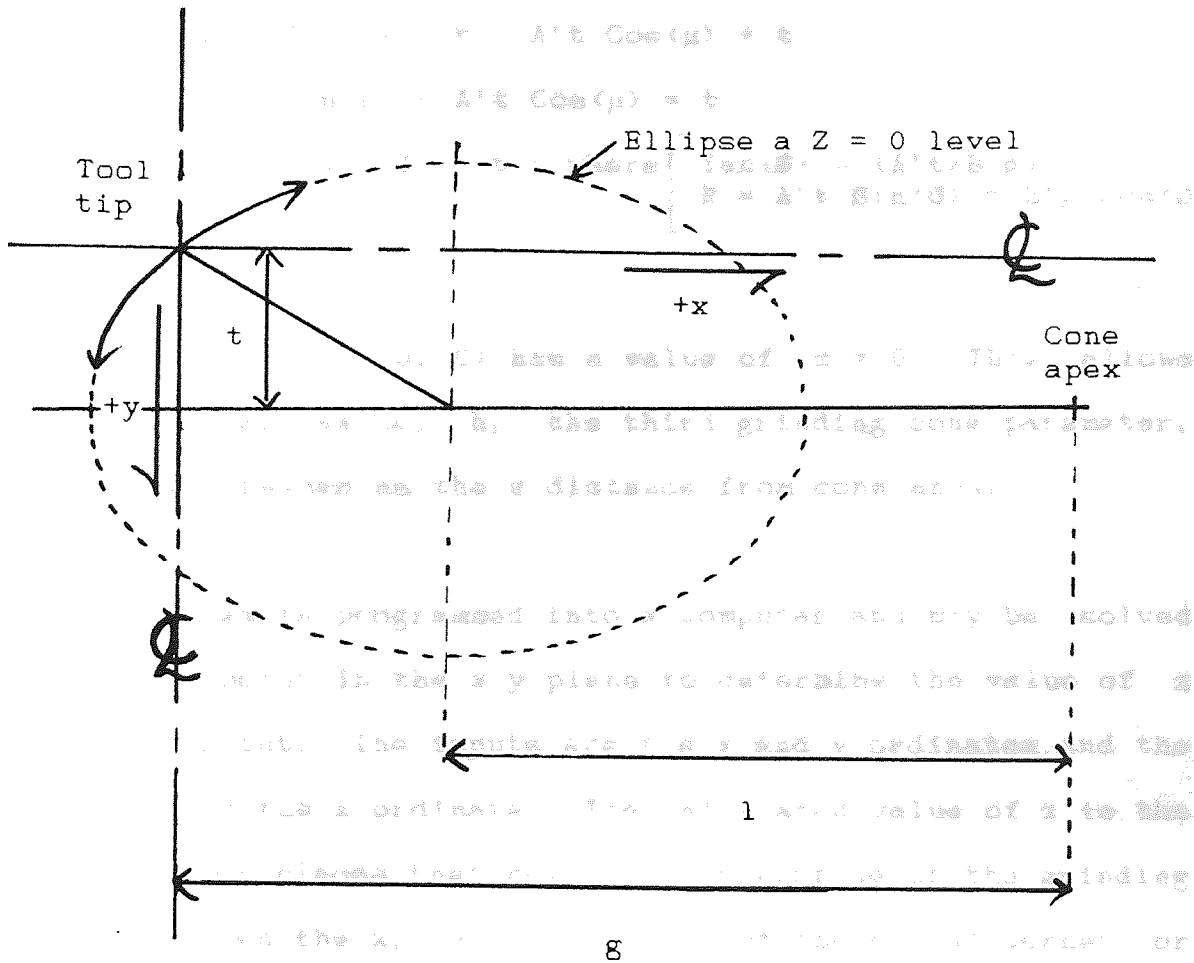


Figure 15 - Geometry of Major and Minor Axes of Ellipse



Tip of tool = (0,0,0)
 Cone apex = (g,t,h)
 Ellipse = [A'l Cos (μ)
 [B'l Sin (μ)

Figure 16 - Z Ordinate Routine for Tool Tip

point, figure 8

$$\Rightarrow 1 = \frac{A't \cos(\mu) + 1}{B'\sin(\mu)} = \frac{t}{B'\sin(\mu)}$$

$$\Rightarrow B'g \sin(\mu) = A't \cos(\mu) + t$$

$$\Rightarrow B'g \sin(\mu) - A't \cos(\mu) = t$$

$$\Rightarrow R \sin(\mu - \emptyset) = t : \text{ where } \begin{cases} \tan(\emptyset) = (A't/B'g) \\ R = A't \sin(\emptyset) = B'g \cos(\emptyset) \end{cases}$$

The drill tip (0, 0, 0) has a value of $z = 0$. This allows the dependent value, h , the third grinding cone parameter, to be determined as the z distance from cone apex.

This system is programmed into a computer and may be solved for any point in the x - y plane to determine the value of z at that point. The inputs are the x and y ordinates and the output is the z ordinate. The calculated value of z is the value which places that point on the surface of the grinding cone. Given the x , y co-ordinates of the chisel corner or the outer corner it is easy to determine the third, z , ordinate and so fix these positions on the cutting lip.

The tip of the drill is initially the only point known that is common to both cone surfaces. The locus of the intersection of the two cone surfaces is the chisel edge of the drill. This locus of intersection is a three dimensional curve but over such a short distance as the chisel length it is reasonable to assume the chisel to be straight in the x - y plane. The chisel at the drill tip is therefore assumed parallel, or tangential, to the curve of either ellipse at

that point, figure 17. The solution of the derivative of the equation of the ellipse at the position $x = 0, y = 0$ gives the gradient of the curve at this point. This is the angle of the chisel edge to the x axis in the x-y plane.

It is now necessary to look at the fluted length of the drill. The two operations, drill flute grinding and drill point grinding, are performed separately on different machines. These operations produce the flute/rake surface and the point/flank surface of the drill form which intersect to produce the cutting lip. The necessary match between the drill flute orientation and the drill point orientation is produced practically by probes or stops which hold the drill shaft by the flutes while the drill point is machined. This match must be reproduced mathematically. One method makes use of the requirement that the cutting lip be straight. Since the only straight line on a cone is a cone generator passing through the cone apex then, as stated by [2], the cutting lip must be a cone generator, figure 18. Having fixed the locus of intersection of the two surfaces their relative orientation is also fixed.

To achieve this effect in the model, the chisel corner is positioned, in the x-y plane, by drawing a cone generator as a straight line passing through the cone apex. This line is drawn tangential to the circle of the semi-web thickness parameter 'W/2'. The intersection of this line with the line of the chisel edge is the position of the chisel corner in x

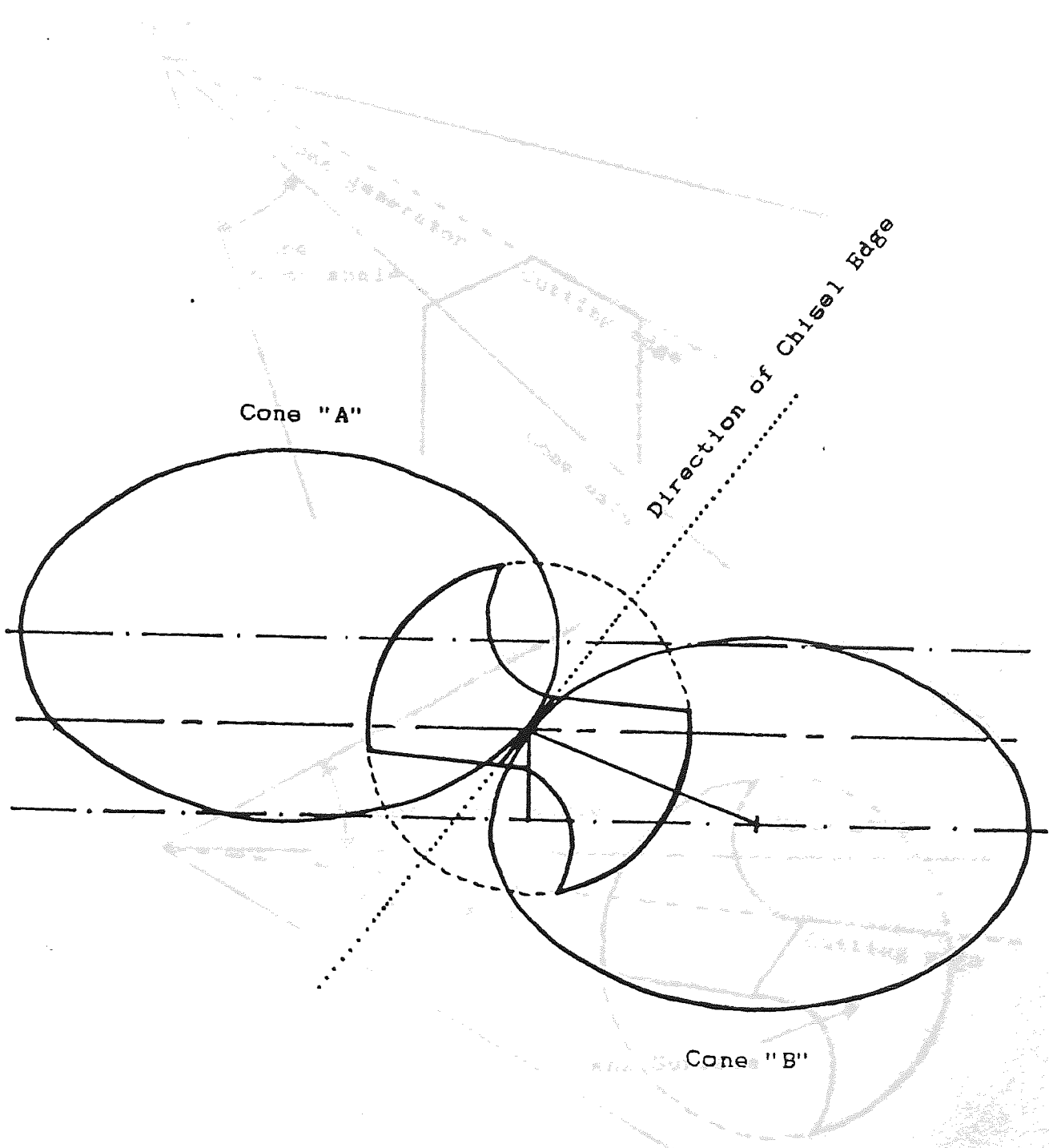
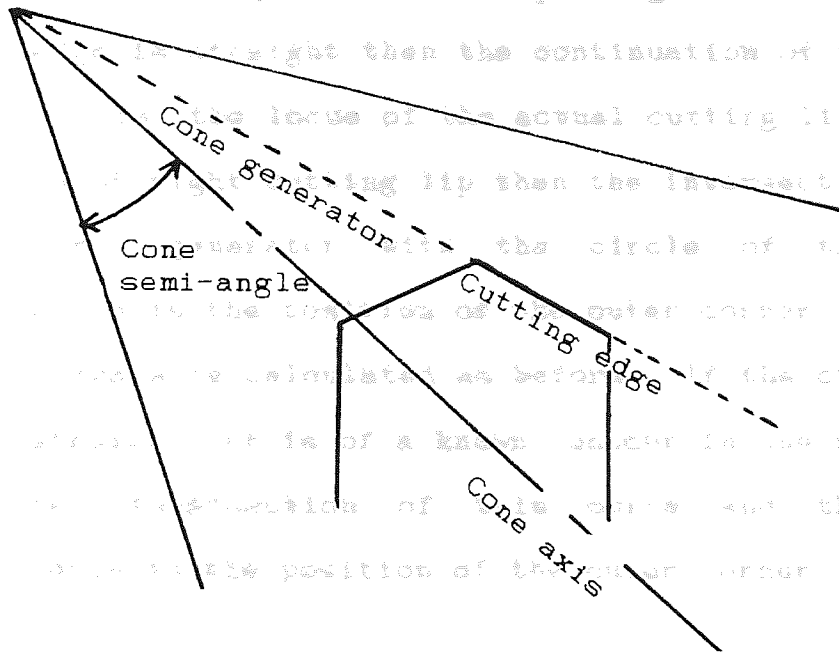


Figure 17 - Intersection of the Ellipses
at the Tool Tip

Apex



Apex

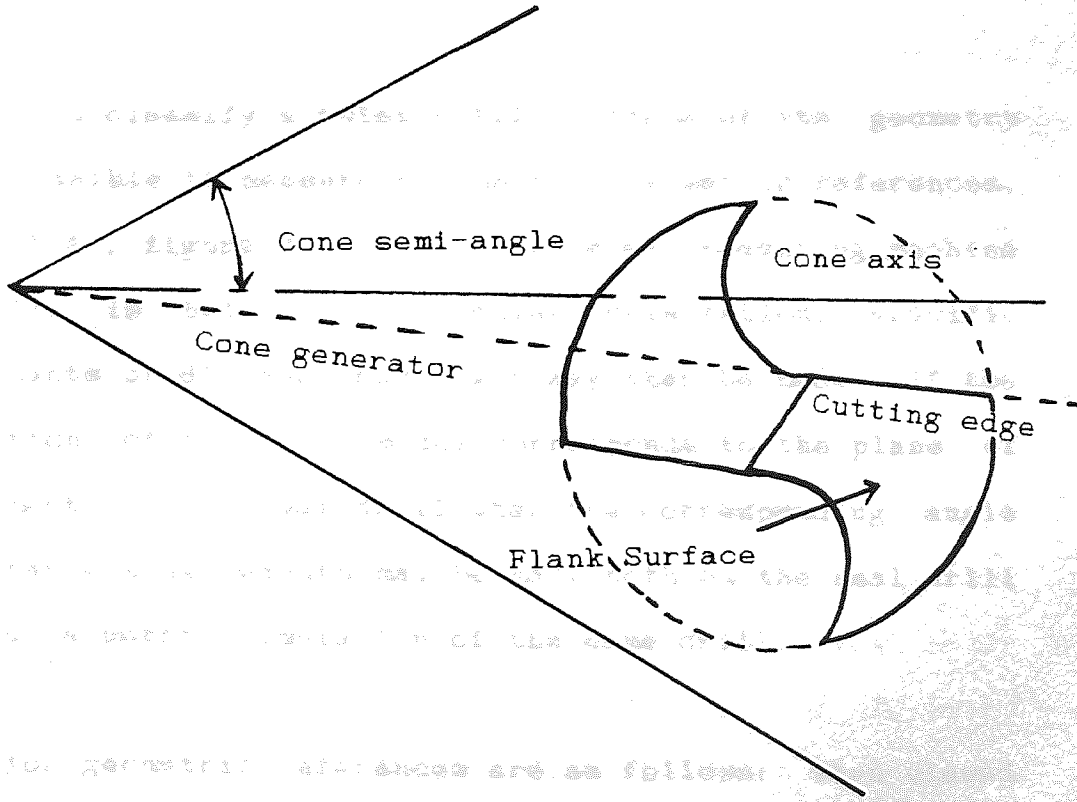


Figure 18 - Cutting Edge as a Cone Generator

and y . The solution of the equation in 1, figure 19, for this position will give the corresponding z ordinate. If the cutting edge is straight then the continuation of this line, (x, y, z) , is the locus of the actual cutting lip. So by assuming a straight cutting lip then the intersection of the above cone generator with the circle of the drill circumference is the position of the outer corner in x and y the z ordinate is calculated as before. If the cutting lip is not straight but is of a known contour in the x - y plane then the intersection of this curve and the drill circumference is the position of the outer corner.

3.2. RELATING THE SOLID GEOMETRY TO A REAL DRILL.

In order to classify a twist drill in terms of its geometry it is possible to measure a number of geometric references, section 1.4., figure 7. Using a universal measuring machine the drill is held in a particular orientation, specific measurements of distance and angle may then be made. If the orientation of the drill model corresponds to the plane of measurement in the real drill then the corresponding angle and distance measurements may be made both on the real drill and on a geometric simulation of the same drill.

The major geometric references are as follows: When viewed from the side of the drill, normal to the cutting lip and the drill axis, the semi point angle as measured on the universal measuring machine, figure 19, is the angle between

the line of the cutting lip and the z axis. This angle is simply that of the line joining the chisel corner to the cone apex, so it is strongly related to the parameters of the grinding cone geometry.

The tool clearance, figure 20, in the circumferential direction, the direction from which the work approaches, may be determined at any radius but as a measured drill property it is generally associated with the outer corner. It is found by determining the z displacement, using the equation in 1, figure 16, for a point on the cutting lip and for a second point a small increment behind it at the same radius. Calculated from the tangent, the angle determined for the drill radius is equal to the drill clearance angle of the outer corner, again equivalent to that measured on the universal measuring machine. The flank clearance angle may be determined by this method for any point on the flank face at any radius on or behind the cutting edge.

The tool rake, figure 21, in the circumferential direction may also be determined at any radius. In the circumferential direction the rake angle is equal to the helix angle. The drill flute has a constant lead which means that the helix angle varies with radius, the value of the lead of the helix being independent of the radius. The lead may be calculated from the nominal flute helix angle and nominal radius by the equation:

$$\text{Lead} = 2 \cdot \pi \cdot (\text{nominal } r) \cdot \tan(\text{helix angle})$$

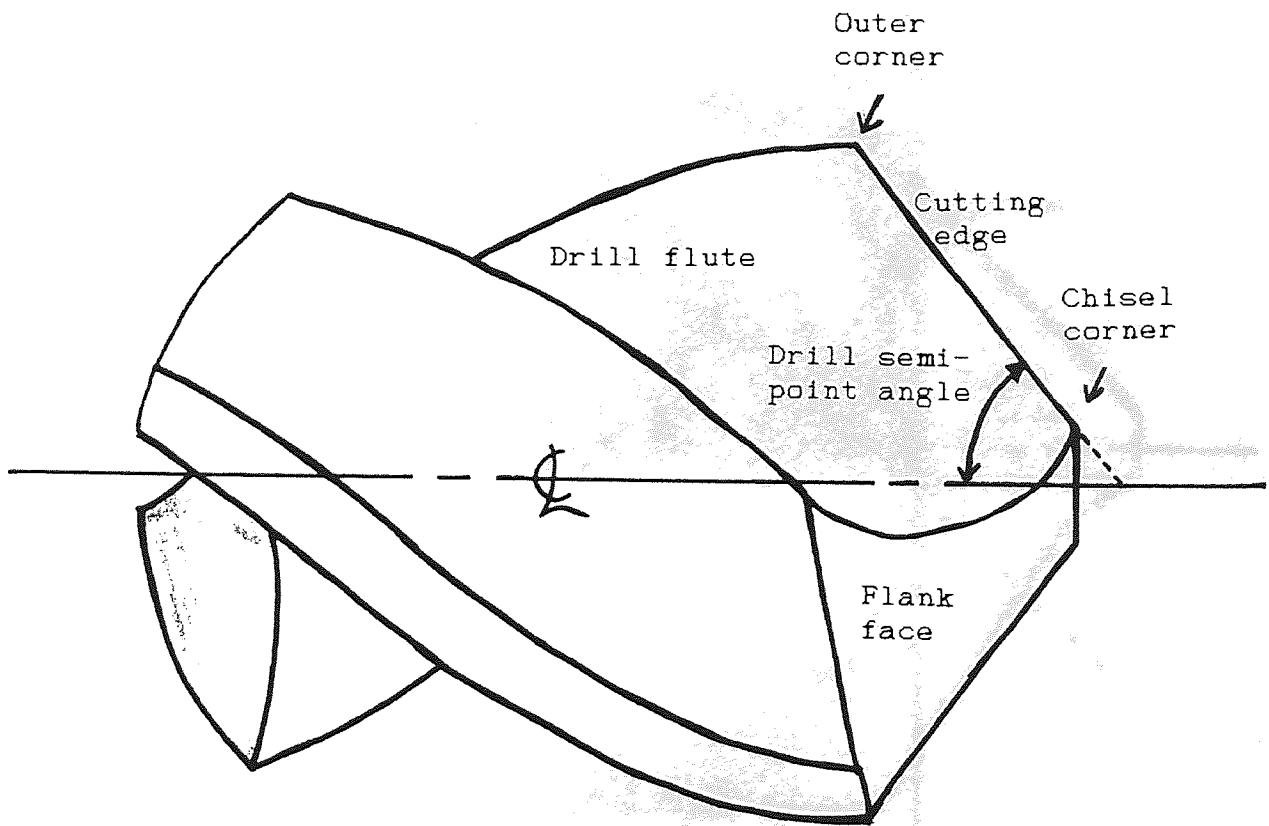


Figure 19 - Side Elevation Normal to Cutting Edge

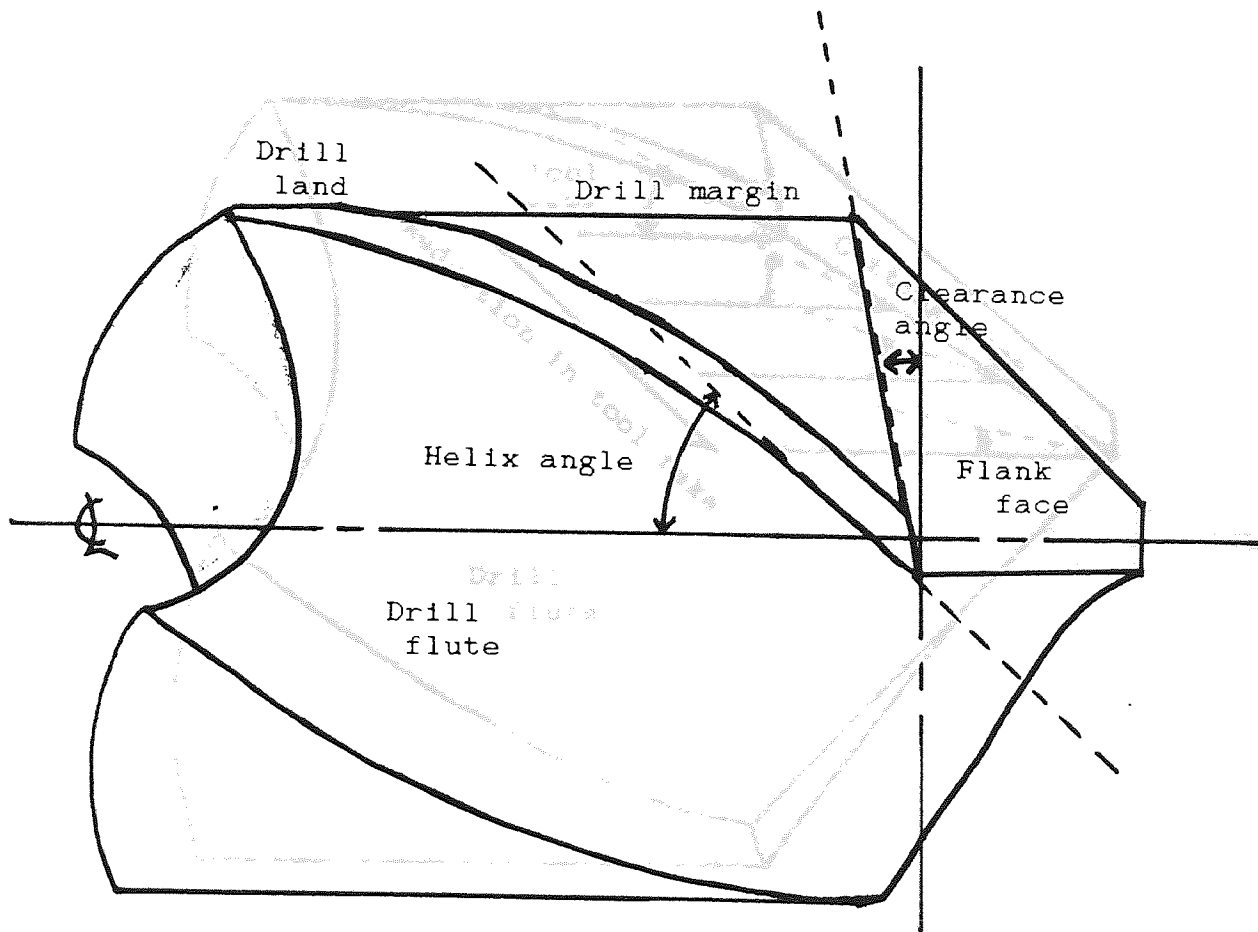


Figure 20 - Side Elevation of Outer Corner

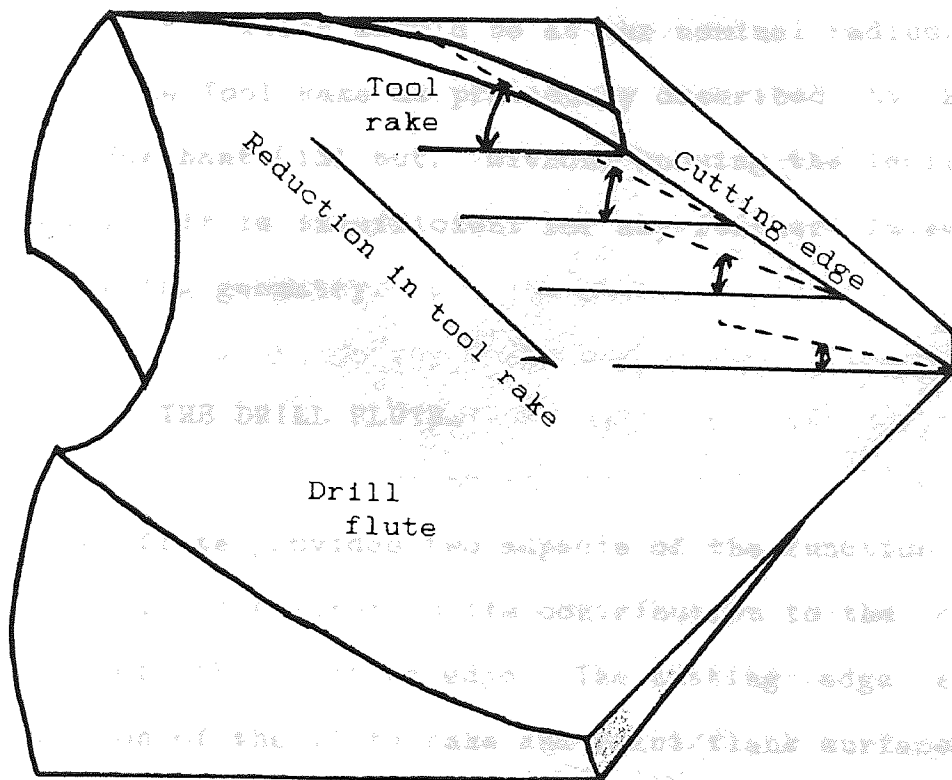


Figure 21 - Tool Rake (not True Rake)

The local value of the helix angle at any radius equals the tool rake angle. The above formula is rearranged to give:

$$\tan(\text{helix angle}) = \text{Lead} / (2\pi \cdot (\text{radius}))$$

This angle increases with radius from a theoretical value of 0° at zero radius, to the actual minimum value at the chisel corner and up to the value of the nominal helix angle at the outer corner, which should be at the nominal radius. This value is the Tool Rake as previously described by Stabler [11] and Merchant [13] but, without knowing the inclination angle [11], it is insufficient for any further calculation of the cutting geometry.

3.3. THE DRILL FLUTE.

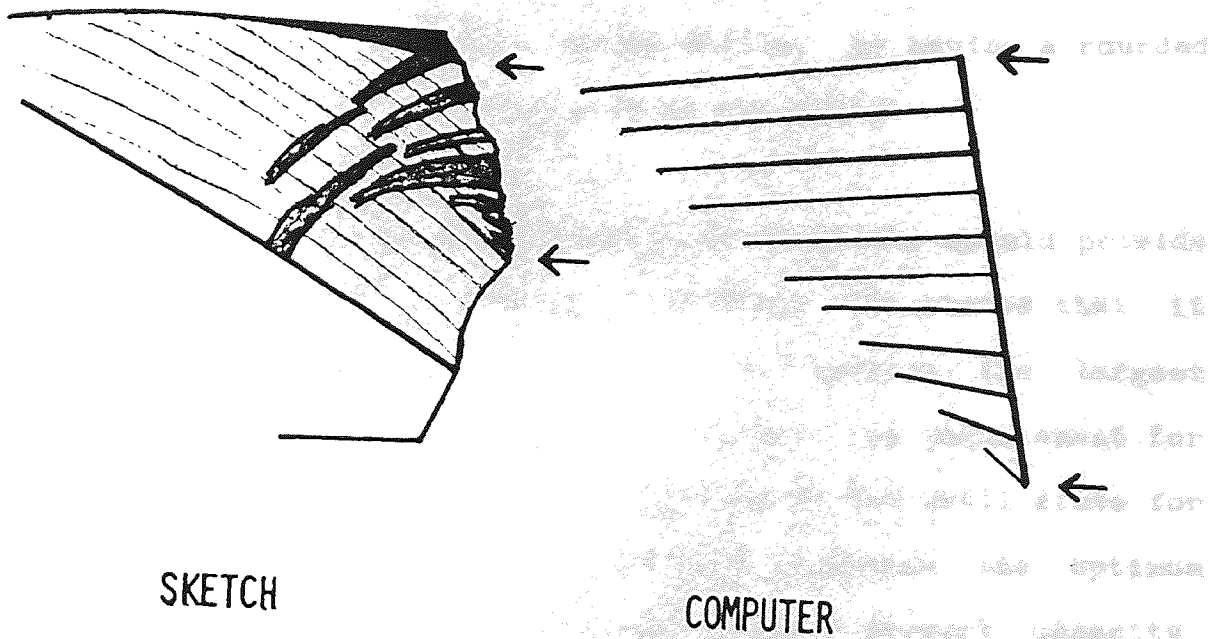
The drill flute provides two aspects of the function of the twist drill. The first is its contribution to the cutting geometry of the cutting edge. The cutting edge is the intersection of the flute/rake and point/flank surfaces. The flute shape must therefore match the designed point shape and will not match an alternative or defective point shape. The second is to provide a path of escape from the cutting edge for the swarf or chip material generated at the cutting edge by the metal cutting, hole generation process. The larger the volume or cross sectional area of the flute space, the better the drill is able to provide adequate chip transport capability.

Reproduced from Webb and Maiden [14], figure 22 is a sketch of the residue deposits of this chip transport process in the flute as it takes place at and immediately after the cutting edge. The computer is able to simulate this process and indicate by vectors the initial directions of chip flow that are present. There is good correlation between these two representations.

The position of the cutting lip has been determined by analysis. This position is a valid line both on the point/flank surface and on the flute/rake surface. The co-ordinates of points on the cutting lip may all be projected to a common x-y plane making due allowance for the flute helix. These points may then be plotted to indicate the cross section of the drill flute. By specifying that the cutting edge be straight and a portion of a cone generator then this is the only flute geometry that will produce the required cutting edge. In this way the form of the leading or cutting half of the flute is determined.

The trailing or second half of the flute shape is remote from the cutting edge and may therefore be of arbitrary shape without affecting the cutting edge. The trailing side of the drill flute may be defined using two criteria:

- 1, As far as is possible, the clearance across the flank face of the drill must be positive to avoid unnecessary thrust force. The shape of the drill point face is



SKETCH

COMPUTER

Figure 22 - Sketch vs Simple Computer

Representation of Chip Flow [14]

determined by the form of its intersection with the flute. This face is one that is subject towards the centre, to a high level of pressure due to lack of cutting clearance. This is the source of the majority of the thrust on the drill shaft while drilling. The heel corner is a second area where such lack of clearance may be found. The drill centre is often modified by the grinding of a secondary relieved surface, point thinning, back from the cutting edge. In the same way the heel corner is often relieved, especially in thick webbed drills, by having a rounded heel on the trailing side of the flute.

- 2, The cross sectional profile of the flute should provide the optimum stiffness. El-Wahib [15] states that it should be sufficient to just enclose the largest possible circle, figure 23. This is the requirement for the optimum cross sectional form of the drill flute for best chip clearance. El-Wahib explores the optimum ratio of drill stiffness : chip transport capacity. Drill stiffness is explored in section two of this work but obviously as more material is removed from the drill cross section so it becomes a weaker structure. El-Wahib proposes the requirement that the minimum material should be removed from the drill cross section. He provides a geometric analysis which is applied to the cross section, it ignores the obliquity of the flute. This is an example of an analysis that

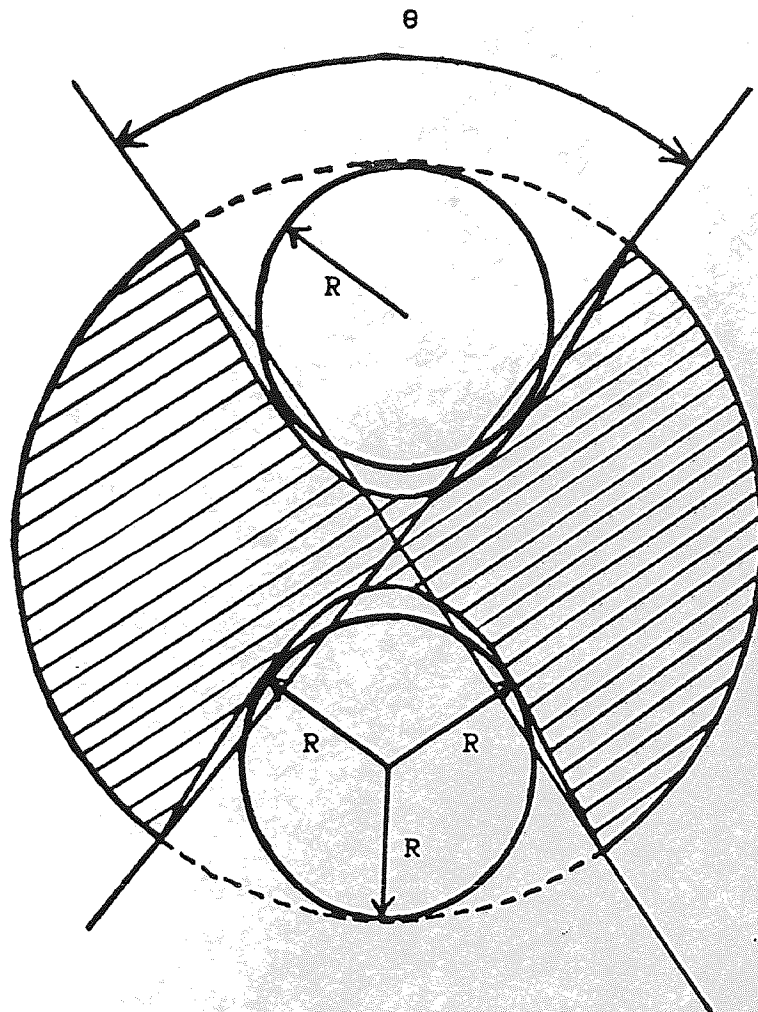


Figure 23 - Optimisation of Drill Stiffness

by Optimisation of Angle θ [15]

allows the drill flexibility without examining any of the effects of such deformation.

It is required to calculate the position of the second half of the flute. The locus of the trailing half of the flute is arbitrary and may be determined as an equation. The two curves of the flute may then be merged to form a continuous line. The method used to describe the heel side of the drill flute is the use of a Bezier curve. The solution of either a parabolic or cubic Bezier curve requires conditions of position and or slope at points on the curve. The parabolic profile is common for simple flute shapes but the rolled heel flute form requires a cubic curve. By the use of the Bezier procedure continuity of position and slope may be achieved, there is no discontinuity of shape as with Radhakrishanan, Kawlra and Wu [5], where a circular or an elliptical curve is used. Examples are given at figure 24.

3.4. CONCLUSIONS.

The kinematics of the drill manufacturing processes may be mathematically described more easily than attempting to interpret the actual form displayed by a finished drill. Once described in terms of the manufacturing processes, the twist drill may be reproduced, geometrically, at will.

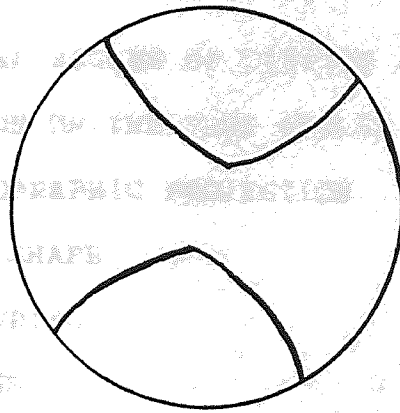
Six parameters are required to describe the point grinding operation. This also defines the cutting edge and the

trailing edge is fixed as a Bezier curve. This information and one further parameter now describes the flute grinding operation. The drill feed rate, mm/rev, is the final parameter required to determine the cutting action of a twist drill.

The modification of the drill form by point thinning or by the grinding of secondary clearance faces does not alter this basic shape. The swept volumes of these secondary finishing operations need only be subtracted from the standard form.

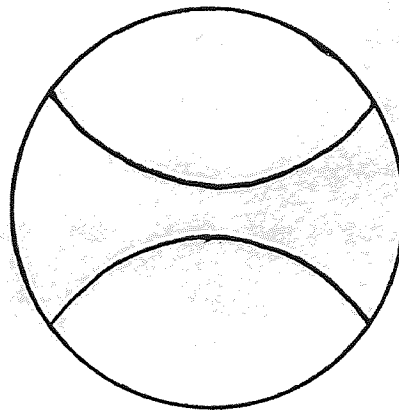
The first part of objective one is to identify the minimum number of parameters by which the computer can uniquely describe the shape of the basic drill form as a geometric model. This aspect has now been achieved.

Curvature of cutting lip fixed,
curvature of trailing side governed by:-



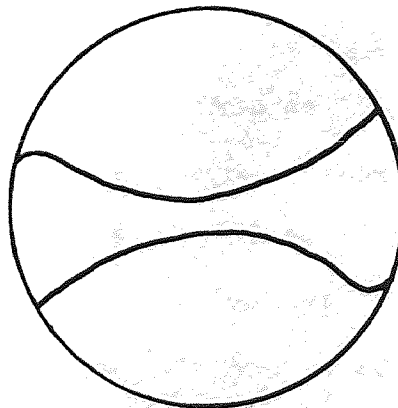
Lack of continuity
at chisel corner

Circular curve - $f(A, B)$



Good continuity
between two
halves of flute

Parabolic curve - $f(A, B, C)$



Heel corner may
be rounded as
required

Cubic curve - $f(A, B, C, D)$

Figure 24 - Examples of Flute X-Section

CHAPTER 4

	PAGE
4. THE FUNDAMENTAL ANGLES OF CUTTING THEORY	87
4.1. CALCULATION OF THE TRUE ANGLES	87
4.2. THE STEREOGRAPHIC PROJECTION	97
4.3. THE FLUTE SHAPE	103
4.4. FLUTE GRINDING	109
4.5. CONCLUSIONS	111

4. THE FUNDAMENTAL ANGLES OF CUTTING THEORY.

4.1. CALCULATION OF THE TRUE ANGLES.

It is necessary to determine the true cutting geometry across the drill cutting edge. A system capable of examining the true, fundamental, geometry of such a complex three dimensional cutting tool does not exist. The basic requirement is therefore for the creation of a system for analysis of the cutting action.

There are two inputs to such evaluation. One, the relative velocity of the drill and workpiece, which is the sum of its rotation and feed, and two, the geometry of the cutting surfaces, which has now been determined as the surface mesh of a geometric model.

The cutting action of the twist drill is a three dimensional problem variable across the whole width of the cutting edges and also across the chisel. It is a system where working with a two dimensional method of trigonometrical analysis imposes many practical constraints on the ability to accurately express the true angles of cutting. The solution must include both the drill geometry and the full relative motion of the drill. In the past feed rate has been largely ignored but at small radii it is of significant importance to drilling thrust. Other factors have also not been represented faithfully to the true situation.

Before starting the analysis it is therefore necessary to reassess the co-ordinate system and the method of trigonometrical analysis.

The homogeneous co-ordinate system is now the best tool to progress from the geometric base. With the homogeneous co-ordinate system matrix type transformations may be performed. The use of matrix type calculations promotes accuracy by ordering the data supplied to the computer. By one such calculation it is possible to determine the plane containing three or more points. The formula produces the homogeneous co-ordinates of the common plane:-

Given n points define their common plane $m = (m_1 + m_2 + m_3 + m_4)$

$$m_1 = \sum_{i=1}^n (y_i - y_j)(z_i + z_j)$$

$$m_2 = \sum_{i=1}^n (z_i - z_j)(x_i + x_j)$$

$$m_3 = \sum_{i=1}^n (x_i - x_j)(y_i + y_j)$$

where $j = i + 1$, except

when $i = n$. Then $j = 1$.

m_4 is determined from $v \cdot \delta = 0$

$v =$ any point
 $\delta =$ any plane
 If true the point v
 lies on plane δ .

Homogeneous co-ordinates consist of four values, these co-ordinates may be normalised by making the final ordinate = 1 and they then are equal to the direction cosines of the vector normal to the plane, i.e. they indicate the intersections of the plane with the x, y and z axis. The

normal to the plane, in three dimensional space, is easily determined from these values. So given three sets of co-ordinates the direction of the normal to their common plane is calculated.

As pictured in figure 25 the geometric model has supplied the co-ordinate descriptions of the flank face and the rake face as a mesh of curvilinear triangles. The true cutting geometry must be measured relative to the orientation of these faces and to the cutting edge. These values describe the true orientation of the various surfaces as a series of numerical values fully understood by the computer.

It is now necessary to examine the method of comparison of pairs of these three dimensional directions. The comparison required is the smallest angle between the two directions. In plane, or two dimensional, trigonometry it is first necessary to know the common plane. Spherical Trigonometry, more usually associated with navigation, works directly in three dimensions. The method calculates the shortest distance across an assumed spherical surface between any two points on that assumed surface, [16] part 1 chapter 3. This distance is determined in degrees and minutes of arc.

In order to apply spherical trigonometry to the normal directions, at present expressed in terms of (x, y, z) co-ordinates, they are converted to a spherical co-ordinate system of latitude and longitude where the polar axis

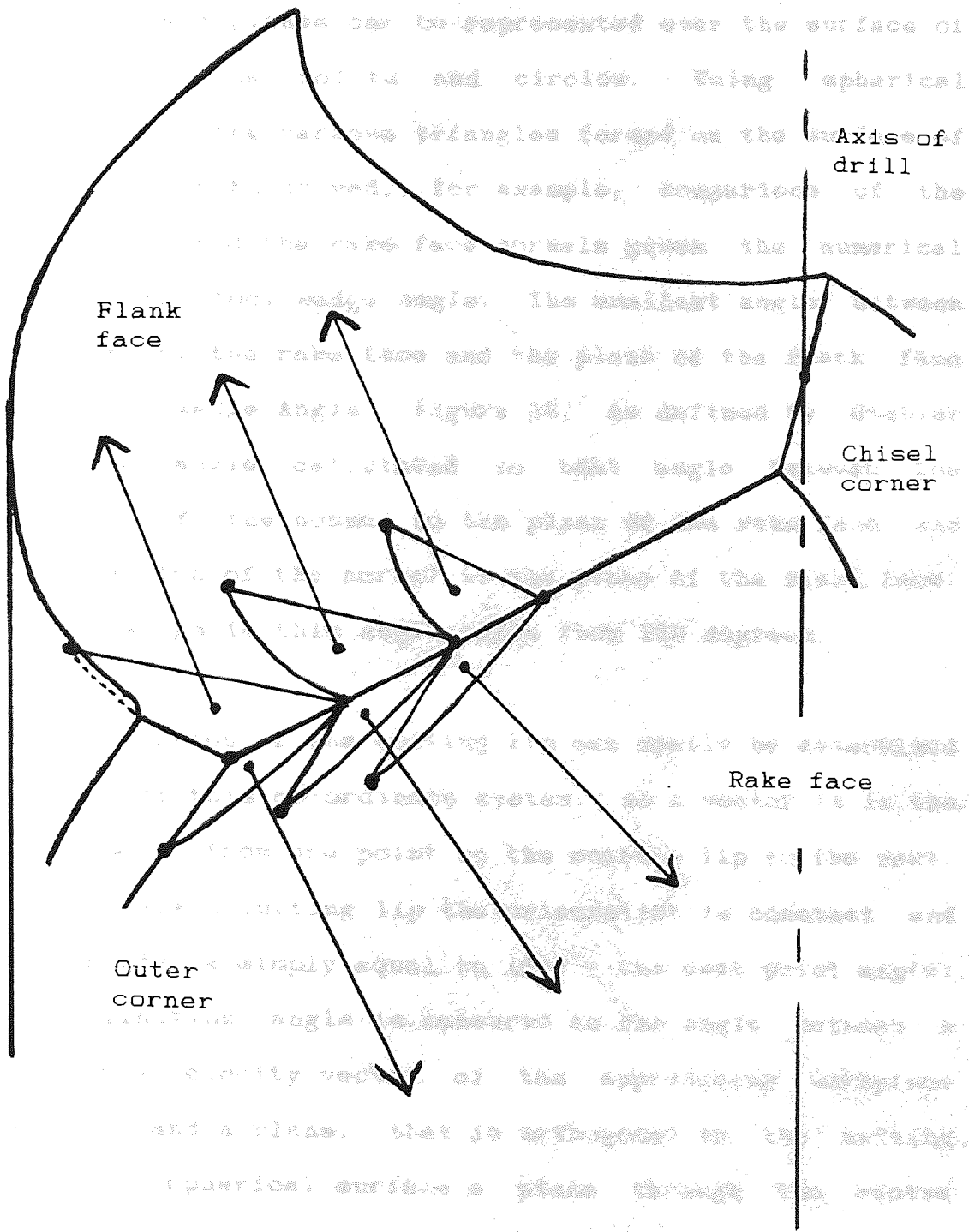


Figure 25 - Figure of Face Normals

coincides with the drill axis and longitude = 0 coincides with the x axis. Assuming an imaginary sphere the various directions and planes can be represented over the surface of that sphere as points and circles. Using spherical trigonometry the various triangles formed on the surface of the sphere may be solved, for example, comparison of the flank face and the rake face normals gives the numerical value of the tool wedge angle. The smallest angle between the plane of the rake face and the plane of the flank face is the Tool Wedge Angle, figure 26, as defined by Stabler [11]. The angle calculated is that angle between the direction of the normal to the plane of the rake face and the direction of the normal to the plane of the flank face. The Tool Wedge is this angle taken from 180 degrees.

The orientation of the cutting lip can easily be determined in terms of this co-ordinate system. As a vector it is the displacement from one point on the cutting lip to the next. For a straight cutting lip the orientation is constant and its latitude is simply equal to $(90^\circ - \text{the semi point angle})$. The inclination angle is measured as the angle between a point, the velocity vector of the approaching workpiece material, and a plane, that is orthogonal to the cutting edge. On a spherical surface a plane through the centre divides the sphere into two hemispheres. In spherical coordinates the apex of either hemisphere is 90° from the plane, it is straight forward to determine the angle between any point and this apex. The apex is numerically identical

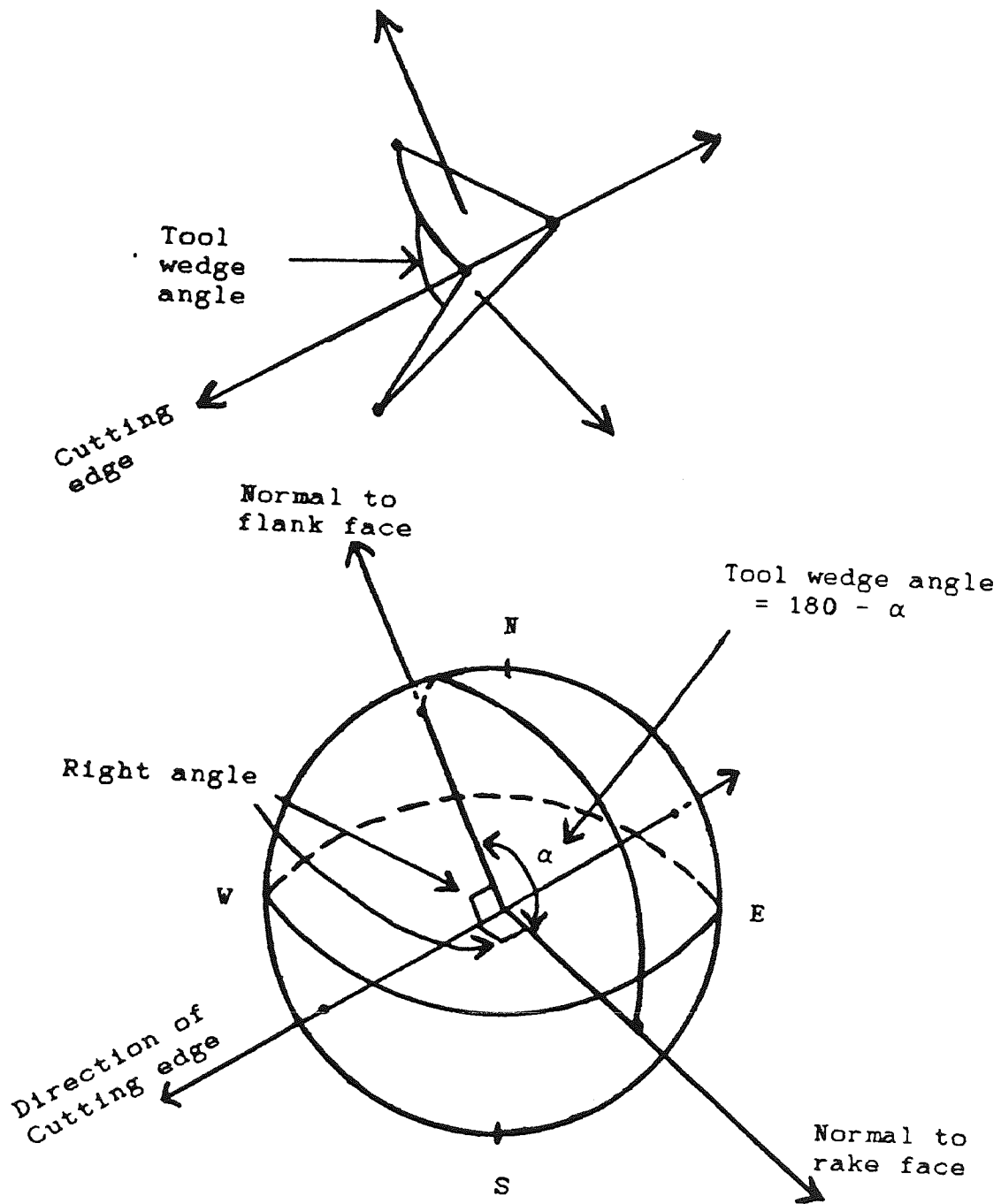


Figure 26 - Spherical Representation
of Tool Wedge Angle

to the displacement vector along the cutting edge. The workpiece velocity vector must be compared with the direction of the cutting edge and the inclination angle is the complement of the result. Obviously the direction of the velocity vector, figure 27, is dependent on spindle speed, radius and feed rate, but whatever its actual direction, one simple calculation determines the inclination angle, figure 28. There is, specifically, no advantage of simplification of the calculations by ignoring the feed.

With the velocity vector as input one may now determine the remaining cutting geometry. The angles between the velocity vector and the normal to the rake face and between the velocity vector and the normal to the flank face give intermediate values which must be corrected for inclination angle to produce true rake and clearance. Stabler [11] provides trigonometric functions to make these corrections but these are derived from plane trigonometry. A simpler correction is the use of right angled spherical triangles which may be simplified by the application of Napiers method of solution, as below, [16] part 1 chapter 4:-

The angle between the velocity vector and the normal to the flank face is related to the clearance angle by the formula:-

$$\text{Arcsin}(\text{Cos}(\text{calculated angle}) / \text{Cos}(\text{Inclination Angle}))$$

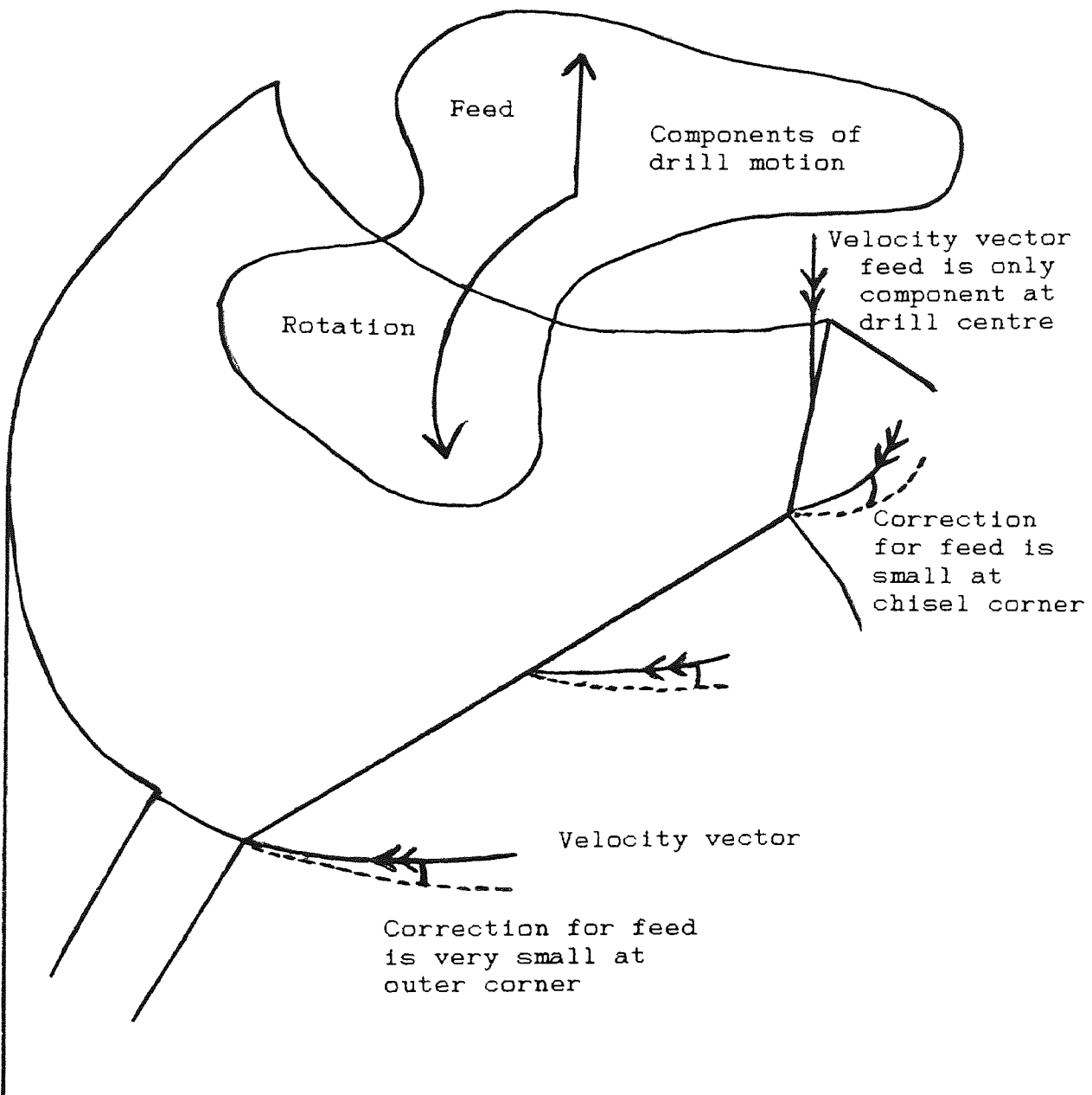


Figure 27 - Velocity Vector

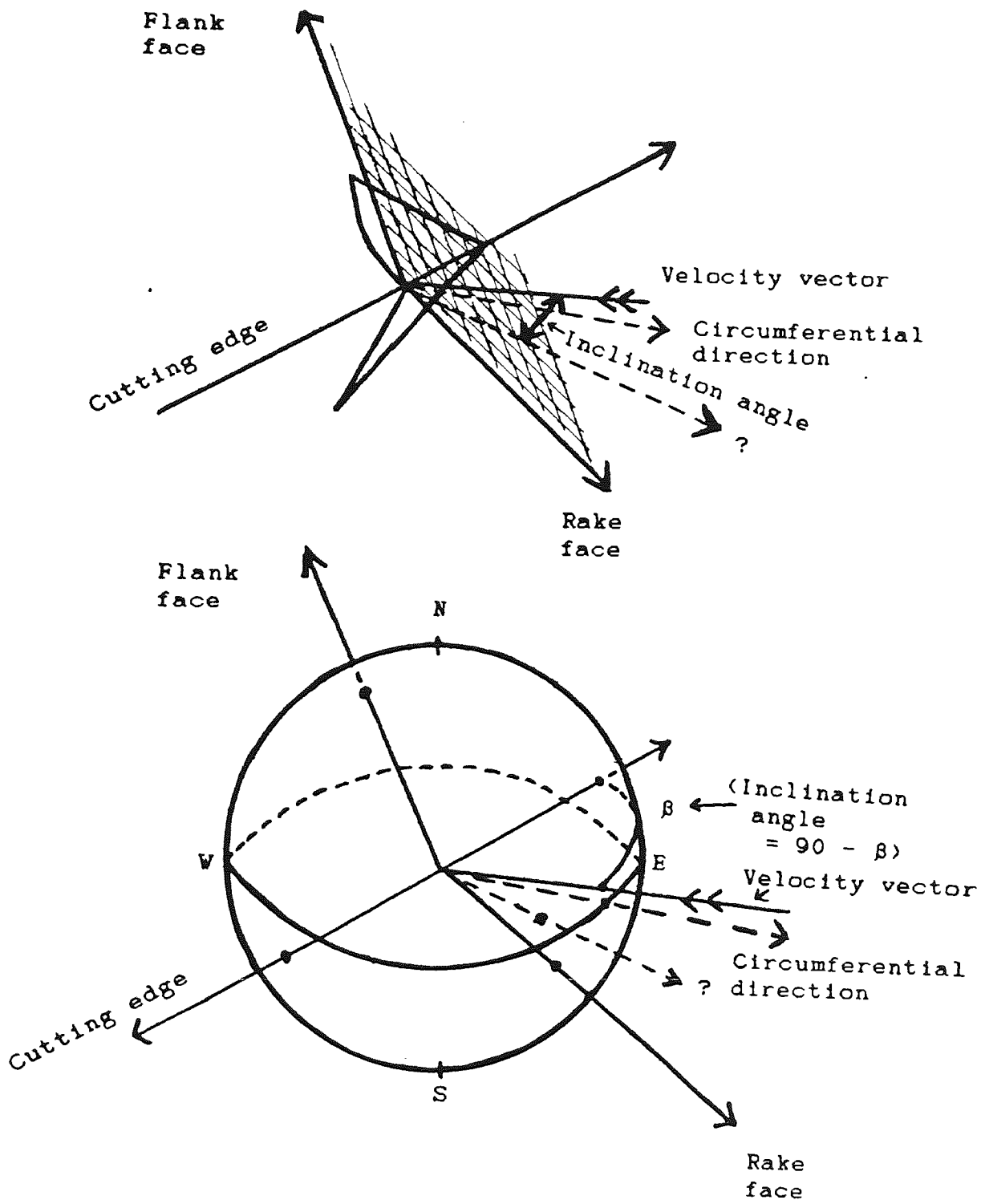


Figure 28 - Spherical Representation
of Inclination Angle

The angle between the velocity vector and the normal to the rake face is related to the clearance angle by the formula:-

$$\text{Arccos}(\text{Cos}(\text{calculated angle}) / \text{Cos}(\text{Inclination Angle}))$$

There is a complication with the rake angle in that it may be positive or negative. The spherical triangle used to calculate this angle is an ambiguous case where the sign is not revealed. Separate calculations of the directions of the cutting lip from the velocity vector and the normal to the rake face from the velocity vector resolve the ambiguity. They reveal that the rake angle starts positive at the outer corner but is negative at the chisel corner.

Stabler [11] proposes a formula equating the inclination angle of the approaching chip, (β), with the inclination angle of the chip leaving the cutting edge (γ). This formula may be used to determine the direction of motion of the chip as it leaves the cutting edge. The motion must be across the rake face, locally a plane that has already been determined. The calculation that remains is to determine which direction in this plane is the direction with an inclination angle of departure equal to the inclination angle of the arriving chip. Once again it is easier to measure this angle from the value of the normal direction. The triangle so produced is right angled and Napier's Rules may be applied to determine the solution. The initial directions and speeds of motion of the departing chip vary and interfere across the width of the cutting edge. The

deformation resulting from this action is restricted by the presence of the rake face and results in bending away from the rake surface. The curled chip seen in drilling operations is consistent with such deformation.

4.2. THE STEREOGRAPHIC PROJECTION.

It is possible to produce diagrams, like those used in the preceding text to represent the three dimensional situation. If they are based on the Stereographic Projection, figure 29, they provide an accurate two dimensional representation of this complex three dimensional situation, [16] part 2 chapter 13. Such a representation, once understood, is extremely informative. The method of stereographic projection may be applied to any spherical triangle and may, therefore, be applied to the problem of representing the true cutting geometry of the cutting edge of the twist drill. As already stated the true cutting geometry is measured between the relative motion of the workpiece material and the orientation of the cutting faces. The variations of these values across the cutting edge are displayed as arcs on the stereographic projection.

The stereographic projection is one of many methods of translating a three dimensional surface onto a two dimensional surface. It may be visualised as a sphere divided into two hemispheres by a plane. When viewed from above the plane the three dimensional surface is the surface

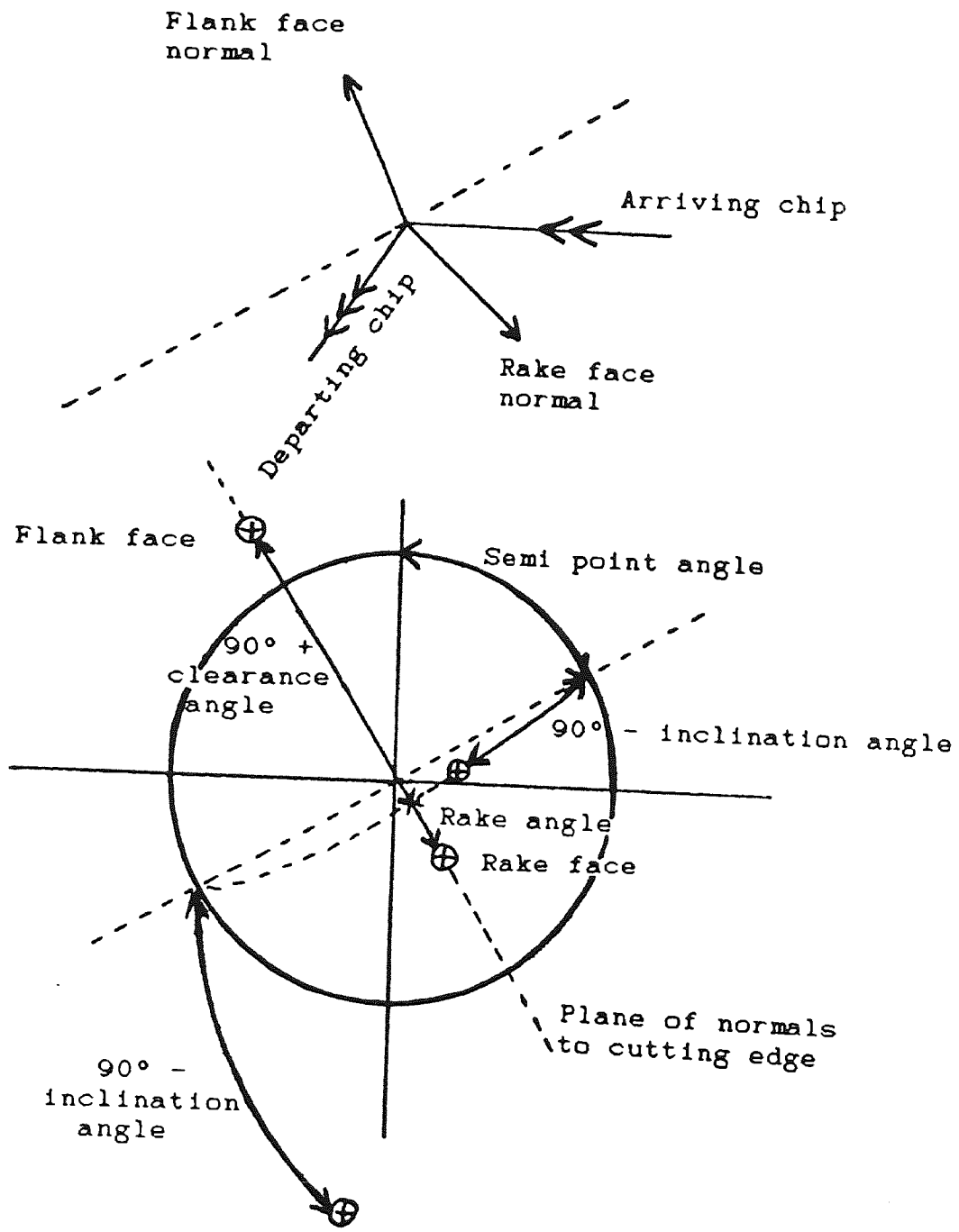
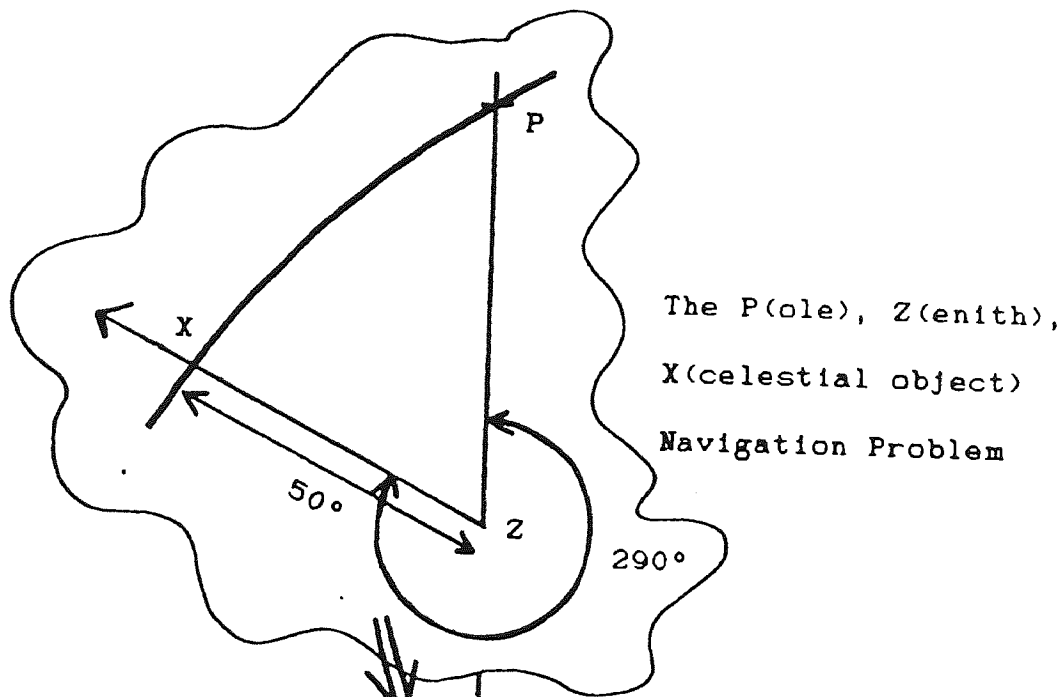


Figure 29 - Stereographic Projection

of the sphere. The two dimensional representation is the plane surface. The circle drawn on the plane represents the locus of intersection of the spherical surface and the plane, the so called horizon circle. One hemisphere is the area within the circle, with the circle centre being the zenith from which the sphere is observed, and the other is the area outside the circle, (theoretically out to infinity but practically to a limited distance 'over the horizon'). Any position defined in terms of Latitude and Longitude may be plotted onto the diagram with the use of protractor, ruler and compass. Once a system is plotted, by the use of the reverse procedure, positional and directional information may be lifted off the diagram.

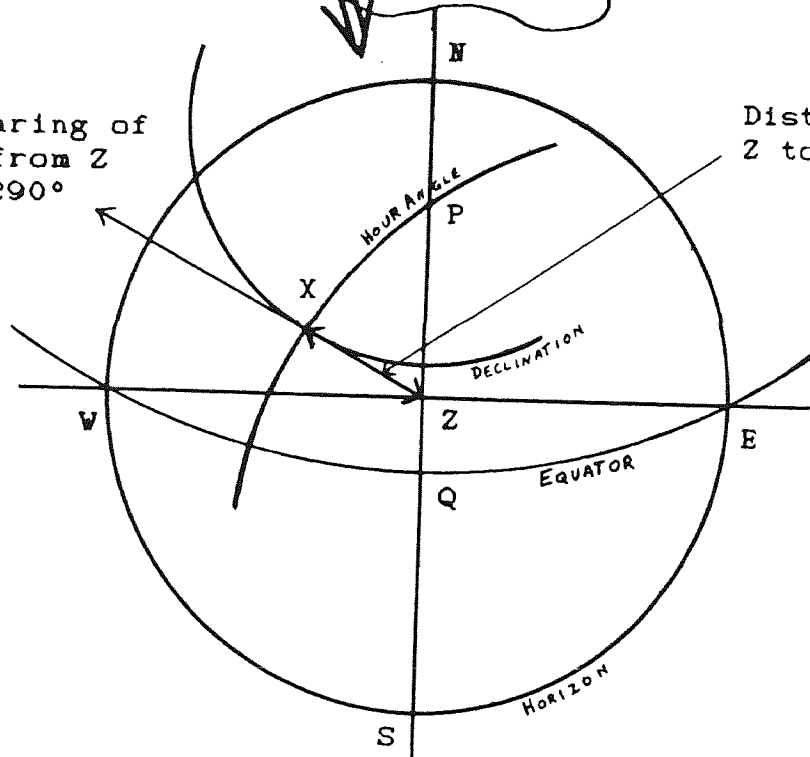
The typical navigational exercise is the P,Z,X triangle. P for pole, Z for the observers zenith and X for the geographical position of a celestial object. The Stereographic Projection of such a triangle is shown at figure 30. The equivalent spherical trigonometric calculation has been programmed into a computer using the spherical cosine rule. Again this is applicable to any spherical triangle no matter what the relative orientation of Z and X.

Given a drill point with a straight cutting lip then a spherical projection may be drawn as viewed from the direction normal to the cutting lip in the x-y plane. Given the co-ordinates of the various directions in terms of



Bearing of
X from Z
= 290°

Distance from
Z to X = 50°



Point of View (Z)

= 30°N 0°W

Position of Object (X)

= 40°N 60°W

Figure 30 - Typical P.Z.X. Triangle

spherical co-ordinates it is possible to map the various directions onto the projection, figure 31. On the diagram all the following geometry may be represented:-

1. The displacement vector along the cutting edge and the semi point angle.
2. The tool wedge angle.
3. The velocity vector, elevation due to feed and horizontal inclination due to the off centre position of the cutting edge.
4. The inclination angle β of the chip approaching the cutting lip.
5. The normal to the flank face and normal clearance angle.
6. The normal to the rake face and primary rake angle.
7. The normal to the rake face and the angle γ which indicates the direction of the chip flow leaving the cutting lip.

All the lines on the projection are circles or straight lines and are equivalent to great or small circles on the surface of the sphere. The straight lines passing through the 'zenith' point, the point of view of the diagram, are special in that the length or, in spherical terms, the angle between any two points on that line may be read off the diagram directly. This is the case with the tool wedge, normal clearance and primary rake angles. The three 'fundamental' cutting angles may be evaluated on this diagram for the conditions at any point on the cutting edge. The diagram offers a quick evaluation of any twist drill geometry, and of changes by comparison or by extrapolation of the diagram.

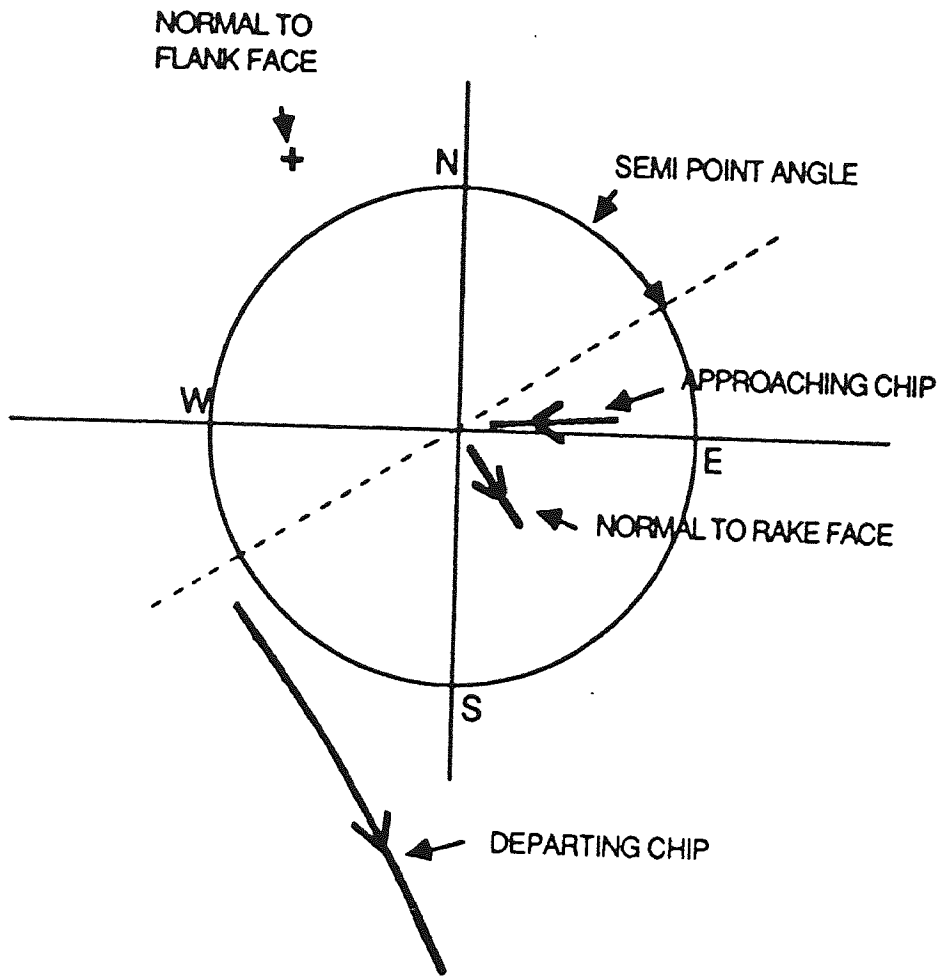


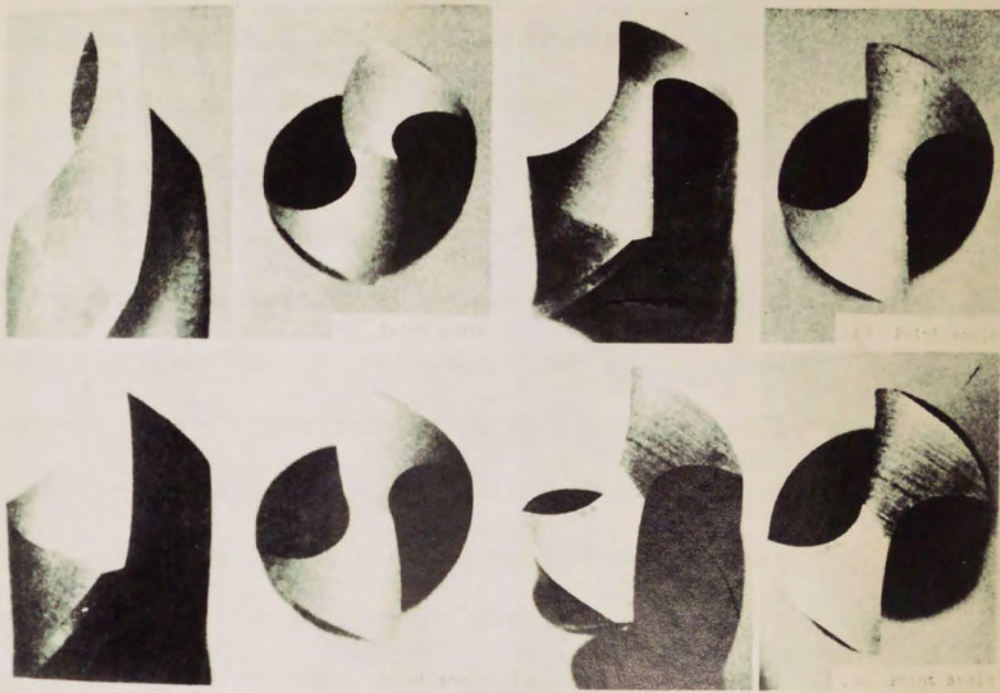
Figure 3 1 Stereographic Representation of the
Cutting Action of a Straight Edge Twist Drill [14]

4.3. THE FLUTE SHAPE.

It has already been stated that the drill flute, although it reduces the drill rigidity, is a necessary element within the structure of the twist drill. First, the cutting edge is the intersection of the flute and flank surfaces. Second, the flute provides the escape path for the chip material produced by metal removal at the drill point. The flute shape must match the design point shape. This was demonstrated by Galloway, [2], by grinding a range of point angles on drills with the same flute shape, figure 32. As one can see only the 'correct' point angle of 118° gives a straight cutting edge.

In order to provide a shape for the arbitrary trailing side of the flute shape with sufficient flexibility to maintain good continuity with the cutting half this research uses a Bezier curve, both parabolic and cubic. The minimum requirement for continuity is that the two curves of the flute be merged to form a continuous line with continuity of both position and slope throughout.

How is the Bezier curve to be applied to the trailing half of the flute? The standard cubic Bezier curve requires the position and slope of the start and end points. The position of the two end points is sufficient data to calculate the linear equation of the straight line between them. If a third parameter is included, it is possible to calculate the



View to the left

View from top

View from side

View from front



View from back

View from bottom

View from side

View from front

Figure 32 - Point Shape [2]

equation of the parabolic curve joining them. This third condition is the slope of the flute profile at the chisel corner and is sufficient to describe a simple drill flute. The use of a parabolic profile is made in [15] to describe the drill flute form.

The Bezier curve is calculated from the two end points and the slope, given as the co-ordinates of an imaginary point a short distance from the chisel corner, along the same slope as the cutting half of the flute profile. The calculated curve will not pass through the position of this third point but it will originate from the chisel corner in the direction of this point so ensuring continuity. This form of curve definition is often described in lay-man's terms as an attraction away from the straight line towards the position of the intermediate point or points. Varying the distance of the third point from the start point varies its influence and, therefore, the shape of the parabola produced.

The calculated equation of the line joining the two points is parametric. Two equations are produced, one for x and one for y as quadratic equations of the parameter t , where t varies from 0 at the start point to 1 at the end point. These equations are found and solved using matrix notation.

Looking now at the rolled heel drill flute form a fourth condition must be introduced. It is then possible to calculate the equation of the cubic curve between the two

end points. The fourth condition is the slope of the flute profile at the intersection with the drill radius. This may or may not be tangential to the radius. The trailing corner is the end point, as before. The 'fourth point' governs the slope of the curve as it reaches this end point. Two cubic parametric equations are produced.

The solution of these equations for successive values of the parameter t provides co-ordinates in the x-y plane of the profile of the trailing edge of the drill flute.

The position of the cutting lip has determined the form of the cutting half of the flute. The second or trailing half of the flute is remote from the cutting edge and may, therefore, be of arbitrary shape. A Bezier curve has been proposed to describe this half of the flute. The shape of the drill point face is determined by the form of the intersection between the point face of the drill and both halves of the flute. The point face is the one that is subject to a high level of pressure due to lack of cutting clearance, this face being the source of the majority of the thrust on the drill shaft present in a drilling operation. For this reason it is often modified, in a generally arbitrary way, by the grinding of a secondary relieved surface or by a point thinning operation, or by the provision of a rounded trailing corner, or heel, by the performance of an additional grinding operation. The Bezier curve format of the trailing half of the flute allows

flexibility in the shape of the trailing half of the flute and allows the effect of change of shape to be explored. These secondary operations are currently developed by trial and experience rather than a true understanding of the material velocities present across the point face.

In the construction of the geometric model the drill cutting edge was originally placed to achieve a web thickness equal to the value of the parameter 'W'. This was determined before the flute profile was defined. It is now necessary to calculate an accurate value for the webthickness as the point of closest approach of the flute profile to the drill centre. This is less than the value of the webthickness parameter 'W', figure 33.

The point of closest approach may be described, taking the more complex example of the cubic Bezier curve, as the point where the local radius, r , is a minimum. As $r^2 = x^2 + y^2$ and r^2 is a minimum when r is a minimum, then the derivative of $x^2 + y^2$ must be equated to zero in order to mathematically determine the location of this minimum. For the cubic curve the derivative is a polynomial in t to the power 5 and may be solved by a Newton-Raphson iteration. The angle at which this occurs is the deepest point of the drill flute and is important when examining the flute grinding operation as it must coincide with the most extreme point of the grinding wheel.

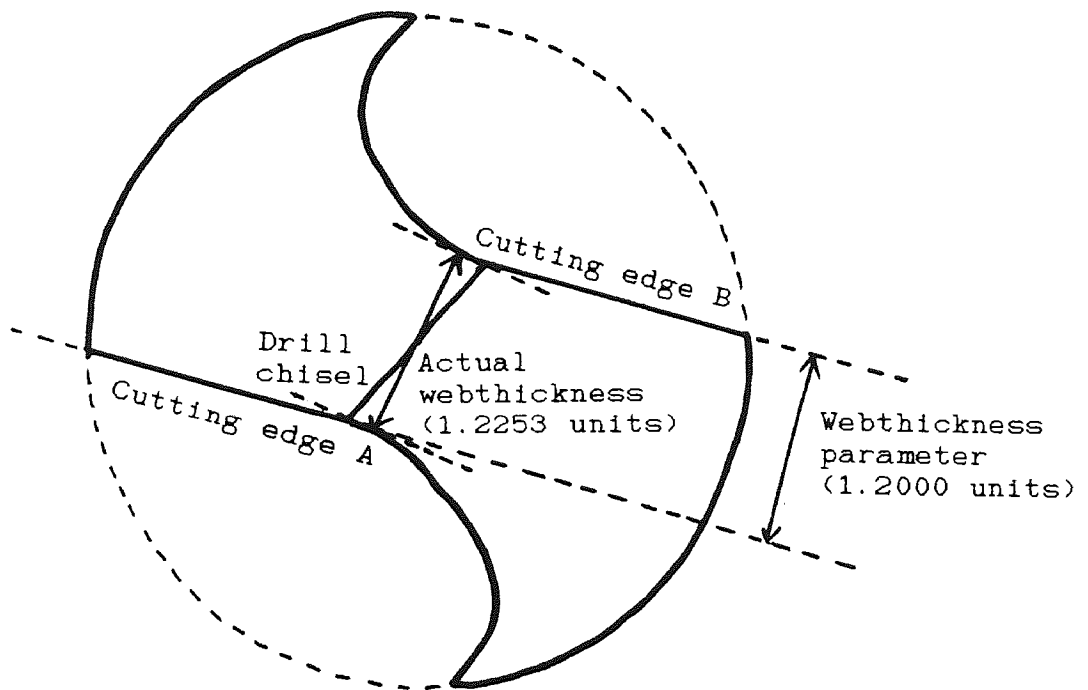


Figure 33 - Webthickness Parameter vs
Actual Webthickness

4.4. FLUTE GRINDING.

The flute is ground with a grinding wheel dressed with a 'v' shaped profile. The 'v' is generally formed by two arcs which meet at a point. The parameters of these arcs have been collected into secret reference books by the various drill manufacturers. This intersection is the most extreme part of the grinding wheel profile. The web thickness is controlled by the penetration depth of this point. The grinding machine is set up so that this extreme point is directly over the drill centreline. The flute helix is controlled by the lead set on the helical grinding machine.

In any helical milling or grinding operation there is an interference effect. This causes significant modification between the profile of the tool being used for cutting and the profile of the generated flute shape. In the drill manufacturing industry, in order to minimise this effect, the tool is set at a helix angle approximately 4 degrees greater than the nominal helix, figure 34. The flute is still ground using the lead which matches the nominal helix. This offset of the wheel partly counteracts the effects of interference but the flute shape produced from a particular wheel profile is still modified and the actual shape produced is known by experience rather than evaluation.

The Grinding Wheel
is Rotating

The Drill Shaft Moves
Longitudinally Past the
Grinding Wheel while
simultaneously being
Rotated at a Synchronised
Rate to create the Constant
Lead of the Helix

Grinding wheel

Offset angle of
grinding tool

Rotation

Translation

New
Flute

Nominal
helix angle

The Offset Angle of the Grinding Wheel =

$90^\circ - \text{Nominal Helix Angle}$

+ 4° Correction for Interference

Figure 34 - Helical Milling

4.5. CONCLUSIONS.

The requirement is for a system able to determine the true or fundamental cutting geometry across the drill cutting edge. Chapter 3 provides the drill as a geometric model or shape. The interaction between that shape and the relative velocity of the workpiece material approaching that shape has now been examined. Spherical trigonometry provides a consistent and unambiguous answer to this interaction.

It is also necessary to introduce the manufacturing process required to generate the drill flute. This is again a process currently known to the drill manufacturer by dint of experience in the form of a book of tables listing the position and radii of the two arcs required to generate a particular flute form.

CHAPTER 5

	PAGE
5. COMPUTER APPLICATION	113
5.1. SUPERCAL 4 -	
COMPUTER SPREADSHEET SOLUTION	114
5.2. TURBO PASCAL -	
SOLUTION WITH GRAPHIC DISPLAY	123
5.3. CONCLUSIONS	151

5. COMPUTER APPLICATION.

The mathematical process to be followed has been outlined by the two previous chapters. It is now necessary to examine the implementation of that mathematics within a computer. The research policy is to avoid the expense of high powered hardware and sophisticated software. The work is intended to look at what is possible using standard software and a standard IBM compatible personal computer. Where appropriate material has been screen dumped from the prototype computer programs to illustrate the text.

By making calculations about the geometry of the twist drill with the use of a discrete mesh of individual co-ordinates, rather than attempting to obtain continuous equations, it is possible to simplify the mathematical calculations compared with researchers [2..5]. The basic reasoning here is that overcomplex mathematics based on continuous equations that only provide limited information, such as [2..5], will find no practical application and will be of esoteric interest only. Whereas a simplified piecewise system, even where it is tied to the use of a personal computer, may be accessed by anyone.

Two separate prototype applications of the method have been programmed, each with separate strengths, and they are described in turn. During the following explanation of the method, example data is generated for a 4.5mm Quick Spiral drill, as would be recommended for use with aluminium. This drill is used as an example but similar data would be

available for any drill by using the individual form parameters of that drill.

5.1. SUPERCAL 4 - COMPUTER SPREADSHEET SOLUTION.

SuperCalc 4 is a "computerised spreadsheet". It is used for the entry, storage, processing and display of numerical data. It may be used passively, where cells are filled with numerical values and where further cells are programmed with formulae. These formulae act on the initial cell data to produce answers. Answers, such as column and row totals, are displayed, as the results of formulae cells, wherever required.

A full range of mathematical functions, including conditional, 'if', statements, is available. SuperCalc 4 may also be used actively, in conjunction with a command file in it's own programming language. Such a command file may access the data on several different spreadsheets, process it through further spreadsheets and collect the data, as required, to yet further spreadsheets. Alternately separate parts of the same sheet may be used. This second mode is primarily designed to overcome the size limitation of a single spreadsheet.

A "computerised spreadsheet" is, therefore, a powerful system capable of processing and displaying large volumes of data with ease.

The equations of the geometric drill solution have been used to construct a SuperCalc 4 spreadsheet. This is an excellent medium for trial and error or, more scientifically, iteration calculations. A short form of the spreadsheet is used to determine the grinding parameters corresponding to a particular drill geometry, figure 35. Being a relatively small spreadsheet it performs very quick re-calculations. The grinding parameters are input as cell values and the effect of varying any parameter is quickly displayed after each change.

For more detailed evaluation these grinding parameter values are transferred to a larger spreadsheet. The eight grinding parameters providing the unique blueprint of an individual drill. A command file is executed to assemble a set of information. This set examines the geometry over a range of radii. At each radius, after performing a re-calculation, the drill geometry variables are transferred to another section of the spreadsheet. The clearance angle is measured by finding the z ordinate of two points close together displaced by a known small angle:-

$$\text{The clearance angle} = \text{Arctan}(\delta Z/r\delta\theta)$$

This set may then be input to SuperCalc 4 graphs. Billau and McGoldrick [4] investigated the presence or otherwise of positive clearance around the periphery of the drill flank face. Figure 36 displays such a distribution produced by the SuperCal program and, as can be seen, at an angular distance

	A	B	C	D	E	F	G
1	Drill R =	2.25		Nom D=	4.5		
2	Web T =	1.3					Theta=
3	G =	20		H =	14.382		x =
4	T =	2					y =
5	Beta =	15	.26179	Helix	30		P =
6	Alpha =	40	.69813	Lead	24.486		R =
7							Mu =
8	Drill Centre			Chisel Corner			
9	X =	0		X =	-.3533		
10	Y =	0		Y =	.62765		
11	Z =	0		Z =	-.0429		
12	Point Angle =		109.47	Chisel Angle=	115.52		
13				Chisel Len =	1.4405		The+1=
14	Outer Corner						x =
15	X =	-2.1929					y =
16	Y =	.503616					P =
17	Z =	-1.3467		Radius	1.2391		R =
18							Mu =
19	Clearance Angle=		21.937				x =
20							z =
A1							
Width: 9 Memory: 85 Last Col/Row: 146							
1>							
READY F1:Help F3:Names Ctrl-Break:Cancel							

Figure 35 - Spreadsheet Display of Drill Data

of 5° behind the...
 relative to zero...
 still would...
 removing that...
 the distribution...
 as at figure 37 for...
 graphs are able to...

Variation of Clearance Angle With Radial Angle from Outer Corner

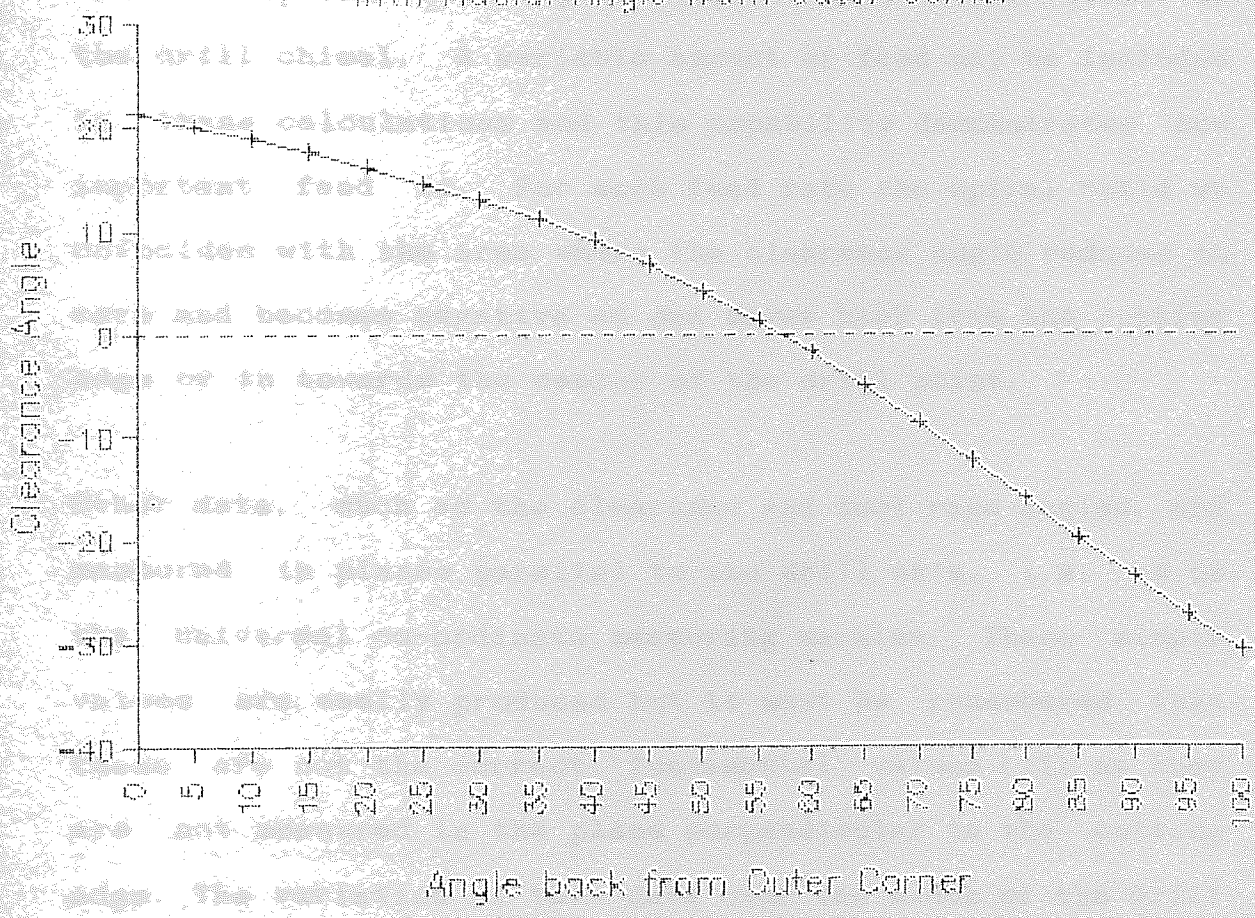


Figure 36 - Periphery Clearance Angle [4]

of 55° behind the outer corner the periphery clearance angle reduces to zero and becomes negative beyond this point. This drill would therefore require a rolled heel flute so removing that portion of the drill flank face. Alternately the distribution along the cutting edge may be investigated as at figure 37 for a series of intermediate radii. These graphs are able to indicate the extent of the area with no positive clearance, an area which is marked by an easily visible spiral built up of material around both sides of the drill chisel. A variable amount of feed may be included in these calculations and this capability demonstrates how important feed is. For each feed rate the spiral build up coincides with the area where the clearance angle reduces to zero and becomes negative as one moves back from the cutting edge or in towards the center of the drill point.

Other data, such as the clearance and tool rake angles, are measured in planes parallel to the drill axis, i.e. as on the universal co-ordinate measuring machine. These simple values are easily produced but it must be remembered that these are not the correct 'fundamental' values [11] as they are not measured in the plane perpendicular to the cutting edge. The variation of this data over the width of the drill cutting edge may easily be displayed on SuperCal 4 graphs, for example helix or tool rake as in figure 38. Currently such information is the only geometric data that is available to the drill designer.

Helix Angle
Range of Clearance Angle
Over Cutting Lip C.C. to O.C.

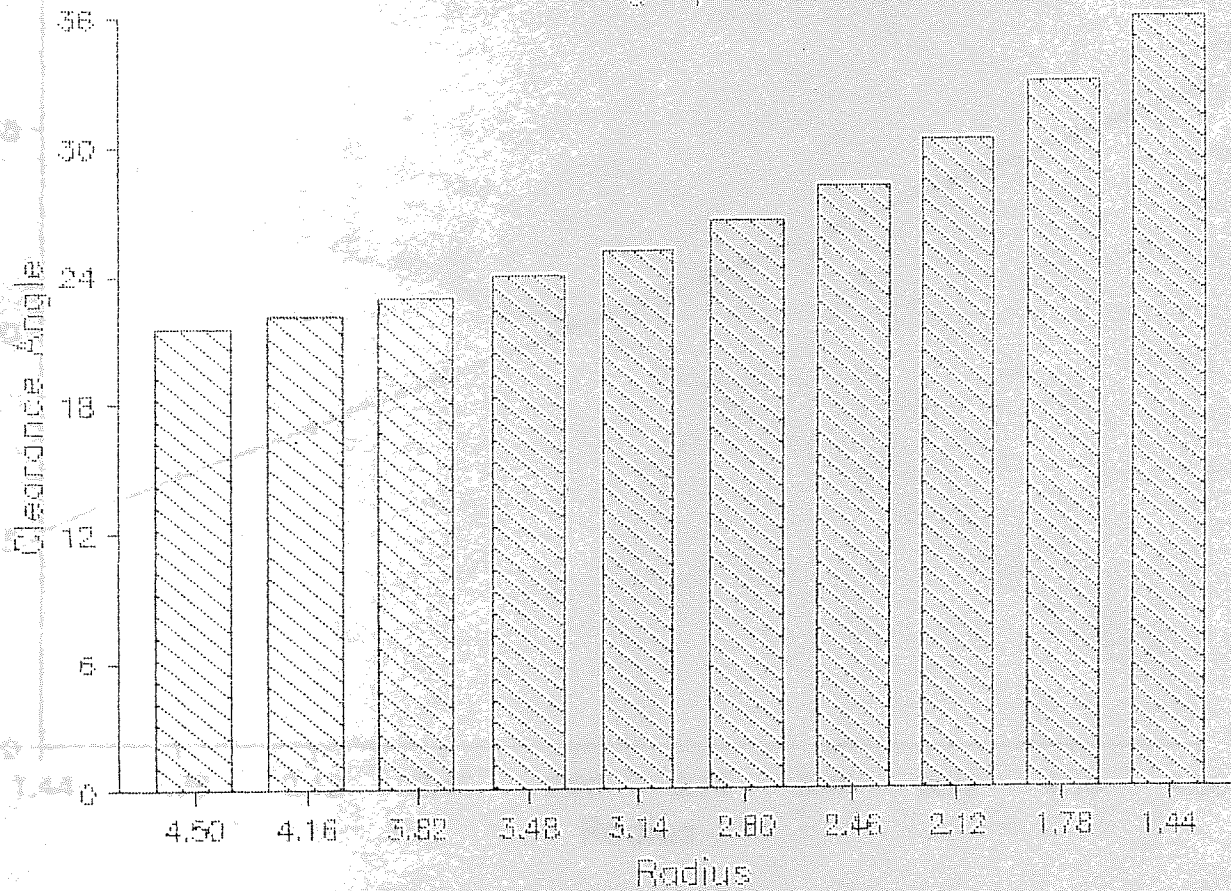


Figure 37 - Spreadsheet Histogram of Clearance Angle

Helix Angle = Tool Rake Angle

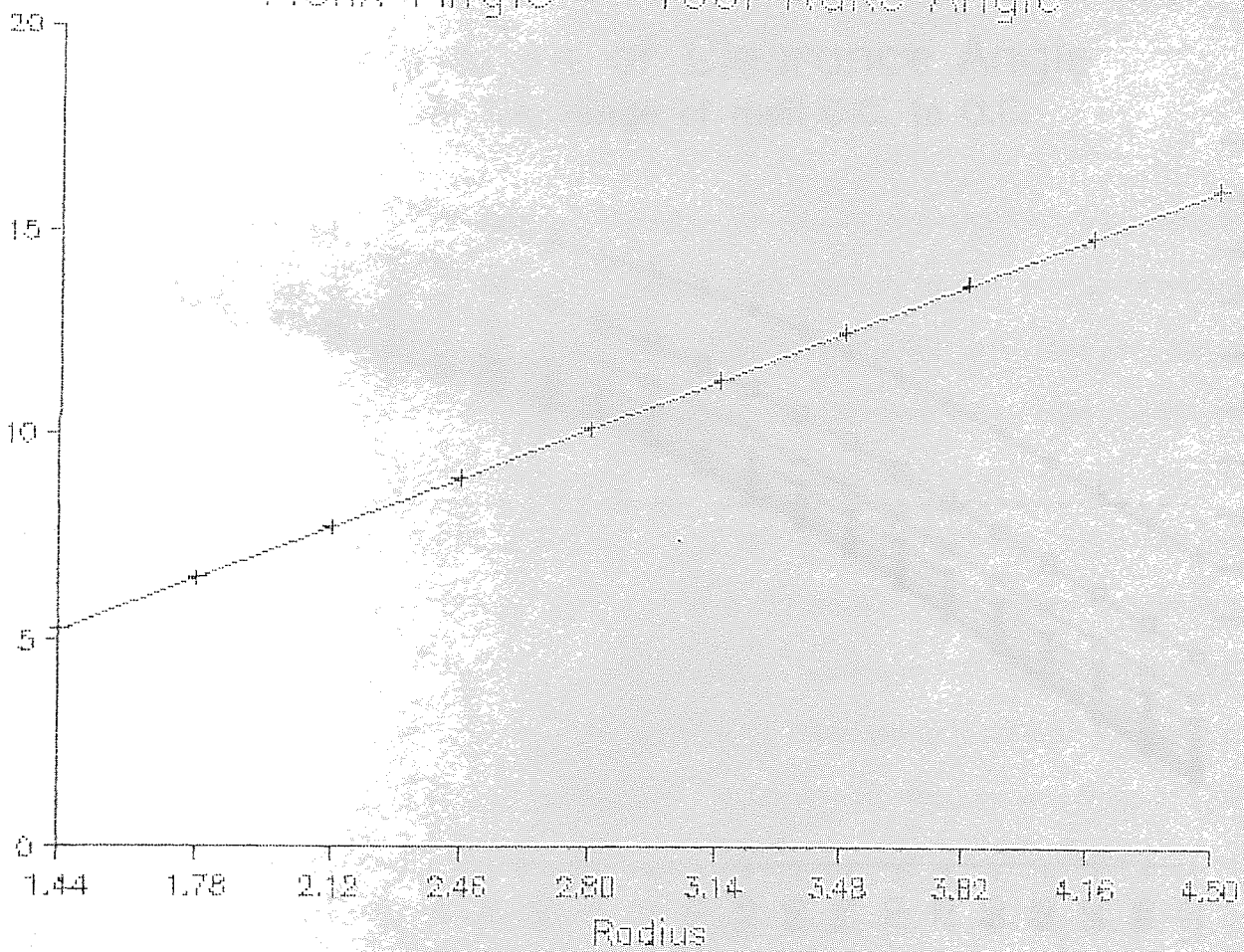


Figure 38 - Line Graph of Helix or Tool Rake Angle

The point clearance angle

specifically by the

figure 39. The

size of the

clearance angle

defined by the

to be straight.

flank face

The

Variation of Clearance Angle

for the range of radii C.C. to O.C.

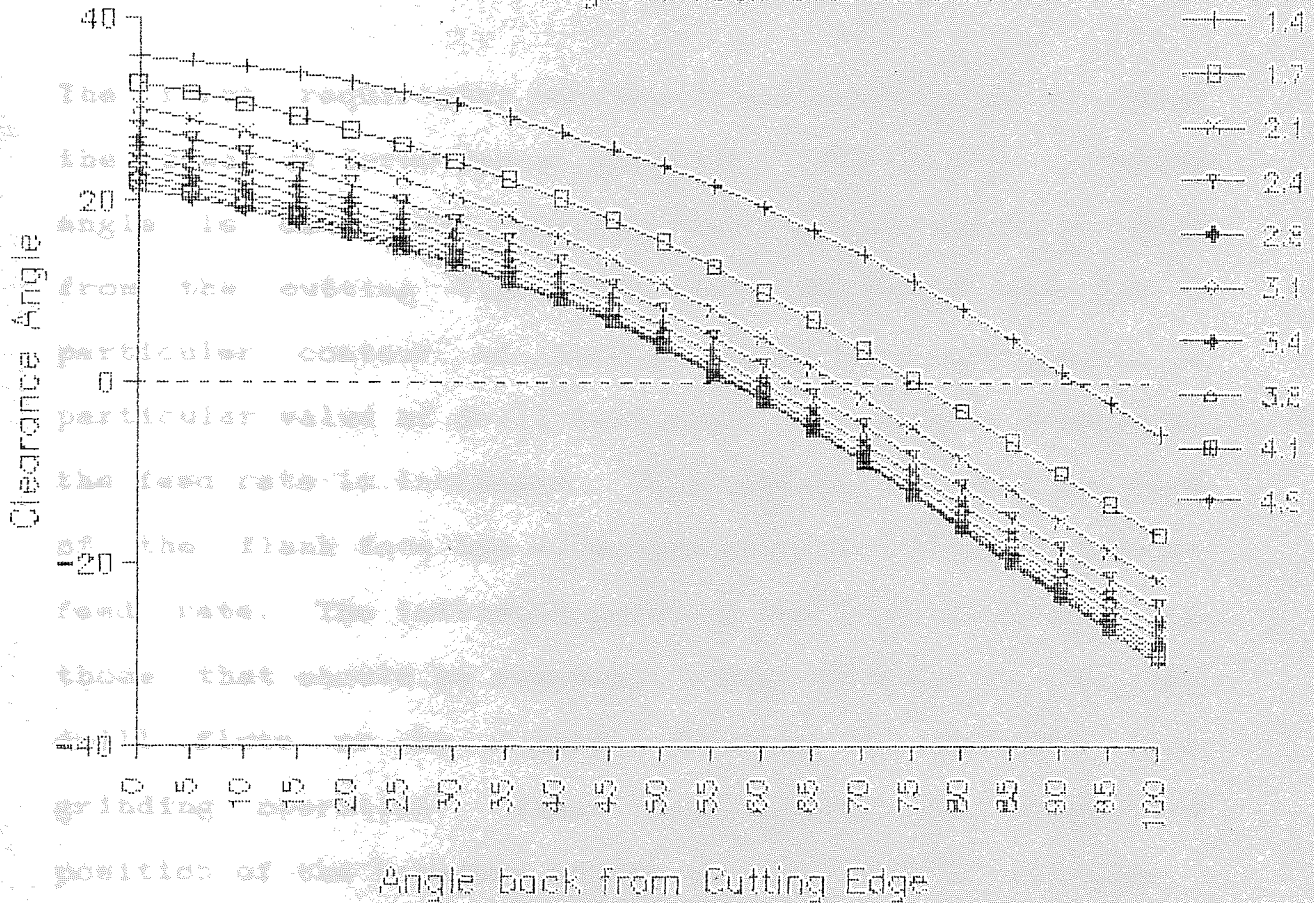


Figure 39 - Range of Point Face Clearance Angles

The graph drawing facility of SuperCalc 4 is used specifically to examine the point/flank face of the drill, figure 39. When examining the parameters that determine the size of the flute space there are two factors in direct competition. The trailing half of the flute has not been defined by the fundamental requirement for the cutting lip to be straight. The shape and position of this side of the flank face must be determined from two other requirements:-

- i. The point/flank face area and contour.
- ii. The drill stiffness.

The first requirement may easily be investigated by using the power of Turbo Pascal graphics. The value of clearance angle is determined over the flank face as one moves back from the cutting lip. This value decreases and has a particular contour of zero clearance corresponding to a particular value of drill feed rate. The contour expands as the feed rate is increased. This contour indicates how much of the flank face has effective clearance at a particular feed rate. The indicated parts of the point/flank face are those that should be removed, either by being part of the drill flute or by a point thinning or secondary face grinding operation. These requirements help guide the position of the boundary of the trailing side of the flute.

Point thinning is an important aspect of drill design as it controls the drill thrust force, especially for thick webbed drills which have high stiffness but would require excessive

thrust for penetration particularly with work hardening materials. The flank clearance angle may be determined at every point on the flank face, on or behind the cutting edge. A diagram of the distribution of clearance on the flank face may be produced.

Figure 39 is such a diagram produced by SuperCal graphics, it is, however, difficult to interpret. An alternative display may use the data created in SuperCal but present it by using Turbo Pascal graphics. Figures 40, 41 & 42 are the displays for zero feed rate, 0.2 and 0.4mm/Rev Feed. This shows the influence of drill feed which is an important aspect of this analysis. Feed has not been incorporated in such an analysis by any of the previous works. SuperCal produces the set of flank face clearance angle data for zero feed and this is corrected by the Turbo Pascal presentation for any level of feed rate. The effect of feed is emphasised by the contours of figure 43. This information on the point shape must, however, be reconciled with the requirements of drill stiffness and chip transport capacity before the true optimum geometry for the trailing edge of the drill flute is approached.

5.2. TURBO PASCAL - SOLUTION WITH GRAPHIC DISPLAY.

Turbo Pascal is an enhanced Pascal language available for the IBM PC. This is a much more flexible medium in the range of forms of data display available.

Positive clearance

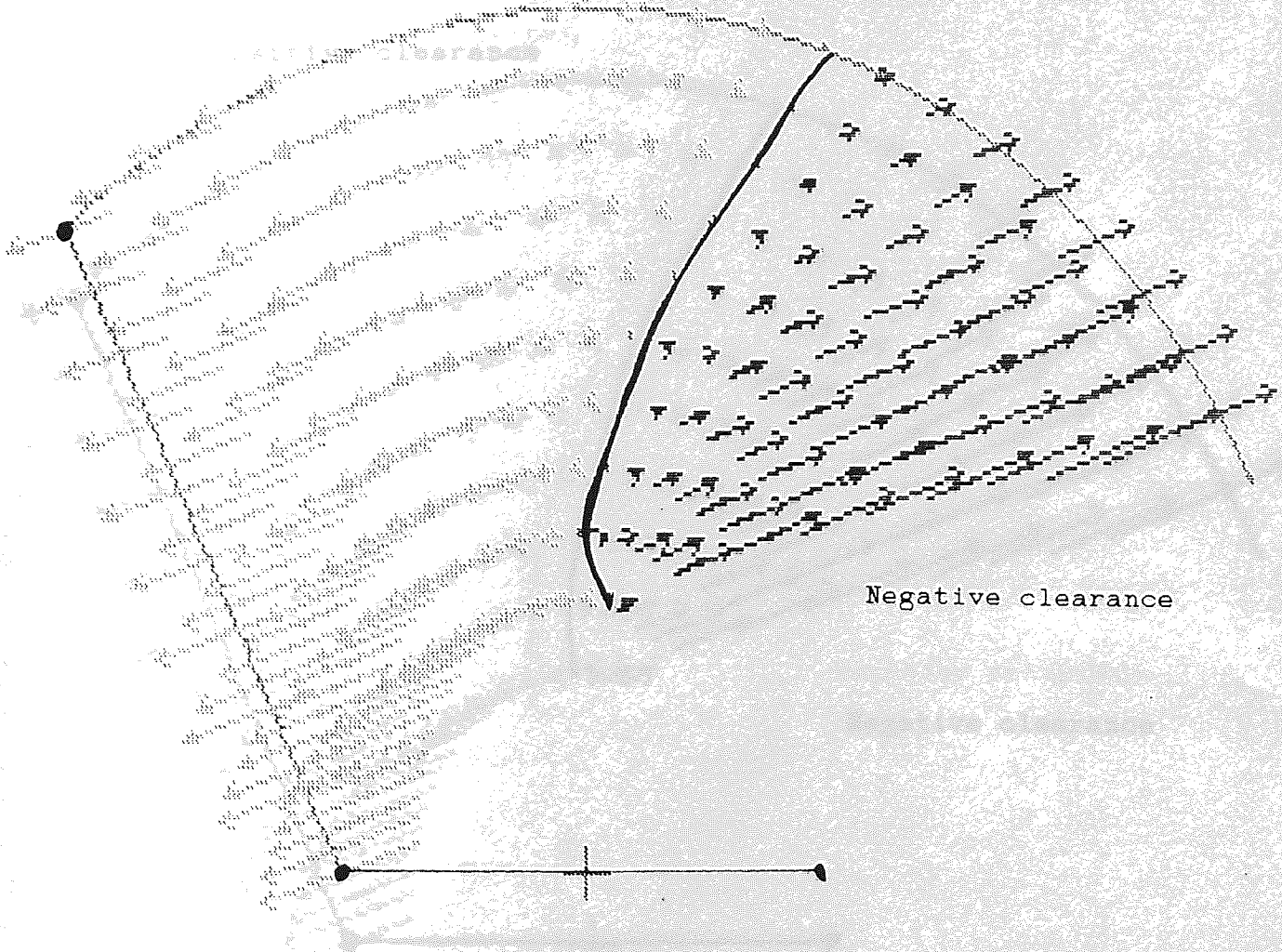
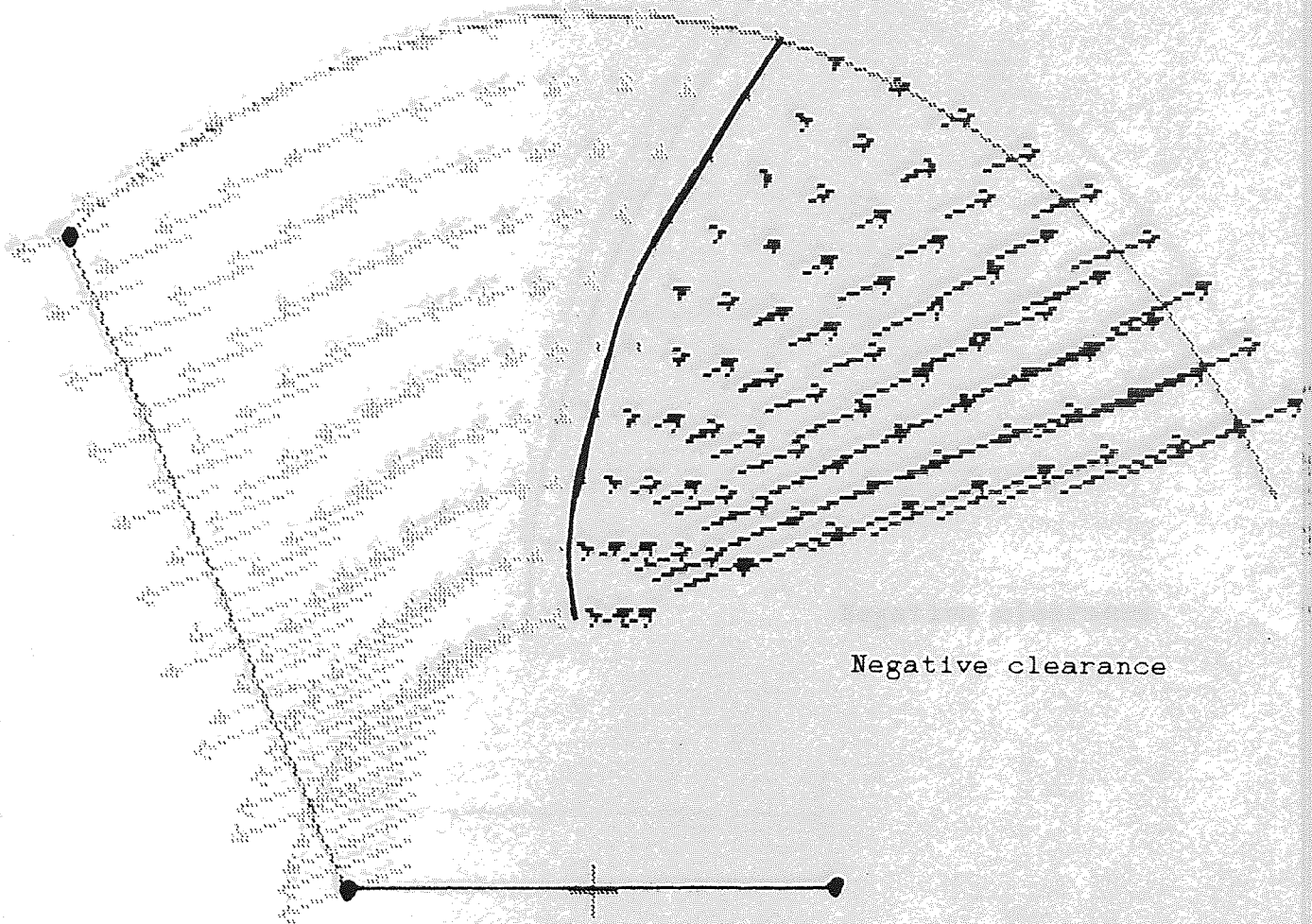


Figure 40 - Representation of Drill Flank Face
Distribution of Clearance Angle for Zero Feed

Positive clearance



Negative clearance

Figure 41 - Representation of Drill Flank Face
Distribution of Clearance Angle for 0.2mm/Rev Feed

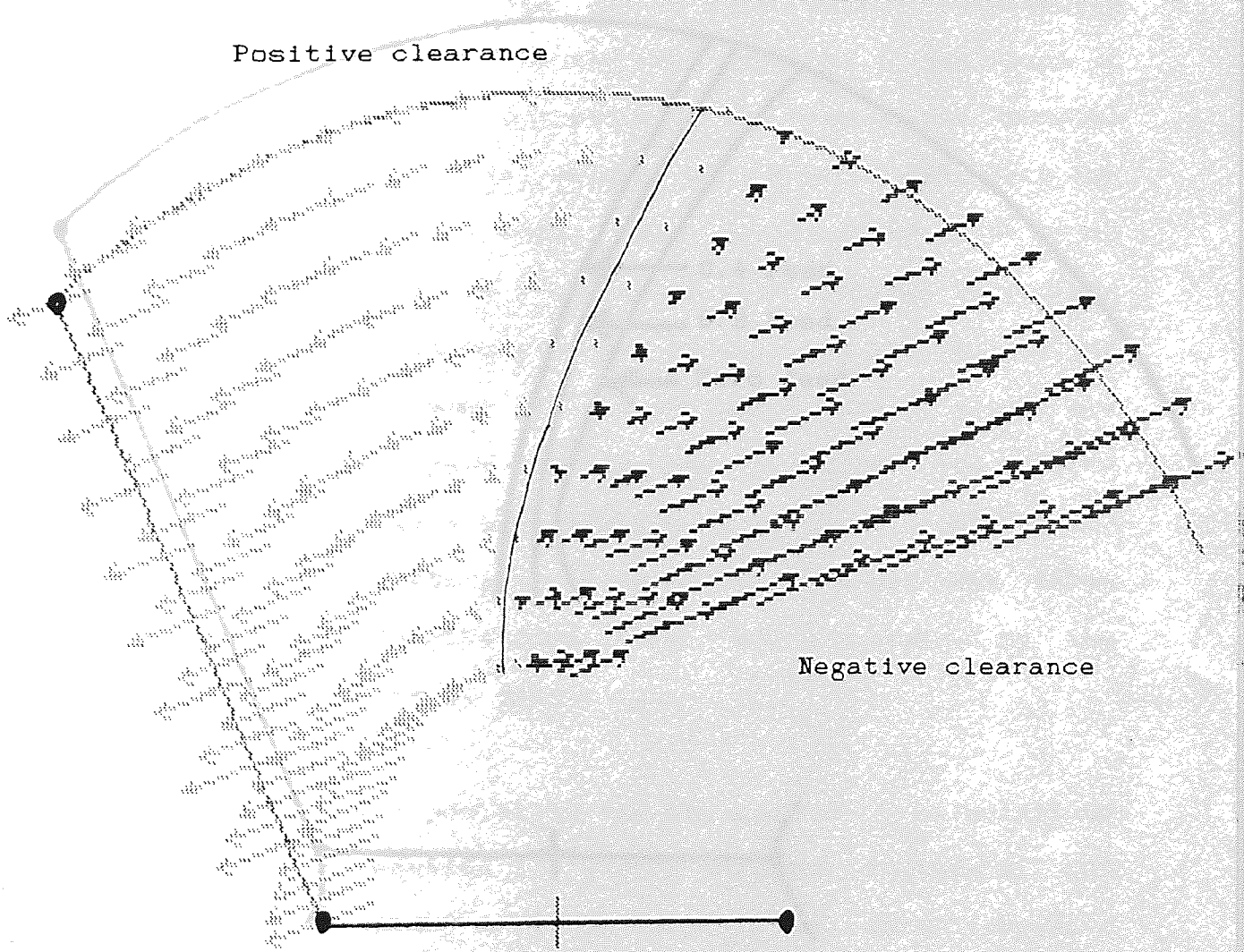


Figure 42 - Representation of Drill Flank Face
 Distribution of Clearance Angle for 0.4mm/Rev Feed

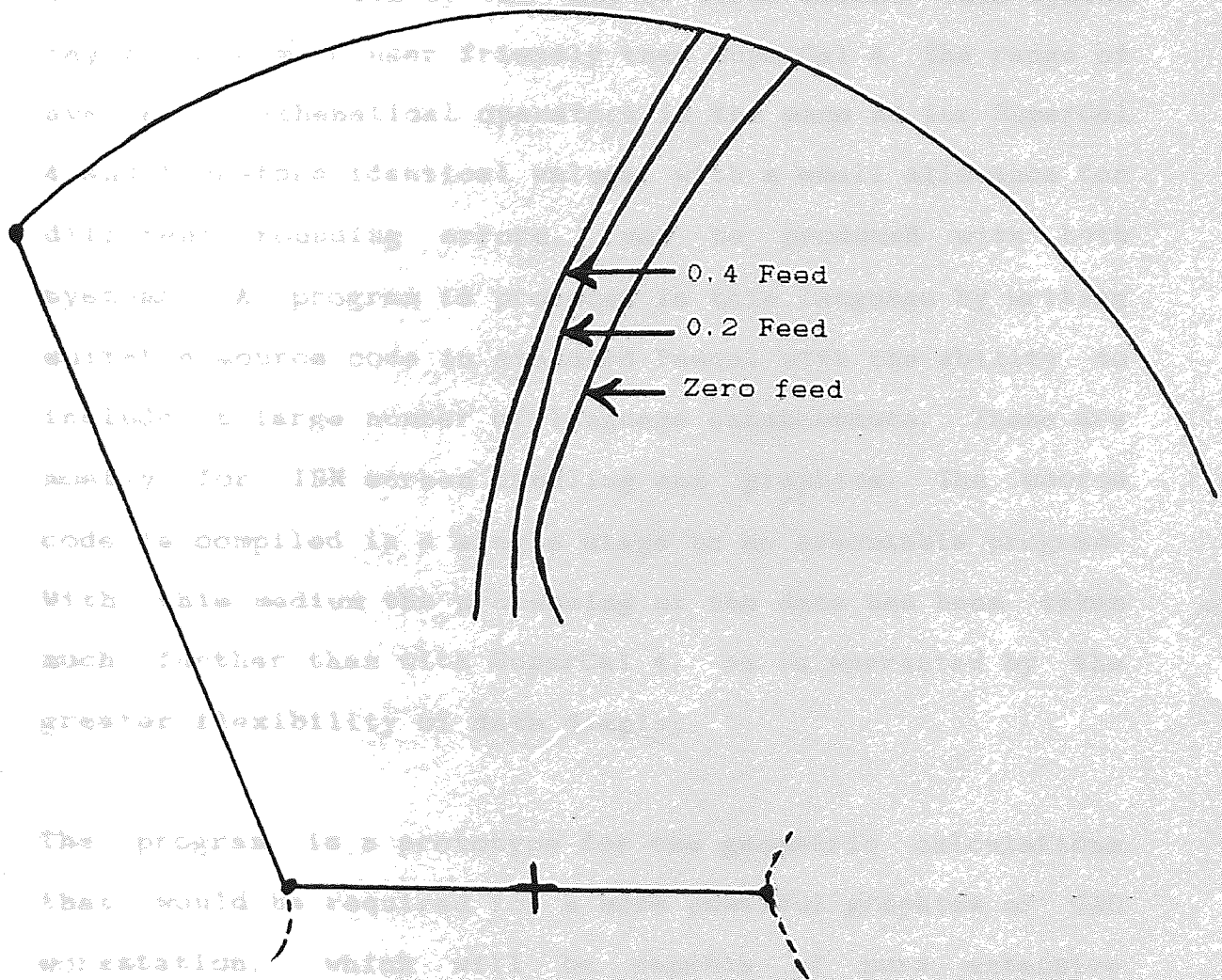


Figure 43 - Representation of Drill Flank Face,
 Comparison of Zero Clearance Angle
 for Range of Feed Rates

It has not been possible to reproduce the drill's helical form with a simple CAD/analysis package although more advanced packages may have this ability. It has proved easier to examine and picture the geometry of the drill on the computer screen by the use of Turbo Pascal. This system may be made more user friendly than SuperCal 4. The range of available mathematical operators is the same as for SuperCal 4 and therefore identical values, with a small allowance for different rounding errors, may be produced with both systems. A program is produced in this language by writing suitable source code in standard Pascal with the ability to include a large number of language enhancements. These are mostly for IBM screen handling and graphics. The source code is compiled in a single stage to an executable program. With this medium the processing of the data has been taken much further than with SuperCal 4, as is warranted by the greater flexibility of data display.

The program is a prototype for the geometric calculations that would be required for a more powerful graphics or CAD workstation, which will be capable of more extensive analysis of the data produced. The program consists of a series of screens of data. The same parameters from the SuperCal 4 system are used again, as applicable to the example 4.5mm Quick Spiral Drill. The start point is the same data, displayed as input data on the first screen. On this screen any value may be altered as required, figure 44. The second screen redisplay some of the parameters together

DRILL PROGRAM

	drill diameter	4.500	
	"t" param	1.200	
	alpha	55.000	
	beta	15.000	
	gparameter	50.000	
	tparameter	2.000	
	drill feed	0.200	
	drill helix	40.000	
Lat File	lead	16.848	
Lat Rail	2-parabolic 3-cubic (present)		parabolic
Lat Rail	length of p2	0.800	
	length of p3	1.000	
	angle of p3	1.000	
	angle of heel	90.000	
	Area of		
	wheel height	15.000	
	wheel offset	4.000	

Figure 44 - Input Parameters

... of the ...
... the ...
... displays ...
... generator ...
... trailing ...
... the program ...
... to modify ...

DRILL PROGRAM

... program is allowed

... of the
Drill Diameter = 4.50
... of
Drill Radius = 2.25
Point Angle = 139.87
...
"T" parameter = 1.200
Helix Angle = 40.000
...
Lead = 16.848
Lat Flank = 69.32 Long Flank = 196.15
Lat Rake O. Cor = -39.97 Long Rake O. Cor = 73.77
Lat Rake Ch Cor = -5.36 Long Rake Ch Cor = 89.64
webthickness = 1.2253
theta[0] = 98.932
Area = 9.1827 units squared
Area of Circle = 15.9043
2nd Mom Area = (15.8458 + 5.0528) =
20.8985 units to the fourth
2nd Mom Area of Circle = 40.2578

... by the ...
... at ...
... bounded ...
... of ...
... by ...
... compared ...
... of the ...
... camera ...
... field is required

Figure 45 - Output Data

with the calculated geometry of the drill point as would be measured by the universal measuring machine, figure 45. The third screen displays the drill flute cross-section with the 'cone generator' cutting side and the 'parabolic' or 'cubic' curve trailing side shown in figures 46 & 47 respectively. The program may now return to the data input screen in order to modify any of the parameters as required.

If the program is allowed to continue the fourth screen is a representation of the end view of the drill, figure 48, consisting of the cutting lip, the chisel and a set of curves which depict the form of the trailing side of the drill point face. This set of information is displayed the same as that described in [3]. This is the most economical way to generate the end view of the drill point. The drill flank contour is a set of elliptical curves obtained from the intersection of a series of planes orthogonal to the drill axis and the conical surface of the drill flank represented by the mathematical model. The flute profile is also mapped at similar levels. The drill point/flank is therefore bounded by these curves in the x,y plane at equal intervals of z. The 'end on' view of the drill point shape is produced by joining up the points of intersection and may then be compared with a real drill. The three dimensional nature of the drill point is difficult to picture optically with a camera or measuring telescope, as sufficient depth of field is required to view in focus both the outer corner and the point.

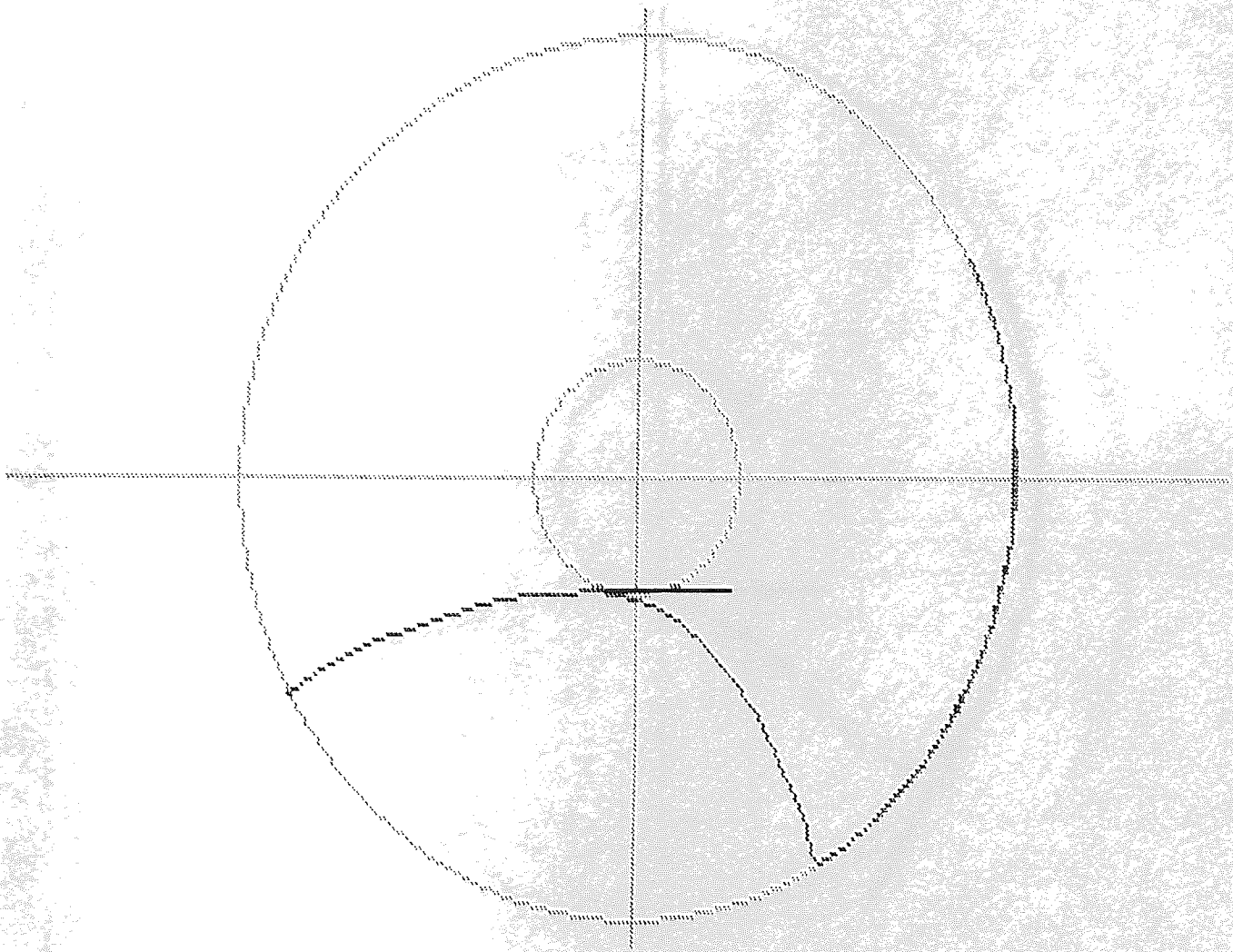


Figure 46 - Parabolic Drill Flute

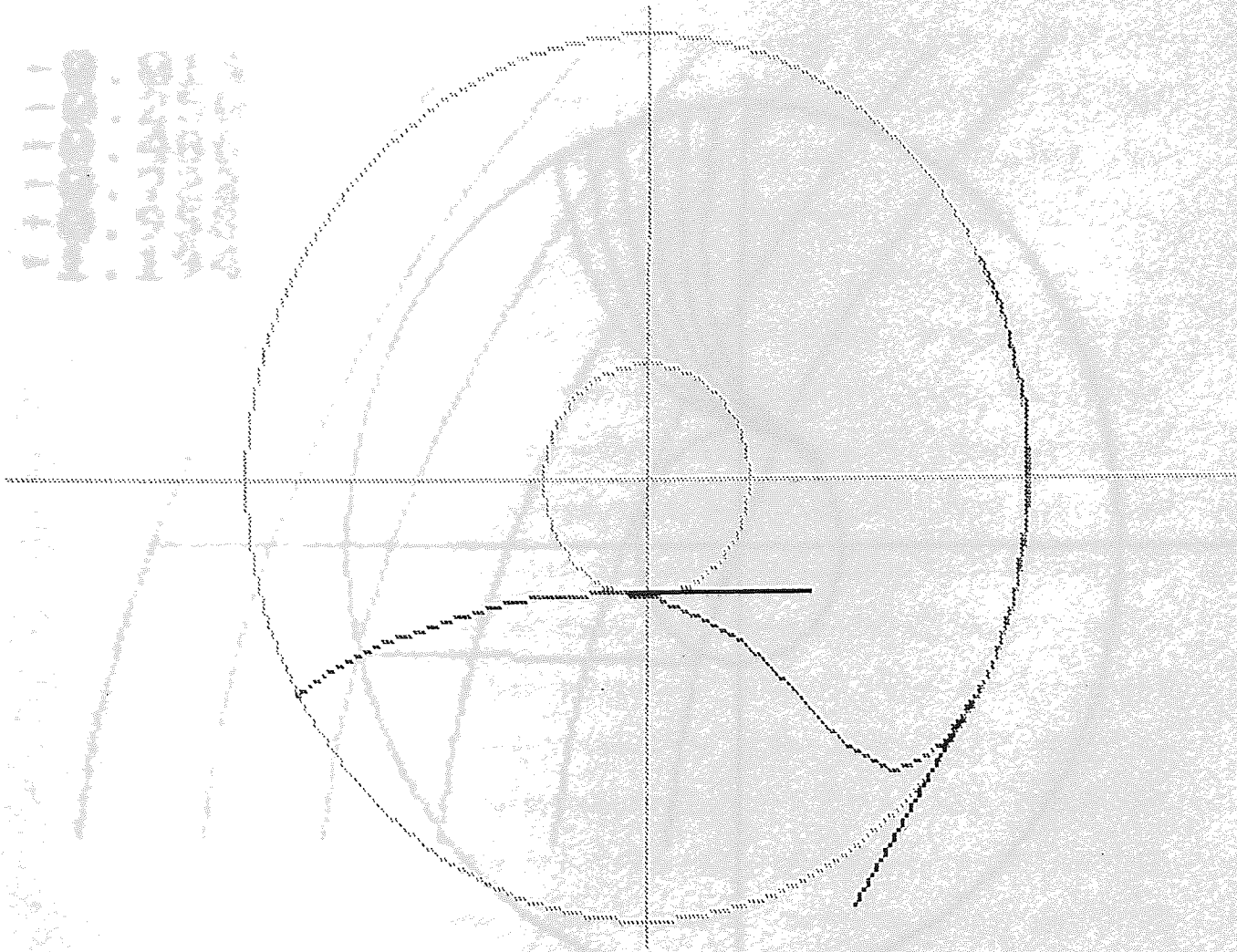


Figure 47 - Cubic Drill Flute

- 0.014
 - 0.250
 - 0.486
 - 0.722
 - 0.958
 - 1.194

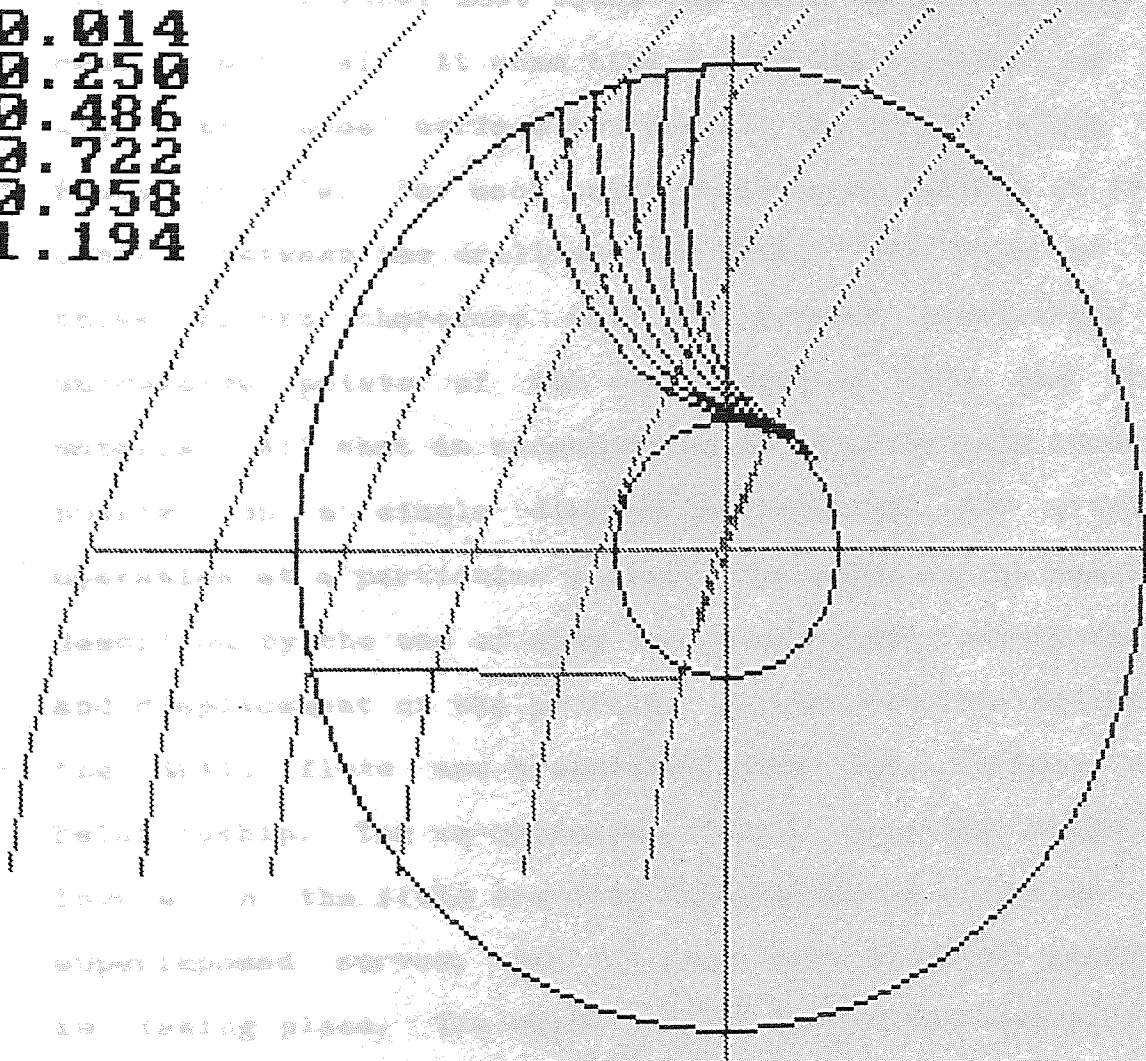


Figure 48 - Wu's Drill Point [3]

The flute shape has been fully described as a set of discrete points. An important industrial requirement is for this shape to be translated to describe the form of the milling cutter or grinding wheel required to generate it.

The grinding wheel must touch the flute surface in order to remove material. At some time during the passage of the wheel the wheel surface touches all the points along the flute profile. For each point there is an instant of final contact between the drill and the wheel. The locus of all these points therefore mark the extreme penetration of successive points of the wheel profile into the drill material. All that is necessary is to describe this locus of points on a single diagram so "freezing" the grinding operation at a particular instant. The shape of the wheel is described by the use of only two co-ordinates, namely radius and displacement of the profile. All the discrete points in the drill flute are translated into this 2-Dimensional relationship. The co-ordinates, (x,r) , over the range of levels in the flute are then represented as a series of superimposed curves, one for each level at which grinding is taking place. The wheel profile is the smallest profile contained within these curves. This is the profile required by the grinding wheel in order to just touch the discrete flute points at their individual deepest points of penetration into the drill material. The generated wheel profile confirms that the maximum depth point of the drill flute, corresponding to the drill webthickness, must be

created by the central and most extreme point of the grinding wheel. This point on the drill flute has been calculated as the radius and angle relative to the drill point where the local flute radius is a minimum. In the manufacturing process the drill flutes are ground before the point. This fluted blank is then held by stops in the flutes so creating the point and therefore the cutting lip at the correct angle relative to the flute form.

This calculation is achieved in the drill program by the generation of a set of flute profile points calculated over a range of z values, figure 49. This array of points is transformed by a matrix multiplication to produce the same set of points but reported in terms of a different co-ordinate axis system, figure 50. This new axis system is that of a suitably placed grinding wheel and is initially in terms of x, y and z. A grinding wheel only requires two co-ordinates to describe it, i.e., disk radius and position of this radius along the wheel axis. The position ordinate is equivalent to the x value, the radius ordinate is found from pythagoras, $\sqrt{y^2+z^2}$. Reducing x, y & z to x & r and plotting these two co-ordinates on the computer screen, for the range of flute levels, gives a series of curves, each corresponding to a different z level on the drill. These enclose the profile of the grinding wheel required to generate the required flute profile, figure 51. The usual problem with helical milling of interference is side stepped so long as the diagram is a progressive overlapping set of

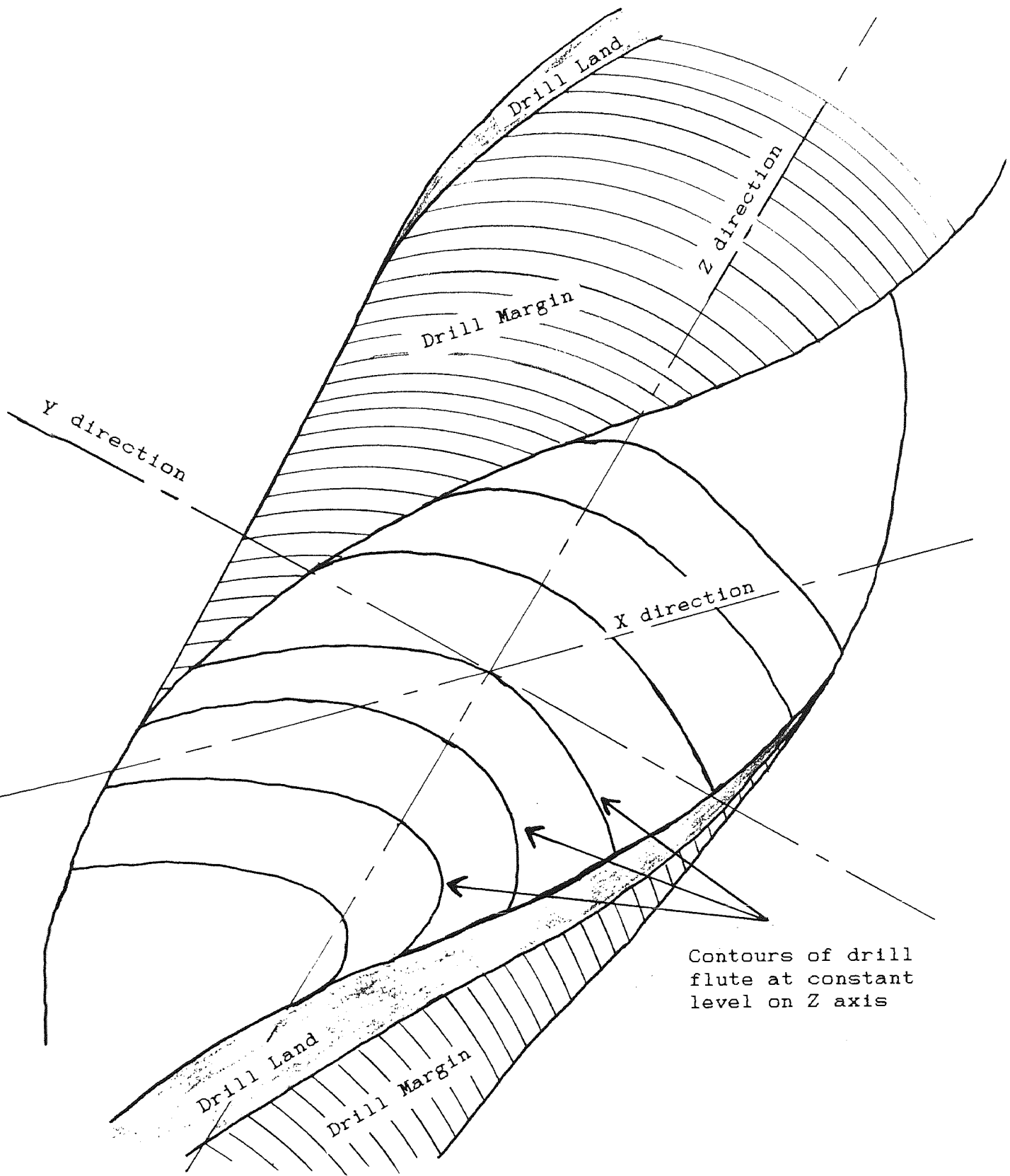


Figure 49 - Set of Drill Flute Data

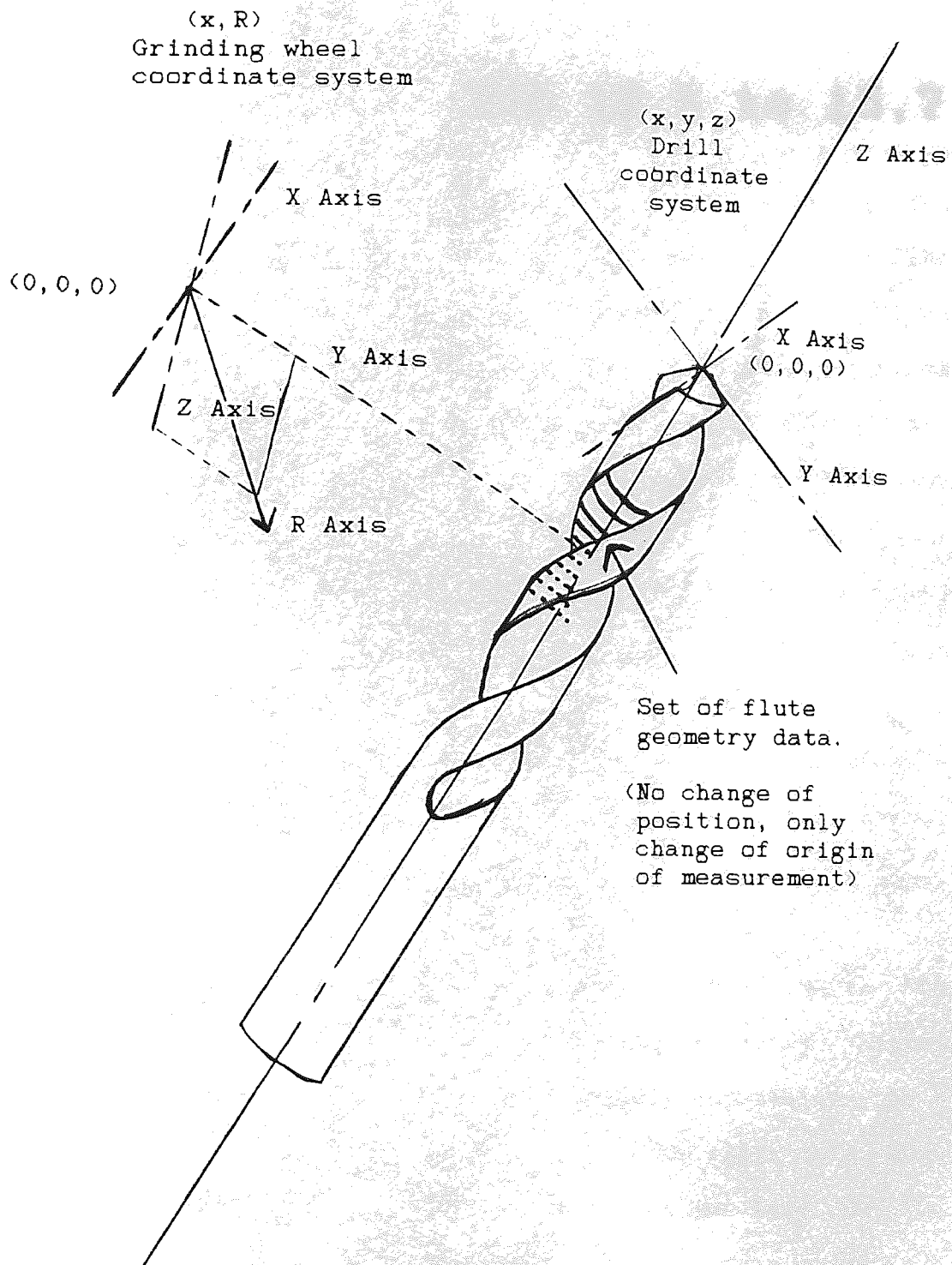


Figure 50 - Flute Data Change of Origin

curves. If however there is random overlapping of the curves then it may be inferred that the profile is not valid. In this case an offset greater than 4° may improve the situation.

As the program continues the following screens each give a histogram representation of some of the tool geometry for the 4.5mm example drill reported over the width of the cutting edge or lip of the drill. The latitude and longitude of the normal to the flank face plane are constant across the cutting edge and reported numerically. The latitude and longitude of the normal to the rake face are not constant and are reported graphically. Similarly Inclination Angle, sensitive to feed rate and as measured from the velocity vector, is displayed, figure 52. The tool wedge angle measured between the two face normals, figure 53. The rake angle and flank clearance angle in the plane normal to the cutting lip, figures 54 & 55. All drill geometry varies across the width of the cutting lip.

A second set of data is also generated referring to the chisel edge where the basic cutting geometry varies considerably, the velocity vector rapidly approaches the z axis as the radius approaches zero. Once again this huge fluctuation demonstrates the need to include feed in the analysis. On the chisel edge the rake and flank faces are both portions of the two conical drill point surfaces, situated immediately on either side of the chisel edge. The

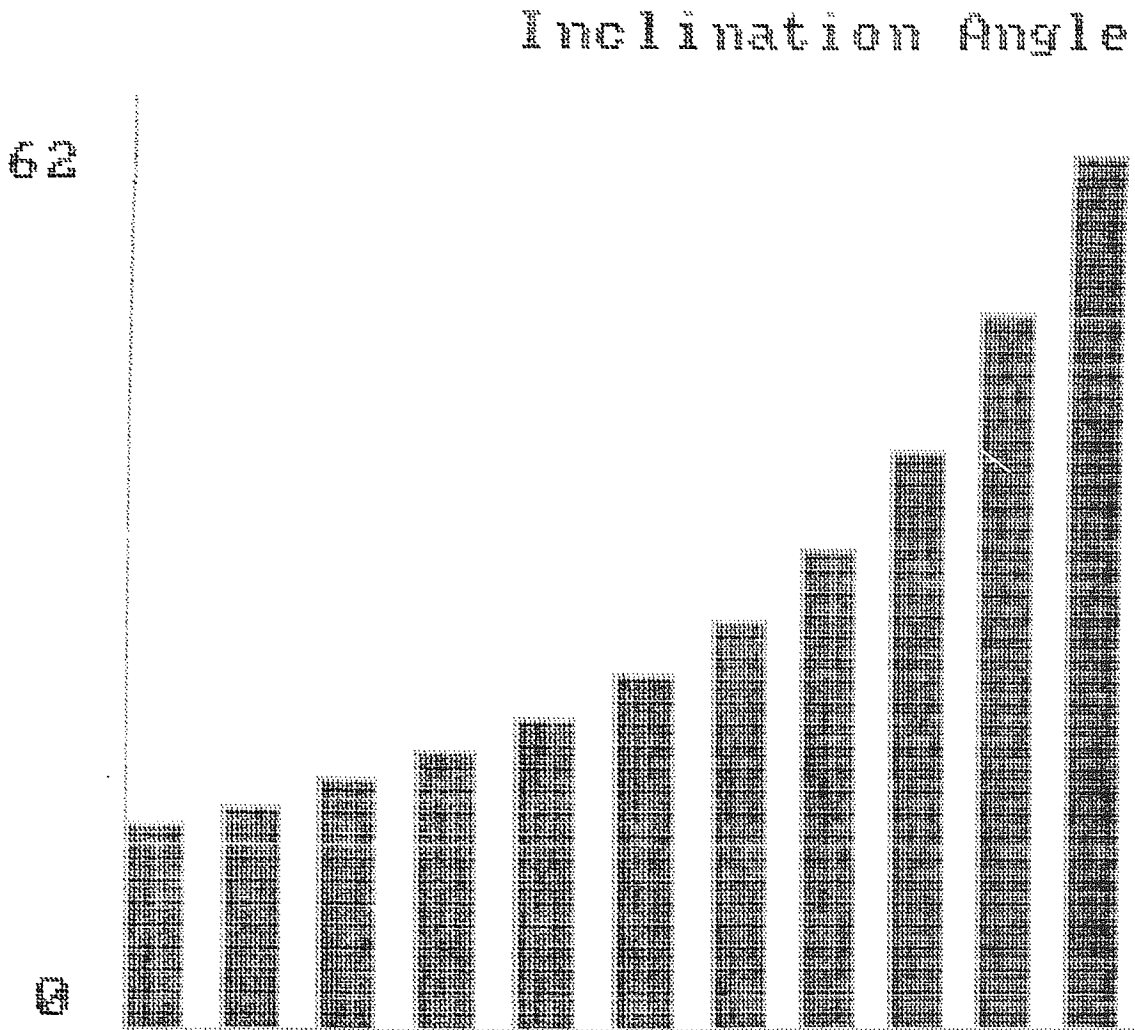


Figure 52

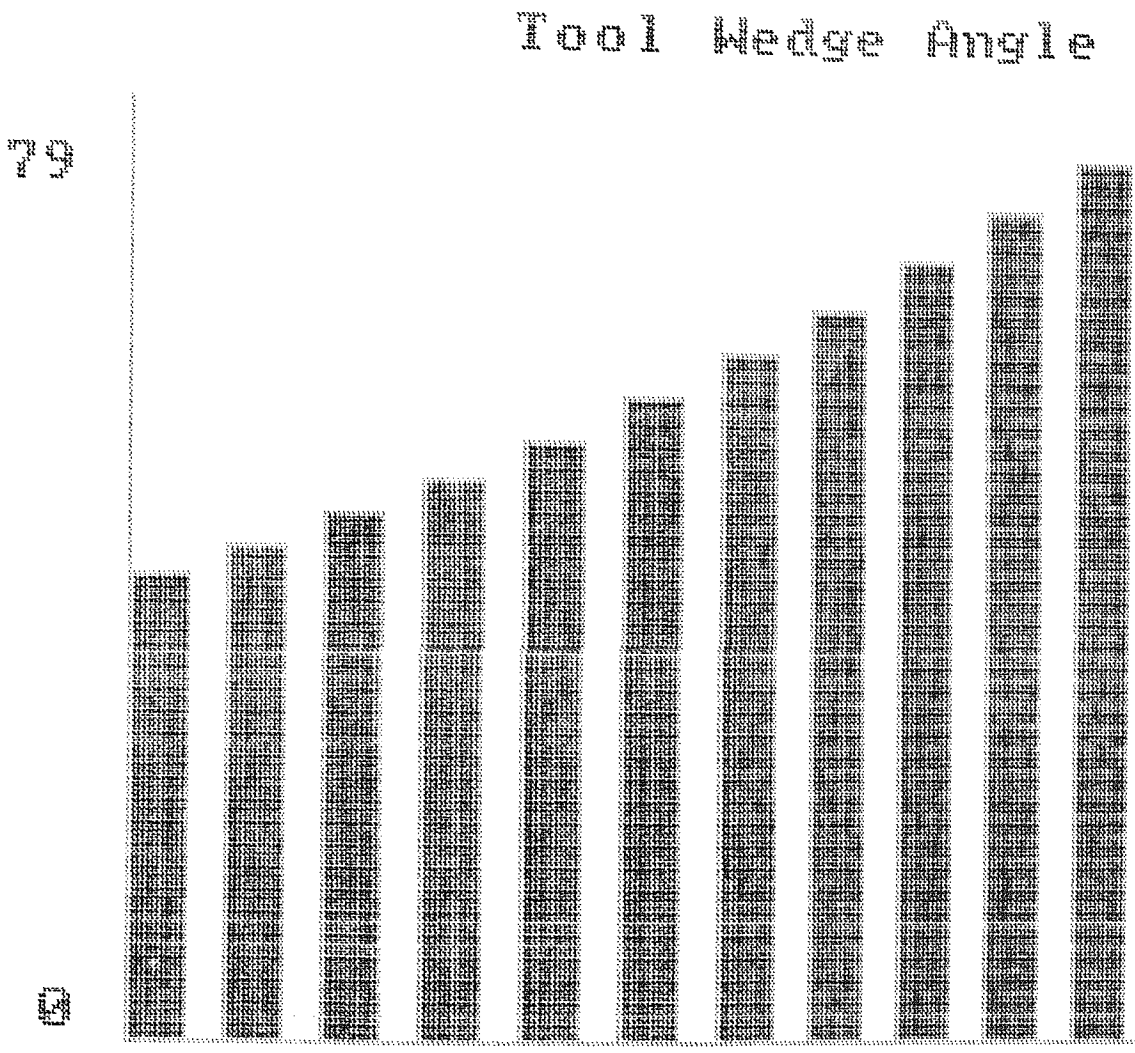


Figure 53

Rake Angle NORMAL

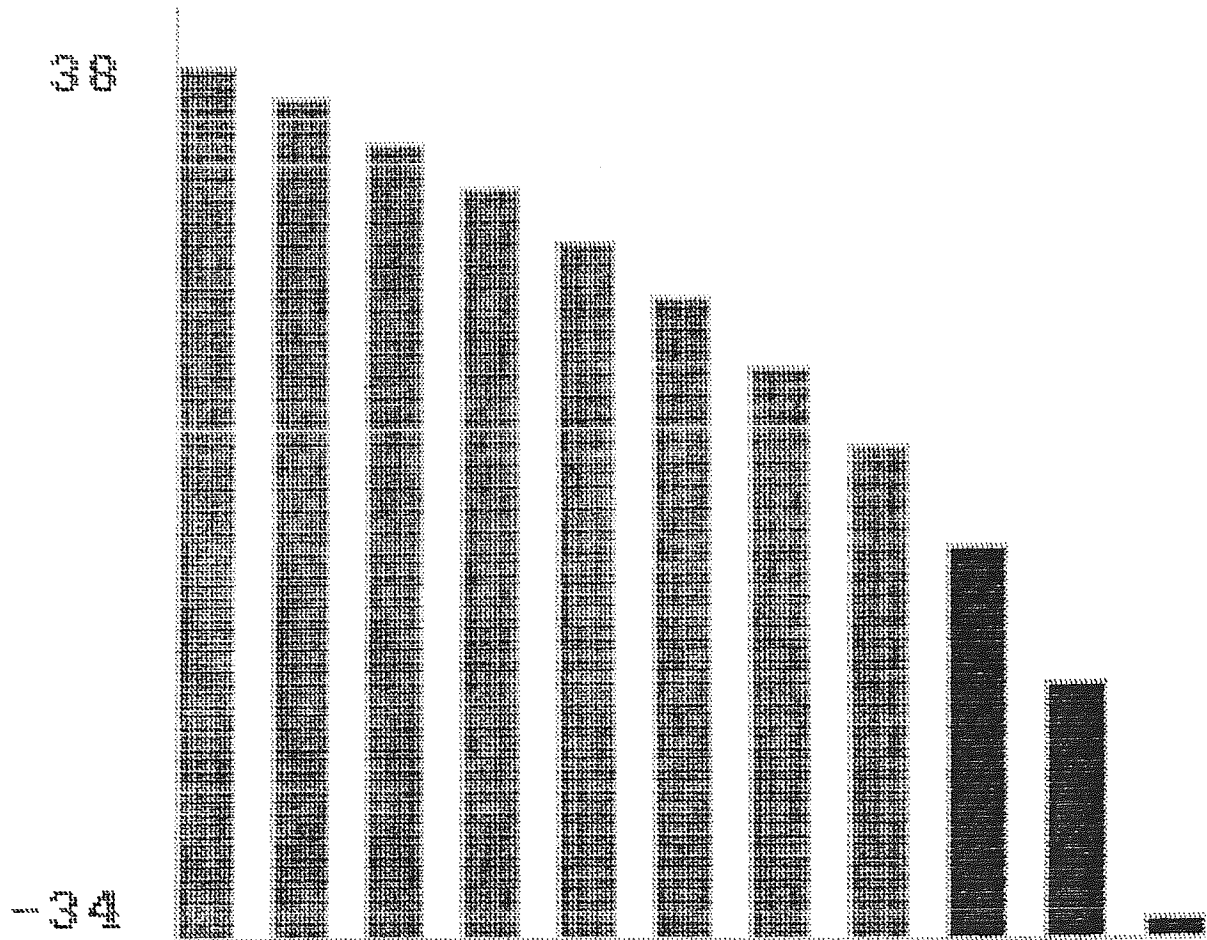


Figure 54

Mark Angle NORMAL

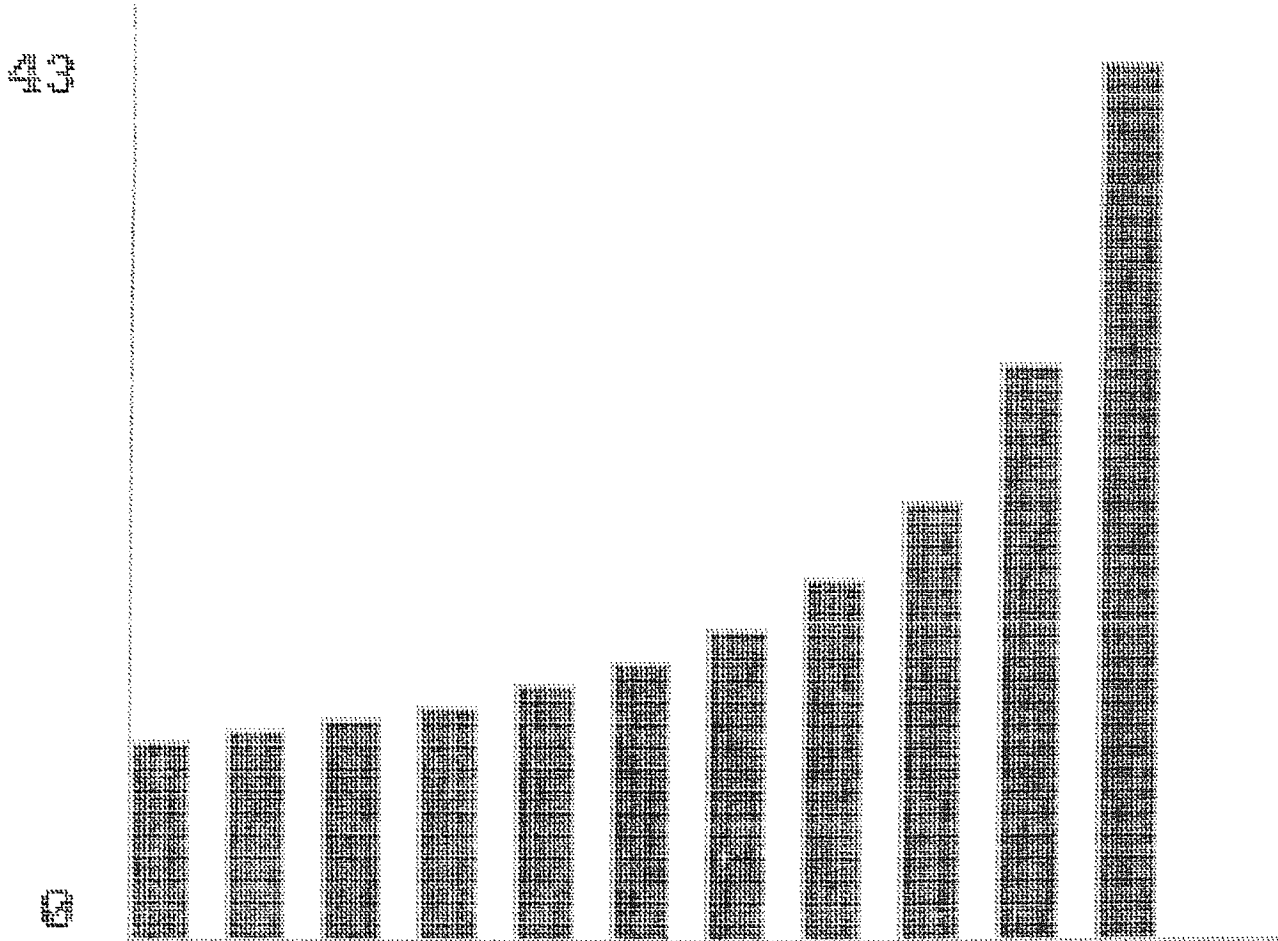


Figure 55

tool is cutting with negative rake angle and the clearance is also highly negative, figures 56-59.

The penultimate screen is a different display of the calculated inclination angle. According to Stabler's Law, [11], the inclination angle of the approaching workpiece material is equal to the inclination angle of the chip material as it moves away from the cutting edge. This allows an assessment to be made of the initial direction of flow of the chip material as it leaves the cutting edge, figure 60. The velocity of this movement is related to the velocity of approach, i.e., the magnitude of the velocity vector, and on the chip thickness ratio. The actual chip thickness ratio is unknown and will vary with the cutting conditions and across the cutting edge. The chip flow away from the cutting edge is plotted by vectors. The vectors originate from a line representing the cutting edge. The vectors are oriented by the individual inclination angles and are of a magnitude proportional to the velocity vectors. This flow is convergent but shows the initial direction and rate of travel of the chips in the flute. The subsequent flow induces curl due, first, to the curvature of the flute and, second, to the convergence of the flow and varying velocity profile across the width of the chip.

The chip flow data is also tabulated on the final screen. The direction of motion is three dimensional, the previous screen being an approximate two dimensional representation,

Chisel Inclination Angle

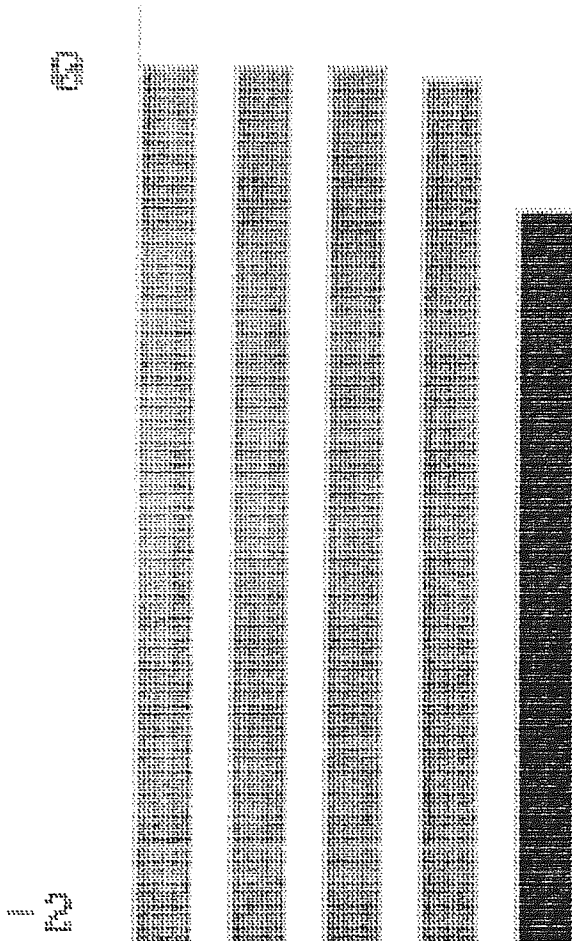


Figure 56

Crime Wave 1991

1991

5

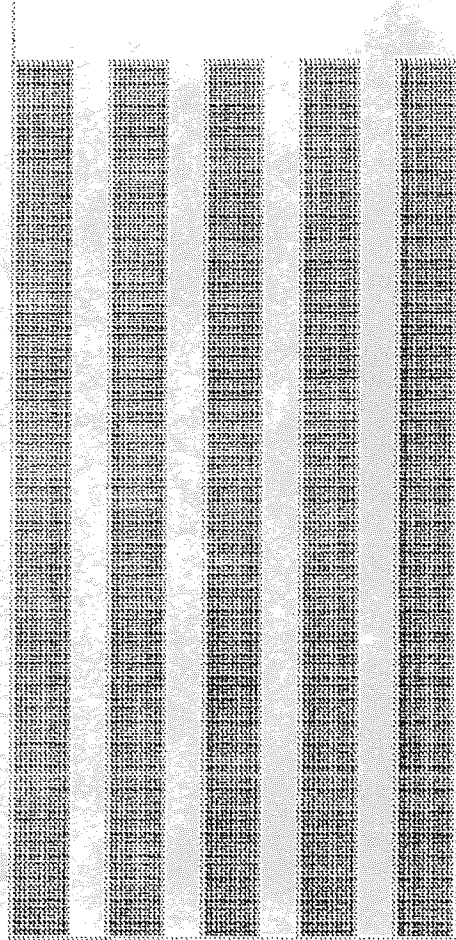


Figure 57

Chisel Blank Angle NORMAL

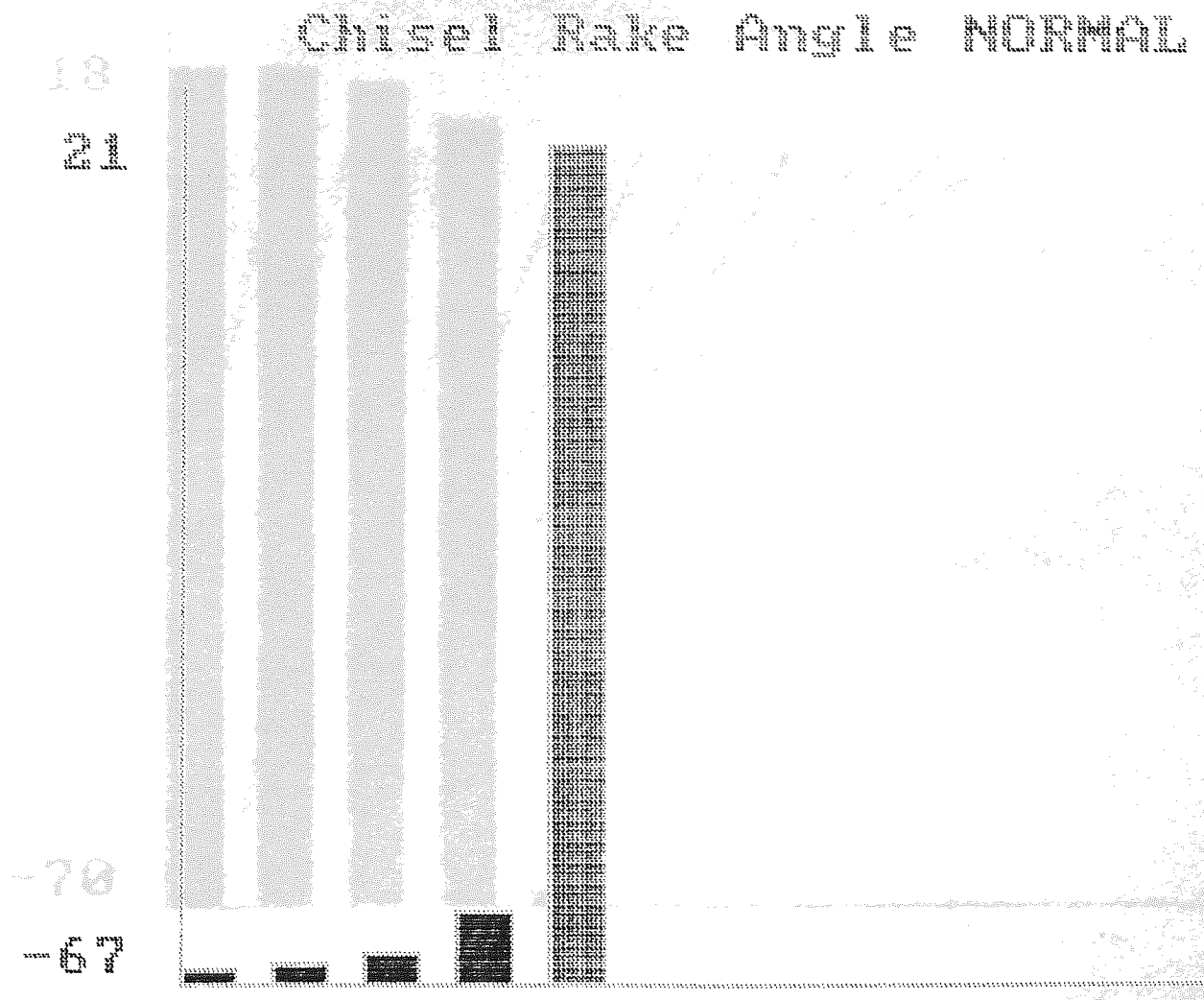


Figure 58

Chisel Flank Angle NORMAL

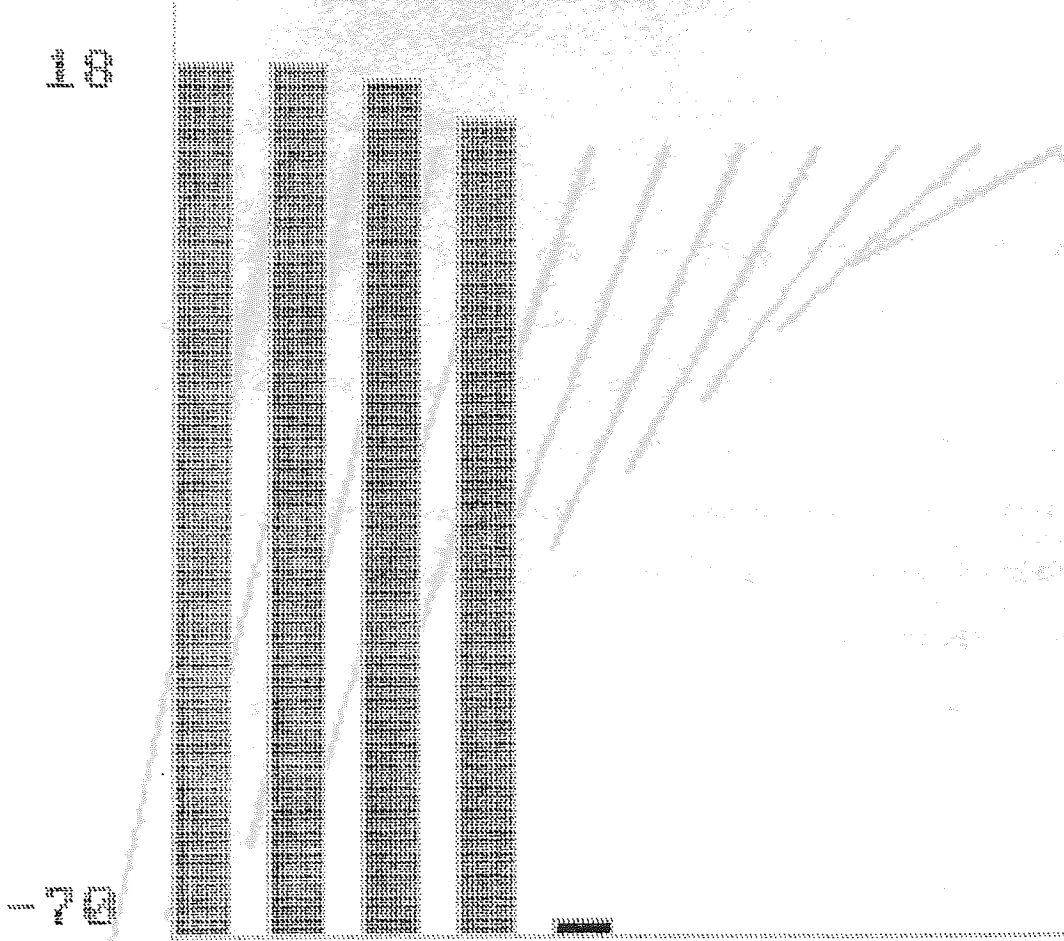


Figure 59

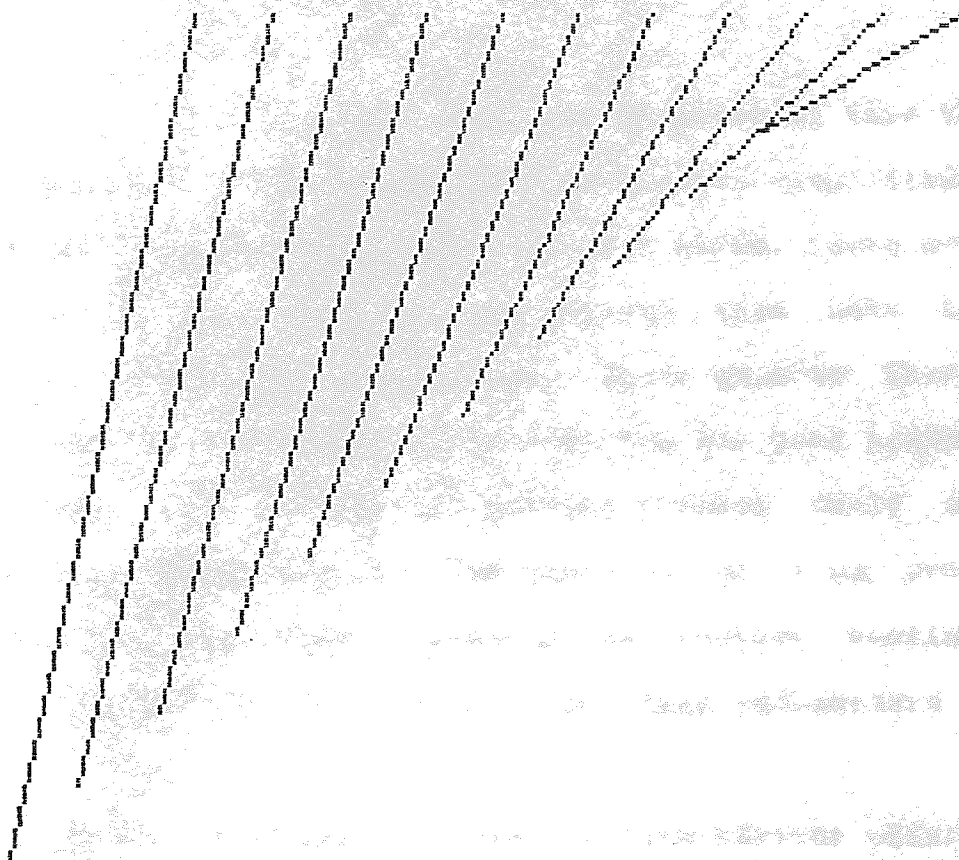


Figure 60 - Chip Flow 2-D Graphic Display

and is given in terms of spherical co-ordinates of the directions of initial chip material flow as it leaves the discrete points on the cutting edge. The spherical co-ordinates may just as easily be quoted as unit vector values in cartesian co-ordinates.

5.3. CONCLUSIONS.

Looked at in the correct way, as proposed by this thesis, the geometry of the twist drill is greatly simplified from the time consuming mathematics of past works. There are many aspects of the manufacturing process that have had no previous numerical explanation. These aspects have been developed by trial and error over the 130 year history of the drill. The fundamental cutting process could not be determined from any of the theories or from practical examination by time consuming destructive testing of individual drills, in anything other than rudimentary form.

The computer programs developed in this chapter offer both understanding of the manufacturing process by translating the generating parameters into equivalent drill forms and understanding of the cutting process by enumeration and display of the fundamental cutting geometry.

CHAPTER 6

	PAGE
6. VALIDATION OF THE METHOD	153
6.1. PUBLISHED DRILLING DATA	154
6.2. PROGRAM OUTPUT, BENEFITS AND FURTHER WORK	158
6.3. EXTENSION OF THE METHOD TO OTHER 3-D CUTTING TOOLS	163
6.4. CONCLUSIONS	166

6. VALIDATION OF THE METHOD.

The sort of drill geometry information contained in papers [2..5], although capable of describing limited aspects of drill geometry, involves complex mathematics. There are no simplified versions of these calculations, none have been attempted by any publications found while researching this thesis. The problem is exaggerated because so little true drill geometry information, either from measuring drills or produced by mathematical methods, has actually been published, nothing is presented by [2..5]. The drill details that have been published are almost invariably measurement of the drill geometric references, figure 7, which are orientated on the drill axis, as may be measured by the universal co-ordinate measuring machine. Past researchers have examined individual aspects of the drill and have compared their relative effects by attempting to alter only one individual aspect of this geometry. The general drill is, however, a complex permutation of half a dozen such geometric characteristics so making fundamental analysis by this method impossible.

The lack of published data and the lack of attempts to interpret the fundamental geometry is assumed to stem from the fact that the true geometry of the drill is hard to visualise and equally hard to determine with accuracy either mathematically or by measurement from real drills.

6.1. PUBLISHED DRILLING DATA.

The geometric references of the drill are reasonably straight forward to assess, given access to a suitable measuring machine. The measurement of a few further properties is possible, for example: Stabler [11] describes a method of measuring the flank clearance angle across the cutting edge by the use of optical sectioning. A shadow is cast across the flank face normal to the cutting edge and the clearance angle of the shadow measured with an optical device, figure 61. This angle may be reproduced by the drill program but it was not considered of value to include example data here.

Such skilled techniques are not possible, however, when used to assess the rake angle as the rake face is enclosed within the flute space. Oxford [17] produces a graph of drill rake angle but the method of obtaining this data is not explained. Here at Aston University the rake of one example drill was assessed by a destructive test, in the work by Upton [18]. A drill was ground with successive plane surfaces normal to the cutting edge. The rake angle was measured optically for each surface. This measuring of one drill took two days and required two men to complete, one man measuring and one man grinding. This measurement is however the 'tool rake', measured in the plane perpendicular to the cutting edge, rather than the true rake, measured from the velocity vector. The graphs of these two

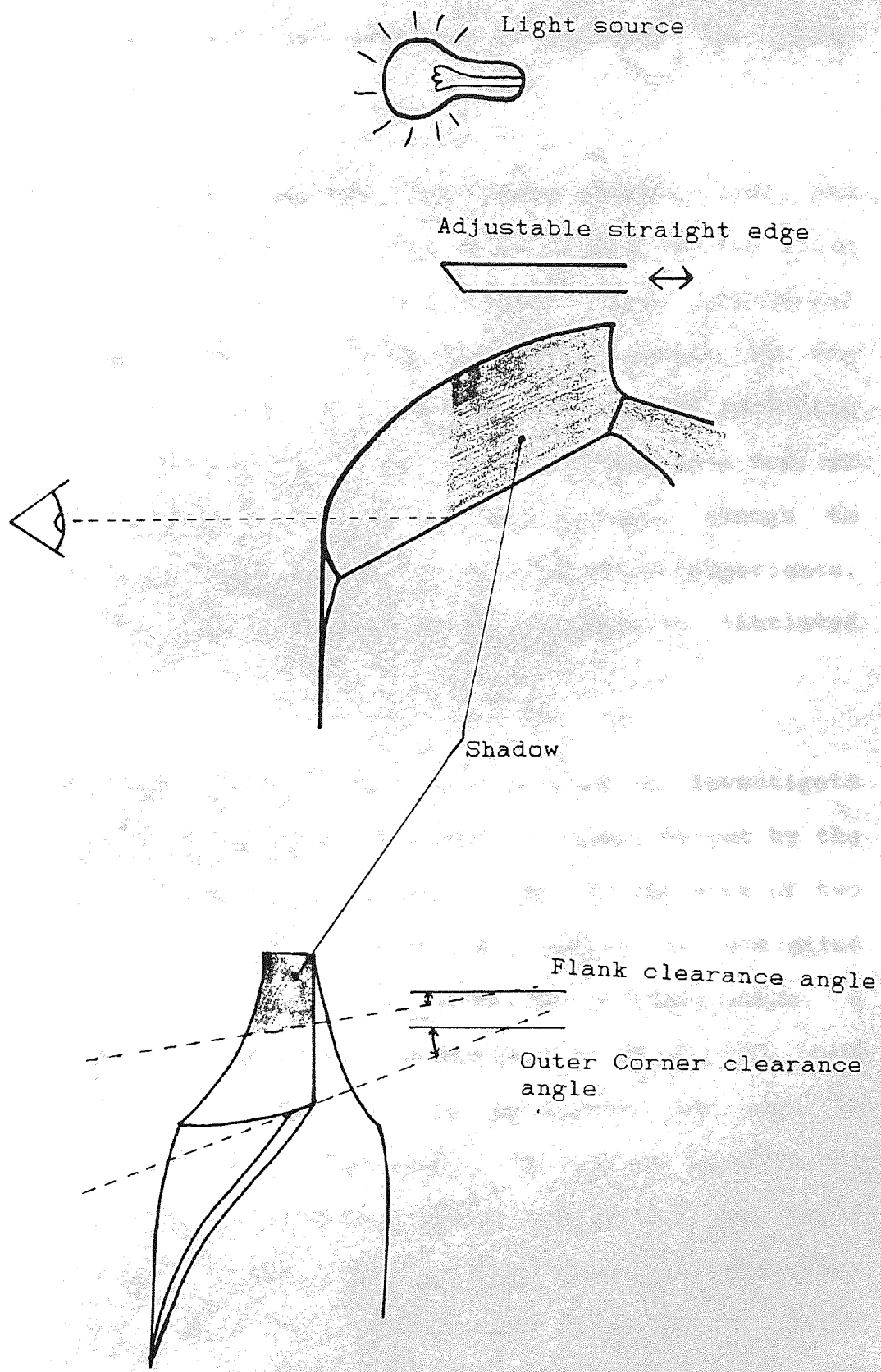


Figure 61 - Optical Sectioning

descriptions of the drill rake are reproduced at figure 62 together with equivalent values as produced by the Turbo Pascal program.

The required profile for the drill flute grinding wheel has been extensively studied, [5]. The relationship between flute shape and wheel shape is not direct. Some commercial computer based systems are available to assist in the selection of the correct grinding wheel profile by providing a solution to this relationship. These systems have not, as yet, proved themselves reliable and accurate enough to replace the historical method of trial and error/experience, (with the data from that experience available in tabulated form).

The Turbo Pascal program has also been used to investigate the flute grinding problem. The general shape output by the program may be simplified, on inspection, to the arcs of two circles, the parameters of which may easily be evaluated from the drill program's representation of wheel shape. A similar shape is suggested by Radhakrishnan et al, [5], and this is also the wheel profile definition as used in practice by drill manufacturers. A narrow profile is expected as the interference effect will widen the drill flute produced during the helical grinding operation. Radhakrishnan does not explain the problem of helix interference and how it is to be allowed for, he looks only at translating the cross section/orthogonal profile to a

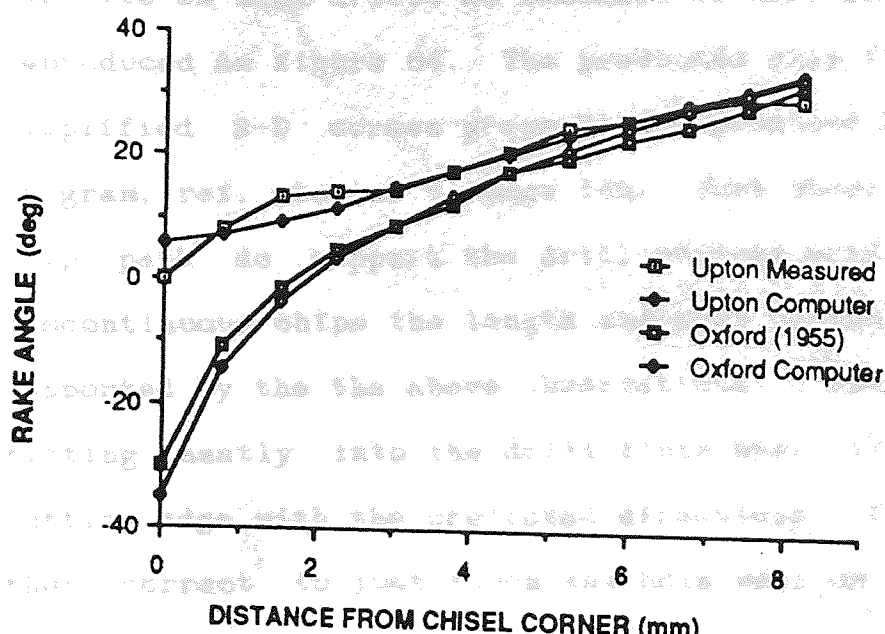


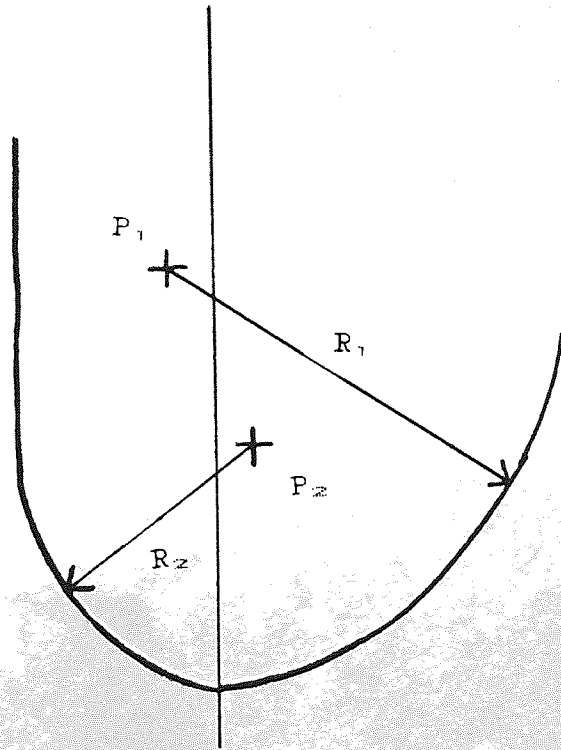
Figure 62 - Graph of Rake Angle [14]

profile across the line of the flute. The wheel profiles suggested by Radhakrishnan are generally wide while the profiles used in drill manufacturing industry are more similar to those produced by the TurboPascal program, figure 63.

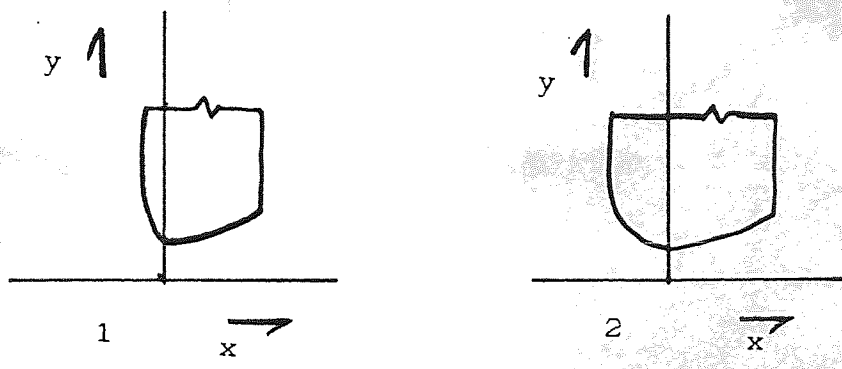
To provide supporting data for the accuracy of the chip flow predictions, it is possible to examine the workpiece deposits on used drills as sketched in Webb and Maiden [14], reproduced as figure 64. The predicted chip flows being the simplified 2-D screen presentation produced by the drill program, ref. chapter 5, page 145. Such observations of the chip path do support the drill program predictions. With discontinuous chips the length and curl of the chips is also supported by the the above observations. A single chip piece fitting neatly into the drill flute when alligned at the cutting edge with the predicted directions. The length is then correct to just touch the hole wall on the opposite side of the drill flute around which it must curl. Touching the far hole wall is assumed to be the chip breaking mechanism. Continuous chips display a helical curve that matches the drill flute perfectly, this curl is, obviously, no longer the initial curl predicted by the drill program.

6.2. PROGRAM OUTPUT, BENEFITS AND FURTHER WORK.

It is of value to summarise the output information generated by the computer programs:



DRILL PROGRAM



These wheels only produce the predicted flute shape over the cutting edge. The profile of the secondary or trailing half is uncontrolled.

Radhakrishanan [5]

Figure 63 - Grinding Wheel Profile

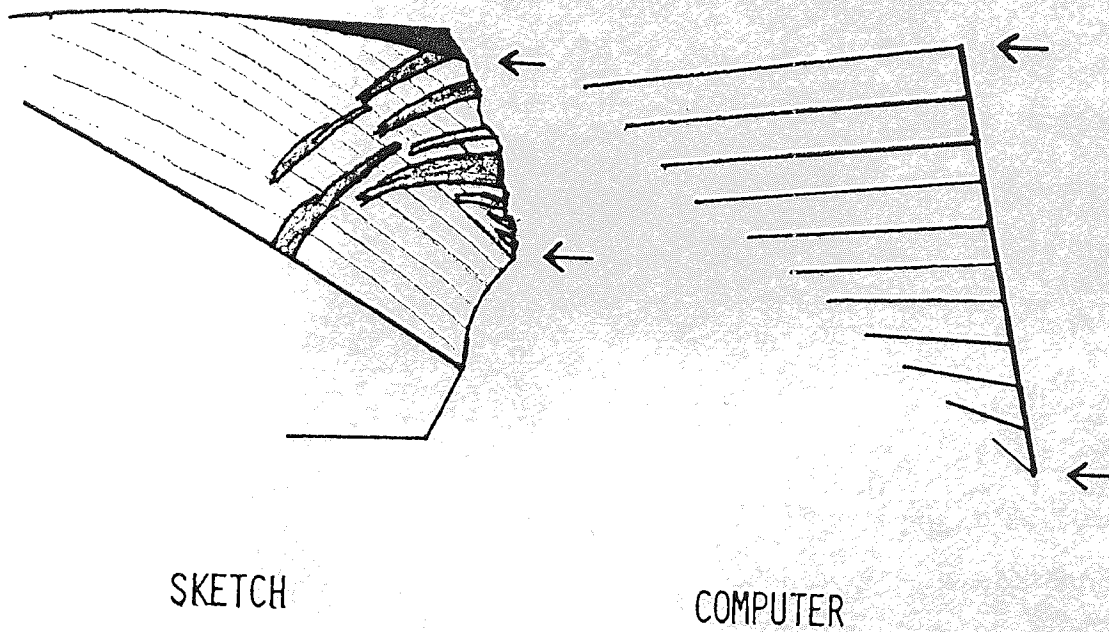


Figure 64 - Sketch vs Simple Computer Representation
of Chip Flow [14]

1. This work has described a method of mathematically defining the basic shape of a twist drill in terms that a computer can understand. This description is in terms of a solid model from which a mesh of co-ordinate data can be generated that details the tool surface. Secondary finishing operations are simply superimposed on this basic shape.

2. From the surface mesh data produced by the model, it is possible to determine the plane orientation of facets or elements of the tool surface. The relationship between this orientation and the incoming velocity vector of the workpiece determines the cutting geometry. This relationship is explored, for the first time, using a direct three dimensional approach.

3. In the geometric model the grinding parameters of the point grinding process are directly translated into the geometric references of the tool point by which drills are described. The helical flute grinding problem is explored, starting from the surface mesh data of the drill flute and producing the required shape of the grinding wheel, by a method that allows for the problem of interference.

It is the author's belief that none of these facilities have been satisfactorily explained or provided in any previously published works.

The logical next stage of the investigation would be two fold, looking first at the drilling forces and second at the drill wear. Further work is required looking at the metal cutting process in terms of the very high inclination and negative rake angles, as determined by the drill programs. Once these relationships are satisfactorily defined they may be slotted into the cutting geometry of the geometric model in order to provide calculations of cutting forces and tool wear rates. This is the means by which the machining data from geometrically more simple metal cutting operations may be utilised.

Geometric modelling or solid modelling is an established technique of three dimensional CAD. After the basic solids are defined within the CAD package the composite shape data may be further analysed by numerical analysis, such as FEA.

One basic CAD package was found unable to provide the cone orientation and helical sweeping required for the drill shape but the prototype programs have proved that the basic mathematics result in a usable drill model. This proof justifies the future use of a more advanced geometric modelling package. The complex shape of the drill could easily be created from it's solid geometry by a CAD system with sufficient capability.

Various forms of numerical analysis are tied to CAD systems and are available to the designer/user, Alternately

numerical analysis may be a separate program but use the same solid model source data or the same set of surface mesh data as produced by the CAD package. The application of numerical analysis to examine the stresses in the drill cross section is the subject of part two of this thesis.

6.3. EXTENSION OF THE METHOD TO OTHER 3-D CUTTING TOOLS.

May any tool be examined in terms of the manufacturing processes used to make it? The approach is applicable for any tool generated by manufacturing processes of known kinematics. Surface orientation data in the form of normal directions is then used to directly calculate the cutting action by the application of spherical trigonometry.

The drill is only one example of a situation where the planes of measurement of the various aspects of cutting geometry are constantly varying. Often with plane trigonometry the determination of the common plane is the most complex step. Each point across the cutting edge has its individual plane of measurement. The common plane depends on the individual situation and has in the past required simplifications, such as the ignoring of drill feed to maintain an artificially constant plane of measurement across the drill cutting edge. These limitations do not apply to a true 3-D method.

There would appear to be no limitation to the application of spherical trigonometry for the general evaluation of such complex three dimensional situations. The advantages of spherical trigonometry are many. Centred on any point it provides a direct method for the calculation of direction. The calculus does not address the aspect of material movement, the equations deal only with direction, however this is not a problem when looking at general material flow at a point as the flow speed and direction at that point are the important factors.

All the faces forming the cutting edges of a milling tool will be created by sweeping grinding motions in the same way as the formation of the drill point. All that is required is to identify the shapes involved. In general this is true of any tool produced by grinding operations. Tool grinding machines are becoming CNC controlled so that the geometry produced on the tool must be known and programmed prior to manufacture. Such geometric information is often 'thrown away' or 'commercially sensitive' and not passed on to the tool user. Once the surface mesh is established it does not matter how many different relative motion components are involved, spherical trigonometry allows direct and accurate calculation of the full cutting geometry with no compromise on planes of measurement.

The calculations predict the initial directions of chip flow. This motion should be designed to avoid interfering

with the cutting process. Drills, taps, and other such fluted tools are provided with flutes in order to allow space for the accumulation of chip material. Most other metal cutting processes are external. With external cutting the volume of chip material is not a limitation as it is generally carried away from the cutting region. Broaching is also an example where like drilling the volume of chip material removed by the process must be catered for by the 'flute space' of the tool design. In all these processes accurate knowledge of the cutting geometry is a valuable aid to good tool design and to the accurate prediction of tool cutting properties. It is very necessary to predict the cutting conditions when implementing modern CNC installations which are all expected to work without the guiding 'sensor' of a human operator.

The special requirement for the analysis of the chip flow away from the cutting edge and down the flute is, however, limited to drilling.

For best application into a general computer numerical analysis system the procedures for the application of spherical trigonometry must become standard matrix type calculations which are applied to vector like co-ordinates. The need for spherical co-ordinates of latitude and longitude would then be masked within these procedures. The advantages of spherical trigonometry for the direct calculation of cutting geometry in three dimensional tools

are too great for this method to be ignored.

6.4. CONCLUSIONS.

The first objective has been achieved in the form of a prototype computer based system. This system is a flexible computer program based on a geometric solid model of the standard twist drill form. The model is driven by just eight parameters and allows the evaluation of the fundamental cutting geometry.

Chapter 7
required
computer
which it
therefore

Chapter 8
been
extracted
there a

Chapter 9
The prototype computer system
ratio and
represents
both cross-sectional effects and longitudinal effects

Chapter 10
dynamic analysis. A simple
solution from the theory of vibrations of elastic bodies
proposed. The information generated is supporting
testing of drills.

The output of prototype computer system
coupled to a printer for display.

PART TWO

This section looks at the static and dynamic analysis of the drill as a flexible structure and how its behaviour is modified by the special shape.

Chapter 7 explores the foundations of the stress analysis required for this examination. A Finite Element Analysis computer system is found wanting in the flexibility with which it can be applied. An alternative system of finite difference equations provides the answer.

Chapter 8 explores the data created by this system. It has been suggested in the literature that such analysis was intractable. This chapter shows this not to be the case and offers a first attempt at solution.

Chapter 9 looks at the prototype computer systems for the static analysis and describes the total system. This represents a first attempt at a coherent system, including both cross sectional effects and longitudinal effects.

Chapter 10 looks at the dynamic analysis. A simplistic solution from the theory of vibration of elastic bodies is proposed. The information generated is supported by physical testing of drills.

The output of prototype computer programs has been 'screen dumped' to a printer for inclusion in the thesis.

	PAGE
7. DRILL RIGIDITY	169
7.1. DRILL STIFFNESS	169
7.2. THE ANALYSIS OF TORSION	171
7.2.1. CIRCULAR SECTIONS	172
7.2.2. NON-CIRCULAR SECTIONS	172
7.3. THE LONGITUDINAL EFFECT	177
7.4. THE DYNAMIC DRILLING MODEL	178
7.5. FINITE ELEMENT ANALYSIS	184
7.6. CONCLUSIONS	188

This chapter discusses the dynamic behaviour of the twist drill during drilling. It is shown that the dynamic behaviour of the twist drill is dependent on the stiffness and angular velocity of the drill. This research indicates that the dynamic behaviour of the twist drill is of an unstable nature, which is unique within metal cutting.

7.1. DRILL STIFFNESS

The angular velocity of the drill is denoted by ω . The stiffness of the drill is denoted by K . The dynamic behaviour of the twist drill is dependent on the stiffness and angular velocity of the drill.

7. DRILL RIGIDITY.

It has been usual in previous work to consider the drill as an essentially rigid object. This is not the case, in fact, and the second part of this thesis will deal with the drill as a flexible structure. The work is divided into consideration of both static response and dynamic response.

The static response is governed by the torsional stiffness which is dependent on the cross section of the fluted shaft of the drill. A rod of similar size to a twist drill, and made out of the same tool steel, has very little torsional flexibility. The fluted shape of the twist drill, however, allows substantial deformation of the drill shape for relatively low states of load. Once the static data is available, the dynamic behaviour may be investigated. The static response is only the mean response of a dynamic system. Dynamic distortion of the twist drill during the drilling process is dependent on the stiffness and also the angular inertia of the drill. This research further proposes that the dynamic behaviour of the twist drill is of an unstable nature, which is unique within metal cutting.

7.1. DRILL STIFFNESS.

The assumption of a rigid drill means that the cutting edges of the drill must exactly copy the motion of the drilling spindle. The introduction of three dimensional flexibility

converts the cutting process of the drill to one where the motion of the cutting edges is of cyclic variation, of continuous slowing down and speeding up of the cutting edge as the drill distorts. The practical effects of this drill flexibility have become common knowledge in manufacturing but no analytical answer has been put forward. The problem is to determine what are the important aspects of drill behaviour that are governed by drill stiffness.

Past research on stiffness has all been based on the behaviour of real drills as determined by various means of measurement, [7,8,9]. Statements have been made such as 'drill chatter is caused by drill flexibility effects'. It is well known that the stability of the cutting forces is improved with a shorter flute length drill. It is therefore important to understand this mechanism before one may attain equivalent stability from drills of longer flute length.

The drill structure has been described as 'flexible', but where the effects of the three dimensional distortions produced have not been examined. Rather the property is assumed related to flute length and is purely to be reduced as much as possible. With larger diameter drills the deformations involved are very small and it is easier to justify not considering the resulting distortion. However it will be demonstrated that with smaller diameter drills, e.g., 4.5mm, the three dimensional distortions present are of the same order as the chip thickness of the metal cutting

process. The three dimensional deformation of this drill is of fundamental importance to its performance.

What may be examined from the drill shaft in cross section? There are obvious cross sectional area differences between thick web and thin web drills which have been partially investigated by, for example Shaterin [7,8] and El-Wahib [15]. In [7,8] the drill webthickness is increased so increasing the tool stiffness. In [15] the effects of tool flexibility are simply assumed to become more prevalent with reduced cross sectional area. In both cases the length of the tool is not considered. Elementary solutions are provided which suggest a particular balance between tool flexibility and flute space, the philosophy being to maximise the twist drill stiffness by providing maximum cross sectional area.

7.2. THE ANALYSIS OF TORSION.

The twist drill is a shaft loaded in torsion. The external torque applied may be measured as: Torque $M(Nm) = \text{Force } F(N) \times \text{Distance } l(m)$. The torque is balanced by the internal property τ , the shearing stress on the transverse plane. Total torque is equal to the intergration:-

$$M = \int_{\text{area}} [\tau_{xy}x - \tau_{yx}y] dA$$

7.2.1. CIRCULAR SECTIONS.

The history of the analysis of torsion goes back to Coulomb, 1787, [19]. He developed the theory for circular cross section shafts which leads to the now common equation:-

$$\frac{\tau \text{ (shear stress)}}{\text{radius}} = \frac{G\theta}{\text{length}} = \frac{\text{Torque}}{\text{Polar 2nd Moment of Area}}$$

Tool steel is unlikely to fail by shear, as would a ductile material, on a transverse plane. A brittle material will fail in tension. Complex stress analysis in 2 dimensions states that the plane of maximum normal stress is orientated at 45° to the plane where the shear stress is at a maximum. This is demonstrated in the helical fracture at approximately 45° commonly seen in twist drills when a shear failure would give a fracture on a transverse plane. The numerical value of the maximum shear stress where normal stress is zero is equal to the numerical value of maximum normal stress where shear stress is zero measured on planes 45° to each other.

The maximum torque that the circular drill shank can withstand will always be greater than the maximum torque of the fluted drill shaft.

7.2.2. NON-CIRCULAR SECTIONS.

The early analysis works for circular shafts because the circular cross section is a special case of symmetry. Along

an axis of symmetry longitudinal displacement due to warping is not present and is therefore not present anywhere in the circular cross section. This necessary assumption is more usually quoted as 'plane sections at right angles to the shaft axis remain plane under the influence of torque'. Navier in 1864, [19], applied this analysis, erroneously, to shafts of non-circular cross section, and deduced that the maximum shearing stress occurred at the points most remote from the centroid of the cross section.

St. Venant [19] realised that the above assumption of plane sections remaining plane was false for the non-circular case. This can be demonstrated by visual inspection of a square rubber shaft. If a grid is drawn on the shaft surfaces and then the rubber shaft is twisted, the grid becomes distorted or warped out of the orthogonal plane. St Venant, in 1855, assumed that the distortion of a shaft due to torsion was divided between two mechanisms:-

1. Rotations of cross sections of the shaft as in the case for a circular shaft.
2. Warping of the cross sections, the shape of which is the same for all cross sections.

Therefore there is a displacement corresponding to rotation namely θ or (x, y) in the plane perpendicular to the shaft axis and a displacement corresponding to the warping namely (z) in the direction parallel to the shaft axis. The warping

displacement is zero on an axis of symmetry and varies + and - cyclically in the areas between such axis.

Mathematically it is possible to analyse the stress distribution over some geometric cross sections, a simple example being an ellipse. St Venant drew two basic conclusions for solid shafts from his investigations:-

1. For a given cross sectional area the circular shaft gives the largest torsional rigidity. For non-circular cross sections as the polar 2nd moment of area increases the torsional rigidity decreases. The following approximate formula is based on the elliptical cross section but has been found to be generally applicable for simple shapes:-

$$C \text{ (torsional rigidity)} = \frac{G \cdot (\text{area})^4}{4\pi^2 \cdot I_p}$$

2. The maximum stress in a solid cross section is found on the boundary, at the point(s) nearest to the centroid of the cross section. The point of highest stress will be in the line of the

Prandtl, in 1903, [19] introduced the concept of 'the stress function' to torsion. It is a function of x & y and describes the distribution of stress across the section. The use of the stress function is a convenient method for application to more complex shapes.

Navier's conclusion, in 1864, was that the maximum shearing stress occurs at the points most remote from the centroid of the cross section. St Venant corrected this error and was supported by Filon in 1900, [19] who investigated a circular shaft with a semi-circular groove cut from it. It is possible to solve the equation of this stress function mathematically, and therefore solve for the distribution of stress across this section by finding an equation to calculate the shear stress, figure 65.

The maximum shearing stress for the circular shaft is given by:-

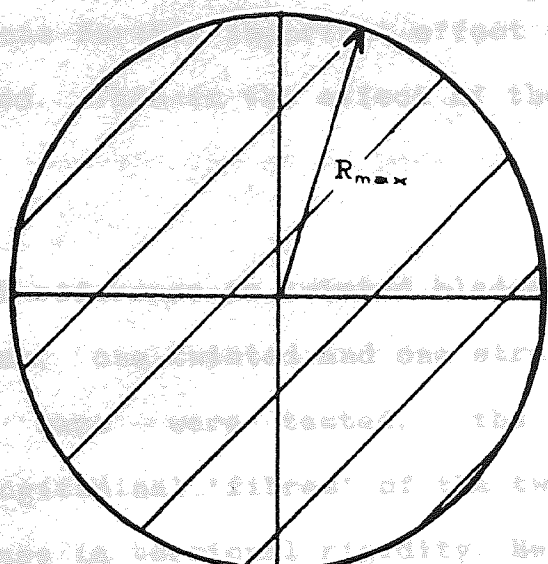
$$\tau_{\text{max}} = G\theta \cdot r_{\text{max}}$$

For point A at the base of the groove the maximum shearing stress is given by:-

$$\tau_{\text{max}} = G\theta \cdot (2a - b)$$

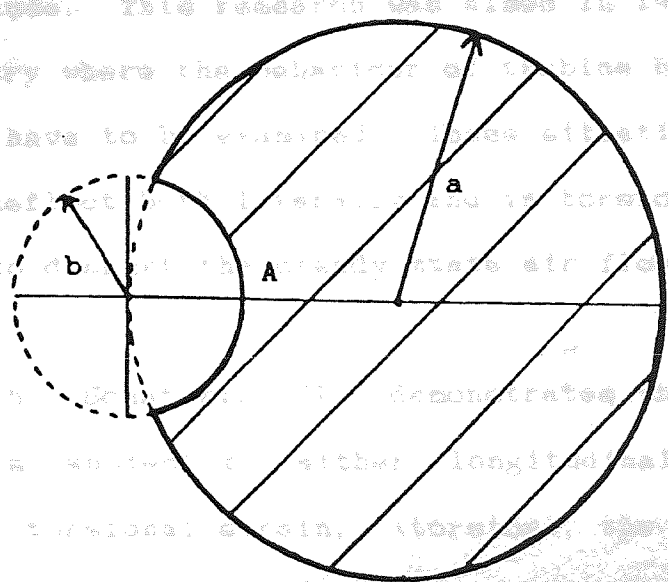
The above indicates that there is a distribution of stress across the cross section of a drill shaft and, firstly, there will be warping of the cross section, secondly, the point of highest stress will be in the base of the groove or flute, the point on the boundary closest to the centre of the shaft. The differential equations required for a similar mathematical solution in terms of a drill cross section with two grooves or flutes may, however, only be solved by numerical methods.

applied on the longitudinal strain across rotational shape
 (11) shaft (12) effect that has
 been multiplied (13) of the helical
 of the drill: (14)
 (15) (16) (17) (18) (19) (20) (21) (22) (23) (24) (25) (26) (27) (28) (29) (30) (31) (32) (33) (34) (35) (36) (37) (38) (39) (40) (41) (42) (43) (44) (45) (46) (47) (48) (49) (50) (51) (52) (53) (54) (55) (56) (57) (58) (59) (60) (61) (62) (63) (64) (65) (66) (67) (68) (69) (70) (71) (72) (73) (74) (75) (76) (77) (78) (79) (80) (81) (82) (83) (84) (85) (86) (87) (88) (89) (90) (91) (92) (93) (94) (95) (96) (97) (98) (99) (100)



Simple Circular Cross Section

equally applicable to (11), but is of
 small magnitude. This research was aimed in 1957 at the
 space industry where the behavior of turbine blades and
 engine wings have to be examined. These elements have
 ability to deflect (12) (13) (14) (15) (16) (17) (18) (19) (20) (21) (22) (23) (24) (25) (26) (27) (28) (29) (30) (31) (32) (33) (34) (35) (36) (37) (38) (39) (40) (41) (42) (43) (44) (45) (46) (47) (48) (49) (50) (51) (52) (53) (54) (55) (56) (57) (58) (59) (60) (61) (62) (63) (64) (65) (66) (67) (68) (69) (70) (71) (72) (73) (74) (75) (76) (77) (78) (79) (80) (81) (82) (83) (84) (85) (86) (87) (88) (89) (90) (91) (92) (93) (94) (95) (96) (97) (98) (99) (100)



Filon's Cross Section with Circular Notch

applied forces (11) (12) (13) (14) (15) (16) (17) (18) (19) (20) (21) (22) (23) (24) (25) (26) (27) (28) (29) (30) (31) (32) (33) (34) (35) (36) (37) (38) (39) (40) (41) (42) (43) (44) (45) (46) (47) (48) (49) (50) (51) (52) (53) (54) (55) (56) (57) (58) (59) (60) (61) (62) (63) (64) (65) (66) (67) (68) (69) (70) (71) (72) (73) (74) (75) (76) (77) (78) (79) (80) (81) (82) (83) (84) (85) (86) (87) (88) (89) (90) (91) (92) (93) (94) (95) (96) (97) (98) (99) (100)

Figure 65

7.3 THE LONGITUDINAL EFFECT.

Superimposed on the influence of the cross sectional shape of the drill shaft is one further important effect that has not yet been mentioned. This is the effect of the helical form of the drill.

Carnegie [20,21], with reference to twisted blades, showed that when two samples, one twisted and one straight, of rectangular section bars were tested, the helical orientation of the longitudinal 'fibres' of the twisted bar gives rise to an increase in torsional rigidity. He provides a mathematical formula to estimate the effect. This increase is equally applicable to the fluted twist drill, but it is of small magnitude. This research was aimed in 1957 at the aerospace industry where the behaviour of turbine blades and aeroplane wings have to be examined. These situations have the ability to deflect both laterally and in torsion, which effect is able to disrupt the steady state air flow.

Further research, Schaterin [7], demonstrates that if a fluted drill is subject to either longitudinal strain, (thrust), or to torsional strain, (torsion), the effect on the drill will not be restricted to deformation in line with that applied force. As the flute is a 'diagonal' member of the structure of the drill the two strains are interrelated. Longitudinal strain will also give rise to twisting and torsional strain will also give rise to change of length.

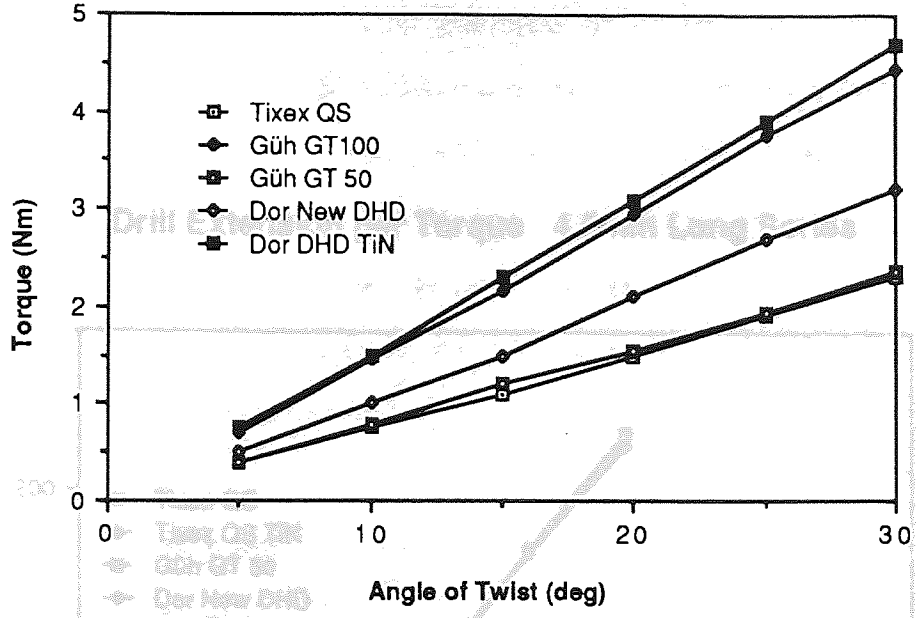
It is easy to measure this change in length against angle of twist which in turn may be measured against static torque. These relationships are linear, see figure 66 & 67 for 4.5mm drills, as measured by the author. Kirilenko [6] reports a mathematical attempt at analysis of this by using complicated factors to describe the cross section and helix.

The earliest references concerned with the measurement of tool flexibility for the twist drill are those of Schaterin [7,8]. In the first of the two papers Schaterin describes the measurement of flexibility in a 20mm diameter twist drill and attributes chatter vibration in drilling to this effect. The second paper measures the dynamic strain deformation of a drill at a variety of cutting speeds, feeds and states of wear. Schaterin's results indicate a relationship between the frequency and amplitude of the vibration and tool life.

7.4. THE DYNAMIC DRILLING MODEL.

All the work in the area of drill flexibility has looked at specific drills and drilling situations. The effects of variation of the drill shape and structure only being investigated by practical experiment, with the influences being inferred. A simple dynamic drilling model is proposed which can be reduced to a two dimensional diagram. The diagram, figure 68, consists of a representative section of the drill structure. The section is produced by

Drill Torque Test 4.5mm Long Series



Drill Twisting 4.5mm Long Series

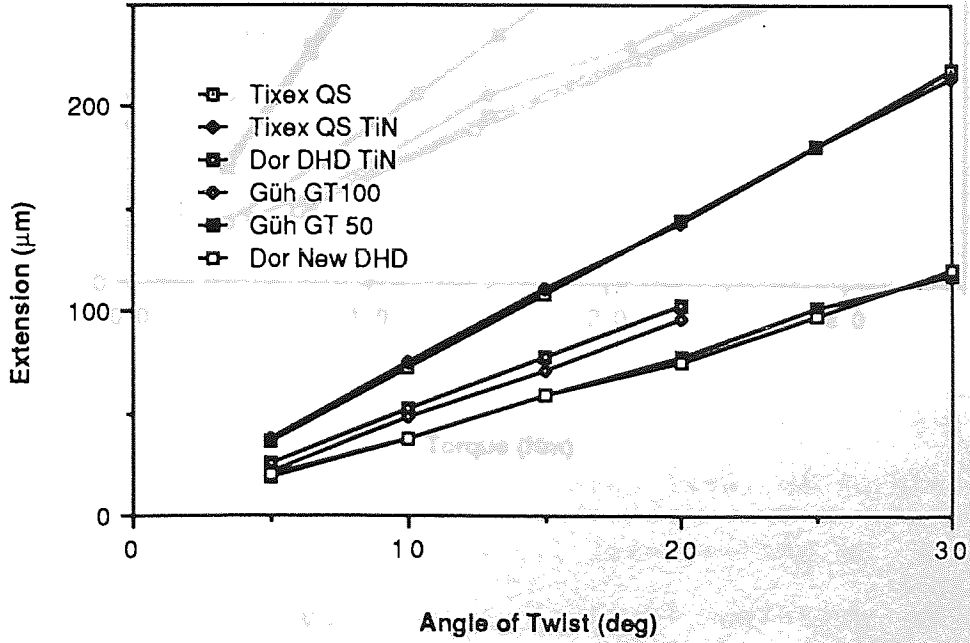


Figure 66 Graphs of Drill Torque Test and Drill Twisting

Drill Extension per Torque 4.5mm Long Series

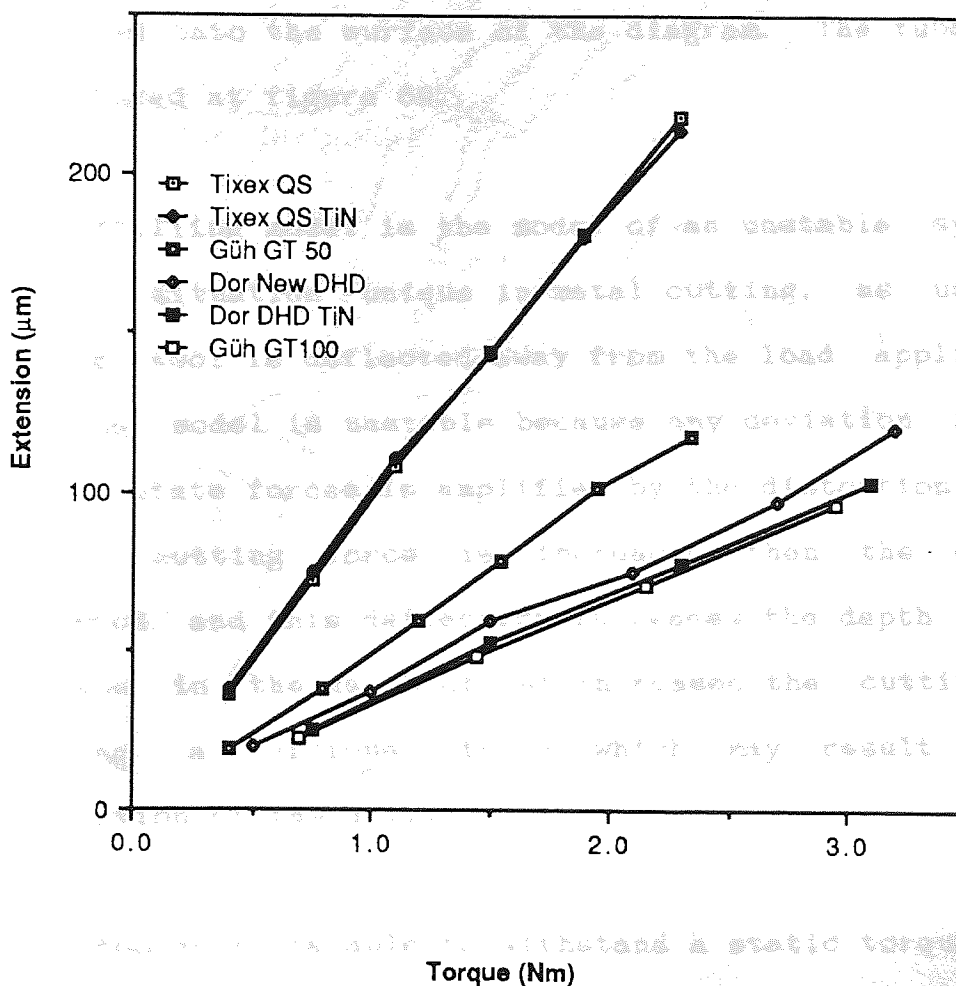


Figure 67 Graph of Drill Extension per Torque

superimposing a co-axial cylinder on the drill with radius between that of the drill outer corner and that of the drill chisel corner. The spiral section of drill is the intersection between the surface of this cylinder and the drill material. This intersection is superimposed onto the surface of this cylinder and is then very similar to the helical strips of cardboard that make up the cardboard tube from the centre of a paper roll. The section is then un-rolled onto the surface of the diagram. The tube section is pictured at figure 69.

This drilling model is the model of an unstable system. A dynamic situation unique in metal cutting, as usually a cutting tool is deflected away from the load applied. The drilling model is unstable because any deviation from the steady state forces is amplified by the distortion induced. If the cutting force is increased then the drill is deflected and this deflection increases the depth of cut. Increase in the depth of cut increases the cutting force creating a vicious circle which may result in the destruction of the drill.

The 4.5mm drill is able to withstand a static torque loading of 6 Nm before failure. The general level of torque that has been measured in standard drill life testing is 0.5 - 1 Nm. At this level of torque, a small variation of cutting torque, of 10-20% or 0.1Nm, will result in deformations of equivalent magnitude to the chip thickness, or depth of cut.

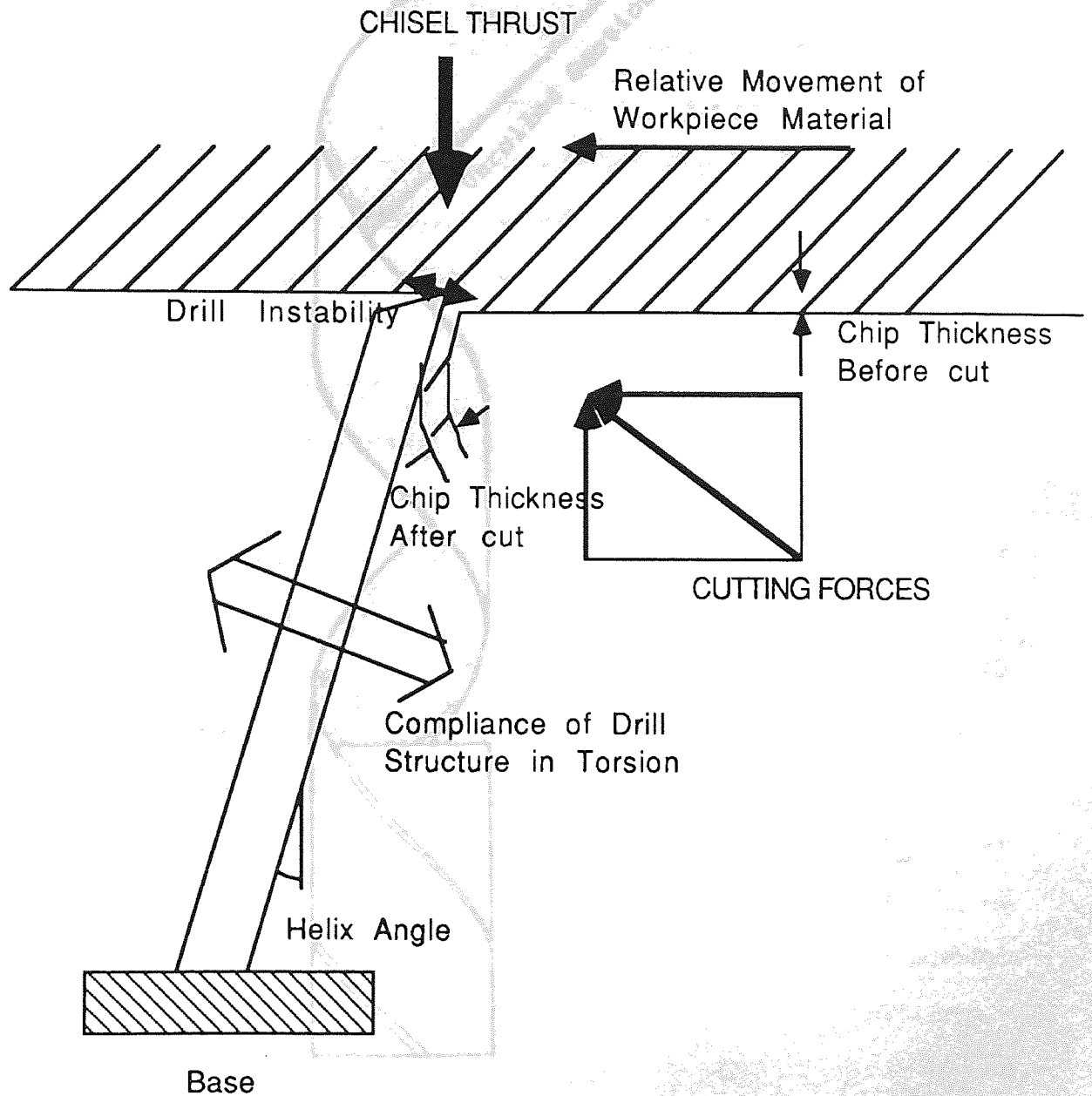


Figure 68 - Dynamic drilling Model

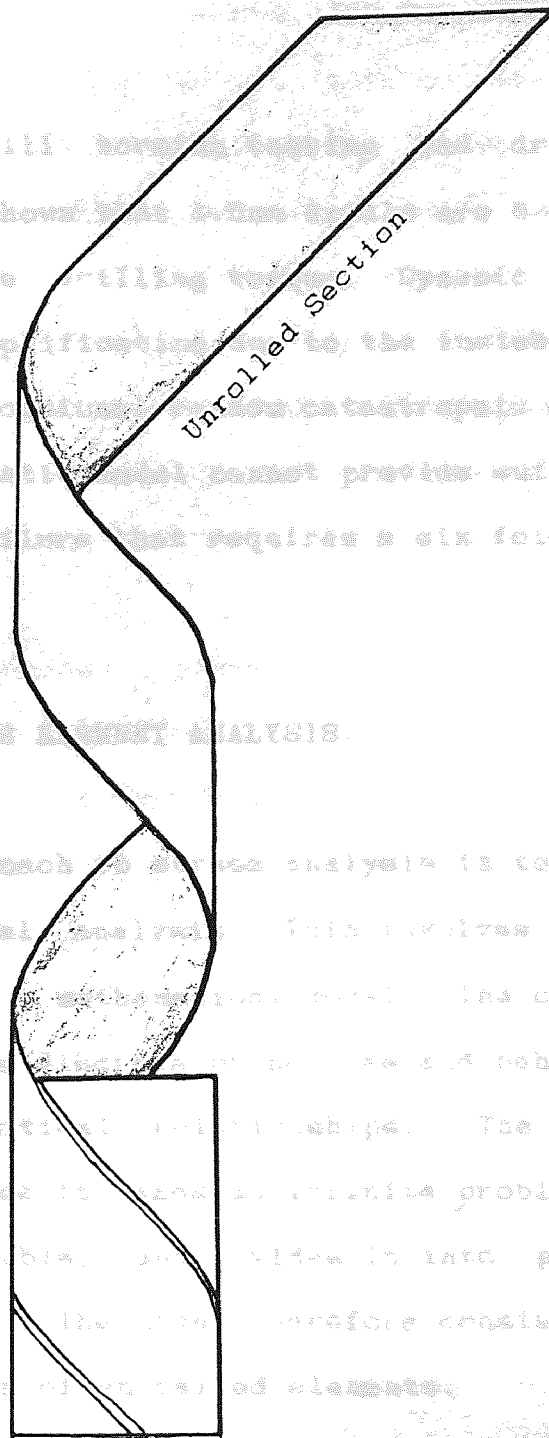


Figure 69 - Helical Tube

These variations may not, therefore, be dismissed as irrelevant.

In this way drill torsion testing and drilling torque measurement has shown that 4.5mm drills are 6 times stronger than the average drilling torque. Dynamic variation, or rather dynamic amplification due to the instability, is able to explain the occasional random catastrophic failure of the twist drill. A static model cannot provide sufficient reason to justify a failure that requires a six fold increase in the torque.

7.5. FINITE ELEMENT ANALYSIS.

The modern approach to stress analysis is to make use of computer numerical analysis. This involves representing a real system with a mathematical model. The component parts of the model have discrete properties and behave according to known mathematical relationships. The process is successful because it takes an infinite problem, which is inherently insoluble, and divides it into parts each of which are soluble. The model therefore consists of a number of building blocks often called elements.

Generally the mathematical analysis is based on matrix manipulation. For example, Finite Element Analysis of a structure can provide numerical data on the distribution of stress within that structure. The behaviour of individual

elements are modelled by equations. These equations are inserted as the rows of a matrix. The matrix then models the behaviour of the whole structure. An approximate solution is available for each individual block, as influenced by the input forces and by interaction with its neighbours. Matching co-ordinates of adjoining blocks are constrained to move in unison and in this way the stress distribution of any cross section may be built up. The sum of the elements models the whole. The matrix manipulations are performed by a computer, using numerical methods.

The use of an established system for numerical analysis such as PAFEC was the first choice for looking at the drill. Although some facilities are available for looking at prismatic shafts in section, a twisted cross section may not be examined in the same way. PAFEC was discounted for two major reasons:-

- i, The most complex 3-D element is required to model a twisted shaft. Three dimensional elements require substantial processing and this processing would be time consuming on any CAD / Numerical Analysis workstation and may even require the power of a mainframe computer system to provide an answer within a reasonable time. It is necessary to weigh this time and cost against any possible benefit. Also the co-ordinates of each node of the elements would require individual evaluation. Even with computer assistance

this is a substantial exercise.

- ii, It would be difficult to load the combined system. There are two distributed loads, thrust plus limited torque over the chisel edge, and torque plus limited thrust over the cutting edges. These loads are three dimensional, applying force from a variety of different directions. The directions must also be made to rotate with the drill point as any twisting distortion is introduced.

These problems may not be as difficult to solve when using a more expensive package, for example one able to look at the flexure and twisting of aeroplane wings.

Chandrupatlia and Webster [10] provide a simplistic attempt to get round these two problems. Their paper examines the deformation present in a twist drill by the use of FEA.

They solve the first problem of the substantial processing time by the simplicity of the three dimensional model. The time is dependent on two factors, one, the complexity of the element blocks used which must be 3 dimensional 20 node bricks, two, the number of elements required. In its simplest form the whole of the end of the twist drill may be modelled by a pair of suitably shaped blocks, only one of which needs to be calculated. They describe how a standard set of simplified co-ordinate values are pre-calculated and

programmed into the FEA analysis as a set of numerical data. The ease of varying this set of co-ordinates is restricted.

The second problem is that of loading the system in a manner that is faithful to the real situation. There are two loadings in drilling, one on the chisel and one on the cutting edge. In this paper the chisel loading is ignored totally. The cutting edge loading is assumed to be purely torque and is divided into three couples applied as forces to the three nodes of the edge of the brick that models the drill cutting edge, this load would be balanced by an equivalent load on the cutting edge of the other brick.

The FEA output is a series of graphs. These deformation / force diagrams all display a strong curvature. The available literature indicates linear relationships. This discrepancy in the reported data stems from a simple acceptance of the data as produced by the model. The accuracy of any FEA program may not be assumed and the nodal values are known to be the points within a FEA structure where the calculated stress function is least accurate. For each element within the FEA, the stress function is a simplified approximation which is assumed to hold across the whole of that element. The simplification gives rise to discrepancies especially at the extremities or nodes of the element.

7.6. CONCLUSIONS.

Dynamic evaluation of the shape of the twist drill has received virtually no attention in the literature. The drill is a highly flexible object and if looked at as such, it is easier to understand many of the confusing aspects of its behaviour.

The proposed dynamic drilling model describes drilling as a unique process among the various forms of metal cutting. It is normal for a tool to be deflected away from the workpiece with increased cutting load. Drilling is the only form of basic metal cutting where the tool deforms into the workpiece as the cutting load is increased. No such basic description of the drill has been found anywhere in the literature.

CHAPTER 8

	PAGE
8. STRESS ANALYSIS	190
8.1. FINITE DIFFERENCE ANALYSIS OF TORSION	190
8.2. ANALYSIS OF LONGITUDINAL STRAIN BY FINITE DIFFERENCE EQUATIONS	202
8.3. CONCLUSIONS	206

8. STRESS ANALYSIS BY NUMERICAL APPROXIMATION.

As stated in the last chapter finite element analysis would be a convenient and direct, three dimensional method of analysis. It is important to allow for three dimensions because, in obtaining the solution, every cross section of the drill must be allowed to warp, i.e. sections must not be constrained to a single plane. Any two dimensional model must therefore encompass the three dimensional nature of the problem.

8.1. FINITE DIFFERENCE ANALYSIS OF TORSION.

Looking first at the development of stress analysis in general, before the evolution of numerical techniques, the evaluation of non circular sections was restricted to special mathematical sections such as the ellipse. In order to progress, various models of the stress function distribution were devised which could be used for more complex cross sectional shapes. These models led to applications which could take advantage of numerical methods. One successful model was the 'Membrane Analogy' which was introduced by Griffith and Taylor in 1917 [19]. Here the Prandtl stress function surface is modelled by a soap film stretched across an opening cut to match the shape of the shaft in cross section. This is a physical technique which was applied to the drill cross section by Neubauer and Boston [22]. Torsion is simulated by the application of a

small pressure difference across the membrane where:-

1. Torque applied $\equiv 2 \times$ volume displaced by the membrane
2. Shearing stress \equiv slope of the membrane

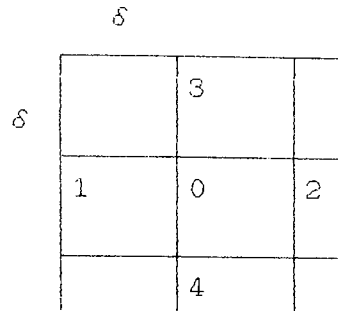
It is possible to mathematically model the deflection of such a soap film. One numerical solution, which predates the computer, is the application of finite difference equations to the solution of the film deflection. It is an iteration system, performed by hand, and may be applied to non-mathematical cross sections. The method is described in Timoshenko and Goodier's reference book [19].

In the finite difference method the equations are applied across a mesh in a similar way to modern FEA. This research has applied the method within the medium of a SuperCal 4 spreadsheet. The spreadsheet allows rapid performance of iteration calculations and gives a quick and accurate numerical evaluation of the stress function distribution.

The torsion 'stress theory' equation is as below:-

$$\frac{\partial^2 \theta}{\partial x^2} + \frac{\partial^2 \theta}{\partial y^2} = -2G\theta$$

Where θ is the stress function, θ is the angle of twist per unit length of the bar and G is the modulus of shear. For a square mesh the finite difference equation is the alternative solution and is:-



Square Mesh

$$\frac{1}{\delta^2} (\phi_1 + \phi_2 + \phi_3 + \phi_4 - 4.\phi_0) = -2G\theta$$

Finite Difference Equation

This is a simple numerical evaluation of the second differential about one central point, P_0 , in the directions of the two co-ordinate (nodal) axes, x & y . Any torsional problem is reduced to finding the set of numerical values which satisfy this finite difference equation at every nodal point within the mesh and become a constant value at the boundary.

To apply this finite difference equation to the SuperCal 4 spreadsheet, first the value of $2G\theta\delta^2$ is assumed at 1000. The finite difference equation then becomes:-

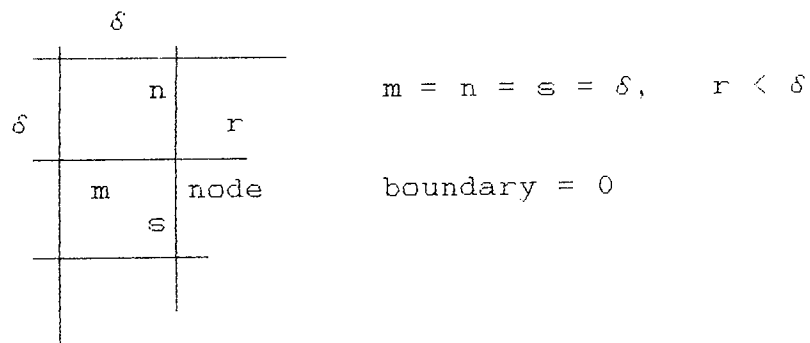
$$\phi_0 = \frac{(1000 + \phi_1 + \phi_2 + \phi_3 + \phi_4)}{4}$$

A suitable area of cells within a SuperCal 4 spread sheet is programmed with the above finite difference equation in each cell. The equation is a function of the four cells surrounding each member, ϕ_0 , of the group. The boundary

value is fixed at zero, i.e. all the boundary cells are set to zero. Where the boundary does not coincide with the nodes, the above equation is modified to allow for the boundary variation:-

$$\theta_0 = \frac{(1000 + \frac{1}{m} \theta_1 + \frac{1}{n} \theta_2 + \frac{1}{r} \theta_3 + \frac{1}{s} \theta_4)}{\left(\frac{1}{m} + \frac{1}{n} + \frac{1}{r} + \frac{1}{s} \right)}$$

m, n, r & s are the fractions of δ between the nodal point and the boundary. Usually only one or two of these fractions are other than 1.



As this alteration is only valid at the boundary and for the examination of torsion the boundary value is fixed at zero, this is a simple adjustment to the spreadsheet equation, i.e., it only requires adjustment to the value of the denominator. This is normally = 4 and will be increased by the change.

The spreadsheet is then allowed to "Recalculate". As the numerical values are functions of other cell values, the software cannot produce a stationary result. It therefore performs a series of iterations either in batches of 100

recalculations or continuously until the variation between recalculations is minimal. After making 100-300 iterations the variation in the value of $-2G\theta$ for the set of finite difference equations across the whole mesh is reduced to less than 1%. The level of deviation may be determined by finding at one sample node the value of:-

$$(\phi_1 + \phi_2 + \phi_3 + \phi_4 - 4.\phi_0)$$

This must be equal to -1000 when the mesh is smooth corresponding to the original assumption of $2G\theta\delta^2 = 1000$. The mesh used is reproduced at figures 70 & 71.

The first element of the membrane analogy was:-

1. The total torque, M_t , is equivalent to the volume of displacement of the membrane.

In mathematical terms:-

$$M_t = 2. \int_{-a}^a \int_{-b}^b \phi \, dx \, dy$$

$$\text{or } M_t = 2.\Sigma \frac{(\text{numerical values of } \phi)}{1000 / (2G\theta\delta^2)}$$

The mesh is one quarter of the whole so that the centre value occurs once, the values along the axes occur twice and the rest four times. This sum gives the relationship between torque applied M_t and angle of twist per unit length θ for a specific diameter of drill shaft:-

$$M_t = K.G\theta \quad [\text{radius of drill} = 20.\delta]$$

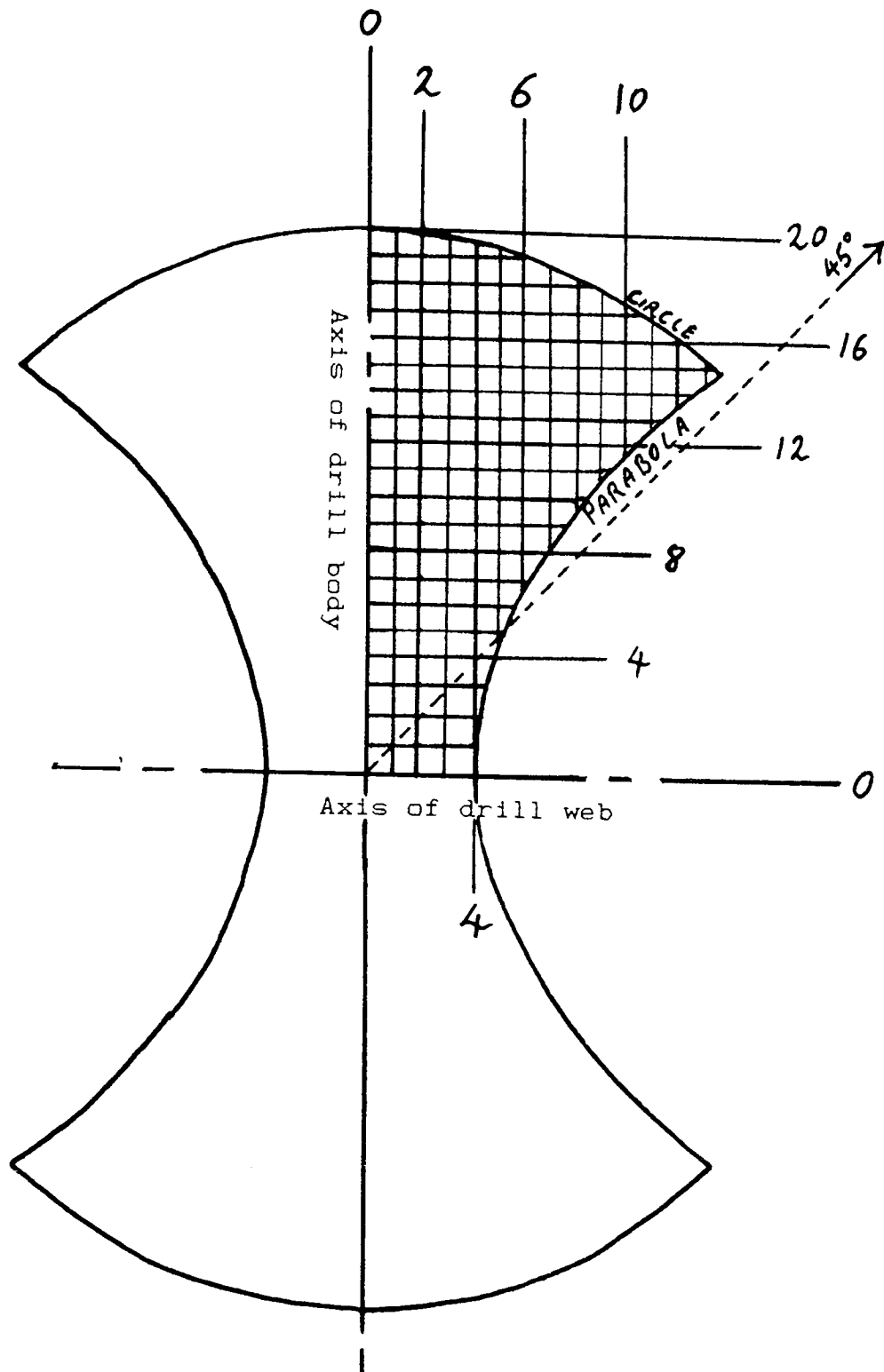


Figure 70 - Cross Section showing the Drill Mesh used for the evaluation of Finite Difference Equations

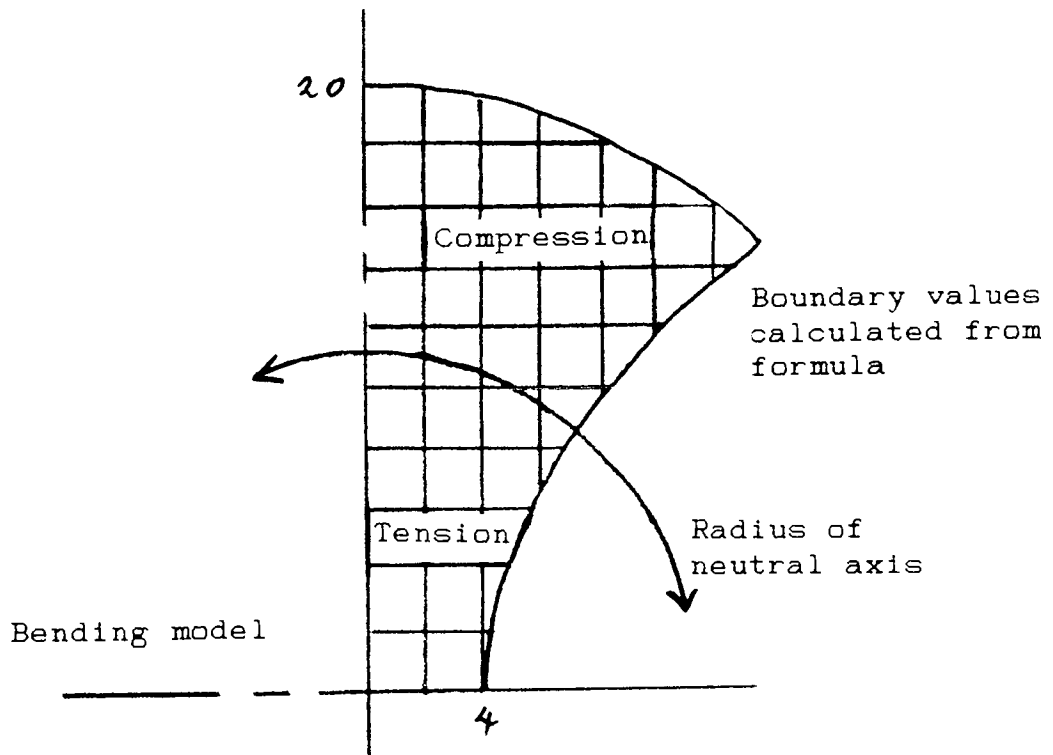
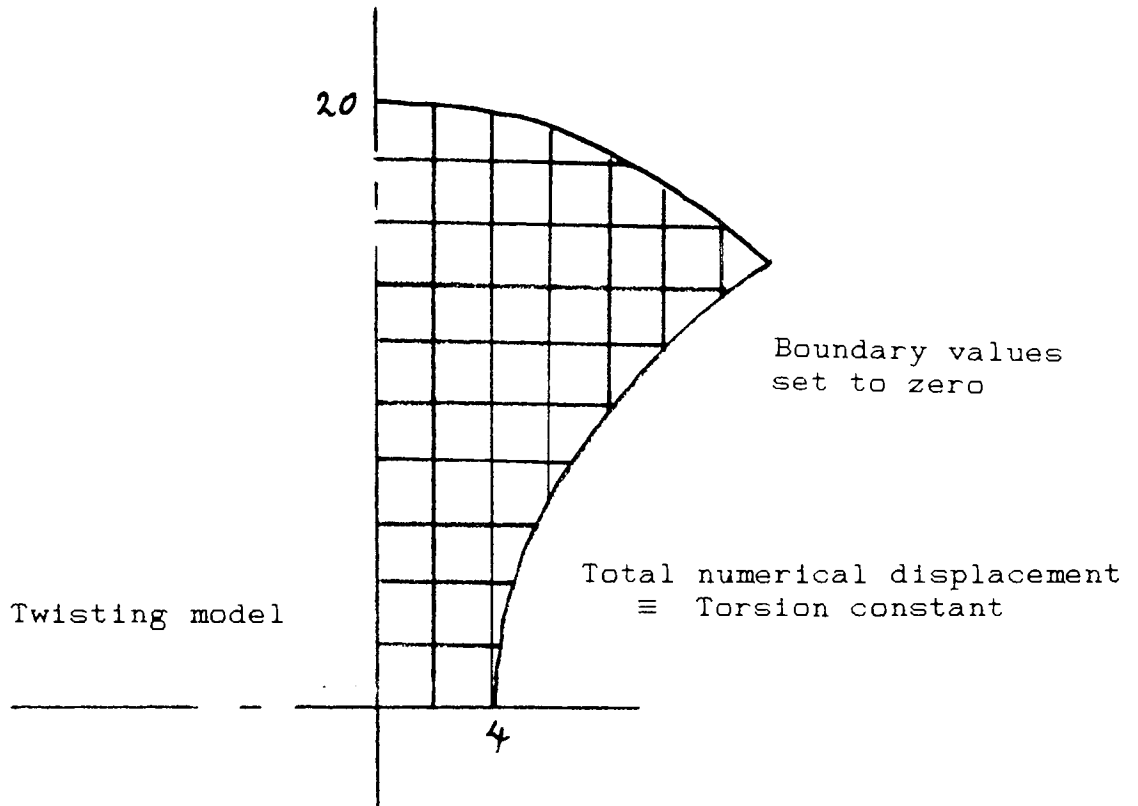


Figure 71 - Cross Section of the Two Drill Models

The second element of the membrane analogy was:-

2. Shearing stress \equiv slope of the membrane

$$\tau_{xy} = \frac{\partial \phi}{\partial y} \quad \text{and} \quad \tau_{yx} = - \frac{\partial \phi}{\partial x}$$

The shearing stress at a node and in a particular direction is equivalent to the variation, or slope, of the stress function at rightangles to that direction. The solution along the axes of the mesh is equivalent to the slope of the smooth curve between the nodes along those axes. From the mesh distribution it is possible to make a numerical approximation of the slope as the difference between the numerical values at adjacent nodes. This gives a numeric value to the two shear stress components at any point within the structure.

A special point within any cross section is the point which has the highest stress. This may then be assumed to be the weakest point within the structure. The external load required to make the stress at this weak point reach the level of failure is the maximum loading that the structure may withstand. These points may be located by looking at the distribution of the resultant shearing stress of the two components, τ_{xy} and τ_{yx} . Figure 72 is a representation of the distribution of the numerical values of Shearing Stress. Figure 73 shows the shape of the deflected membrane. Figure 74 is the distribution of Shearing Stress along the surface of the flute.

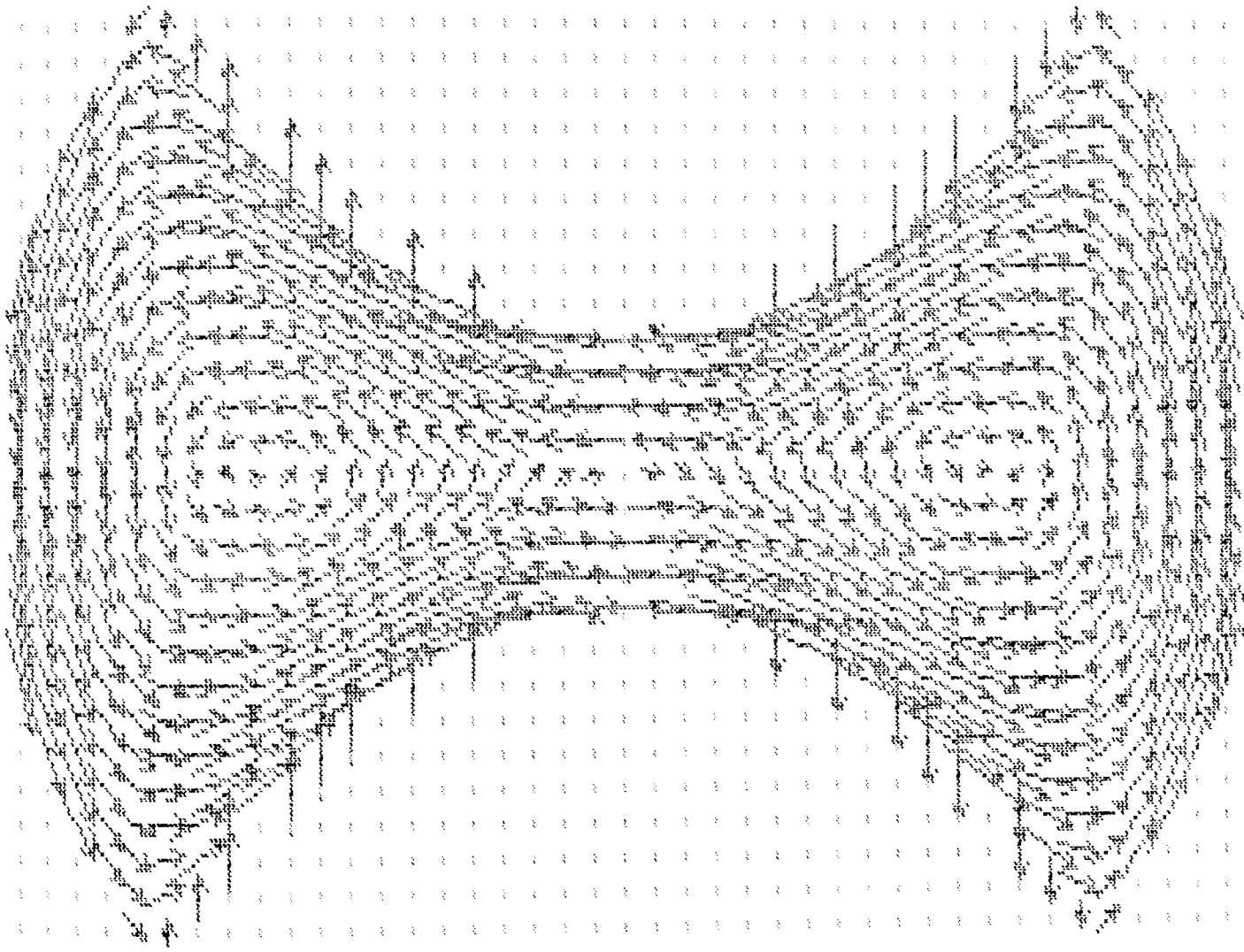


Figure 72 - Turbo Pascal Display of Torsional
Shear Stress Distribution

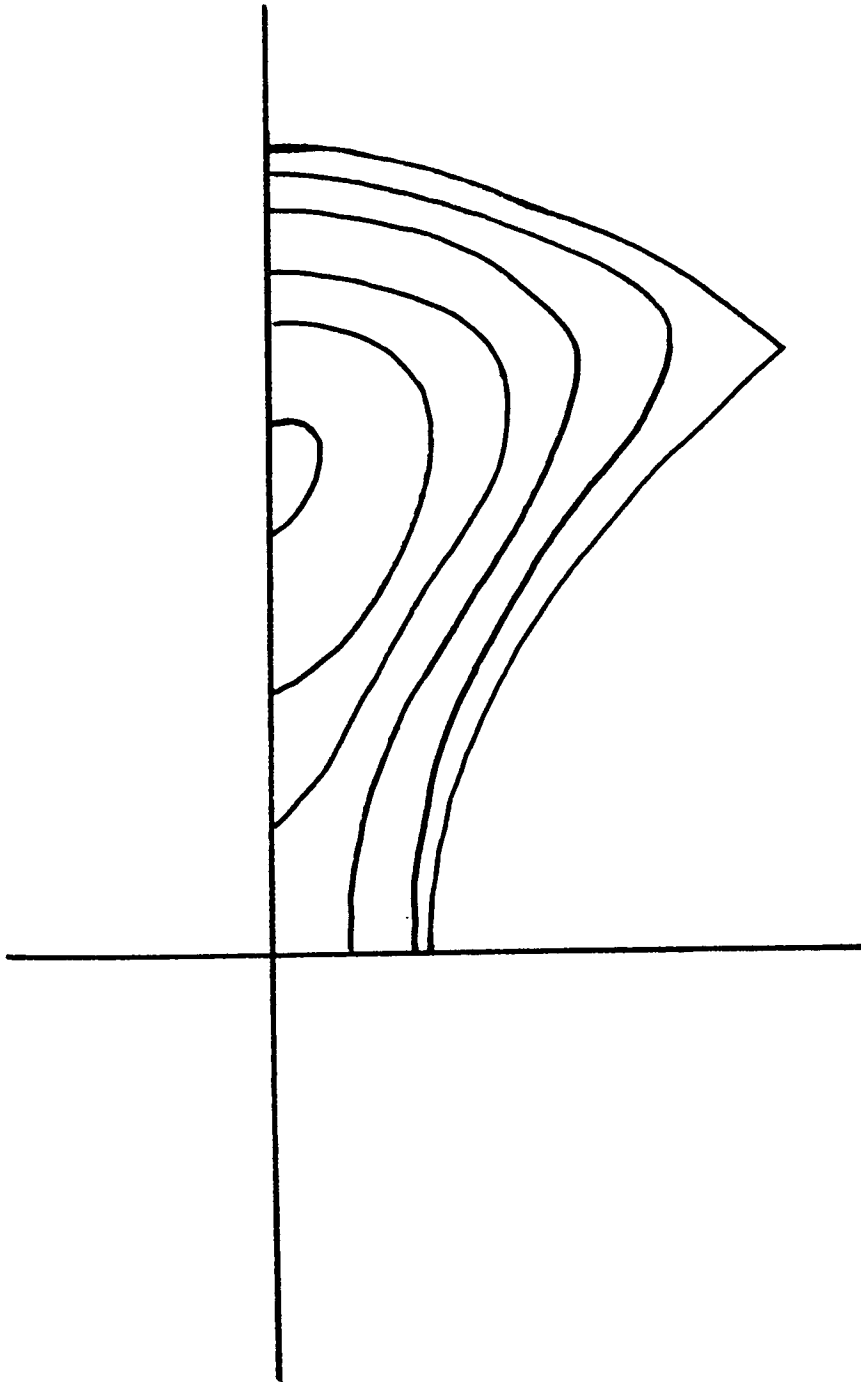
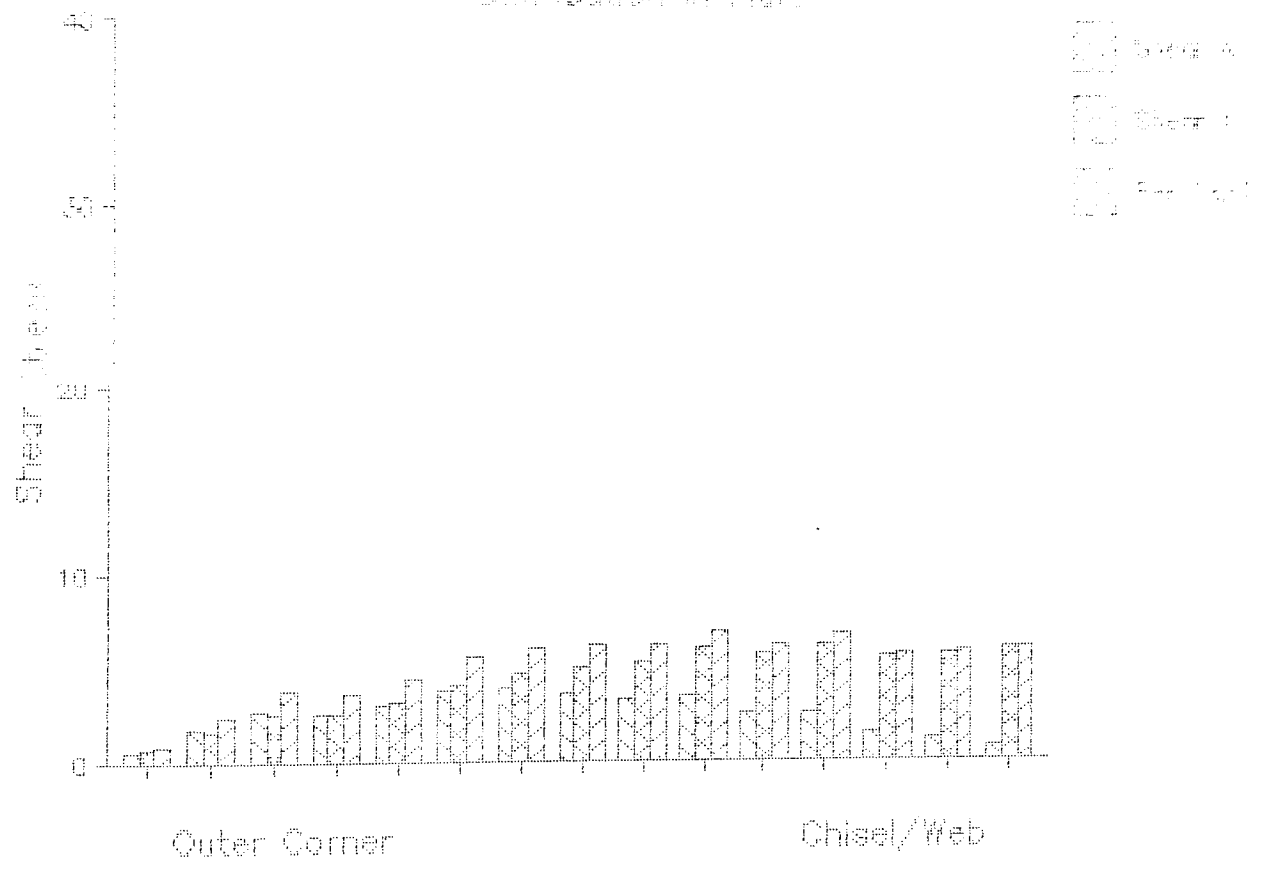


Figure 73 - Contour Lines of Membrane
under the Influence of Torsion

SHEAR STRESS TORSION MODEL
 Distribution in Flute



Shear stress in terms of the slope of the numerical distribution of stress function

Figure 74 - SC4 Display of Torsional

Shear Stress in Flute

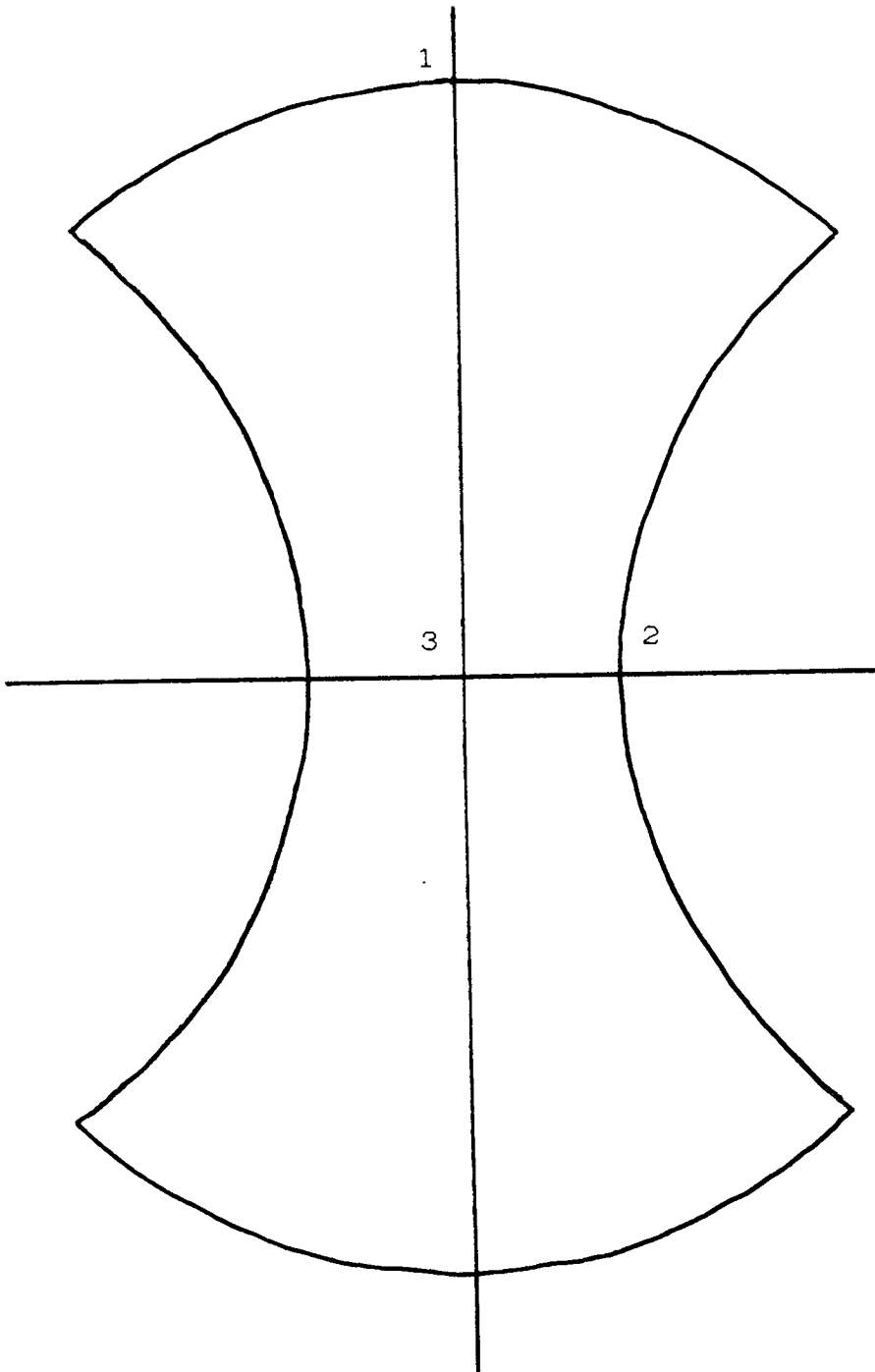


Figure 75 - Points of Interest

Within the cross section of the drill three points are of special interest, namely 1, the extreme radius, 2, the bottom of the flute and 3, the central point, figure 75. In order to improve the estimation of the slope at points 1 and 2, one may use Newton's interpolation formula to find the equation of the line of the membrane deflection and differentiate it for its origin, i.e. at the boundary. At points 1 and 2 there is only one shear stress component present, that aligned with the boundary of the section. Point 3 is a 'saddle', there is no slope and therefore no shearing stress at this point. The two 'highest' points of the stress function distribution, also points of no slope, are located towards the centre of each of the two lobes of the drill structure. This form of distribution agrees with that of Neubauer and Boston [22].

8.2. ANALYSIS OF LONGITUDINAL STRAIN BY

FINITE DIFFERENCE EQUATIONS.

The major basic error in the proposition of Neubauer and Boston's paper [22], and repeated by the above, is that this form of analysis assumes a prismatic bar, i.e. there is no allowance for the drill helix. This aspect will now be examined.

In this research the calculation of the longitudinal or end strain is simplified to the requirement to calculate a radius of neutral axis where the longitudinal strain is

assumed zero. Longitudinal tension will occur inside this radius and longitudinal compression outside.

The differential equation for the solution of the direct stress function is given below:-

$$\frac{\partial^4 \phi}{\partial x^4} + 2 \frac{\partial^4 \phi}{\partial x^2 \partial y^2} + \frac{\partial^4 \phi}{\partial y^4} = 0$$

This equation resolves the distribution of longitudinal direct stress in the cross section of a shaft or beam. The soap film only solves a differential equation to the power 2 so the above equation to the power 4 may not be solved by a soap film method.

In 1917 Griffith and Taylor [19] proposed a different method for the solution of bending problems where the same soap film method may be applied. A stress function is again used to describe the distribution of the shear stresses in the cross section of a cantilever. These stresses are due to a bending force applied to the end of the cantilever. Longitudinal direct stress is also present in such a section but is not included in this form of analysis. The differential equation is given below:-

$$\frac{\partial^2 \phi}{\partial x^2} + \frac{\partial^2 \phi}{\partial y^2} = 0$$

where:-

$$\tau_{xx} = \frac{\partial \phi}{\partial y} - \frac{Px^2}{2I} + \frac{\nu}{2(1+\nu)} \frac{Py^2}{I} \quad \text{and} \quad \tau_{xy} = - \frac{\partial \phi}{\partial x}$$

In this research and by using the above analogy, the drill cross section is modelled as a beam which is exposed to a bending moment. The magnitude of the bending moment is made equivalent to the longitudinal strain imposed by the twisting action. In a loaded cantilever individual fibres are loaded longitudinally with respect to their distance from the neutral axis across the width of the beam section. In the same way individual longitudinal fibres of a twisted drill are loaded with respect to the change in length effect which varies with radius from the drill centre to the extreme radius of the drill.

This stress function distribution may be solved in a similar way as for the torsional problem. It is necessary to make one simplification. The longitudinal stress effect is proportional to the radius, zero at the centre and maximum at the drill radius. In order to use this model it is necessary to assume that the longitudinal stress effect will be proportional to the perpendicular distance from an axis through the drill web.

The mesh used is the same shape as for torsion but this time there is an initial boundary displacement. The individual values of this may be calculated from the equation:-

$$\frac{\partial \phi}{\partial s} = \left[\frac{Px^2}{2 I_x} - \frac{\nu}{2(1+\nu)} \frac{Py^2}{I_x} \right] \frac{dy}{ds}$$

P = Load or Force
 I_x = 2nd Mom of Area
 ν = Poisson Ratio

Starting from one point on the boundary the change in value moving along the boundary, $d\phi/ds$, to the next point may be calculated. These calculations may be continued all round the edge producing a continuous curve. As the shear stresses are found from the slope of the soap film the starting point and initial numeric value may be chosen at random.

As stated above the shear stress values are calculated from the following:-

$$\tau_{xz} = \frac{\partial \phi}{\partial y} - \frac{Px^2}{2I} + \frac{\nu}{2(1+\nu)} \frac{Py^2}{I}$$

$$\tau_{yx} = - \frac{\partial \phi}{\partial x}$$

The slopes may be found from the mesh in the same way as for the torsion mesh. To determine the τ_{xz} value the rest of the above equation is calculated and added to the slope value.

The longitudinal stress is related to the radius. The average radius of the shear stresses is then calculated.

This is taken as the value of the neutral axis with reference to the Dynamic Drill Model. The helix angle of the model is calculated for this radius and is used to determine the extent of the change in length by assuming zero longitudinal stress, i.e. the overall length of the helical fibres of the drill that compose the drill at this radius

maintain the same length while those inside are elongated and those outside are shortened. The same displays of the shear stress distribution as provided for pure torsion are given at figures 63 and 64.

8.3. CONCLUSIONS.

The use of a computer iteration technique allows data of the deformation effects present in the twist drill to be generated quickly and accurately by the use of finite difference equations.

The three dimensional nature of the problem is divided into two parts. The first part is calculation of the torsion constant for the drill cross section. The second part is calculation of the longitudinal effects of drill deformation for the same cross section. The two components described in this chapter are a good representation of this three dimensional problem.

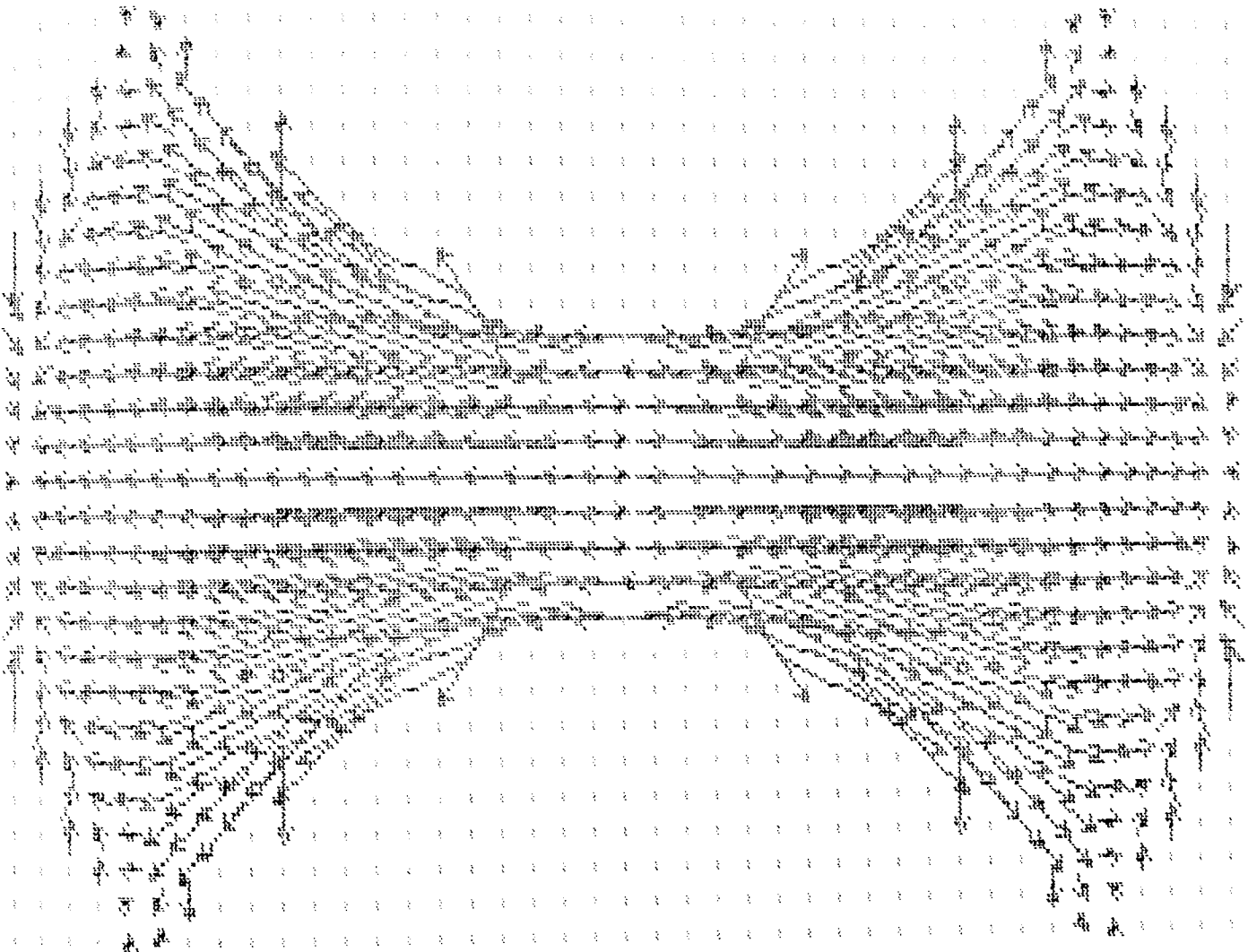
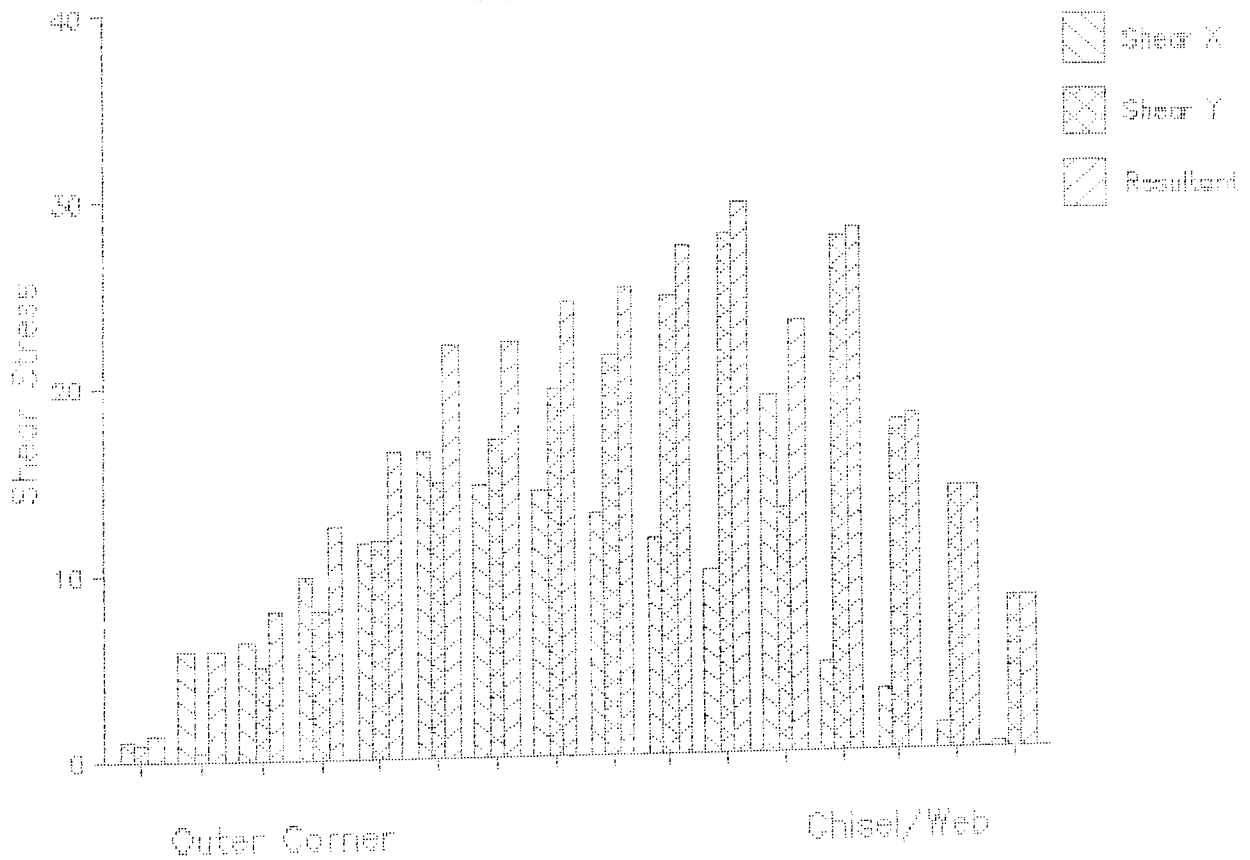


Figure 76 - Turbo Pascal Display of Longitudinal
Shear Stress Distribution

SHEAR STRESS BENDING MODEL

Distribution in Flute



Shear stress in terms of the slope of the numerical distribution of stress function

Figure 77 - SC4 Display of Longitudinal

Shear Stress in Flute

CHAPTER 9

	PAGE
9. TOTAL DRILL DEFORMATION	210
9.1. THE TOTAL SOLUTION	210
9.2. TORSION AND BENDING MODELS	211
9.3. WARPING FUNCTION OF THE TORSION MODEL	229
9.4. CONCLUSIONS	230

9. TOTAL DRILL DEFORMATION

Two aspects to the total deformation of the twist drill have been identified. One is the resistance of the structure to twisting which is approximated by the Torsion Constant. Two is the longitudinal change of length as modelled by The Drill Dynamic Model, figure 68.

There are two parameters to the dynamic model:-

1. The compliance of the drill structure. - This is provided by the twisting model. The angular twisting in the circumferential direction is unwound to the linear direction so indicating the side displacement of the dynamic model.
2. The helix angle of the model. - This item is taken to be the local helix angle at the radius of zero longitudinal strain as indicated by the bending model. This radius is the mean radius of the bending model shear stresses, which puts equal stresses inside and outside the radius.

9.1. THE TOTAL SOLUTION.

The two component solutions are:-

- i, Cross sectional shear stress due to pure torsion.
- ii, Cross sectional shear stress due to the longitudinal effect.

In order to investigate the probable distribution of stress

across the drill in section these components may now be combined by superposition.

This superposition is best explained by working through the figures for a sample drill. In the prototype analysis a drill with parabolic flutes is used with a diameter : webthickness ratio of 5 : 1. This drill has been evaluated by the above two finite difference equation methods. It is easy to apply the methods to find the two separate distributions of shear stress, figures 72, 74, 76 & 77. Comparison may then be made but before any conclusions may be drawn the following question must be addressed: What is the relationship between the torsion model in terms of torque T and the longitudinal, (bending), model in terms of force P?

9.2. Torsion and Bending Models

In the torsion model, the SuperCalc solution provides a value for ϕ_1 . ϕ_1 is the numerical value of the stress function. This is the predicted stress distribution which is then corrected as below:-

$$\phi = \frac{2G\theta\delta^2}{1000} \cdot (\phi_1, \text{ the numerical value from spreadsheet})$$

G = Modulus of Elasticity in Shear
 θ = Angle of Twist per Unit Length
 δ = the size of the mesh

or as in the prototype $\delta = r/20$, $\delta^2 = r^2/400$. Where r = drill radius:-

$$\phi = G\theta r^2 \cdot \frac{\text{(the numerical value from spreadsheet)}}{200000}$$

ϕ is then the true distribution of the stress function. The total torque load of the cross section is carried by the numerical value of twice the volume of the membrane displaced. \int (The numerical values of ϕ) is calculated as $K_1 \cdot G\theta r^2$. This gives the equation for total torque:

$$T = K_1 \cdot G\theta r^2 \quad r = 2.25$$

$$\text{For this drill } K_1 = \frac{6232907}{200000}$$

$$\Rightarrow \text{Torque} = 157.77 \cdot G\theta \quad (\text{Nmm})$$

This is the torque to achieve 1 turn in unit length of 1mm. When calculated out for a twist of 140° in 100mm length, assuming $G = 6000$, it gives:-

$$157.77 \times 6000 \times \frac{140^\circ}{360^\circ} \times \frac{1\text{mm}}{100\text{mm}} = 3681 \text{ Nmm}$$

Or 3.68 Nm to twist a 4.5mm drill having a 100mm flute length by 140° . This compares with a measured value of 6Nm which was the failure load and twist for a similar drill.

The equation relates torque to angle of twist per unit length, θ . So the torque applied is directly related to the angle of twist. The value of angle of twist so found also governs the values of the individual shear stresses created across the component:

$$\tau_{zx} = \frac{\partial \phi}{\partial y} \quad \text{and} \quad \tau_{zy} = - \frac{\partial \phi}{\partial x}$$

These have numeric values of $\phi_1 - \phi_0$ and $\phi_2 - \phi_0$ of the form $K_1 \cdot G\theta r^2$.

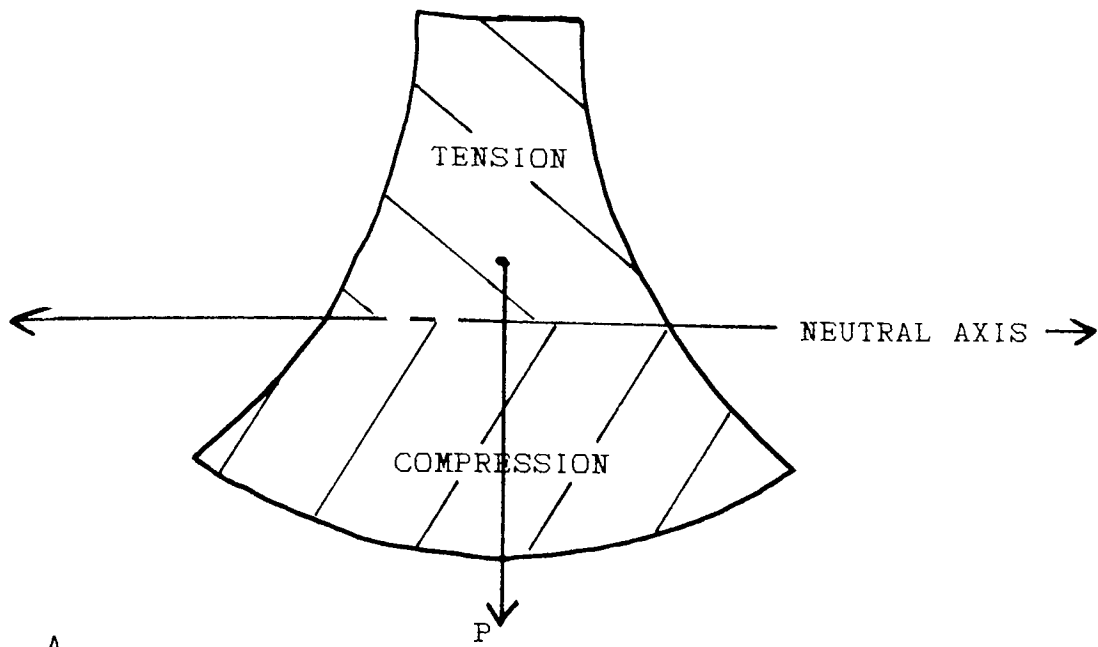
The failure shear stress is known. The point of maximum value of K_1 is read from the shear stress distributions. The maximum value of angle of twist, θ , and also the maximum torque that may be applied before failure, M_t , will be calculated by applying this limiting shear stress at the indicated weak point.

The point of maximum K_1 is in the base of the flute, point 2 in figure 75, and the accuracy of the value may be enhanced by determining its value using Newton's Interpolation Formula. For this drill, where $r = 2.25$, the value of K_1 at point 2 gives:-

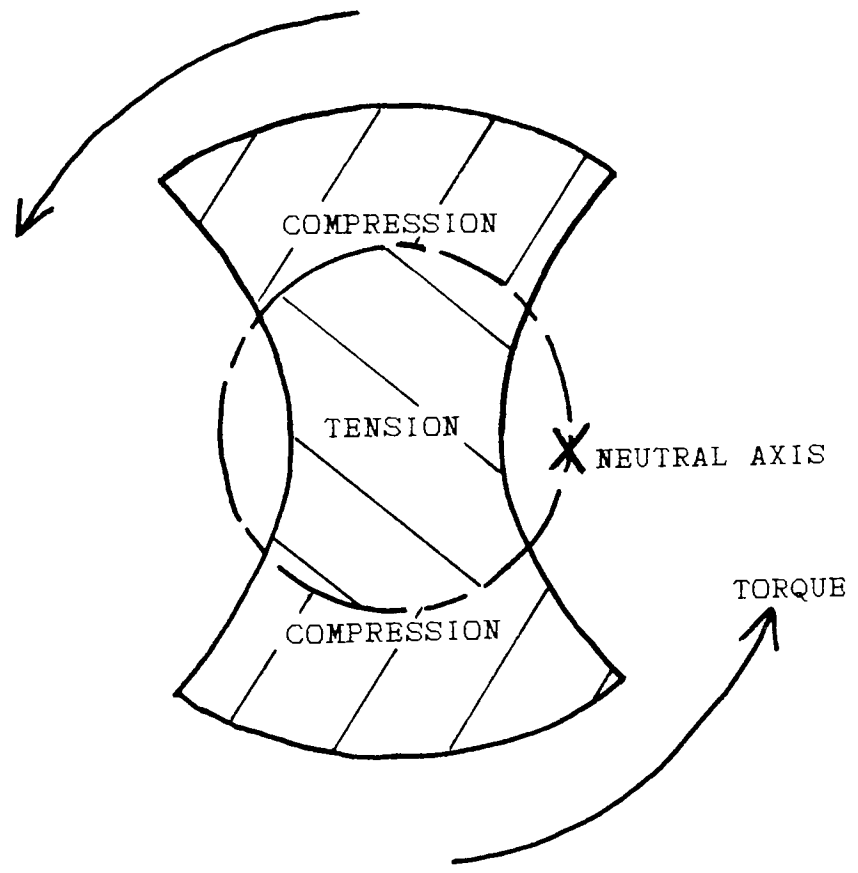
$$\text{shear stress} = 0.140 \cdot G\theta \text{ (N/mm}^2\text{)}.$$

In the bending model the bending membrane analogy is based on the deformation of a cantilever by the application of a force P at the free end. The result of the deformation is to cause the cantilever to distort from a straight line to a curve with maximum curvature at the fixed end.

Once again the SuperCalc solution provides a value for θ . This is the predicted shear stress distribution created



A.



B.

Figure 78 - Bending Model Strain Distribution & Cross Section of Drill under the Influence of Torsion

Deflection

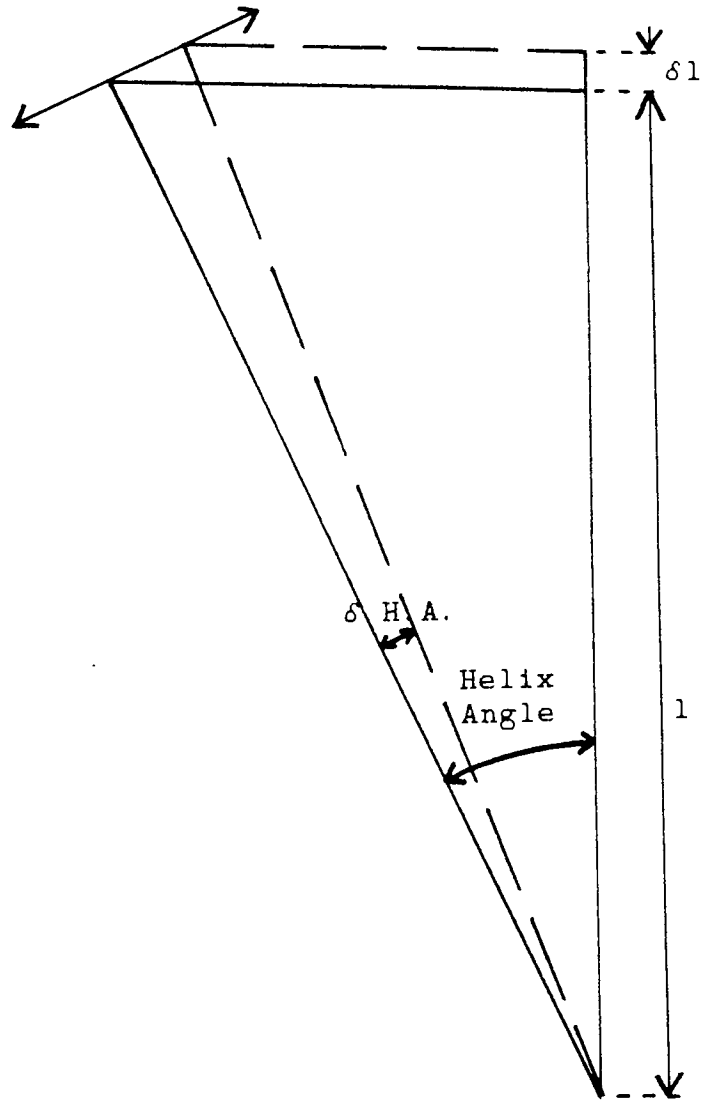


Figure 79 - Triangle of Helix Angle & Drill Extension

across the component by the longitudinal distortion.

Relating P to Torque is performed in two stages. The first is to relate the radius of curvature of the bending model cantilever to the helix angle of the real drill. These are in each case the parameter which controls the distribution of the longitudinal stresses. The second stage is to relate the force P to the radius of curvature of the bending model using bending theory.

The cantilever curvature may be described by its radius. This deformation produces longitudinal stress, figure 78A, tension on the opposite side to the centre of curvature and compression on the same side, so corresponding to the real system. For this bending model the strain is determined by the local value of radius:-

$$\text{Strain} = e/l = ((R+t).\theta - R.\theta)/R.\theta$$

$$\Rightarrow t/R$$

θ = angular length of beam segment
 R = the Radius of curvature of the neutral axis.

t is measured from the neutral axis, positive away and negative towards the centre of curvature.

$$\text{or } \frac{\text{radius} - \text{radius of neutral axis}}{\text{Radius of Curvature}}$$

For the real drill the longitudinal strain varies with radius out from the centre of the drill. This means the drill centre will be in tension while the extremities of the

Comparison of Stress Distribution

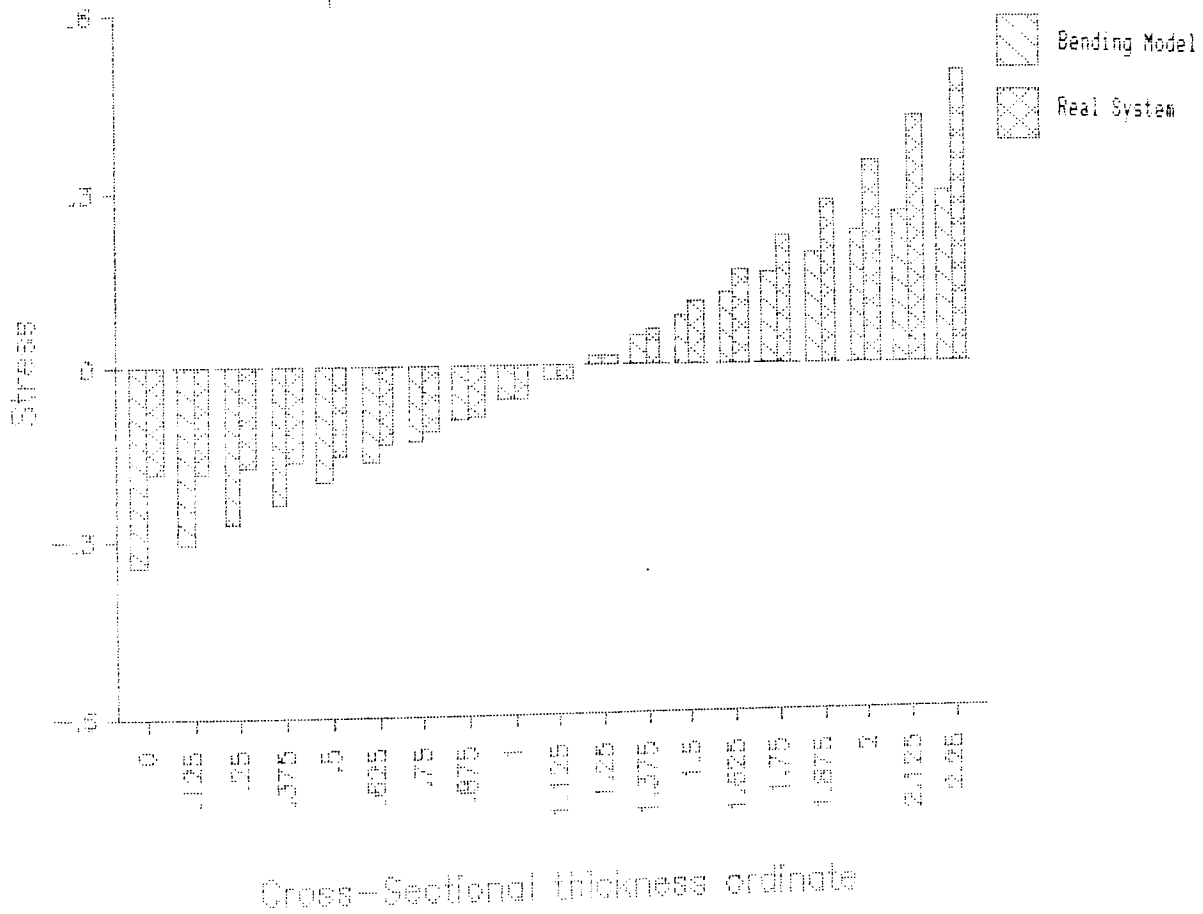


Figure 80 - Bending Model / Real System

Longitudinal Strain

drill will be in compression, figure 78E. The strain is determined from the local value of helix angle, (dependent on the local radius), figure 79.

From the twist drill model:-

$$\begin{aligned} \text{Strain} &= e/l \\ \alpha &= \theta \cdot r / \text{Radius} \\ \theta &= \text{angle of shear strain} \end{aligned}$$

$$\text{and } \frac{1}{e + 1} = \frac{\cos(\text{Local value of Helix Angle})}{\cos(\text{Local value of Helix Angle} - \alpha)}$$

$$\frac{e}{1} = \frac{\cos((\text{N.H.A.}) \cdot r / \text{Rad} - \alpha) - \cos((\text{N.H.A.}) \cdot r / \text{Rad})}{\cos((\text{N.H.A.}) \cdot r / \text{Rad})}$$

$$\frac{\cos(\text{Neutral Axis H.A.} - \alpha) - \cos(\text{Neutral Axis H.A.})}{\cos(\text{Neutral Axis H.A.})}$$

$$\Rightarrow \frac{\cos(\alpha) + \tan((\text{N.H.A.}) \cdot r / \text{Rad}) \sin(\alpha) - 1}{\cos(\alpha) + \tan(\text{Neutral Axis H.A.}) \sin(\alpha) - 1}$$

For small θ , $\alpha = \theta \cdot r / \text{Radius}$:

$$\Rightarrow \sqrt{1 - \alpha^2} + \tan((\text{N.H.A.}) \cdot r / \text{Radius}) \cdot \alpha - 1 - \theta \cdot K_{\alpha}$$

$$\Rightarrow \theta \cdot r / \text{Radius} \cdot \tan((\text{N.H.A.}) \cdot r / \text{Radius}) - \theta \cdot K_{\alpha}$$

$$K_{\alpha} = (r \text{ of neutral axis}) / \text{Radius}$$

$$\tan((\text{N.H.A.}) \cdot (r \text{ of neutral axis}) / \text{Radius})$$

The bending model is an accurate model of twisting when:-

$$(r - r \text{ of neut axis}) / R \equiv \theta$$

$$(r / \text{Radius} \cdot \tan \left[\frac{r \cdot (\text{Nom. H. A.})}{\text{Nom Radius}} \right] - K_{\alpha})$$

Graph of Twist - Radius of Curvature

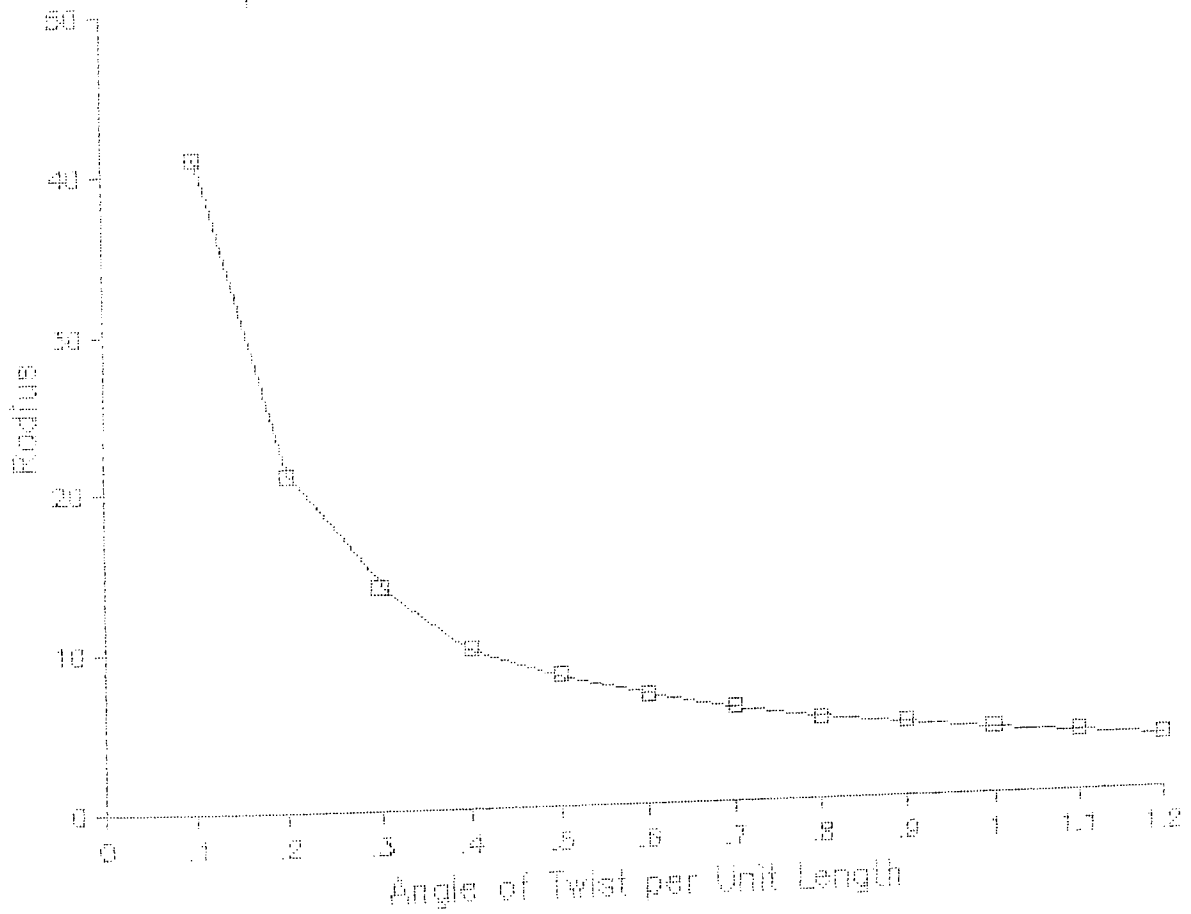


Figure 81 - Bending Model Radius of Curvature : Drill Twist

Graph of Twist - Curvature
(Linear Relationship)

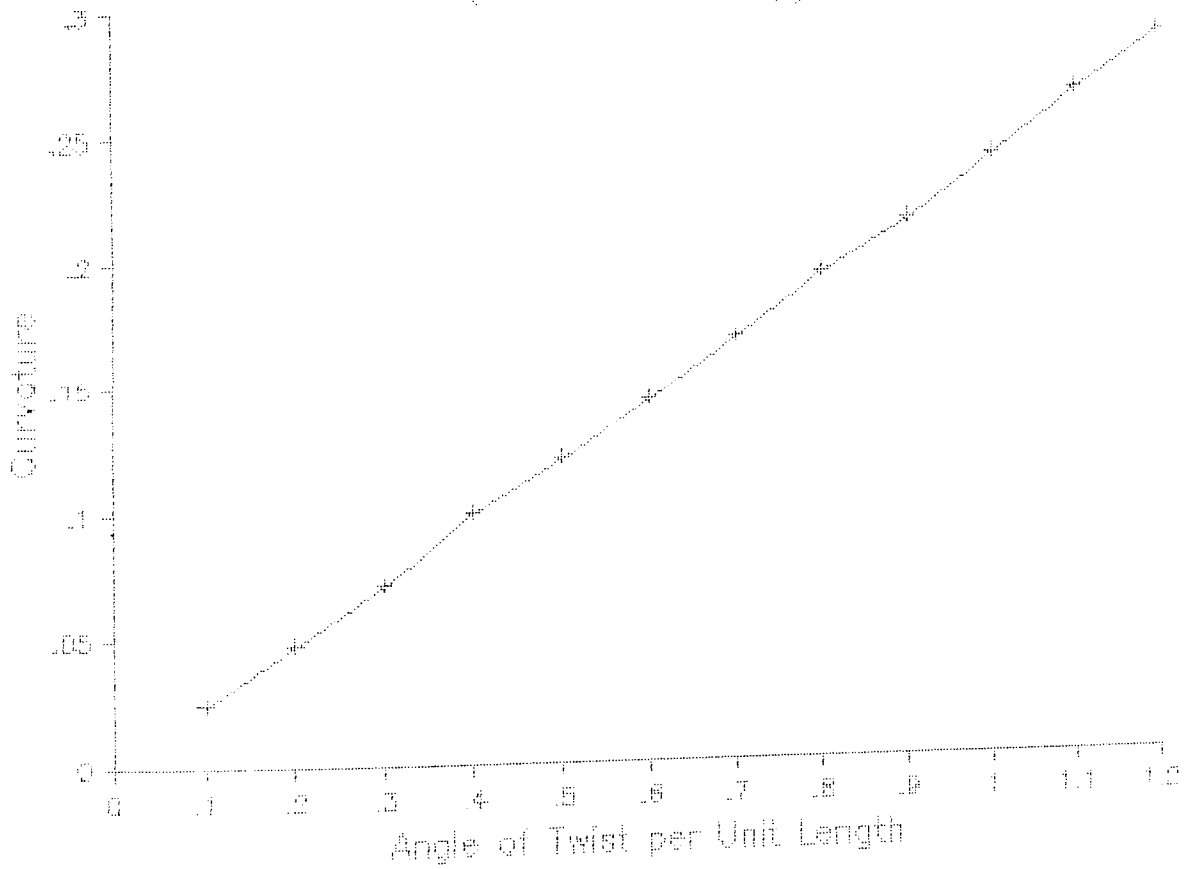


Figure 82 - Bending Model Curvature : Drill Twist

$$\text{or } r / (\text{Rad of Curv}) \equiv \theta \cdot \left(\frac{r / \text{Radius} \cdot \text{Tan} \left[\frac{r \cdot (\text{Nom. H. A.})}{\text{Nom Radius}} \right] }{r} \right)$$

This relationship may be used to equate Radius of Curvature to Nominal Helix Angle.

The term r occurs once on the left hand side and twice, $(r \cdot \text{Tan}(r))$ on the right hand side. The two distributions are not therefore equivalent but as can be seen from figure 80 the model strain is sufficiently similar to the strain of the real drill. If the two sides are programmed into a SuperCalc spreadsheet then they may be evaluated over the range of radius allowing a best fit Radius of Curvature to be found at each specific drill angle of twist. If a range of angles are investigated, the best fit being found each time, then a graph of radius of curvature against angle of twist is generated, figure 81. The graph of Angle of Twist against $(1/\text{Radius of Curvature})$ or 'Curvature' is linear passing through the origin, figure 82.

Radius of curvature in advanced bending theory is equal to the following:-

$$\frac{1}{r} = \frac{M}{EI} [1 - K]$$

This equation also represents the centreline curvature of a cantilever beam. K , in general, is a very small value, of the order $(\text{thickness})^2 / (\text{length})^2$. It is therefore not

unreasonable to use the simplified formula from elementary bending theory in order to examine the curvature of a cantilever at its fixed end. (This is the point of maximum curvature, the curvature reduces to zero at the free end, as does the bending moment.):-

$$\frac{1}{r} = \frac{M}{EI} = \frac{Pl}{EI}$$

E = Youngs modulus
 I = Second moment of area
 M = Bending moment
 or P = Bending load
 l = Length of cantilever

This relates 1/(Radius of Curvature) to the bending moment and therefore to the deflecting force P, the length of cantilever assumed to be unity.

The spreadsheet was programmed with a Helix angle of 30 degs and a radius of neutral axis of 1.2 for the example drill. From the SuperCal spreadsheet the curvature for a twist of 1 is 1/4.1 units or a curvature of 0.244 per unit twist. The value of E is that for tool steel and the value of I_y for the 4.5 unit diameter 5.1 webthickness ratio is 10.063 units⁴. The bending moment and the numeric value of P is therefore 0.244.E.θ.I_y. P/I_y is the factor used in the bending model equations which is equal to 0.244.E.θ.

$$P/I_y = (0.244).E.θ$$

$$G = E / 2.(1 + ν) ≈ E / 2.6$$

$$P/I_y = (0.5344).G.θ$$

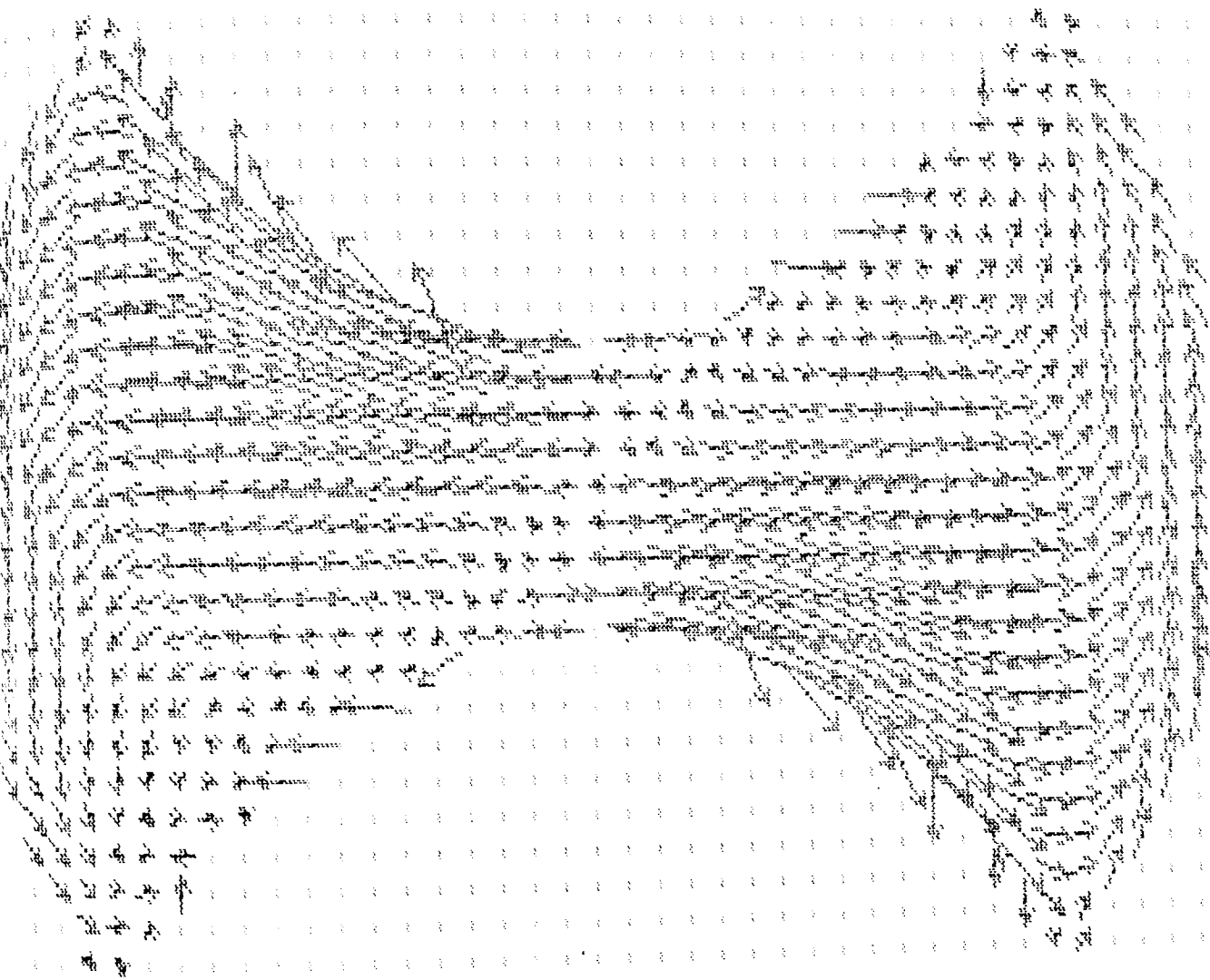


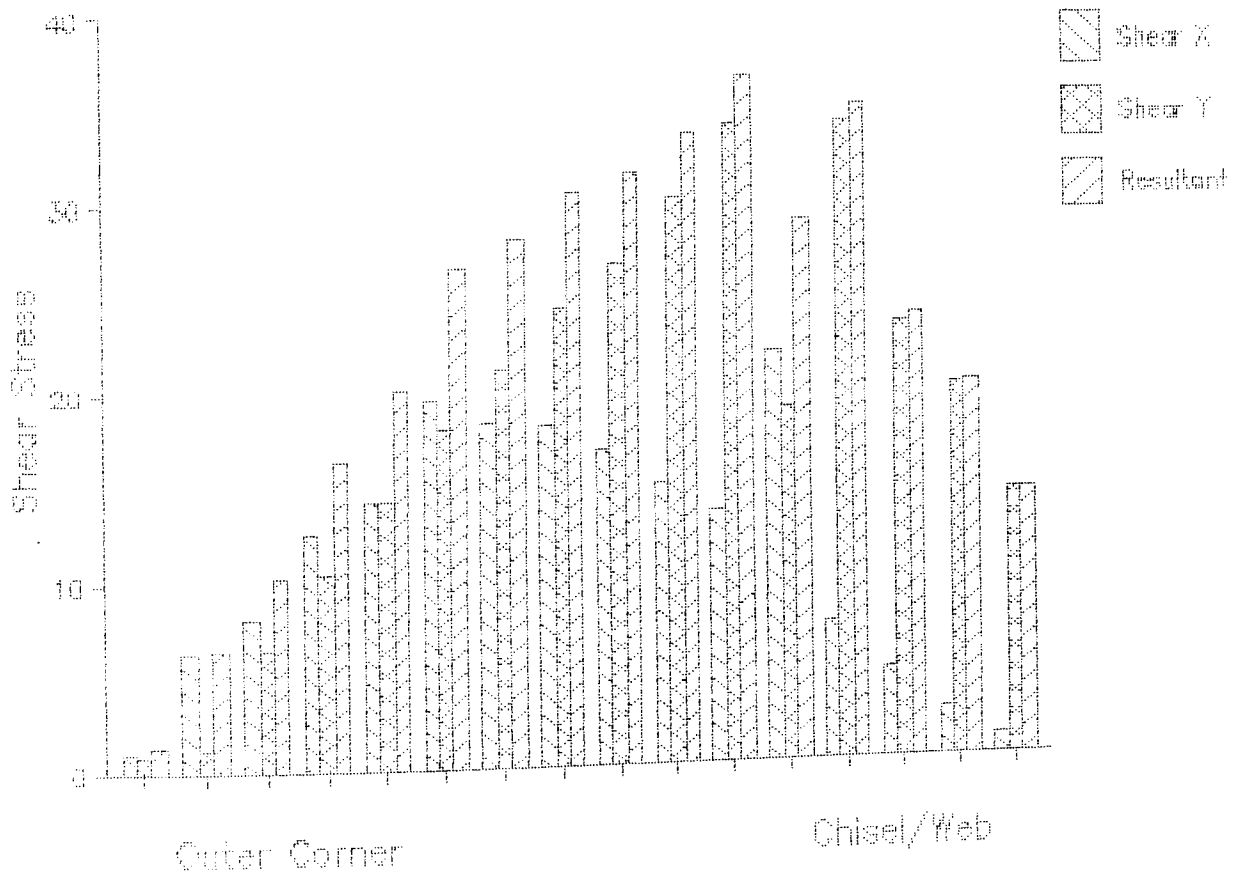
Figure 83 - Turbo Pascal Display of Combined

Shear Stress Distribution

- Quick Spiral Helix

SHEAR STRESS COMBINED

Distribution in Flute



Shear stress in terms of the slope of the numerical distribution of stress function

Figure 84 - SC4 Display of Combined Shear Stress in Flute

ϕ , the value of the stress function distribution in the bending model, is governed by the value of P/I_y . There is a simple linear relationship and a standard value of 1000 for P/I_y is again used in the spreadsheet. The true value of the spreadsheet value and so the values of the shear stresses are found by multiplying by $P/1000 \cdot I_y$.

The perimeter values of the distribution are found from the equation:-

$$\frac{\partial \phi}{\partial s} = \left[\frac{Px^2}{2I} - \frac{\nu}{2(1+\nu)} \frac{Py^2}{I} \right] \frac{dy}{ds} = K_d \cdot \left[\frac{1000x^2}{2} - \frac{\nu \cdot 1000y^2}{2(1+\nu)} \right] \frac{dy}{ds}$$

The shear stresses are found from:-

$$\tau_{xz} = \frac{\partial \phi}{\partial y} = \frac{Px^2}{2I} + \frac{\nu}{2(1+\nu)} \frac{Py^2}{I}$$

$$\Rightarrow \tau_{xz} = K_d \cdot \left(\frac{\text{Num Val}}{y} - \frac{1000x^2}{2} + \frac{\nu \cdot 1000y^2}{2(1+\nu)} \right) \cdot G \cdot \theta$$

$$\tau_{yx} = - \frac{\partial \phi}{\partial x}$$

$$\Rightarrow \tau_{yx} = - K_d \cdot \left(\frac{\text{Num Val}}{x} \right) \cdot G \cdot \theta$$

Where $K_d = (0.5344)/1000$. These values for the shear stress due to bending are then equivalent to those obtained from the torsion model.

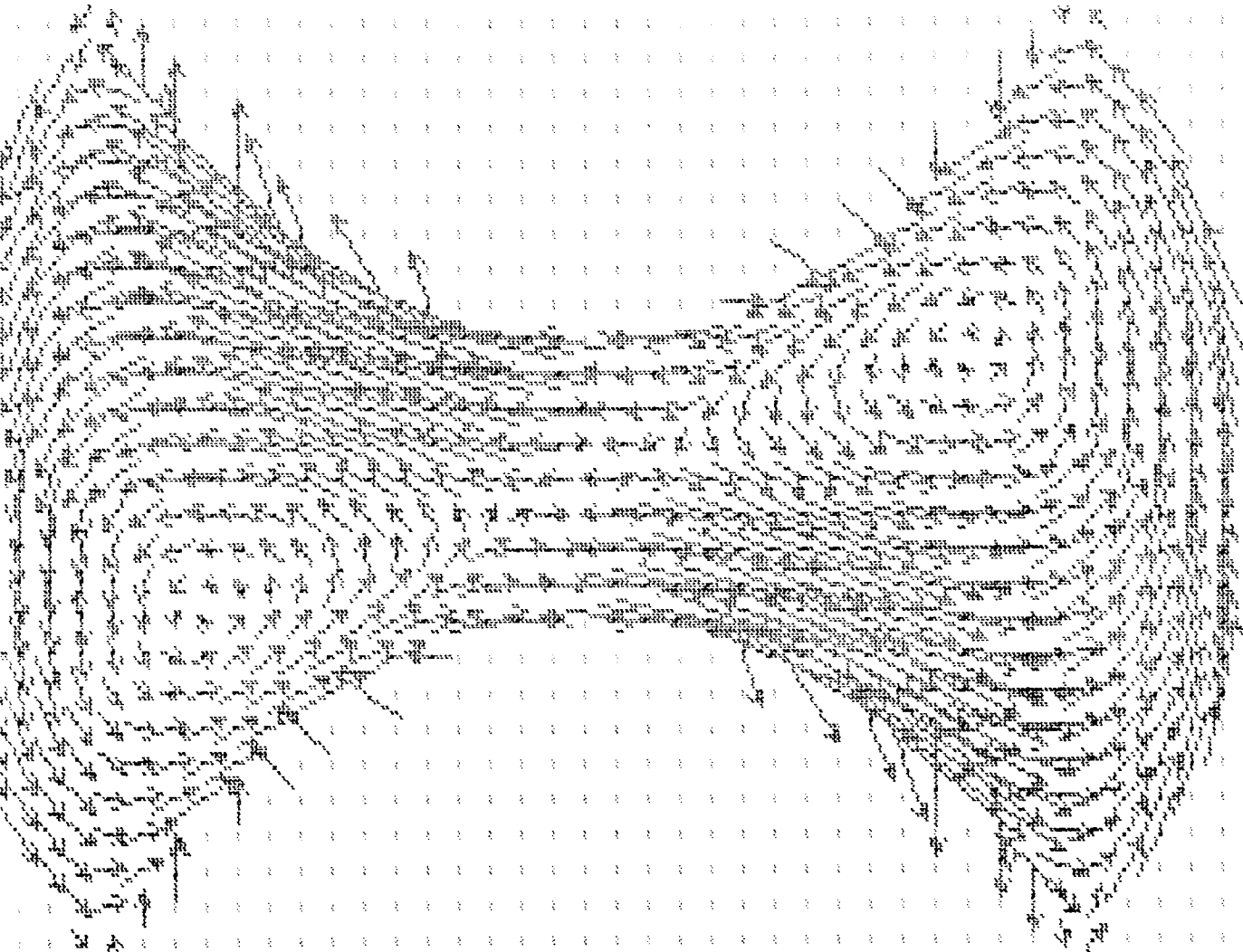


Figure 85 - Turbo Pascal Display of Combined
Shear Stress Distribution- Slow Helix Drill

The torsion model has been displayed at figures 72 & 74. Here the resultant directions of the x and y ordinate values have been determined along with their magnitude. The shear stress directions are then displayed with equivalent arrows. A similar display for the bending model is seen at figures 76 & 77. Having determined the equivalence between the two models it is a simple matter to superimpose the two systems as at figure 83 & 84. This form of display shows how the torsional system, first demonstrated by Neubauer & Boston, [21] for a prismatic drill shaft, must be modified to allow for the helix angle. These are examples of drills with a high or quick helix angle. The figures show a torsional distribution that has been totally swamped by the longitudinal effect. For a drill with a standard helix angle or lesser helix angle this is not the case as can be seen at figure 85 for a drill with a slow helix. The torsion distribution is still visible but modified by skewing its centres from the drill body axis.

The value of shear stress at the drill centre is still zero, the value at the base of the flute is still $(0.140) \cdot G \cdot \theta$ but this is not now the maximum. The maximum value is also off set a short distance around the flute. The shear stress is still $(0.137) \cdot G \cdot \theta$ at the extreme radius of the drill body where the longitudinal shear stress is small.

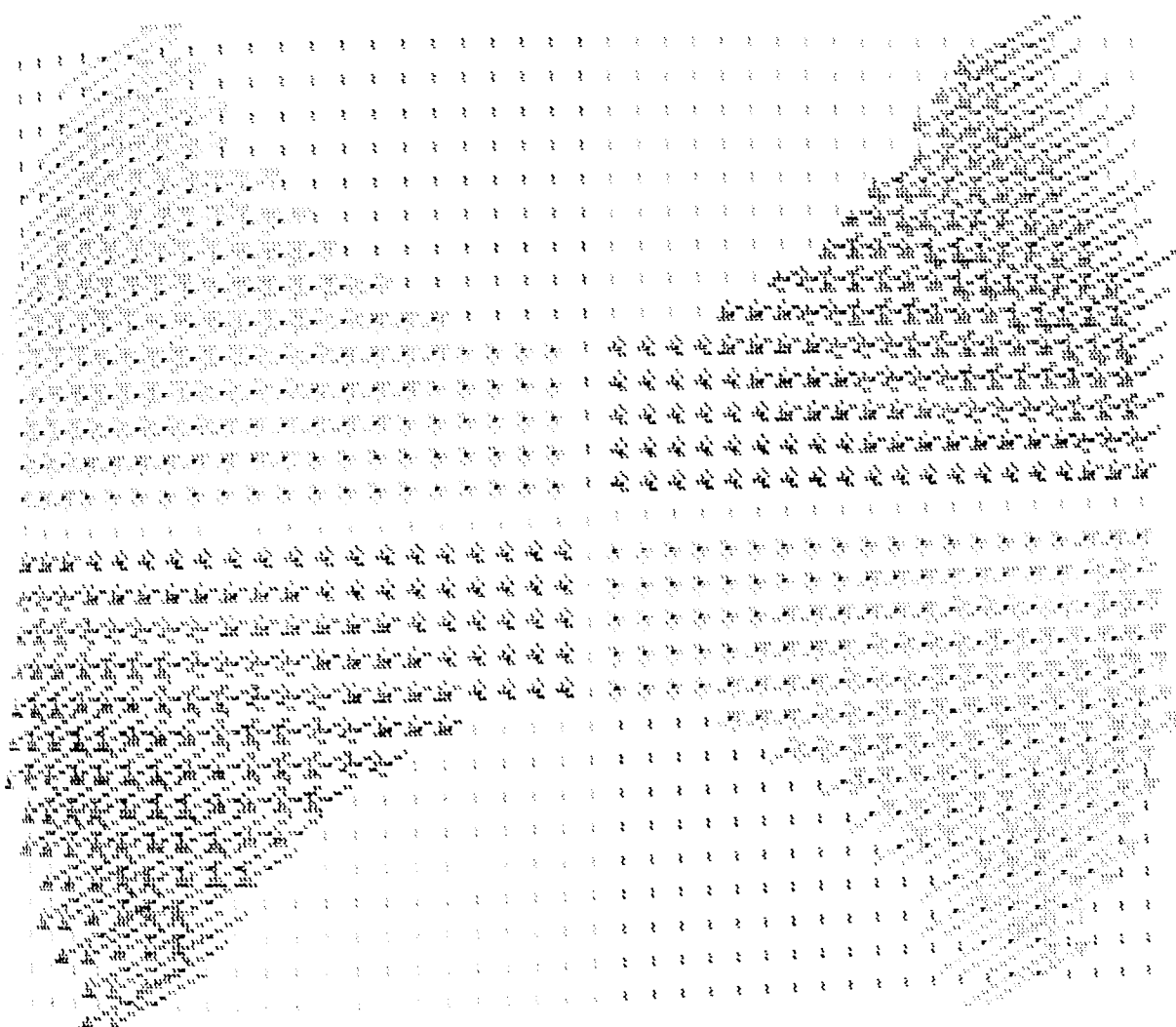


Figure 86 - Warping Distribution

9.3. WARPING FUNCTION OF THE TORSION MODEL.

The warping present in the cross section is described by St Venant's warping function which is related to the torsion model stress function:-

$$w = \theta \bar{\Phi}(x, y)$$

w = warping (displacement in the z direction)

θ = Angle of Twist per unit length

$\bar{\Phi}(x, y)$ = Warping Function as a function of x and y

This distribution is purely related to the torsion model and may be estimated by numerical integration from the numeric values of the shear stresses. In order to include the longitudinal warping effect a further spreadsheet must be programmed with the equations:-

$$\tau_{xz} = G\theta \left(\frac{\partial \bar{\Phi}}{\partial x} - y \right) \quad \text{and} \quad \tau_{yz} = G\theta \left(\frac{\partial \bar{\Phi}}{\partial y} + x \right)$$

Spreadsheet equations are worked out to provide a simplified summation in the two primary directions starting from zero warping. The two values are then added:-

The x effect, $\frac{\partial \bar{\Phi}}{\partial y}$. Scale Factor - y + previous value

The y effect, $\frac{\partial \bar{\Phi}}{\partial x}$. Scale Factor + x + previous value

The total effect = x effect + y effect

Using the numerical values from the torsion stress function distribution this gives a distribution as given at figure 86

for the longitudinal warping. The maximum value of longitudinal warping:-

$$\Rightarrow \frac{23.45}{200000} \times 60 \text{ mm.}$$

Again this is for a twisting of 1 turn per unit length for the drill twisted 140° in 100mm flute length it is:-

$$\frac{23.45}{200000} \times 6000 \times \frac{140^\circ}{360^\circ} \times \frac{1\text{mm}}{100\text{mm}} = 0.002738\text{mm}$$

$$\Rightarrow 2.738 \mu\text{m at the outer corner}$$

9.4. CONCLUSIONS.

The static analysis of the drill is not simply a problem of torsion. This chapter describes how the two component system described in the last chapter may be unified to give the total system. The problem of the torsion constant is basically easy to solve. The important aspect is the incorporation of the second component, in a simple form and based on the same cross section and mesh as the torsion problem.

The maximum torque before failure is an important parameter of a drilling control system. The drill stiffness data produced is available to drive an examination of the dynamic behaviour of the drill and, therefore, an examination of the torque amplification effects which lead to random drill failure.

CHAPTER 10

	PAGE
10. DRILL DYNAMIC RESPONSE	232
10.1. NATURAL FREQUENCY AND THE VALUE OF VIBRATION ANALYSIS	232
10.2. SUPPORTING OBSERVATIONS FROM DRILL TESTING	238
10.3. CONCLUSIONS	244

10. DRILL DYNAMIC RESPONSE.

One may now look at the drill in terms of its dynamic response to a transient loading. It is difficult to imagine tool steel as a flexible material, it is even more difficult to imagine it as 'springy'. In a solid structure such as rod or bar it is very rigid, however, the fluted shape has the effect of turning the twist drill into a structure more closely resembling a coil spring. A 4.5mm dia x 100mm flute length drill is able to twist 140° before failure and at the same time extend by over 1.0mm. This degree of flexibility has not been studied or even described in any of the literature found.

10.1. NATURAL FREQUENCY AND

THE VALUE OF VIBRATION ANALYSIS.

Drill natural frequency has been measured for the case of 20mm dia standard length twist drills as 1400Hz [8]. It is obvious that a large and relatively short drill will have a high natural frequency but that as the drill diameter become smaller and the drill becomes much longer relative to the diameter the natural frequency will reduce. This effect is compounded because when drilling with large drills generally low spindle speeds are used, for example 600 R.P.M., 10Hz, but with smaller diameter drills higher spindle speeds are used with a trend towards very high spindle speeds of up to 10,000 R.P.M., 167Hz, for modern ceramic coated drills.

Modern vibration theory is based on Computer Aided Dynamic Analysis. This assumes that any real system may be modelled by a discrete System with discrete properties. The number of nodal properties that are unconstrained governs the degree of freedom. A real system, in comparison, has its properties distributed throughout and has innumerable degrees of freedom.

The properties that are modelled are selected from the following:-

MASSES	to represent	INERTIA
SPRINGS	to represent	FLEXIBILITY
DAMPERS	to represent	ENERGY DISSIPATION

Governed by a set of ordinary differential equations.

A continuous system leads to a single partial differential equation that is generally insoluble. A model of the same system leads to a set of ordinary differential equations and this set may be solved. There are three basic requirements for a suitable mathematical model of a real system:-

- the model must be adequate but not unnecessarily detailed.
- the results depend on the accuracy of the parameters:-
 - mass, stiffness, damping,
 - boundary conditions, input forces.
- the time and effort expended must reflect the requirements.

The twist drill does not lead to an obvious model. The shaft of a twist drill in torsion is a real system with two properties. A stiffness distributed throughout the fluted section and a mass distributed throughout the drill. It is

less easy to model distributed properties as point masses and springs which have direct effect only at their individual points.

The theory of vibration of elastic bodies provides an equation for the motion of a rod in torsional vibration. The equation is dependent on the torsional stiffness and on the angular inertia. In a rod of circular section, stiffness is given by the product Polar Moment of Inertia I_p times Shear Modulus of Elasticity G and the mass moment of inertia is given by I_p times Density of the rod ρ divided by g . The resulting differential equation is a version of the wave equation for which a mathematical solution is possible:-

$$\frac{\rho}{g} I_p dx \frac{\partial^2 \theta}{\partial t^2} = I_p G \frac{\partial^2 \theta}{\partial x^2} dx$$

or:-

$$\frac{\partial^2 \theta}{\partial t^2} = \left[\frac{G \cdot g}{\rho} \right] \frac{\partial^2 \theta}{\partial x^2}$$

The solution for the natural frequencies, w , of this rod fixed at one end and free to rotate at the other is:-

$$\cos \left[w \sqrt{\left(\frac{\rho}{G \cdot g} \right) l} \right] = 0$$

l = length of rod

$$w \sqrt{\left(\frac{\rho}{G \cdot g} \right) l} = \frac{\pi}{2}, \frac{3\pi}{2}, \frac{5\pi}{2} \dots (n + \frac{1}{2})\pi$$

$$w = (n + \frac{1}{2}) \frac{\pi}{l} \sqrt{\left(\frac{G \cdot g}{\rho} \right)}$$

Applying the first equation to the drilling situation. For the left hand side, the polar moment of inertia is known from the previous geometric analysis, Chapter 5. The density of tool steel is known. For the right hand side a numeric value for the torsional stiffness has been calculated in the static analysis. For the sample drill the equation $T = K_t \theta r^2$ gives Stiffness = 157.77G. The differential equation of the free vibration of the 4.5mm drill is therefore given below:-

$$\frac{\rho}{g} 20.9 \, dx \frac{\partial^2 \theta}{\partial t^2} = 157.77G \frac{\partial^2 \theta}{\partial x^2} \, dx$$

or, by the equation above for the fundamental frequency of the sample drill:-

$$w = \frac{1}{2} \frac{\pi}{0.150} \sqrt{\left(\frac{157.77Gg}{20.9\rho} \right)}$$

$G = 6000$
 $g = 9.81$
 $\rho = 7.0$

$$\Rightarrow w = 2638 \text{ Rad/Sec} \quad \Rightarrow 419 \text{ (Hz)}$$

No method for the measurement of drill natural frequency has been reported in the literature and no method has been developed here at Aston to be available for comparison.

Wu's paper of 1977 titled "Dynamic Data System - A New Modelling Approach", [23], describes some of the many advantages of a method for the monitoring of the dynamic variation of the cutting forces. It is a method that has

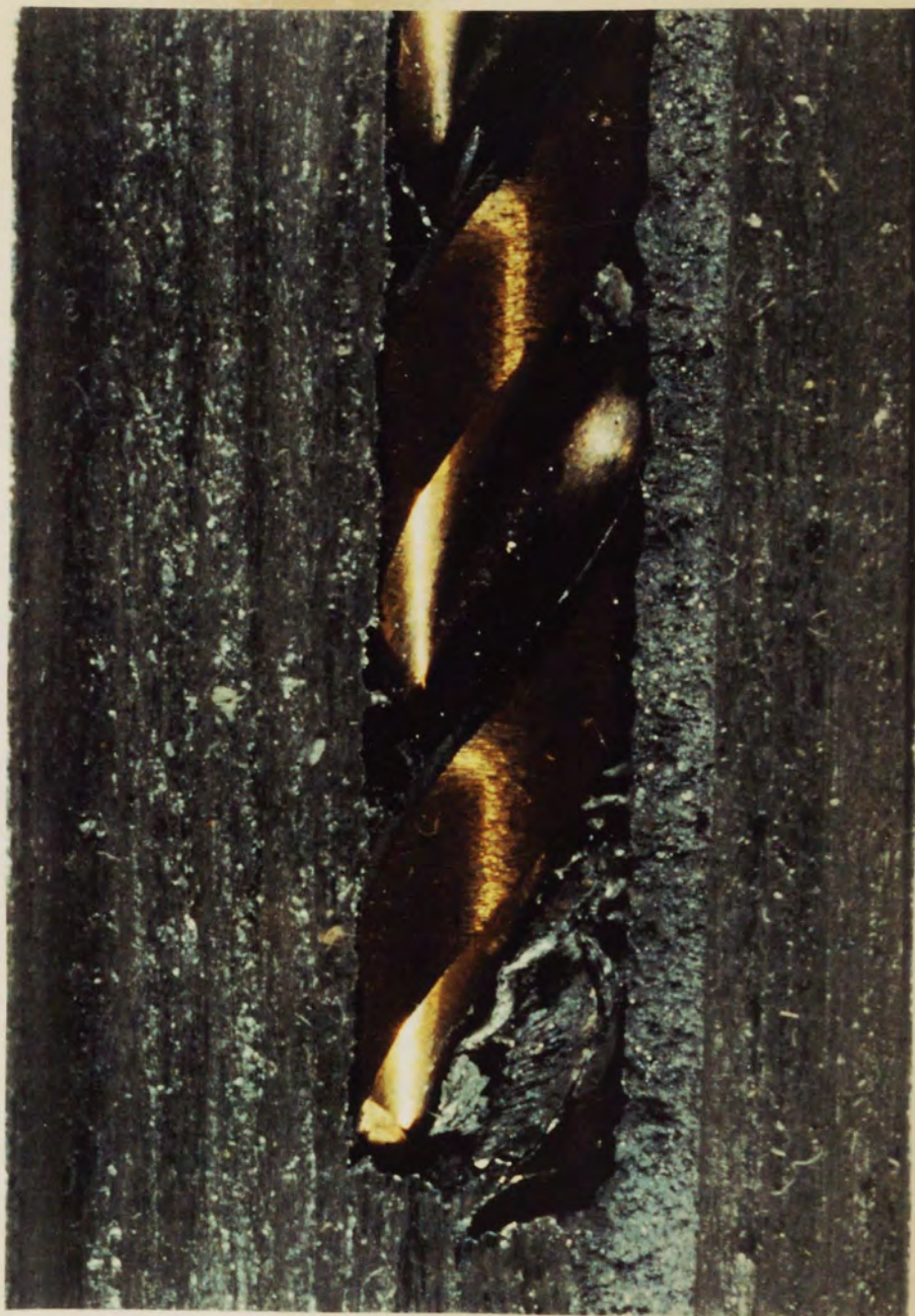


Figure 87 - Photograph of Broken Drill in Test Block

been tested for the monitoring of the drilling process and a strong correlation has been identified between the dynamic signal and the drill wear at the frequency of twice the spindle speed. This correlation remains unexplained but such vibration effects offer many prospects for the future control of machining if only the dynamic properties can be understood.

Stick-slip vibration effects have also been measured, Schaterin [8], related to the spindle speed but also related to the drill natural frequency in torsion.

Understanding the dynamic behaviour of the drill is becoming increasingly important. The modern machining centres in use today are equipped for adaptive control either by torque monitoring, (static load or dynamic low frequency response), or by acoustic monitoring, (high frequency response). Torque monitoring often senses the load on the spindle motor and in this form is inappropriate for drilling with small diameter drills as the drilling torque is relatively insignificant for such a large and powerful motor. However other forms of torque monitoring are available, for example strain sensors. Acoustic monitoring equipment could be utilised for drill wear monitoring provided the necessary details of what frequencies and frequency variations to monitor are first established.

10.2. SUPPORTING OBSERVATIONS FROM DRILL TESTING.

The behaviour of twist drill as described by the dynamic drilling model, figure 68, is important because it is a logical explanation of the mechanism of catastrophic drill failure where previously no logical explanation was available. A drill, that failed catastrophically during routine testing for no obvious reason, is shown in the photograph at figure 87. The point of the drill is intact and still has good cutting edges. The dynamic nature of drilling is indicated by the fact that the drill tip is firmly wedged into the workpiece material but is not located at the bottom of the hole. The separation is a distance of 1.0 mm back from the chip it was cutting at the time of failure. The photograph was obtained from the workpiece in which the drill point became firmly wedged. Material from one side of the drilled hole has been cut away from the workpiece so exposing the drill. The drill remains firmly wedged in the hole due to chips compacted in the flutes. This gap at the bottom of the hole was common with drills that suffered such random failure. The following paragraph is a description of the suggested mechanism:-

When the drill is wound up by a period of increased resistance to the cutting action the length of the drill is extended so exaggerating the situation by increasing the chip thickness. This action slows down the cutting edge also exaggerating the situation. This combination of effects

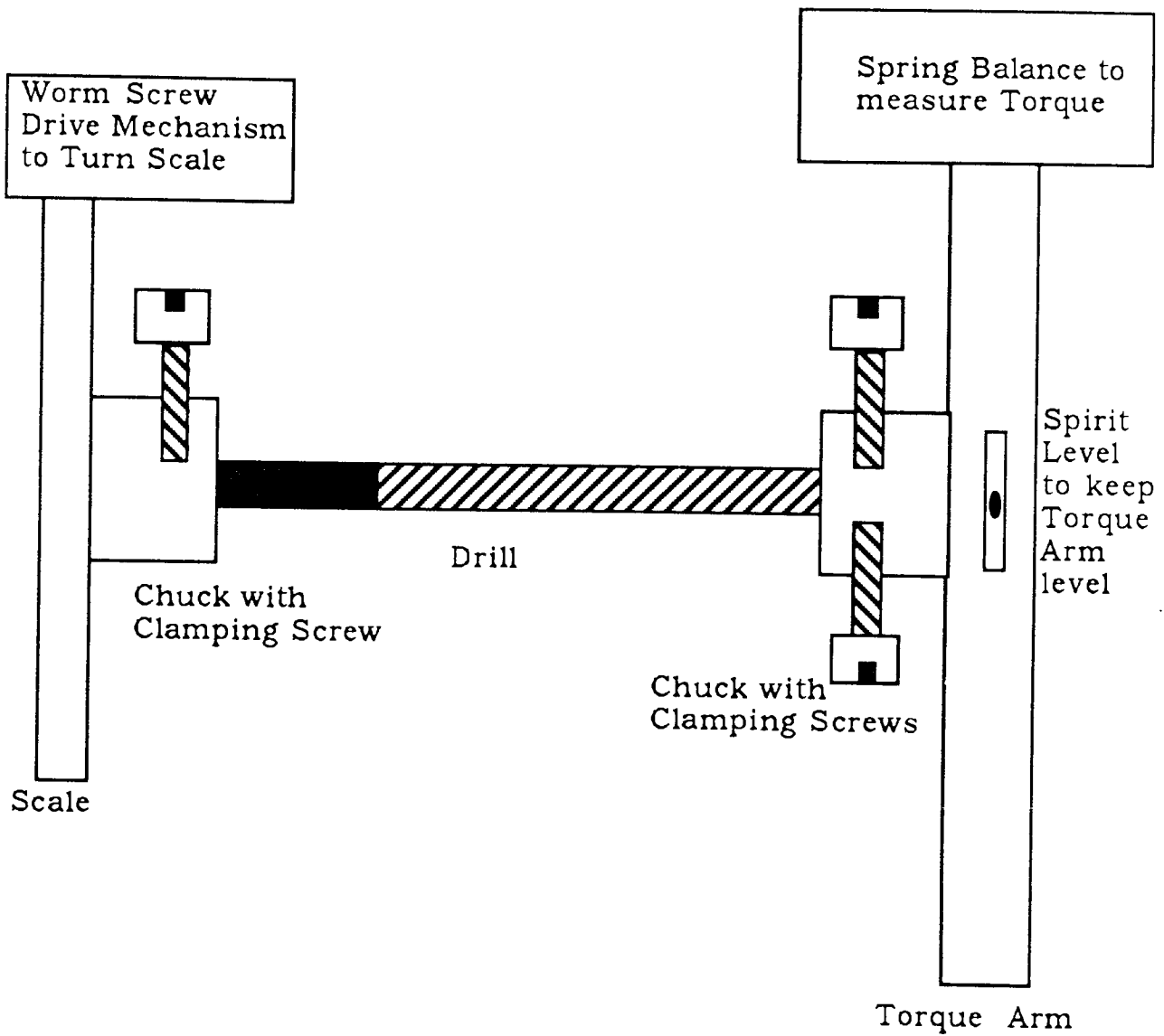


Figure 88 - Drill Torque Testing Machine

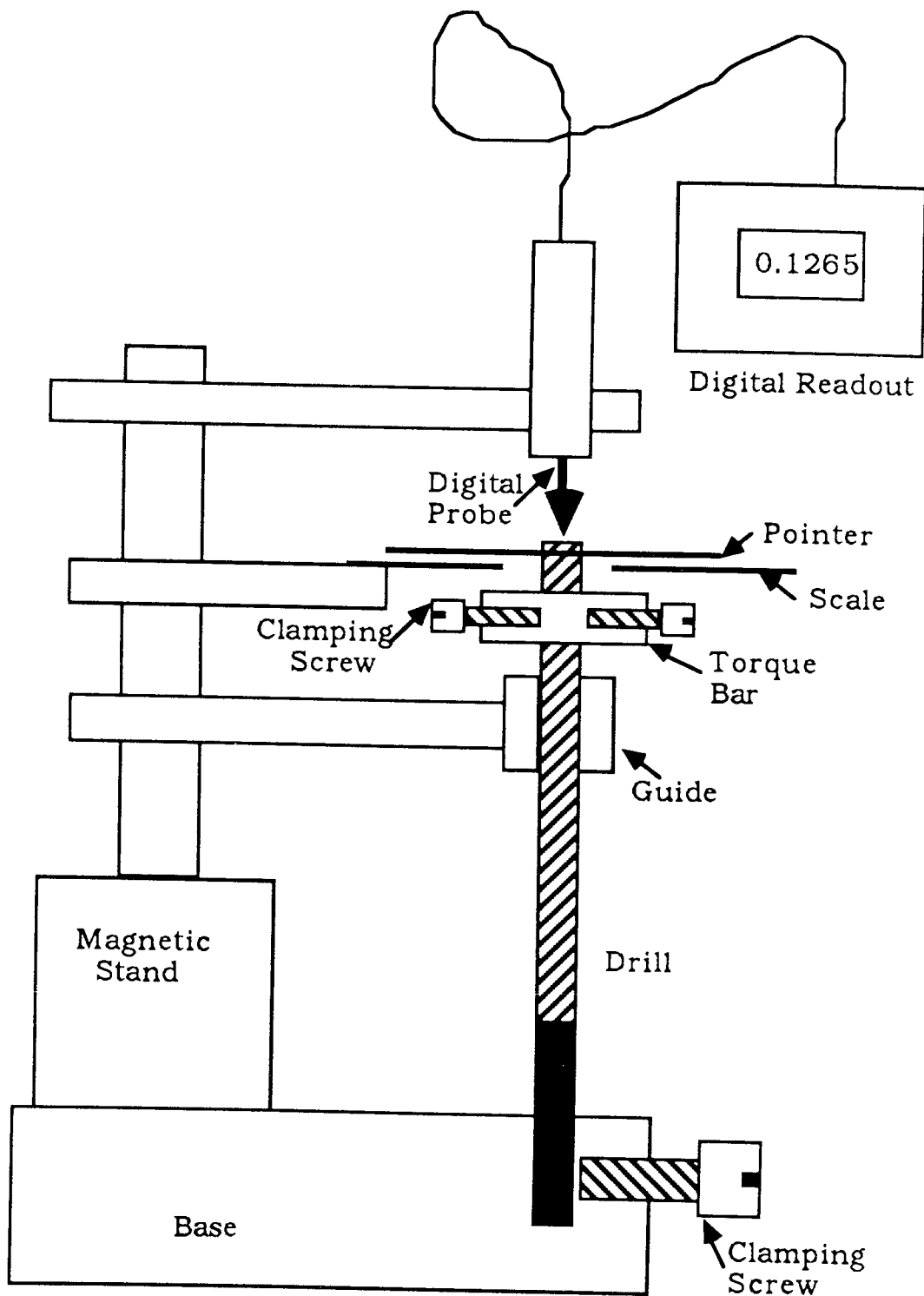


Figure 89 - Drill Extension Testing Machine

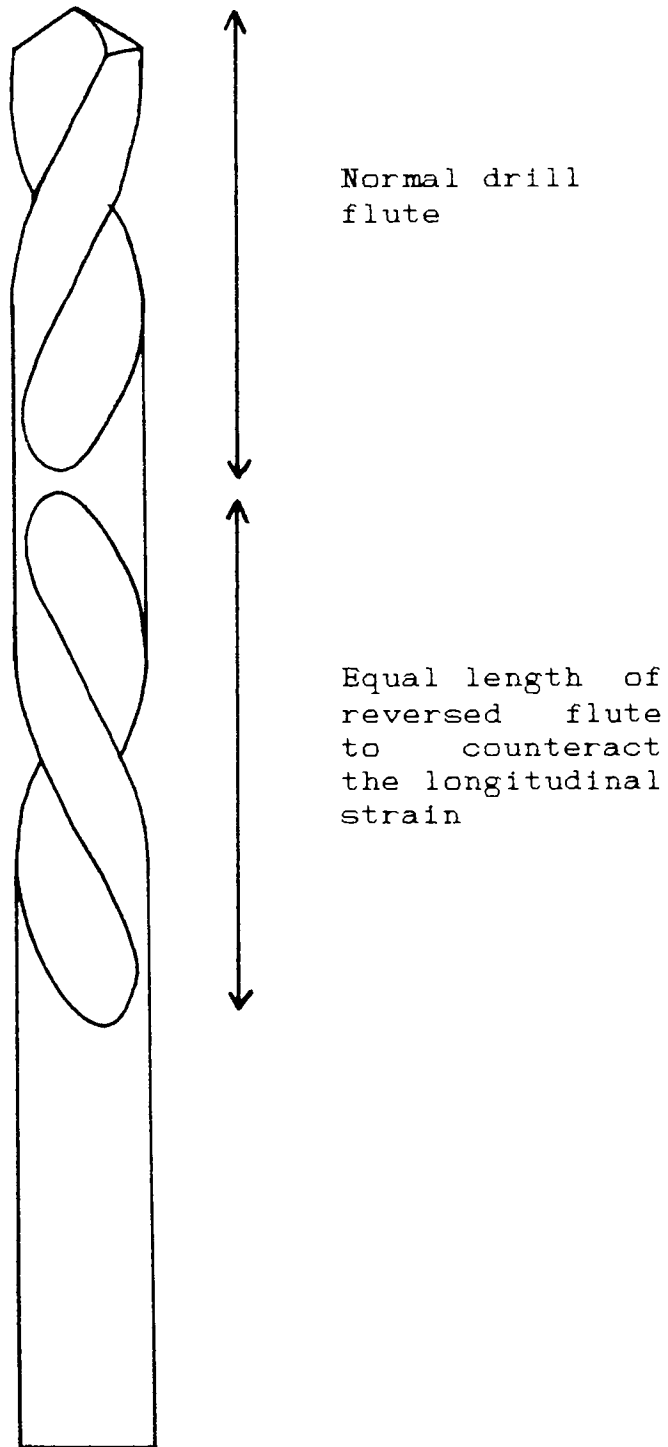


Figure 90 - Drill Modification Design

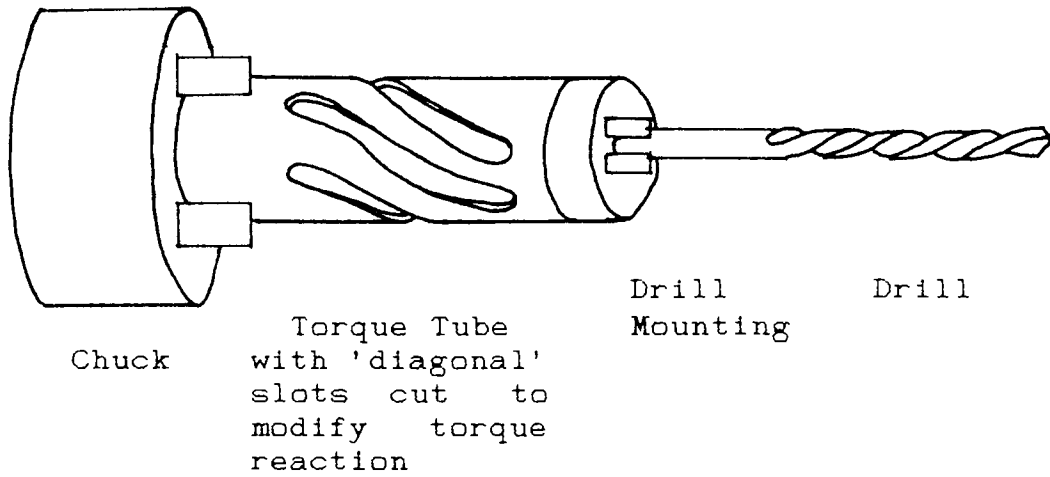


Figure 91 - Drill Mounting Design

gives rise to transient amplification of the cutting torque to many times the mean value, sufficient to provide the six times increase before failure described previously. Alternately, if the drill does not fail due to this increased load, then, when it starts cutting more freely, the twist unwinds and the length reduces so reducing the chip thickness and allowing the cutting speed to increase. This sudden unloading of the drill may also lead to drill failure.

Torque amplification can be a problem on tool entry and re-entry into the work at which point the cutting edges start cutting. When the torque is taken up the drill extends suddenly into the work. Torque amplification is also present at the time of breakthrough in through holes. As the drill chisel emerges the majority of the drilling thrust is removed so causing a sudden initial extension of the drill. The increased torque load is then amplified causing further extension. This is also a common instant when drill failure occurs.

Two experiments were set up to practically examine the flexible behaviour of 4.5mm Quick Spiral twist drills. The first experiment looked at the twisting torque required for specific angles of twist. It measured the torque load at one end of the drill while the other end is twisted through a range of angular deformations, figure 88. The second experiment mounted the drill on a base and then twisted the

end through the same range of angular deformations while measuring the longitudinal extension with a digital measuring probe, figure 89. The two sets of data may then be put together to obtain the torque : longitudinal extension behaviour. The results are given at figures 66 & 67.

Given that the adverse longitudinal effects exist as described by the dynamic drilling model, it would clearly be beneficial to reduce this effect by some external method. This was attempted by two designs for drill mountings with a similar arrangement of structures linking torsion and length but arranged in the opposite direction to counteract the drill action. It would therefore reduce in length when increased torque is applied and increase in length when torque is reduced, figure 90 & 91. These designs have yet to be proven.

10.3. CONCLUSIONS.

Why when using modern, unmanned CNC machine tools is it necessary to drill holes excessively slowly in order to provide a high level of tool protection? The only reason is that drilling is not fundamentally understood.

The dynamic behaviour of all metal cutting is becoming more important as our ability to monitor vibration in real time improves. The mathematics are time consuming but the computers doing the calculations are becoming ever faster.

This chapter assembles some of the available information and makes logical sense of this information by using the dynamic model of drilling proposed in chapter 7.

CHAPTER 11

	PAGE
11. DISCUSSION AND CONCLUSIONS	247
11.1. DEFINITION OF THE GEOMETRIC PROBLEM	248
11.2. ENUMERATE TOOL GEOMETRY	248
11.3. IDENTIFY THE CUTTING ANGLES	249
11.4. MODIFICATION FOR TOOL FLEXIBILITY	251
11.5. SUMMARY OF CONCLUSIONS	255
11.6. FUTURE WORK	256

11. DISCUSSION AND CONCLUSIONS.

This thesis is produced as the result of a research contract to investigate industrially relevant improvements in drill tooling and drilling technique. The geometric research reported in this thesis has been taken up by a major international drill manufacturing company for use in drill design and research. Drilling technique research has been reported in the thesis of I. Kavaratsis [24] who was also working at Aston University during this period. Some of the improvements described have been used successfully in the engineering industry.

The motivation for pursuing the geometric nature of the drilling process in this way was based on the shortcomings of the practical testing as described in chapter one, especially in the attempts to analyse drilling data.

This thesis proposes a new solution to the complex geometry of the twist drill which offers equivalent numerical information about any drill form and therefore offers mathematical predictability. The dynamic instability of the drill cutting process is then superimposed on this basic drill geometry.

11.1. DEFINITION OF THE GEOMETRIC PROBLEM.

The Twist Drill is a well established tool with a history going back to the 1860s. In modern times research and development in the industry has been restricted by a reluctance on the part of the drill users to pay any more for a tool thought of as tried and tested and also by a prolonged period of savage international competition. The current explosion of materials to be cut by drills, to make drills from and to coat drills with, does however require a whole new generation of twist drills and the current trend towards unmanned computer controlled machine tools requires a complete rethink of drilling technique.

Practical testing of drills identified the need to enumerate in detail the individual cutting geometry of a particular twist drill. Part one explains a new, simple method which, with the use of a personal computer, is able to put accurate figures to the problem of drill geometry.

11.2. ENUMERATE TOOL GEOMETRY.

The basic question is: What is the shape of the tool? This question must be answered simply and in terms that the computer may understand.

The system selected for this work is the generation of the three dimensional solid model described in part one. By

examination of the drill manufacturing process the description of the shape may be considerably simplified. Galloway's grinding cones [2] provide a simple basis for the model. Galloway's original axis orientation has been changed and the mathematics totally reworked and extended far beyond any previous work. This solid model is described by only 8 parameters and is able to comprehensively describe the shape of any drill form. This work uses the power of the computer to calculate a complete numerical solution.

11.3. IDENTIFY THE CUTTING ANGLES.

A scheme of measurement is required to apply to the drill model. This is provided by the definitions of Merchant and Stabler. Defining the drill geometry in these terms has been tried before but only as a theoretical mathematical exercise, a comprehensive method that is simple and accurate was not previously available.

Determining the fundamental cutting angles of the twist drill is a 3-dimensional problem for which in the past a 2-dimensional solution has been applied. Because of the use of plane trigonometry previous work has not been able to address the effect of drill feed. The presence of feed complicates the mathematics by taking the relative velocity vector out of the plane orthogonal to the drill axis. Spherical Trigonometry is a point centered analysis which allows the direct, 3-dimensional calculation of the angle

between any two random directions emanating out from that central point. The use of Spherical Trigonometry is proposed and it has three major advantages:-

1. It allows direct calculation with a single, simple formula. Cumulative errors of a multi-staged operation are therefore avoided.
2. The formula is invariable making its application to a computer a simple exercise. A standard computer sub-routine may perform this function without the user knowing that spherical formulii have been used.
3. Additional effects such as the feed rate of the drill may be included in the analysis of the cutting situation with no effect on the degree of calculation required.

The drill form is generated as a mesh of data. The facets of surface between these points are assumed to be part of a plane and the normal direction to this plane is calculated. This is the form in which the surface data is compared with the relative velocity vector of the workpiece motion. The comparison is made using spherical trigonometry and provides the cutting angle data.

In a 3-dimensional tool such as the drill there is a range of tool shape and of velocity vector across the width of the cutting edge. The TurboPascal program described in part one allows rapid quantification of the range of tool cutting

angles for any shape of twist drill. This allows various aspects of the drill to be examined, including the cutting edge, the chisel edge, the flute and the shape of the flute heel. By a similar method the evaluation of any geometrically complex cutting tool is possible.

This improvement in cutting information will allow interpolation to be made between existing data rather than require the running of new experiments for each and every new situation. Chip flow may also be examined and good agreement is seen between computer chip flow predictions and evidence of the actual chip flow across the cutting edge.

11.4. MODIFICATION FOR TOOL FLEXIBILITY.

Applying the geometric work to the cutting action of the twist drill without modification assumes the stability and general rigidity of the structure of the drill. It is easy to make this assumption but it is erroneous. Much evidence of drill flexibility is provided, for the author the most convincing example is that of tool failure while drilling. When a drill fails while drilling the broken portion often remains firmly wedged in the hole. If the surrounding material is milled away the drill is revealed and it is never at the very bottom of the hole, figure 87 page 232. In order to explain this phenomena it is necessary to examine the twist drill for its dynamic properties and to facilitate this a new dynamic drilling model is introduced, figure 68

The Twisting Model

$$\frac{\partial^2 \phi}{\partial x^2} + \frac{\partial^2 \phi}{\partial y^2} = -2G$$

At the boundary : $\phi = \text{Constant (Zero)}$

$$\tau_{xz} = \frac{\partial \phi}{\partial y}$$

$$\tau_{yx} = - \frac{\partial \phi}{\partial x}$$

The Bending Model

$$\frac{\partial^2 \phi}{\partial x^2} + \frac{\partial^2 \phi}{\partial y^2} = 0$$

At the boundary : $\frac{\partial \phi}{\partial s} = \left[\frac{Px^2}{2I} - \frac{\nu}{2(1+\nu)} \frac{Py^2}{I} \right] \frac{dy}{ds}$

$$\tau_{xz} = \frac{\partial \phi}{\partial y} - \frac{Px^2}{2I} + \frac{\nu}{2(1+\nu)} \frac{Py^2}{I}$$

$$\tau_{yx} = - \frac{\partial \phi}{\partial x}$$

Figure 92 - Boundary Value Partial Differential Equations

page 182.

Part two examines two aspects of the static stress analysis of the drill in cross section. The first is the cross section torsional rigidity or Torsion Constant, which is called the twisting model. The second is to account for the helical orientation of the drill and is called the bending model.

The twisting model is a straight forward application of elasticity, however the bending model requires a little explanation. It is a first attempt at a mathematical solution to the longitudinal effect where the drill cross section is divided into two across the drill web. Each half may then be modelled as a cantilever bent by the application of a load at the free end. The distribution of longitudinal strain in the case of the cantilever is reasonably similar to the distribution of longitudinal strain in the real drill when twisted.

The equations for the torsion model and for the bending model are similar and are applied to the same cross section so allowing the two results to be compared. The two 'boundary value partial differential equations' are shown in figure 92.

Both systems are solved in terms of their components of shear stress in the cross section, τ_{xz} and τ_{xy} , and combined

to produce the distribution of total shear stress. The Torsion Constant, Maximum Shear Stress Concentration and the Warping Distribution are also produced.

The dynamic drilling model requires two parameters to describe the drill deformation. First the effective helix angle and second the Torsion Constant. The resulting action of the tool tip is a motion towards the workpiece when the torque loading increases, so exaggerating or amplifying the change, and a motion away from the workpiece when the torque loading is reduced, again amplifying the change. Drilling is therefore an unstable process and no previous research has described the twist drill in this way.

The dynamic behaviour of the drill may be examined by using the equation from the theory of vibration of elastic bodies for torsional vibration in rods. It is possible to calculate the fundamental natural frequency of torsional vibration of the fluted length of the drill shaft from the torsional stiffness and the mass per unit length. Dynamic measurement of the drilling process has indicated the importance of this frequency.

Drilling, when described in this way as a dynamic process, is an uniquely unstable metal cutting process when compared with the full range of other metal cutting processes.

11.5. SUMMARY OF CONCLUSIONS.

The Geometric Analysis defines (for the first time):-

1. The Drill Geometry.

This thesis provides an analytical link between the current definition of a drill in terms of geometric references and the numerical data required to define that drill form to a CAD design computer or to a CNC machine tool prior to manufacture.

2. The Cutting Angles.

Current drill testing only provides information applicable to the particular drill workpiece combination examined. The ability to define the fundamental cutting geometry of a twist drill is provided by this thesis and this ability allows drilling data to be compared on equivalent terms between two different drills and with other forms of metal cutting.

The Dynamic Analysis provides:-

3. An insight into the dynamic behaviour of the twist drill.

The first half of this thesis works towards the calculation of cutting angles but this geometry is only applicable to steady state conditions. Before the information is of use for the adaptive control of twist drilling it must be modified for the dynamic distortion

of the twist drill.

11.6. FUTURE WORK.

The reported work explores some of the basic geometric concepts of three dimensional cutting processes through a detailed examination of the geometry of the twist drill. The research indicates two basic directions for future work.

The first direction for future work is in drill design. The only method currently available for looking at the performance of the cutting geometry of the drill is a system of trial and error backed up by human intuition. Some analytical aids are available, for example, a computerised system to predict the drill flute form from a particular grinding wheel form, but there is no overall drill design package and there is no analytical method for looking at drill performance.

What is the true cutting geometry of the cutting edges of the twist drill? There is a flank face and a rake face with a flow of workpiece material across them. This thesis shows that it is possible to describe this cutting geometry in numerical terms. The immediate advantage is an accurate analytical assessment of the influence of changes in the drill form. It is no longer necessary to isolate the various aspects of drill geometry as any two drills are described in equivalent numerical terms.

The various aspects of the geometric calculations of this thesis will form the nucleus of a complete drill design and analysis system. This system must include the ability to allow for the material properties of the workpiece and so make possible the calculation from the known cutting geometry of the cutting forces and chip behaviour.

The second direction for future work is in the utilisation of drills or what has been termed drilling technique. The flexibility work has taken a system that was described by J. R. Masuha [25] as mathematically impossible in the introduction to his rework of Schaterin's investigations [7,8]. The analysis has produced strength, stiffness and frequency data for the dynamic distortion of the twist drill in very simple terms.

There is no doubt that drill stiffness has strong influence over the two most important aspects when drilling deep holes. These are to maintain the stability of the drilling process so avoiding random failure and to control the runout of deep holes which are often oilways carefully sited to avoid other machining and requiring accurate linking to oil galleries in the workpiece.

LIST OF REFERENCES

- [1] Tools and Product Quality when using TiN Coated Drills
D.P. Upton & R.H. Thornley
Plasma Assisted Coatings Technology Seminar, National
Centre of Tribology, UKAEA, 11/12 June 1986.
- [2] Some experiments on the influence of various factors on
drill performance
D.F. Galloway
Transactions of the ASME, February, 1957, pp 191-231
- [3] Computer Analysis of Drill Point Geometry
W.D. Tsai & S.M. Wu
Int J of M T Des & Res, Vol 19, 1979, pp 95-108
- [4] An Analysis of the Geometry of the Periphery of the
Flank Face of Twist Drills Ground with Cylindrical and
Conical Forms
D.J. Billau & P.F. McGoldrick
Int J of M T Des & Res, Vol 19, 1979, pp 69-86
- [5] A Mathematical Model of the Grinding Wheel Profile
required for a specific Twist Drill Flute
R.K. Radhakrishnan, R.K. Kawlra & S.M. Wu
Int J of M T Des & Res, Vol 22, 1982, pp 239-251
- [6] Importance of Flute Helix-Angle of Twist Drills
A.L. Kirilenko
Machines & Tooling, vol XLIII No.1 p. 48 1972
- [7] Wendelbohrer mit erhöhter Steufigkeit
Michail A. Schaterin
Werkzeugmaschine International, No. 6, December 1971.
- [8] Das Schwingungsverhalten von Wendelbohrern im Schnitt
Michail A. Schaterin
Werkzeugmaschine International, No. 1, February 1972.
- [9] An Investigation into the Influence of Helix Angle
on the Torque-Thrust Coupling Effect in Twist Drills
K. Narasimha, M.O.M. Osman, S. Chandrashekhara and
J. Frazao.
The Int. Journal of Advanced Manufacturing Technology,
2 (4), 1987, pp 91-105
- [10] Effect of Drill Geometry on the Deformation of a Twist
Drill
Tirupathi R. Chandrupatlia and William D. Webster, Jr
GMI Engineering and Management Institute
Proc of the 25th International MTDR Conference
April 1985

- [11] The Fundamental Geometry of Cutting Tools
G.V. Stabler
Proc of the I Mech E Vol 165, 1951 pp 14-26
- [12] Some Practical Aspects of Cutting Tool Nomenclature
D.F. Galloway, Discussion by G.V. Stabler
Proc of the I Mech E Vol 168, 1954
- [13] Basic Mechanics of the Metal Cutting Process
Merchant M.E.
Transactions of the ASME, Vol 66, 1944, pp A-168
- [14] The Application of Spherical Trigonometry to the
Evaluation of the Cutting Action of a Tool
with Complex Three Dimensional Geometry
Webb P.M. and Maiden J.D.
Dept of Mech and Prod, University of Aston in B'ham
Proc of the 4th Nat Conf Prod Research,
Sheffield, Sept 1988
- [15] The influence of tool geometry on the
performance of drilling tools
El-Wahab A.I.
PhD Thesis, University of Aston, 1985
- [16] A Treatise on Spherical Trigonometry with Applications
to Spherical Geometry and Numerous Examples
McClelland W.J. & Preston T.
London MacMillan & Company, Second Edition, 1897
- [17] On the Drilling of Metals I -
Basic Mechanics of the Process
Oxford C.J.
Transactions of the ASME, vol 77, p103, 1955
- [18] Some aspects of Drill Performance
Upton D.
PhD Thesis, University of Aston, 1987
- [19] Theory of Elasticity
Timoshenko S.P. and Goodier J.N.
McGraw-Hill Book Company, Third Edition, 1970.
- [20] The Static Bending of Pre-Twisted Cantilever Blading
Carnegie W.
Proc Ins Mech Eng, Vol 171 No 32 pp 873-894, 1957
- [21] Vibrations of Pre-Twisted Cantilever Blading
Carnegie W.
Proc Ins Mech Eng, Vol 173 No 12 pp 343-374, 1959
- [22] Torsional Stress Analysis of Twist
Drill Sections by Membrane Analogy
Neubauer, E.T.P. & Boston, O.W.
Transactions of the ASME 69 (1947) 18, S. 29-34

- [23] Dynamic Data System - A New Modelling Approach
Wu S.M.
ASME Jour of Eng for Ind, Vol 99, B, No 3,
pp 708-714, Aug 1977.
- [24] Control of the Twist Drilling Process
Kavaratsis I.
PhD Thesis, University of Aston, 1990
- [25] Torsionsteifigkeit und Bohrverhalten von
Spiralbohren mit Sonderprofilen
Masuha J.R.
Carl Hanser Verlag, München 1980, ISBN 3-446-13274-0